F_1F_0 ATP Hydrolysis is a Determinant of Metabolic Rate, a Correlate of Lifespan, and a Weakness of Cancer

Michael David Forrest Ph.D., *(mikeforrest££hotmail.com (££=@))*

ABSTRACT

Body temperature decrease, in mice administered with a drug that selectively inhibits F_1F_0 ATP hydrolysis (which doesn't inhibit F_1F_0 ATP synthesis), is evidence that F_1F_0 ATP hydrolysis is used for metabolic heat generation *in vivo*. It being pivotal to homeothermy, which is a new discovery. This drug, capable of dose-dependently lowering body temperature, might slow aging and extend lifespan (combating all age-related diseases thereby). Because slightly lower body temperature corresponds with a much longer lifespan in mice and humans. Alzheimer's, a disease of aging, can cause a higher body temperature (that accelerates its progression), which this drug might counteract. Across twelve investigated species, less F_1F_0 ATP hydrolysis correlates with greater maximal lifespan. A case for causality is made. Selective drug inhibition of F_1F_0 ATP hydrolysis exerts potent anti-cancer activity *in vitro*. Teaching F_1F_0 ATP hydrolysis as a new cancer drug target.

SIGNIFICANCE

Different species age at different rates, conferring different maximal lifespans. For example, the maximal lifespan of a mouse is 4 years, while that of a bowhead whale is 211 years. So, aging is modifiable. But how? A clue might be body size: smaller mammal species tend to age faster than larger ones. In geometry, smaller objects have a greater surface-area-to volume ratio than larger objects. Meaning smaller mammal species lose more of their metabolically generated heat. And so, each gram of a smaller mammal species needs to generate more metabolic heat than each gram of a larger mammal species. To keep their body temperature at 37°C. The chemical reactions that the body uses to obtain energy from food (e.g., to keep the body warm) produce harmful by-products: Reactive Oxygen Species (ROS). That cause molecular damage. The accumulation of which might be aging. Each gram of a smaller mammal species generates more metabolic heat, uses more food, produces more ROS, and ages faster.

Herein reported is a chemical reaction (F_1F_0 ATP hydrolysis) that mammal species use to generate heat. Showing that each gram of smaller (shorter-living) mammal species use it more than each gram of larger (longer-living) mammal species. A drug that selectively inhibits it (which doesn't inhibit F_1F_0 ATP synthesis) is shown to decrease metabolic heat generation in mice. Higher doses decrease it more. The human body (in typical clothing) is most comfortable at an ambient temperature of around 20.3°C. But much of the world is hotter than that (for at least part of the year). Conceivably, this drug can, by decreasing metabolic heat production (in a dose-dependent manner), increase the ambient temperature that someone is comfortable at, increasing comfort in hot climates/seasons/rooms. If this drug is applied to only part of the body (e.g., in a face cream), heat transfer from the remainder of the body (via blood flow) is expected to maintain this part at 37°C, no matter the ambient temperature.

In the literature, lower body temperature extends the lifespan of mice (0.34°C lower increases lifespan by 20%) and corresponds with a longer human lifespan and healthspan. Moreover, calorie restriction, which slows aging and increases the lifespan of model organisms, reduces body temperature. This drug can (dose-dependently; *if* the ambient temperature is permissively low) reduce body temperature.

This drug is predicted to slow aging (whether reducing body temperature or not). Indeed, in mice, its mechanism of action (selectively inhibiting F_1F_0 ATP hydrolysis) is shown to safely decrease intracellular ROS concentration. This drug is shown to have anticancer activity *in vitro*. Thence (prospectively) here is an anticancer drug that helps, rather than harms, normal cells.

INTRODUCTION

Different species age at different rates and have different maximal lifespans [1]. If we could discover why, elucidating how nature modulates aging, we might be able to harness this power for ourselves.

A well-known thesis is that chemical reactions in the body (those for obtaining energy from food) produce harmful by-products [2-5]. Called Reactive Oxygen Species (ROS). And these cause molecular damage, which accumulates over time, which is aging. This paper adds to this thesis. With new experimental data and analysis.

Aerobic respiration converts the chemical energy of food into the chemical energy of ATP [6]. An intermediate in this process is the generation of an electrochemical gradient of protons, a proton motive force (pmf), comprising ΔpH and voltage (Ψ_{IM}) components, across the inner mitochondrial membrane. ATP synthase is located in this membrane. It can use the pmf to generate ATP from ADP and inorganic phosphate (Pi). But ATP synthase is reversible. Depending on its substrate and product concentrations, and the pmf value, operating forwards (passing protons, making ATP) or backwards (pumping protons, consuming ATP). Its forward and reverse modes respectively. Which may also be termed F_1F_0 ATP synthesis and F_1F_0 ATP hydrolysis respectively.

IF1 protein is an endogenous protein that selectively blocks the reverse mode of ATP synthase (F_1F_0 ATP hydrolysis), which does *not* block the forward mode of ATP synthase (F_1F_0 ATP synthesis) [7-12] (Figure 1). It is widely considered irrelevant during aerobic respiration because (*i*) ATP synthase is solely performing F_1F_0 ATP synthesis, and (*ii*) IF1 protein activity is pH sensitive [13], being low at the normal mitochondrial matrix pH (~pH 8). But it is considered significant upon matrix acidification. Caused by collapse of the pmf across the mitochondrial inner membrane. Which causes ATP synthase to reverse its operation, performing F_1F_0 ATP hydrolysis instead, consuming cellular ATP. This can occur, for example, during ischemia [14-15]. When a tissue, or part(s) thereof, is completely/partially cut off from blood flow, foregoing respiratory substrates and O_2 delivery. So, the present consensus is that IF1 protein is a safety device. Important in mitigating pathology, but irrelevant normally.

By contrast, I herein report that F_1F_0 ATP hydrolysis ***does*** occur normally. It being important for generating metabolic heat. Whilst IF1 protein activity, although subdued by the normal alkaline pH of the mitochondrial matrix, is *usefully* non-zero. Wherein the amount of IF1 protein activity constrains the amount of F_1F_0 ATP hydrolysis (metabolic heat generation). And I propose that the different maximal lifespans, in different mammal species, are (at least partially) because of different specific F_1F_0 ATP hydrolysis rates, set by different specific IF1 protein activities. I show, in a species set, (larger) longer-living mammal species have more specific IF1 protein activity, and less specific F_1F_0 ATP hydrolysis. Consistent with IF1 protein activity being a molecular determinant of maximal lifespan. Hinting that a drug mimicking IF1 protein activity, which selectively inhibits F_1F_0 ATP hydrolysis, might slow

aging and extend the lifespan of mammals. If administered when the ambient temperature (and/or bodily insulation) ensures no, or only a safe, body temperature drop. Such drugs are taught in my US patent applications [16-17]. Examples therefrom are used in experiments reported herein. Preprint versions of this paper were published on bioRxiv in 2021 [18-19].

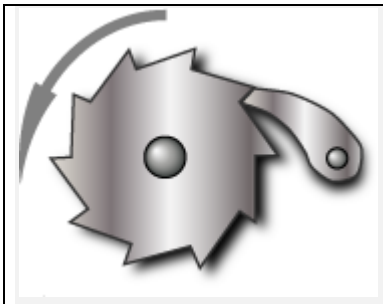

Figure 1 - A ratchet and pawl mechanism, wherein the pawl ensures that the ratchet cog can only rotate in the direction shown by the arrow [20]. IF1 protein's inhibition is unidirectional. Only of F_1F_0 ATP hydrolysis, it not inhibiting F_1F_0 ATP synthesis [7-12]. ATP synthase comprises a molecular rotor, which rotates one way when performing ATP synthesis [21]. And the opposite way when performing ATP hydrolysis. But F_1F_0 ATP hydrolysis is not simply the reverse of F_1F_0 ATP synthesis, because they follow different molecular pathways [22-24]. Reflected, for example, by azide inhibiting F_1F_0 ATP hydrolysis and not F_1F_0 ATP synthesis [25-26] (*N.B., azide also inhibits Complex IV [27] and so is a metabolic poison*). IF1 protein can only bind ATP synthase when it is hydrolysing ATP. When bound it acts analogously to a pawl, blocking the rotational direction of ATP hydrolysis, but not that of ATP synthesis. It being driven off/disassociated by the action/rotation of ATP synthesis.

IF1 protein binding to ATP synthase blocks the rotational direction of ATP hydrolysis directly (by its N-terminal section directly binding ATP synthase's central shaft γ subunit [12]). And indirectly by preventing ATP hydrolysis (by its binding imposing, at one of ATP synthase's three catalytic centres, the structure and properties of the β_{TP}-α_{TP} interface upon the β_{DP}-α_{DP} interface that it binds, thereby preventing this centre hydrolysing its bound ATP [9-12]).

RESULTS

This Results section comprises new experimental data. Presented first. Thereafter, in the light thereof, novel analysis/interpretation of publicly available data. Then, disclosed at the end,

more new experimental data. Methods are presented later, as the penultimate section of this paper, before References.

New experimental results

Systemic inhibition of F_1F_0 ATP hydrolysis: If F_1F_0 ATP hydrolysis is a drive of metabolic heat generation, then systemic, selective drug inhibition of F_1F_0 ATP hydrolysis (without inhibition of F_1F_0 ATP synthesis) should reduce metabolic heat generation in a subject. Which should, *if* the ambient temperature is lower than their normal body temperature, reduce their body temperature towards the ambient temperature. This is experimentally observed in Figure 2.

The drug administered to mice to produce Figure 2 was developed decades ago by Bristol Myers Squibb (BMS), a leading pharmaceutical company, to treat ischemia [28-29] (but it was never tested in humans. It is orally bioavailable, with good pharmacokinetics, in rats [28]). This drug potently inhibits F_1F_0 ATP hydrolysis. But ***not*** F_1F_0 ATP synthesis. As shown by assays with Sub-Mitochondrial Particles (SMPs; formed by sonicating mitochondria). Where F_1F_0 ATP hydrolysis is assayed by a spectroscopic assay for NADH fluorescence, which incubates SMPs with reagents that include pyruvate kinase and lactate dehydrogenase enzymes (*F_1F_0 ATP hydrolysis confers ADP for pyruvate kinase to convert phosphoenolpyruvate to pyruvate, producing ATP thereby, whilst lactate dehydrogenase converts pyruvate to lactate, and NADH to NAD^+. So, the amount of F_1F_0 ATP hydrolysis can be read out by the decrease of NADH fluorescence*). F_1F_0 ATP synthesis is assayed by a spectroscopic assay for NADPH fluorescence, which incubates SMPs with reagents that include hexokinase and glucose-6-phosphate dehydrogenase enzymes (*F_1F_0 ATP synthesis confers ATP for hexokinase to convert glucose to glucose 6-phosphate, producing ADP thereby, whilst glucose-6-phosphate dehydrogenase converts glucose 6-phosphate to 6-phosphogluconolactone, and $NADP^+$ to NADPH. So, the amount of F_1F_0 ATP synthesis can be read out by the increase of NADPH fluorescence*). A drug shown to inhibit F_1F_0 ATP hydrolysis, and not inhibit F_1F_0 ATP synthesis, in SMPs has been shown to do the same in isolated (*ex vivo*) rat heart [30]. Shown to conserve ATP during ischemia. Without reducing [ATP] under normal conditions. Thence shown to be distinct from drugs that inhibit both modes of ATP synthase (such as oligomycin) which, by contrast, are shown to reduce [ATP] under normal conditions.

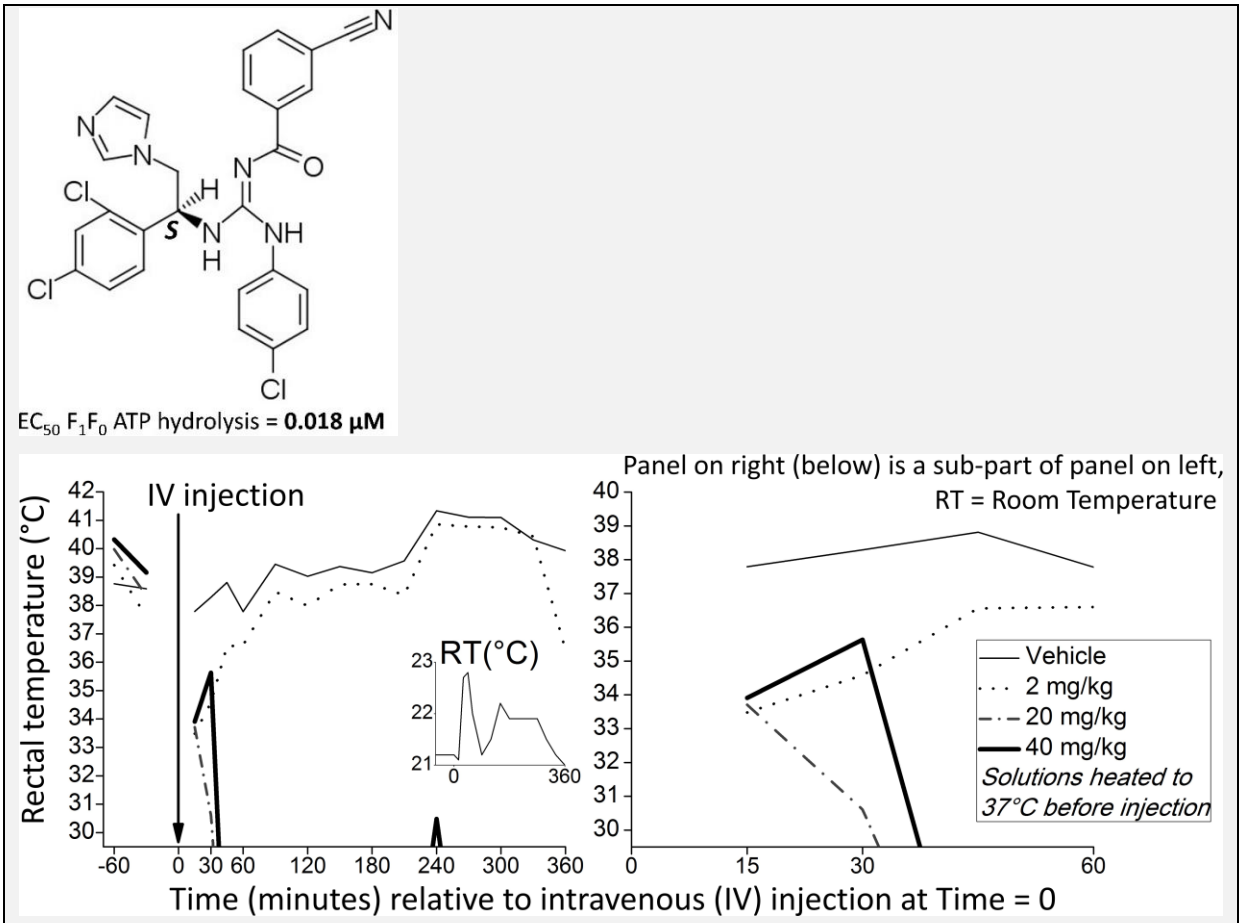

Figure 2 - Selectively inhibiting F_1F_0 ATP hydrolysis (without inhibition of F_1F_0 ATP synthesis) in mice reduces their rectal temperature towards room temperature. Room temperature (RT) was around 22°C. Drug structure shown (with enantiomeric excess (ee) of *S* stereoisomer ≥97%) was systemically (intravenously) administered to mice, whose rectal temperatures were monitored. This drug selectively, and potently, inhibits F_1F_0 ATP hydrolysis (EC_{50} = 0.018 µM [=18 nM], in a Sub-Mitochondrial Particle {SMP} assay {in which *no* inhibition of F_1F_0 ATP synthesis by this drug was observed}) [28-29]. Four mice were used. One was administered vehicle (control), and the other three differing doses of the drug: 2 mg/kg, 20 mg/kg, and 40 mg/kg (all solutions heated to 37°C before administration). Rectal thermistor used couldn't measure rectal temperatures lower than 30°C. Both 20 and 40 mg/kg (but not 2 mg/kg) drug doses made rectal temperature fall below 30°C and out of range. Although the ensuing uncertainty is bounded because rectal temperature cannot fall below room temperature (RT): RT ≤ rectal temperature < 30°C. Rectal temperature was recorded every 15 minutes in the 1st hour after dosing, and every 30 minutes in the later hours shown. It was also recorded at 60 and 30 minutes before dosing. For each mouse, the 1st rectal temperature recording is typically of an atypically high body temperature. Which is

associated with the stress of being handled, which a mouse typically becomes habituated to during the course of the experiment. This handling effect has been reported in other rectal thermistor studies of rodents, e.g. [31].

Statistics upon this data: For the 360 minutes (6 hours) after intravenous (IV) injection: comparing data for vehicle (mean rectal temperature = 39.50°C, *median = 39.41, standard deviation = 1.16, standard error of the mean, SEM = 0.3104, data does not differ significantly from that which is normally distributed by the Kolmogorov-Smirnov test of normality*) and 2 mg/kg drug (mean rectal temperature = 38.06°C, *median = 38.43, standard deviation = 2.31, standard error of the mean, SEM = 0.6175, data does not differ significantly from that which is normally distributed by the Kolmogorov-Smirnov test of normality*): independent t-test [degrees of freedom=(N1-1)+(N2-1)=(14-1)+(14-1)=26)]: t-value = 2.08873, one-tailed (because alternative hypothesis is directional) p-value = 0.023333, i.e. statistically significant at $p<0.05$ (Using Welch's t-test instead: t-value=2.0887, one-tailed p-value= 0.023335. Mann-Whitney U Test: U-value = 58, z-score = 1.81493, one-tailed p-value = 0.03515). With a large effect size [32-36]: Cohen's d = 0.787833, Hedges' g = 0.787833, Glass's *delta* = 1.241379. Given that the 20 mg/kg and 40 mg/kg data are even more distinct from the vehicle data (than the 2 mg/kg data is), they must also each be (by t testing) significantly different than vehicle data at $p<0.05$. And also with, clearly (by visual inspection), a larger effect size. For the 360 minutes after intravenous (IV) injection: comparing the rectal temperature data of all the mice (abstracting rectal temperatures below 30°C to all be 29.5°C, which probably subtracts from the differences to vehicle control {and to each other}, attenuating statistical significance and effect size) using the Kruskal-Wallis H Test (*which, unlike one-way ANOVA, doesn't assume normality of data*): H statistic = 39.0917, p-value = 0.00000002. With a large effect size: η^2 (eta–squared, its classical formulation [37]) = 0.77.

Figure 2 indicates that F_1F_0 ATP hydrolysis is a major determinant of metabolic heat generation (and so of metabolic rate). Its data suggests that during normal aerobic respiration, ATP synthase synthesizes ATP, but also hydrolyses a fraction of the ATP synthesized, which means more ATP needs to be synthesized. Which is a futile cycle, dissipating proton motive force (pmf) to heat, because of the inherent inefficiency of any energy conversion (2^{nd} Law of Thermodynamics). And because it, by conferring a proportion of ATP synthase molecules not passing protons, but instead pumping protons back, increases the rate of proton leak. Wherein pumped protons return to the mitochondrial matrix outside of ATP synthase. Their potential (electrochemical) energy dissipated as heat rather than (partially) captured in ATP. All of this drives a higher rate of aerobic respiration. Where the amount of F_1F_0 ATP hydrolysis, increasing the rate of aerobic respiration (metabolic rate), is constrained by the amount of IF1 protein activity (per the amount of ATP synthase).

A prediction atop of Figure 2, for future testing, is that if the ambient temperature was instead at the mouse's normal body temperature (around 37°C [1]), or safely higher, then no body temperature drop would occur. Even at high drug doses. Because a mouse's body temperature cannot be at a lower temperature than its surround (2nd Law of Thermodynamics). To illustrate, by analogous example, anaesthetic can dramatically reduce a mouse's body temperature, but *not* when the mouse is kept at an ambient temperature of 37°C [38]. At an ambient temperature of 37°C (or higher), the body doesn't have to generate any heat to maintain a body temperature of 37°C. So, an ambient temperature of 37°C (or higher) counteracts any drop in metabolic heat production, of any magnitude.

Any drop in metabolic heat production is drug dose-dependent and is predicted inconsequential if the mice are kept at an accordingly higher ambient temperature to compensate. To illustrate: if after the selected drug dose is administered, body temperature drops by 3°C, increasing the ambient temperature by 3°C (or safely more) counterbalances, meaning body temperature remains 37°C. Or if after a *greater* selected drug dose is administered, body temperature drops by 7°C, increasing the ambient temperature by 7°C (or safely more) counterbalances, meaning body temperature remains 37°C. Where the ambient temperature never needs to be in excess of 37°C, no matter how large the administered drug dose. If the mouse were already at a higher ambient temperature (e.g. 35°C), for example because of a tropical location, the drug's dose-dependent decrease in metabolic heat generation (thereby increase of thermoneutral temperature) could increase the mouse's thermal comfort. Indeed, this drug may have utility in humans for increasing thermal comfort in hot climates (e.g. close to the equator) and in the summer of seasonally hot climates.

In this experiment, the drug-treated mice's body temperature couldn't have fallen to less than room temperature, which was ~22°C. Mice can survive a body temperature of as low as 16°C, which can occur during their torpor [39]. Torpor, characteristic of many small mammal species, is a period of metabolic depression. Where body temperature is below 31°C. And O_2 consumption is less than 25% of that during normal, normothermic inactivity. With diminished responsiveness to stimuli. Prompted by low food intake and/or low ambient temperature (<20°C). Can occur frequently, even daily, depending on food regime and/or the time course of ambient temperature.

A prediction is that this drug can slow aging and increase lifespan. For example, regularly administering it to a mouse (at a dose that can slow its metabolic rate per unit mass to that of a human {slowing its heart rate from 600 to 60 beats per minute}), with the ambient temperature set accordingly, is predicted to make this mouse live much longer. Perhaps even as long as a human.

I own patent claims for methods of using this drug for various non-ischemic indications/applications. Moreover, I've invented better (potency) selective F_1F_0 ATP hydrolysis inhibiting small-molecule drugs (*that don't inhibit F_1F_0 ATP synthesis*). Disclosed in a series of patent applications across all major (and many minor) jurisdictions, e.g. [16-17] in the USA. One of these applications has already been granted (i.e. determined novel and inventive) in Australia [40]. A novel drug therefrom is used later herein (Figure 13).

Novel analysis/interpretation of publicly available data *(in light of the new experimental data above)*

Less specific F_1F_0 ATP hydrolysis correlates with longer maximal lifespan

Figure 3 shows that, across twelve different (mammal and bird) species, less specific F_1F_0 ATP hydrolysis (*in vitro*, in Sub-Mitochondrial Particles {SMPs}; a nuanced assay described in the Methods section) correlates with larger body mass, lower specific basal metabolic rate, slower heart rate, and greater maximal lifespan. The underlying data of this figure is in a table in the Methods section. With data sources disclosed there.

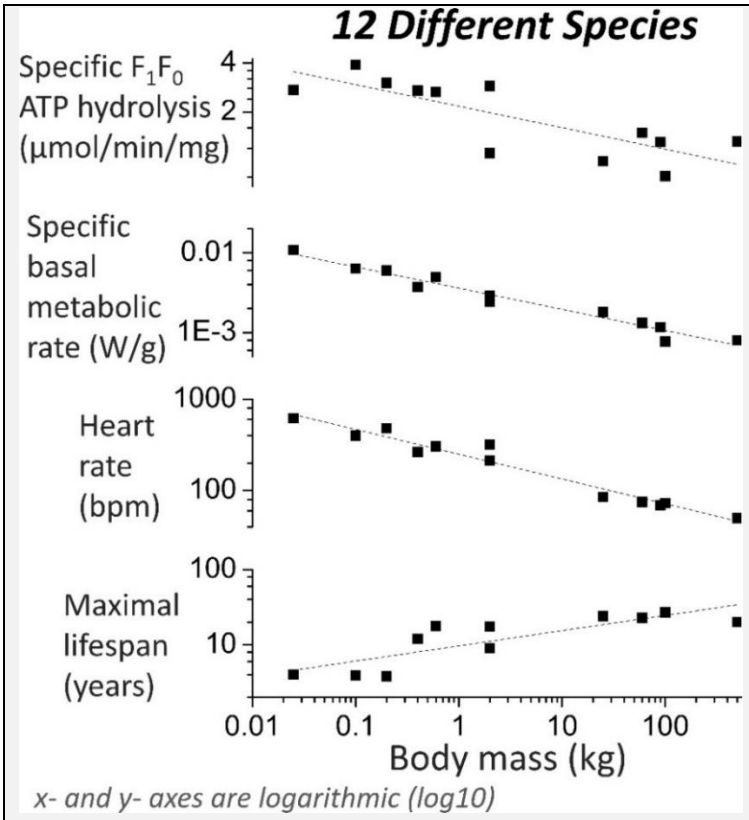

Figure 3 - 1st (top) panel shows a negative correlation between species body mass and specific F_1F_0 ATP hydrolysis (mg is of mitochondrial protein). 2nd panel shows a negative correlation between species body mass and specific basal metabolic rate. 3rd panel shows a negative correlation between species body mass and heart rate (bpm is beats per minute). 4th panel shows a positive correlation between species body mass and maximum lifespan.

Shown best fit lines to the plots of Figure 3 are of the form:

$\log_{10}(y) = \log_{10}(a) + b \cdot \log_{10}(x)$, where b is gradient:

	$\log_{10}(a)$	b		Adjusted R^2
1st panel	0.33791 (±0.04411)	-0.13213 (±0.03077)		0.61323
2nd panel	-2.44192 (±0.02381)	-0.26591 (±0.01661)	≈ *-0.25*	0.95872
3rd panel	2.39875 (±0.02593)	-0.27123 (±0.01808)	≈ *-0.25*	0.95318
4th panel	0.98595 (±0.06233)	0.20246 (±0.04528)	≈*+0.25*	0.65512

Pearson correlation coefficient (R), and associated p-values (one-tailed, because each alternative hypothesis is directional), for the log-log data of Figure 3:

		$\log_{10}$(y1)	$\log_{10}$(y2)	$\log_{10}$(y3)	$\log_{10}$(y4)

R	$\log_{10}(x)$	-0.80523	0.98105	-0.97849	0.83043
p		0.000788	0.0000000093	0.000000017	0.0007755

Where x=body mass, y1=specific F_1F_0 ATP hydrolysis, y2=specific basal metabolic rate, y3=heart rate, and y4=maximal lifespan.

Figure 4 recasts some of the data of Figure 3 (omitting body mass data).

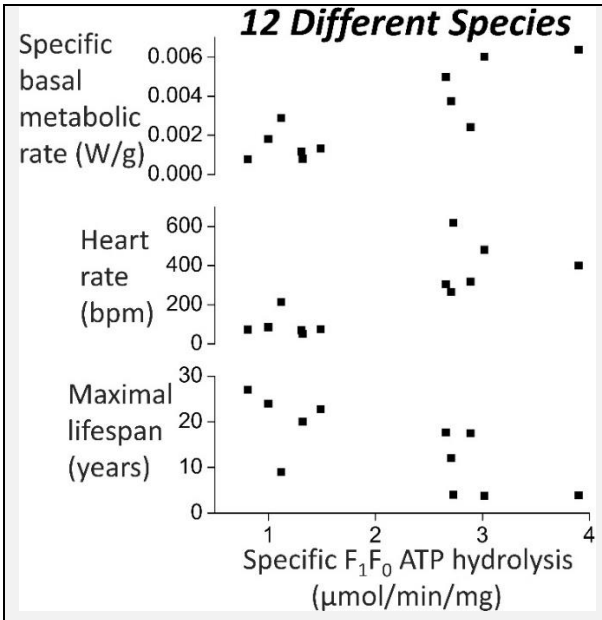

Figure 4 - 1st (top) panel shows, across species, a positive correlation between specific F_1F_0 ATP hydrolysis (mg is of mitochondrial protein) and specific basal metabolic rate. 2nd panel shows, across species, a positive correlation between specific F_1F_0 ATP hydrolysis and heart rate. 3rd panel shows, across species, a negative correlation between specific F_1F_0 ATP hydrolysis and maximal lifespan. Herein proposed, the 1st panel correlation drives the 2nd and 3rd panel correlations.

For the data used to produce Figure 4, the following table presents Pearson correlation (R) coefficients, and associated p-values (one-tailed, because each alternative hypothesis is directional), for its inter-relations:

Pearson correlation coefficient (R)				
	Specific basal metabolic rate	Heart rate	Maximal lifespan	
Specific F1F0 ATP hydrolysis	0.7016	0.8007	-0.7192	
	Specific basal metabolic rate	0.9476	-0.8144	
		Heart rate	-0.8572	
p-value (one-tailed)				
	Specific basal metabolic rate	Heart rate	Maximal lifespan	
Specific F1F0 ATP hydrolysis	0.0054965	0.0008765	0.0063065	
	Specific basal metabolic rate	0.0000015	0.001136	
		Heart rate	0.0003725	
Asymptotically exact harmonic mean p-value for combining independent/dependent tests				
Of all the p-values above (in this present table) = 0.000008933458 = **0.000009**				
Fisher's combined probability test				
Using p-values for [Specific F1F0 ATP hydrolysis vs. Maximal lifespan] (=0.0063065) &				
[Heart rate vs. Specific basal metabolic rate] (=0.0000015) = 0.0000002				

The p-values are small, despite the small values of *n*, in testament to the high *R* values. The asymptotically exact harmonic mean p-value was calculated according to the method of [41] (its post-published corrected method, as corrected on 7 October 2019). All the p-values are smaller than 0.05, and so all are *significant*.

Local inhibition of F_1F_0 ATP hydrolysis

I postulate that if F_1F_0 ATP hydrolysis is inhibited locally in a subject, i.e. only in a body region, then there is no appreciable body temperature drop. Not even in the affected body region, because of heat transfer (especially via blood flow) from other body regions. Indeed, supporting, [42] has shown the safety of local inhibition of F_1F_0 ATP hydrolysis *in vivo*. Wherein, in forebrain neurons of mice, they reduced the amount of F_1F_0 ATP hydrolysis by ~35%. By increasing their IF1 protein amount by 300%. Wherein the extra IF1 protein was actually human IF1 protein, with a single amino acid substitution that increases its inhibitory potency against F_1F_0 ATP hydrolysis at pH 8. These mice were "normal in appearance, home-cage behaviour, reproduction, and longevity up to 1-year follow-up".

[43] showed the *in vivo* safety of locally decreasing F_1F_0 ATP hydrolysis, by locally increasing IF1 protein amount, in mouse liver (especially in perivenous hepatocytes): locally, extra IF1 protein decreased F_1F_0 ATP hydrolysis by 40% and decreased State 3 respiration rate by 44%. Wherein these mice had "no differences in weight, life span and cage behavior when compared to controls after one year of follow up".

[44] showed the *in vivo* safety of locally decreasing F_1F_0 ATP hydrolysis, by locally increasing IF1 protein amount, in mouse intestine: locally, this extra (human) IF1 protein decreased the F_1F_0 ATP hydrolysis capability by 35%, which decreased the oligomycin sensitive respiration rate by 60%. All safely.

Inhibiting F_1F_0 ATP hydrolysis decreases [ROS]

Data herein suggests that metabolic rate confers life, but that some correlate to it causes aging, which ultimately takes life away. This correlate might be Reactive Oxygen Species (ROS) [2-5]. Produced by electrons leaking from the respiratory chain during oxidative phosphorylation. If so, one would expect inhibition of F_1F_0 ATP hydrolysis to reduce the rate of ROS generation. This is experimentally observed. In *reinterpreted* data of [42].

[42] interpret their data as showing that increased IF1 protein amount, and decreased F_1F_0 ATP hydrolysis, *increases* [ROS]. But this is in error. What their data actually shows is that increased IF1 protein amount, and decreased F_1F_0 ATP hydrolysis, *decreases* [ROS]. [42] transgenically increased IF1 protein amount, which decreased F_1F_0 ATP hydrolysis, in the forebrain neurons of mice. This manipulation furnished these cells with a lower respiration rate (lower O_2 consumption rate). And a more hyperpolarized membrane potential across their mitochondrial inner membrane (Ψ_{IM}; presumably because of less proton motive force dissipation to heat by futile cycling of F_1F_0 ATP synthesis and F_1F_0 ATP hydrolysis). Because of this greater hyperpolarisation (rendering a more negative mitochondrial matrix), these cells accumulate more positively charged ROS (superoxide) reporting MitoSOX^{TM} probe. Which means they have greater ROS signal. Which [42] mistakenly take at its face value, interpreting this as meaning greater [ROS]. However, once the Ψ_{IM} disparity is factored in, which is a contribution of the present paper, then one can see that these cells actually have *lower* [ROS].

[42] assay Ψ_{IM} by assaying TMRM accumulation. And assay [ROS] by MitoSOX probe fluorescence. But they don't realize that MitoSOX, like TMRM, is also a Delocalized Lipophilic Cation (DLC). And so its accumulation in the mitochondrial matrix is dependent upon Ψ_{IM}. Indeed, to an even greater degree than TMRM:

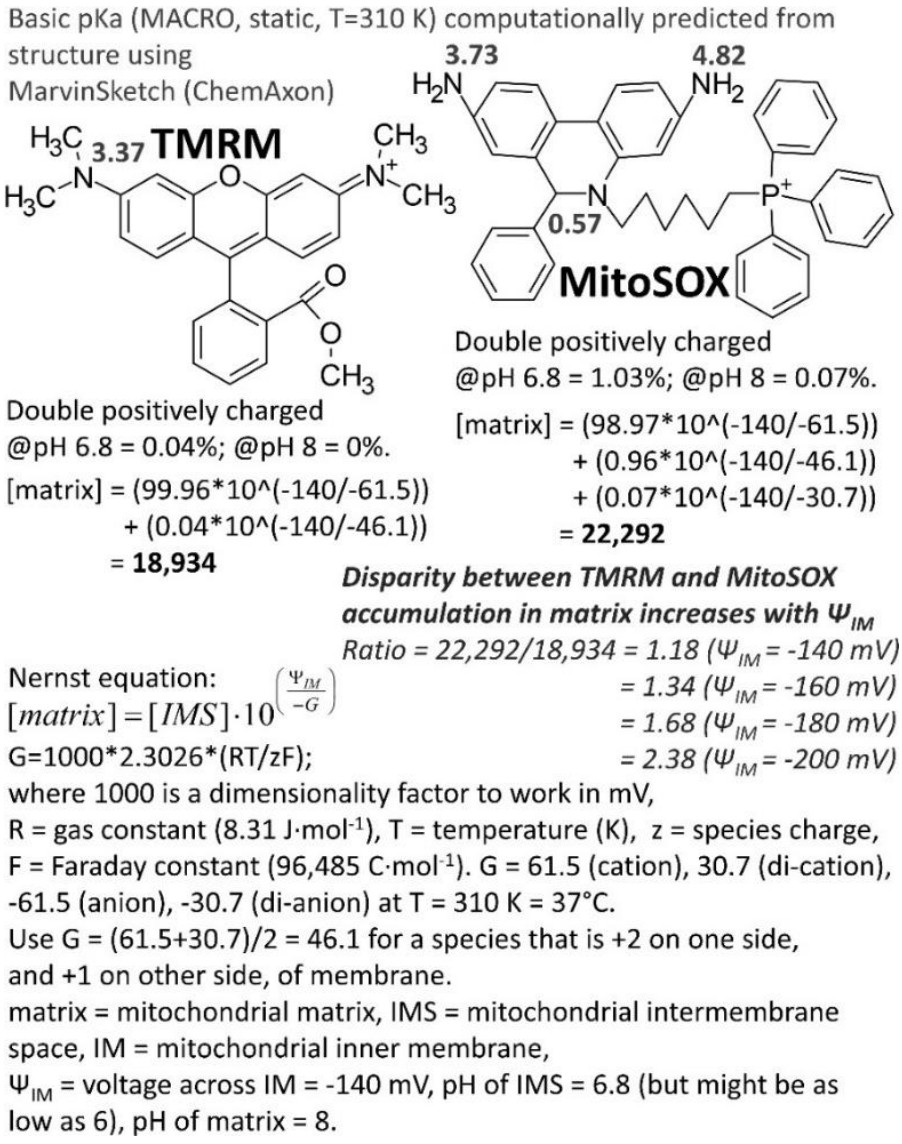

References for voltage across IM [45], pH of IMS [46-47], and pH of mitochondrial matrix [48]. Constraint in the User Interface (UI) of MarvinSketch meant that pH 6.8, rather than 6.88 or 6.9 [46], was used for the IMS. But pH 6.8 is within the observed range, wherein [46] reports 6.88±0.09.

Figure 5 herein, using data from [42], shows

(a) the disparity in TMRM accumulation (Ψ_{IM}) between cells that have elevated IF1 protein and those that don't; and

(b) by my calculation, the predicted disparity in MitoSOX fluorescence signal that this disparity in Ψ_{IM} should cause; and

(c) the actually observed disparity in MitoSOX fluorescence signal.

Wherein the observed is 66% less than what is predicted by the disparity in Ψ_{IM}. So, then the cells with elevated IF1 protein (and thence decreased F_1F_0 ATP hydrolysis) must have 66% lower [ROS].

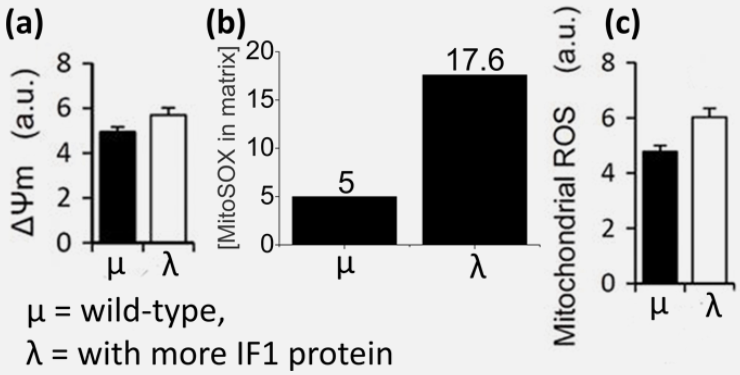

Figure 5 - Compared to wild-type mouse cells (μ), transgenic mouse cells, with more IF1 protein (λ), have a lower Reactive Oxygen Species (ROS) concentration. **(a)** Experimental data [42]: membrane potential across the inner mitochondrial membrane, Ψ_{IM} (or Ψ_M), as measured by TMRM accumulation. A typical value for Ψ_{IM} in normal mitochondria is -140 mV [45]. If we equate the 5 a.u. value for μ with -140 mV. Then the 6 a.u. value of λ is -168 mV. So, transgenic mouse cells, with more IF1 protein, have a more hyperpolarized membrane potential than wild-type cells. **(b)** Calculated data: predicted differential in MitoSOX accumulation in the mitochondrial matrix because of the different Ψ_{IM} values. **(c)** Experimental data [42]: Reported [ROS] by MitoSOX fluorescence. The MitoSOX fluorescence of transgenic mouse cells, with more IF1 protein, is 6 a.u. But wherein, because of their more hyperpolarized Ψ_{IM}, the MitoSOX fluorescence is expected to be greater than this, at 17.6 a.u. The fact that they have less MitoSOX fluorescence than this expected amount shows that they must have less [ROS]: ({17.6-6}/17.6)*100 = 66%. So, [ROS] is 66% lower in transgenic mouse cells, with more IF1 protein, than wild-type.

Some past approaches in the literature have tried to decrease [ROS] by increasing ROS mitigation [49-51]. By administering an antioxidant compound(s). Wherein I suggest that the potential in this ROS mitigation approach is constrained. Because when administering an antioxidant compound into a biological system, there are inherently so many more biological molecules (some of which are incredibly large e.g. DNA) than administered antioxidant molecules. That a ROS is always more likely to collide with a biological molecule, causing

damage, rather than collide with an exogenously introduced antioxidant molecule, and be mitigated. For an exogenous antioxidant to efficaciously outcompete at scale, for ROS collision, with the *huge* number of biological molecules, so much antioxidant compound would have to be administered that toxicity is likely. Moreover, at least some antioxidants, e.g. vitamin C (ascorbic acid, ascorbate), are pro-oxidants also [52] (vitamin C mitigates ROS species by reduction [electron donation]. But this means that it can also reduce Fe^{3+} to Fe^{2+}. Priming the Fenton reaction to produce, from H_2O_2, arguably the worst ROS species of all: the hydroxyl radical, $^{\bullet}OH$ {Fenton reaction: $H_2O_2+Fe^{2+} \rightarrow {}^{\bullet}OH+OH^-+Fe^{3+}$, thereafter OH^- collects a proton to become H_2O}. Where this harmful pro-oxidant action may outweigh the benefit of anti-oxidant action at higher vitamin C concentrations).

In summary, ROS mitigation is a constrained/flawed approach. By contrast, the present paper proposes a different approach to decreasing [ROS]. By decreasing ROS generation. Where, as observed in the data herein, decreasing ROS generation can dramatically decrease [ROS].

[ROS] increases with body age [53-55]. Indeed, hair greying/whitening is reportedly because of increased [H_2O_2] (i.e. hair is bleached by the hydrogen peroxide) [56]. So, decreasing the [ROS] of an old animal, if only to the [ROS] of a young animal, is interesting. Moreover, keeping the [ROS] of a young animal at the same level throughout its life.

<u>IF1 protein does not inhibit F_1F_0 ATP synthesis, misreports that it does are hereby explained</u>

[42-44] interpret increased IF1 protein amount decreasing respiration rate in mice as evidence that IF1 protein directly inhibits F_1F_0 ATP synthesis. This is misinterpreted. Newly revealed herein (*moreover in my corresponding patent applications, e.g.* [16-17]): in mice (especially; and in other mammals), substantial F_1F_0 ATP hydrolysis is occurring under normal conditions (Figure 2). Hydrolysing a fraction of the synthesized ATP, meaning more ATP needs to be synthesized. Which sets oxidative phosphorylation (OXPHOS) at high rate, to generate heat. Increased [IF1 protein] inhibits F_1F_0 ATP hydrolysis more, so less ATP needs to be made by F_1F_0 ATP synthesis, thence less OXPHOS is required, and less O_2 is consumed. So, more IF1 protein *does* decrease F_1F_0 ATP synthesis. But this is by inhibiting F_1F_0 ATP hydrolysis. <u>*Not*</u> by inhibiting F_1F_0 ATP synthesis. This reinterpretation, of the data of [42-44], distinctively aligns with the interpretation of structural data by [9-12] (summarized in Figure 1 herein), which conclude that IF1 protein can only block F_1F_0 ATP hydrolysis, and *not* F_1F_0 ATP synthesis.

Across different species, greater specific F_1F_0 ATP hydrolysis correlates with more mitochondrial ROS detected

This section correlates the variables listed down the left-hand-side of the table below (their data is presented in a table in the Methods section) to data from [57]. [57] consolidates superoxide ($O_2^{\bullet-}$) and H_2O_2 measurements from a number of different species, across a number of different studies. The superoxide measurements are from Sub-Mitochondrial Particles (SMPs), the H_2O_2 measurements from isolated mitochondria. Herein, both these measurements can be termed "mitochondrial ROS" measurements. Utilizing the mitochondrial ROS data from [57]:

Pearson correlation coefficient (R)								
	[SUPEROXIDE] DETECTED (nmol superoxide/minute/mg of protein)							
	A	B	C	D	E	F		
Specific F1F0 ATP hydrolysis	0.7711	0.6714	0.7724	0.7815	0.7995	0.7937		
Specific basal metabolic rate	0.7489	0.9415	0.8734	0.9449	0.7904	0.7891		
Heart rate	0.8573	0.9667	0.8327	0.9241	0.786	0.779		
Maximal lifespan	-0.7362	-0.7372	-0.6732	-0.7322	-0.7114	-0.6662		
	[H2O2] DETECTED (nmol H2O2/minute/mg of protein)							
	B	C	D	G	H	I	J	K
Specific F1F0 ATP hydrolysis	0.865	0.8675	0.8226	0.712	0.7665	0.719	0.703	0.7945
Specific basal metabolic rate	0.8288	0.525	0.6127	0.5542	0.6065	0.5804	0.6945	0.6866
Heart rate	0.813	0.5486	0.627	0.5808	0.7646	0.621	0.6553	0.7057
Maximal lifespan	-0.8191	-0.7059	-0.7755	-0.7878	-0.8073	-0.8246	-0.6642	-0.7533

In the table, please note that the lower section (for H_2O_2) has a different selection of capital letter headings than the upper section (for superoxide). Because it wasn't possible to calculate columns H, I, J, K for superoxide, and columns A, E, F for H_2O_2, from the data available in [57] (or the primary papers it pulls data from). Below is a key to the table above. Within it, primary source papers are referred to as they are in Tables 1 and 2 of [57]. In this key, *n* is the number of species that overlap with the species that I have specific F_1F_0 ATP hydrolysis data for (from [58]). And thence the number of species included to generate the Pearson correlation coefficients in that particular (capital letter headed) column. The highest value of *n* is 8, wherein this consists of cow, pig, rabbit, pigeon, guinea pig, rat, hamster, and mouse. The data in [57] from "Sohal et al. 1993b" (as [57] refers to it) was excluded. Because its values are over 1,000 times different from the values of the other studies. That primary paper aside, all the other mitochondrial ROS data in [57], for species I have specific F_1F_0 ATP hydrolysis data for (from [58]), was included to make the table above. If a primary source

paper's data, sourced from [57], had more than 4 species overlapping with the species I have specific F_1F_0 ATP hydrolysis data for, Pearson correlation coefficients were calculated. For primary source papers with 4 or less species of overlap, their data is only incorporated into the means. In total, via [57], mitochondrial ROS data from 7 different primary papers is used, from 3 different organs (liver, kidney, heart), from 3 different research groups, from studies separated by up to 18 years (by publication date).

A = Liver, "Sohal et al. 1989"; n=5
B = Kidney, "Ku et al. 1993"; n=7 (n=6 for H202 assay)
C = Heart, "Ku et al. 1993"; n=7
D = mean of B and C; n=7
E = mean of A, B, C; n=7
F = mean of E and [kidney and heart, "Ku and Sohal 1993"]; n=8
G = mean of D and [kidney and heart, "Ku and Sohal 1993"]; n=8
H = Liver, "Sohal et al. 1990)"; n=6
I = mean of G and H; n=8
J = mean of I and "Lambert et al. 2007"; n=8
K = mean of J, "Herrero and Barja 1997", "Herrero and Barja 1998"; n=8

Using the mean of *all* the superoxide data, across all the used studies, is column F; using the mean of *all* the H_2O_2 data, across all the used studies, is column K. To report p-values (one-tailed, because each alternative hypothesis is directional) for these columns:

p-value (one-tailed)		
	Superoxide	H2O2
	F	K
Specific F1F0 ATP hydrolysis	0.009347	0.0092445
Specific basal metabolic rate	0.009949	0.0300005
Heart rate	0.011355	0.0252435
Maximal lifespan	0.035629	0.015467

These p-values are small, despite the small value of n (8) for each, in testament to the high R values. All these p-values are smaller than 0.05. So all are *significant*.

Reporting from the table: the greater the specific F_1F_0 ATP hydrolysis, the more mitochondrial ROS detected. The greater the specific basal metabolic rate, the more mitochondrial ROS detected. The greater the heart rate, the more mitochondrial ROS detected. The greater the maximal lifespan, the less mitochondrial ROS detected.

[57] only reports, and so the table above only uses, data from isolated mitochondria and SMPs. What is the situation in a more complete system? In whole cells respiring glucose?

[59] shows that, in *ex vivo* brain slices, respiring glucose, ROS (superoxide) production increases with age. And that the gradient of this increase is steeper in shorter living species. "The rate of age-related increases of superoxide dependent chemiluminescence was inversely related to the maximum lifespan of the animals". At least for the species they looked at. Wherein there aren't enough shared species to calculate a Pearson correlation coefficient with the data herein unfortunately. In the present study, an implemented rule is that the Pearson correlation coefficient isn't employed for any cases that there aren't at least 5 pairs (x,y) of data.

Across different species, greater specific F_1F_0 ATP hydrolysis correlates with more ROS damage detected

The following table correlates the variables listed along its top (their data is presented in a table in the Methods section) to data from [60]. Showing Pearson correlation (R) coefficients (and p-values, one-tailed because each alternative hypothesis is directional) to data from [60], which reports, from a number of different species, the urinary excretion of (probable) repair products of oxidative DNA damage: 8-oxo-7,8-dihydroguanine (8-oxoGua), 8-oxo-7,8-dihydro-2'-deoxyguanosine (8-oxodG), and 5-(hydroxymethyl)uracil (5-HMUra).

		Specific F1F0	Specific basal		Maximal	
		ATP hydrolysis	metabolic rate	Heart rate	lifespan	log10(body mass)
R	**8-OxoGua**	**0.8455**	**0.9019**	**0.9488**	**-0.972**	**-0.9889**
p		0.0169805	0.0069815	0.001933	0.002801	0.000092
R	**8-OxodG**	**0.838**	**0.9955**	**0.9626**	**-0.7675**	**-0.9289**
p		0.01862	0.000015	0.001036	0.064891	0.0037015
R	**5-HMUra**	**0.7053**	**0.9545**	**0.8704**	**-0.6204**	**-0.8665**
p		0.0587375	0.001529	0.012053	0.13209	0.012772
R	**MEAN**	**0.8223**	**0.9779**	**0.9609**	**-0.8453**	**-0.9775**
p		0.02228	0.0003635	0.001132	0.035661	0.000377
	Unit: nmol/mmol creatinine					

A rationale of [60] appears to be that bigger species have more cells. Thence these species have more DNA, and they produce more creatinine. So [60] reasons that the disparity in DNA amount can be washed out of the data by dividing its values by the amount of creatinine. With this standardization, smaller species are observed to have higher values of (probable) DNA repair products in their (per unit of) urine. Reflecting greater specific DNA repair. Presumably reflecting greater specific ROS damage of DNA. Perhaps reflecting greater specific [ROS] more directly, if these oxidized products can be produced by ROS

interaction with the corresponding free substrates (guanine, deoxyguanosine, uracil), which aren't incorporated into DNA/RNA.

Oxidative damage to DNA increases with age [61-62]. In [60], the "biological age" of the individuals from the different species was constant (around 20% of maximal lifespan for each species) *except* for pig (4% of maximal lifespan). Removing pig data didn't change the direction of any of the correlations, or majorly change any of their R values (data not shown; three biggest changes in R value, upon removal of pig data, were 0.0546, 0.0402, 0.0213; without pig data, correlations to maximal lifespan couldn't be computed because of insufficient number of data points [atop of omission of human data for maximal lifespan correlations, by rationale given in the Methods section]).

In the table (most immediately) above, all the correlations to the mean of data are *significant* (p-value < 0.05).

The following table correlates the variables listed along its top (their data is presented in a table in the Methods section) to data from [63]. Showing Pearson correlation (R) coefficients (and p-values, one-tailed because each alternative hypothesis is directional) to data from [63], which reports, from a number of different species, upon the amount of a ROS damage product, 8-oxo-7,8-dihydro-2'-deoxyguanosine (8-oxodG) (standardized to the amount of deoxyguanosine, dG; per 10^5 dG), in mitochondrial DNA (mtDNA).

	8-oxodG/10^5dG	Specific F1F0	Specific basal		Maximal	
	in mtDNA	ATP hydrolysis	metabolic rate	Heart rate	lifespan	log10(body mass)
R	**Brain**	**0.885**	**0.8837**	**0.9246**	**-0.7369**	**0.7531**
p		0.022999	0.0233855	0.012286	0.07772	0.070845
R	**Heart**	**0.7335**	**0.9509**	**0.9642**	**-0.7438**	**-0.9575**
p		0.030316	0.0004995	0.000229	0.02764	0.0003495
R	**MEAN**	**0.8212**	**0.9738**	**0.9867**	**-0.8533**	**-0.9157**
p		0.044142	0.0025355	0.000919	0.03297	0.0145035

The mean only includes species for which *both* brain and heart data is in the data set. Data was extracted from graphs in [63] using WebPlotDigitizer, https://apps.automeris.io/wpd/. [63] optimized more for a constant chronological, rather than "biological", age. All the individuals, from the different species, were around one to two years old: "the mean age of the animals was 8 months (mice), 11 months (rat), 1.4 years (guinea pig), 1.5 years (rabbit), 1 year (pig), and 1.5–2.5 years (sheep, cow, and horse)" [63].

In the table (most immediately) above, all the correlations to the mean of data are *significant* (p-value < 0.05).

The following table correlates the variables listed along its top (their data is presented in a table in the Methods section) to data from [64]. Showing Pearson correlation (R) coefficients (and p-values, one-tailed because each alternative hypothesis is directional) to data from [64], which reports, from a number of different species, upon DNA substitution (mean of SBS1, SBSB, and SBSC types), indel (somatic insertions and deletions), and mtDNA mutation, rates per year. Data was sourced from Supplementary Table 4 of [64].

		Specific F1F0	Specific basal		Maximal	
		ATP hydrolysis	metabolic rate	Heart rate	lifespan	log10(body mass)
R	**DNA substitution rate per year**	**0.9155**	**0.9332**	**0.9595**	**-0.7817**	**-0.8878**
p		0.0052045	0.003272	0.001214	0.0591735	0.0090885
R	**Indel rate per year**	**0.9109**	**0.9569**	**0.9667**	**-0.7511**	**-0.9038**
p		0.0057775	0.001373	0.000823	0.071684	0.0067185
R	**mtDNA mutation rate per year**	**0.906**	**0.9619**	**0.9592**	**-0.7238**	**-0.8857**
p		0.0064195	0.001075	0.001232	0.0834205	0.009425
	N.B. Substitution rate per year = SBS1 + SBSB + SBSC rate per year					

The following table correlates the variables listed along its top (their data is presented in a table in the Methods section) to data from [65]. Showing Pearson correlation (R) coefficients (and p-values, one-tailed because each alternative hypothesis is directional) to data from [65], which reports, from a number of different species, upon the amount of a ROS damage product, malondialdehyde (MDA), formed by lipid peroxidation.

		Specific F1F0	Specific basal		Maximal	
		ATP hydrolysis	metabolic rate	Heart rate	lifespan	log10(body mass)
R	**LP**	**0.8976**	**0.9221**	**0.909**	**-0.8075**	**-0.8191**
p		0.0030475	0.001559	0.002283	0.01403	0.0120945
	LP = *in vivo* Lipid Peroxidation (mmol MDA/g tissue)					

Data was extracted from Fig. 5 in [65] using (aforementioned) WebPlotDigitizer. “All animals used were young adults with an age within 15–30% of their MLSP” [65], wherein MLSP is maximum lifespan.

In the table (most immediately) above, all the correlations are *significant* (p-value < 0.05).

The following table correlates the variables listed along its top (their data is presented in a table in the Methods section) to data from [66]. Showing Pearson correlation (R) coefficients (and p-values, one-tailed because each alternative hypothesis is directional) to data from [66],

which reports, from a number of different species, protein degradation rate constants (K_{deg}) for a number of different proteins, the median of which was taken for each species. K_{deg} data was obtained by personal communication with the first author of [66] (ages of the animals used were unknown, except for mouse [6 month old female]).

		Specific F1F0 ATP hydrolysis	Specific basal metabolic rate	Heart rate	Maximal lifespan	log10(body mass)
R	**Median Kdeg**	**0.9465**	**0.8369**	**0.9065**	**-0.9884**	**-0.9446**
p		0.0021085	0.0188665	0.0063525	0.0007485	0.0022595

In the table (most immediately) above, all the correlations are *significant* (p-value < 0.05). So, shorter living species have faster protein turnover (greater median K_{deg}). I suggest this is because, as a function of greater specific F_1F_0 ATP hydrolysis (driving greater specific basal metabolic rate), they have greater intracellular [ROS], and so a greater rate of ROS damage of proteins, and so their rate of protein replacement needs to be greater. Compounding because protein replacement itself requires ATP energy, requiring ATP synthesis, (if ATP is synthesized aerobically) generating ROS, increasing the requirement for protein replacement. The correlation of median K_{deg} to maximal lifespan across species, at -0.99 in the table above, is particularly high.

In this headed section, a correlative link has been shown between specific F_1F_0 ATP hydrolysis and damage to DNA, lipids and (by inference) proteins. The asymptotically exact harmonic mean p-value [41] (*its post-published corrected method, as corrected on 7 October 2019*) for all the p-values of this section (excluding those using means of data) is 0.0005027958 = 0.0005. Very significant.

Numerical prediction observed

Kleiber's law is that an adult animal's basal metabolic rate scales to $M^{0.75}$, where M is the animal's adult body mass [67-68]. Thence an adult animal's specific basal metabolic rate scales to $M^{0.75}/M = M^{-0.25}$. Therefore the log-log plot of adult body mass (x-axis), and specific basal metabolic rate (y-axis), has a gradient of -0.25. Indeed, this is observed in the 2nd panel of Figure 3 herein (refer to the corresponding table of its best fit line equations). Moreover, its 3rd and 4th panels also conform to "quarter-power scaling". In which its heart rate and maximal lifespan data both scale to body mass with the same exponents as (is typical) in the literature. $M^{-0.25}$ and $M^{0.25}$ respectively [69-70]. However, in Figure 3 herein, it is notable that

specific F_1F_0 ATP hydrolysis, which I suggest is a drive to specific basal metabolic rate (which scales to $M^{-0.25}$), does *not* have the -0.25 exponent itself. Its exponent is instead -0.13213 (±0.03077). This suggests that something might be missing. Specific F_1F_0 ATP hydrolysis data in prior figures, e.g. in Figure 3, is actually from Sub-Mitochondrial Particles [SMPs] (data from [58]). In which all the intricate internal structure of mitochondria is lost. I suggest that this is what is missing in the exponent. In intact mitochondria, across different species, [71] reports that [mitochondrial inner membrane surface area/mitochondrial matrix volume] ($cm^2/\mu l$) scales to $M^{-0.102}$.

Selecting data from [71], for species that I have specific F_1F_0 ATP hydrolysis data for (from SMPs, from [58]), the product, *g*, of [specific F_1F_0 ATP hydrolysis (from SMPs)], multiplied by [mitochondrial inner membrane surface area/mitochondrial matrix volume], scales to **precisely** $M^{-0.25}$. As shown in Figure 6.

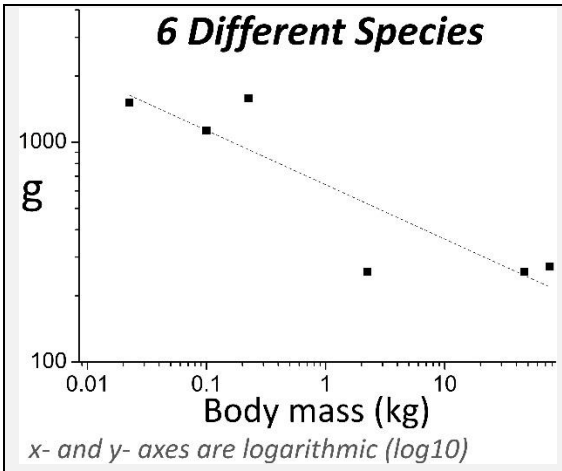

Figure 6 - On the y-axis, *g* is

$$g = h \cdot (s/v)$$

wherein *h* is specific F_1F_0 ATP hydrolysis in Sub-Mitochondrial Particles [SMPs] (μmol/min/mg; mg is of mitochondrial protein), *s* is mitochondrial inner membrane surface area (cm^2), *v* is mitochondrial matrix volume (μl). Data for *h* is from [58] (and has been used in prior figures herein, e.g. Figure 3). Data for *s* and *v* is from [71]. In this figure, each species' body mass value is the mean of pooled body mass values, for the particular species, from [58] and [71].

Across species, *g* decreases with body mass (M). With an **exponent of -0.25**.

The best fit line in Figure 6 is:

$\log_{10}(y) = \log_{10}(a) + b \cdot \log_{10}(x)$, where b is gradient:

$\log_{10}(a)$	b	Adjusted R^2
2.80659 (±0.08226)	-0.24725 (±0.06192) ≈ ***-0.25***	0.74928

Pearson correlation coefficient (R), and its p-value (one-tailed, because the alternative hypothesis is directional), for the log-log data of Figure 6:

		$\log_{10}$(g)
R	$\log_{10}$(body mass)	-0.8941
p		0.0081

I suggest that *g*, defined in the Figure 6 legend, can be (abstractly) interpreted as being specific F_1F_0 ATP hydrolysis in mitochondria (μmol/min/mg·cm^2/μl). So, whereas *h* is specific F_1F_0 ATP hydrolysis in Sub-Mitochondrial Particles [SMPs] *in vitro*, *g* is (interpreted to correspond to) specific F_1F_0 ATP hydrolysis in intact mitochondria *in vivo*. Wherein *g* and *h* are interrelated by the equation in the legend of Figure 6.

More mitochondrial inner membrane surface area, per mitochondrial matrix volume, is to say the mitochondrial inner membrane has more and/or larger invaginations (cristae). Sacrificing mitochondrial matrix volume for greater mitochondrial inner membrane surface area. This greater surface area of the mitochondrial inner membrane means there is more proton leak across it. Furthermore, cristae locally increase proton concentration on the intermembrane side of the mitochondrial inner membrane, which increases the Ohmic (or supra-Ohmic) drive for proton leak. Wherein more and/or bigger cristae increases this more. A cristae is bigger by longer protrusion into the mitochondrial matrix.

As aforementioned, Figure 6 shows that specific F_1F_0 ATP hydrolysis combines with mitochondrial inner membrane surface area (per mitochondrial matrix volume) to confer, *precisely*, the expected -0.25 exponent. That this relation is because of proton leak is suggested by specific F_1F_0 ATP hydrolysis combining with the rate of proton leak to confer, within the margin of slope error, a -0.25 exponent also. As shown in Figure 7.
In overlapping support, [71] uses data from more species than are represented in Figure 7, and finds body mass and proton leak related with an exponent of -0.129 (±0.049). Which,

when added to the aforementioned exponent relating body mass and specific F_1F_0 ATP hydrolysis (-0.13213±0.03077), yields an exponent of -0.26, with -0.25 within its margin of error.

Pearson correlation coefficient (R), and its p-value (one-tailed, because the alternative hypothesis is directional), between *l*, the rate of proton leak ([nmol of H^+]/min/mg protein) across the inner mitochondrial membrane {when the membrane potential across it is -170 mV, with ATP synthase blocked by oligomycin}, and (s/v); where *s* is mitochondrial inner membrane surface area (cm^2) and *v* is mitochondrial matrix volume (µl); data from [71]:

		(s/v)
R	l	0.861
p		0.014

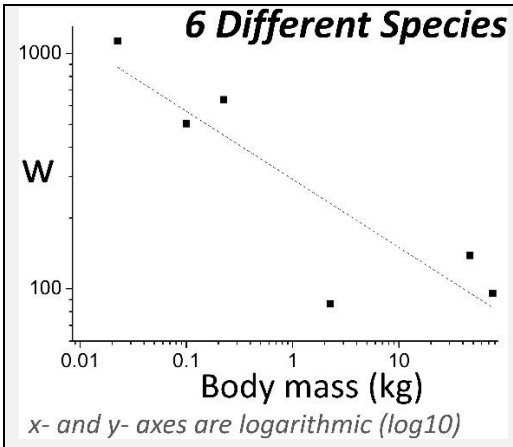

Figure 7 - On the y-axis, *w* is

$$w = h \cdot l$$

wherein *h* is specific F_1F_0 ATP hydrolysis in Sub-Mitochondrial Particles [SMPs] (µmol/min/mg; mg is of mitochondrial protein), *l* is proton leak rate across the inner mitochondrial membrane, when the membrane potential across it is -170 mV, and ATP synthase is blocked by oligomycin ([nmol of H^+]/min/mg protein). Data for *h* is from [58] (and has been used in prior figures herein, e.g. Figure 3). Data for *l* is from [71]. In this figure, each species' body mass value is the mean of pooled body mass values, for the particular species, from [58] and [71].

Across species, *w* decreases with body mass (M). With (within the margin of slope error) an exponent of -0.25.

The best fit line in Figure 7 is:

$\log_{10}(y) = \log_{10}(a) + b \cdot \log_{10}(x)$, where b is gradient:

$\log_{10}(a)$	b	Adjusted R^2
2.46545 (±0.10233)	-0.28943 (±0.07704) ≈ *-0.25*	0.72399

Pearson correlation coefficient (R), and its p-value (one-tailed, because the alternative hypothesis is directional), for the log-log data of Figure 7:

		$\log_{10}$(w)
R	$\log_{10}$(body mass)	-0.8827
p		0.0099

Pearson correlation coefficients (R), and their p-values (one-tailed, because each alternative hypothesis is directional), between *h, g* and *w* (variables as defined in the legends of Figures 6 and 7):

		g	w
R	h	0.8323	0.6779
p		0.020	0.069
R		g	0.9036
p			0.0067

Pearson correlation (R) coefficients, and their p-values (one-tailed, because each alternative hypothesis is directional):

		Specific basal metabolic rate	Heart rate	Maximal lifespan
R	***h***	**0.7016**	**0.8007**	**-0.7192**
p		0.0054965	0.000877	0.006307
R	***g***	**0.8816**	**0.9466**	**-0.7942**
p		0.010099	0.002101	0.029586
R	***w***	**0.9691**	**0.9442**	**-0.6952**
p		0.0007085	0.002292	0.062598

The correlations with *h*, where *h* is specific F_1F_0 ATP hydrolysis (from [58]), are as presented in an earlier table. Its correlations are calculated with more species, and so a higher value of *n*, than the correlations to *g* and *w*. And thence its correlations have a smaller p-value for any given value of R.

Looking at R values only, the correlations of *g* are superior to those of *h*. Those of *w* are superior to those of *g*. Except for the correlation to maximal lifespan.

When *h* is correlated to the same, smaller data set as *g* and *w*, its correlation to maximal lifespan doesn't worsen but improves (-0.7842), and its correlation to specific basal metabolic rate and heart rate is 0.7318 and 0.7706 respectively.

Comparing the table below, to the table most immediately above, one can see that the correlations of each of *g* and *w*, are *much* superior to those of (*s*/*v*) and *l* (variables as defined in legends of Figures 6 and 7). To specific basal metabolic rate, heart rate, and maximal lifespan (data for these variables is presented in a table in the Methods section). R is the Pearson correlation coefficient and p-values are one-tailed, because each alternative hypothesis is directional. Incidentally, proton leak, *l*, negatively correlates with maximal lifespan (at least across species, for these species). Although not significantly so.

		h	Specific basal metabolic rate	Heart rate	Maximal lifespan
(*s* /*v*)	R	0.4445	0.7588	0.8193	-0.5301
	p	0.188581	0.040125	0.023015	0.1396655
l	R	0.4159	0.8794	0.8283	-0.496
	p	0.20606	0.01047	0.020845	0.158506

Considered in totality, the data of this present Results section (encompassing Figures 6 and 7) suggests that it might be the combination of F_1F_0 ATP hydrolysis ***and*** proton leak, which sets specific basal metabolic rate (setting heart rate), which dictates maximal lifespan.

Why might F_1F_0 ATP hydrolysis, and proton leak, *both* be important?

Oxidative phosphorylation synthesizes ATP. F_1F_0 ATP hydrolysis hydrolyses a fraction of this ATP. At a level constrained by IF1 protein activity. Wherein smaller, shorter living species have less specific IF1 protein activity. This F_1F_0 ATP hydrolysis pumps protons out of the mitochondrial matrix, across the inner mitochondrial membrane, into the mitochondrial intermembrane space. A fraction of these protons return to the mitochondrial matrix via proton leak. Wherein smaller, shorter living species have greater proton leak because of a greater mitochondrial inner membrane surface area (per volume of mitochondrial matrix).

And because of their greater rate of F_1F_0 ATP hydrolysis, pumping more protons per unit time into the mitochondrial intermembrane space. A fraction of the ATP synthase proton conduits in the mitochondrial inner membrane, actively pumping protons energetically "uphill", instead of passing protons energetically "downhill", can explain how so much proton leak can occur. Why so many protons cross the mitochondrial inner membrane at a point of higher resistance. Dissipating their potential energy as heat. Rather than just passing through the lower resistance conduit, ATP synthase, which can capture (a fraction of) their potential energy loss in the chemical energy of ATP. *(But these ATP synthase complexes are available for "forward", proton passing, ATP synthesizing [instead of "reverse", ATP consuming, proton pumping] action if cellular ATP demand increases)*.

This proton leaking is especially pronounced when there is particularly high [ATP] in the mitochondrial matrix, which happens when cellular energy demand is low. Elegantly, when the cell is hydrolysing much ATP to perform much useful work, inherently generating heat as a by-product (2nd Law of Thermodynamics), [ATP] in the mitochondrial matrix is lower and F_1F_0 ATP hydrolysis, and proton leak, is lower. But when the cell isn't performing much work, [ATP] in the mitochondrial matrix is higher and so F_1F_0 ATP hydrolysis, and proton leak, is higher. Which generates heat to keep the body at 37°C. So, when useful work can generate heat, the spurious processes are less. But when not, they are more. For emphasis, this is recast in the next paragraph.

When the body is resting and so isn't performing much work, F_1F_0 ATP hydrolysis (and its drive to F_1F_0 ATP synthesis and metabolic rate) confers endogenous heat production. But when the body is active and performing appreciable work, ATP is consumed to do this work (inherently generating heat as a by-product, 2nd Law of Thermodynamics), and so there is less ATP available to F_1F_0 ATP hydrolysis, which is reduced as a result. So when performing work, which inherently generates heat, the futile (no work) process to generate heat is decreased, affording more energy to actually perform work, and reducing the chance that the body will overheat. So, in the resting state, heat generation is (fractionally) by a futile process, until more work is required, after which the heat generation by the actual performing of work substitutes for a reduction in heat generation by the futile process.

Quarter-power scaling

It is interesting to contemplate that the observed quarter-power scaling, between novel variable, *w*, and body mass, might be the fundamental drive to the quarter-power scaling observed (e.g., in Figure 3 herein) between body mass and each of specific basal metabolic rate (-0.25), heart rate (-0.25), and maximal lifespan (+0.25). Indeed, the basis might be at the cellular or sub-cellular level because the specific metabolic rate of liver slices, sourced from different sized species, adheres to quarter-power scaling (-0.25) *in vitro* [72]. Curiously, *w* has a geometric component, via its proton leak rate, which is a function of inner mitochondrial membrane surface area, which is a *non-Euclidean* shape. Because of its invaginations (sacrifices some volume for greater surface area). A longstanding mystery is why, across species, where M is adult body mass, basal metabolic rate scales with $M^{0.75}$ (Kleiber's law), instead of $M^{0.67}$, which is what is expected on the basis of how surface area scales with volume for a *Euclidean* object [69]. "One cannot but wonder why the power formula, in general, and the mass exponents of 3/4, 1/4 and -1/4, in particular, are so effective in describing biological phenomenon" [69].

Equation for maximal lifespan in terms of specific F_1F_0 ATP hydrolysis

Recasting afore-presented experimental data, Figure 8 shows (across different species) specific F_1F_0 ATP hydrolysis, specific basal metabolic rate, and heart rate for different values of maximal lifespan.

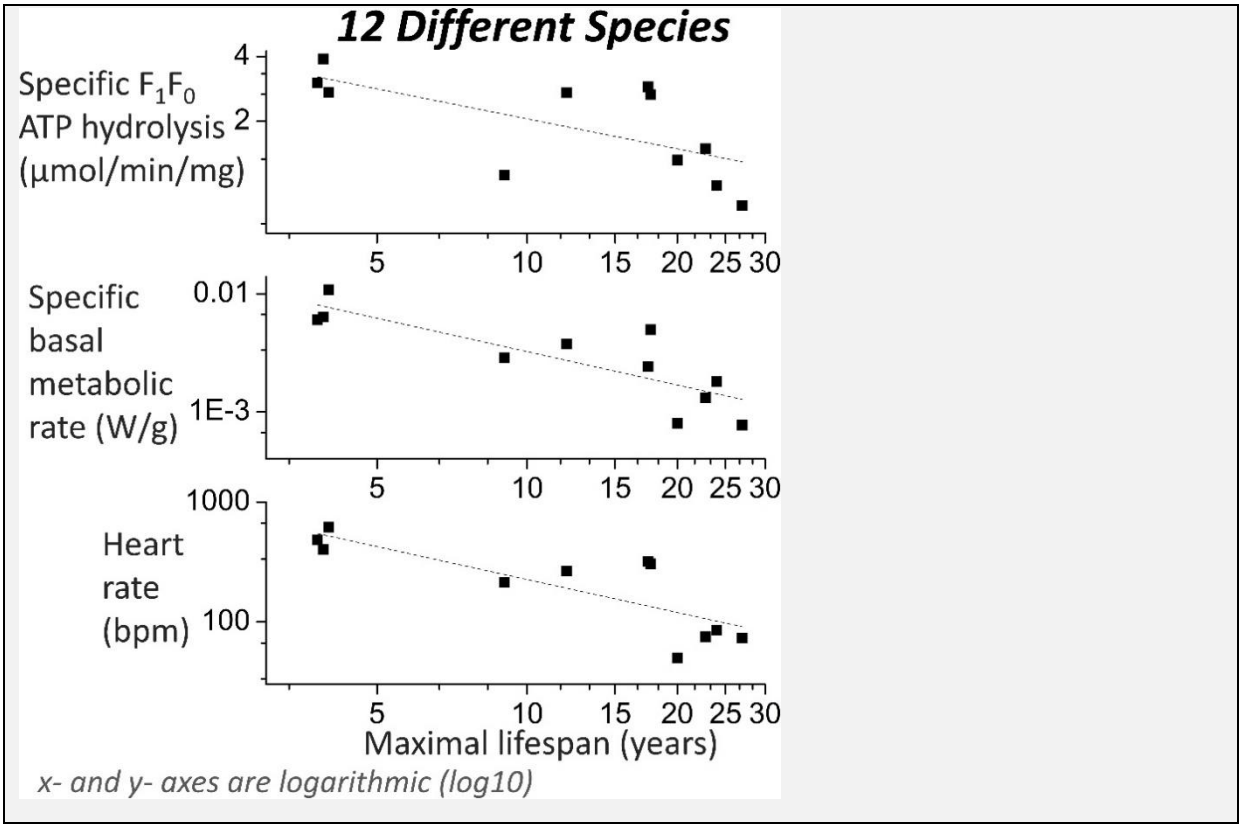

Figure 8 - Across different species, specific F_1F_0 ATP hydrolysis, specific basal metabolic rate, and heart rate for different values of maximal lifespan.

Shown best fit lines in Figure 8 are of the form:

$\log_{10}(y) = \log_{10}(a) + b \cdot \log_{10}(x)$, where b is gradient:

	$\log_{10}(a)$	b	Adjusted R^2
1st panel	0.77685 (±0.19253)	-0.46465 (±0.17242)	0.3851
2nd panel	-1.5502 (±0.22922)	-0.93884 (±0.20528)	0.66575
3rd panel	3.26704 (±0.247)	-0.91411 (±0.2212)	0.61654

Rearranging the plot equation from the 1st (top) panel in Figure 8, gives an equation for maximal lifespan (*years*), x, in terms of specific F_1F_0 ATP hydrolysis ($\mu mol/min/mg$), y:

$$x = 10^{(\{\log_{10}(y) - 0.77685\}/-0.46465)}$$

Mediation analysis

I performed mediation analysis, summarized in Figure 9, in the JASP software (version 0.14.1; https://jasp-stats.org/; developed by a team at the University of Amsterdam; it runs atop of R {https://www.r-project.org/}). Selecting a bootstrap method. Called "Percentile" in JASP, which corresponds to "Percentile bootstrap (PC)" in [73]. Run with 10,000 replications (ten times greater than the default number of replications = 1,000). Note that for the data inputted, I multiplied all the specific basal metabolic rate values by 10,000 (rescaled this variable) to prevent "numerical underflow" in the underlying computations performed by lavaan [74], an R package for Structural Equation Modelling [SEM], which JASP runs for SEM (mediation analysis). Such re-scaling of an input variable(s) for SEM is a good and common practice. Because it is preferable for the different input variables to have a similar order of scale. And it is absolutely needed in this case because the variable with very small numbers (specific basal metabolic rate in W/g) causes even smaller numbers to occur in the internal computations (e.g. in the computations/manipulations of variances, covariances, Hessian, gradients, etc.). Causing "numerical underflow". An alternative method to prevent this "numerical underflow" is to select the option of "Standardized estimates" in JASP. To standardize (mean = 0, standard deviation = 1) all the variables before estimation (standardization: independently for each variable: for each of its values: subtract value from

this variable's mean and then divide this output by this variable's standard deviation). But this method is arguably inferior. Because it is manipulating each variable with quantities, the mean and standard deviation, which are *estimated*, with an error. Instead of manipulating a single variable with a constant, which is *precisely known* (10,000). Regardless, the results from this alternative method, utilizing "Standardized estimates", are presented at the end of this section. From which the same conclusions are drawn.

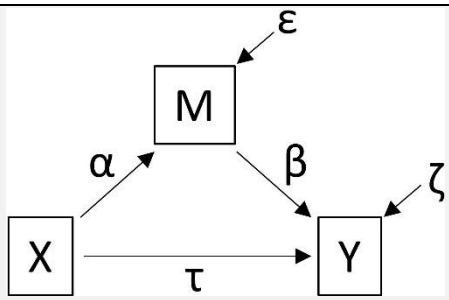

Figure 9 - An indirect effect (mediation) exists when an independent variable (X) acts upon a dependent variable (Y) through an intervening/mediating variable (M). Represented by two regression equations [73]:

$$M = b_M + (\alpha \cdot X) + \varepsilon$$

$$Y = b_Y + (\beta \cdot M) + (\tau \cdot X) + \zeta$$

b_M and b_Y are regression intercepts. ε and ζ are random disturbance terms. α, β and τ are regression coefficients.

Indirect effect (*effect of X upon Y, via M*) = **α·β**.

Direct effect = τ.

Total effect (*of X upon Y*) = (α·β) + τ.

For the table below, using the notation of Figure 9 (*with the data of these variables as presented in a table in the Methods section*), *X* is specific F_1F_0 ATP hydrolysis, *M* is specific basal metabolic rate (*10,000), and *Y* is maximal lifespan.

			95% Confidence	
			Interval (CI)	
α	β	**Indirect effect (α·β)**	Lower	Upper
20	-0.17	-3.452	-9.512	-1.201
		Direct effect (τ)	Lower	Upper
		-2.554	-6.266	4.124

Evidence for an effect is when zero (0) is not within the range of the 95% confidence interval. The data in the table suggests that there is no direct effect between specific F_1F_0 ATP hydrolysis and maximal lifespan. That the effect of specific F_1F_0 ATP hydrolysis upon maximal lifespan is solely indirect, via specific basal metabolic rate.

Figure 10 presents the proposed model of mediation. Mediation data supporting its [specific F_1F_0 ATP hydrolysis → specific basal metabolic rate → maximal lifespan] arm has already been presented. Mediation data supporting its [specific F_1F_0 ATP hydrolysis → specific basal metabolic rate → heart rate] arm is below. (*With the data of these variables as presented in a table in the Methods section*), where *X* is specific F_1F_0 ATP hydrolysis, *M* is specific basal metabolic rate (*10,000), and *Y* is heart rate.

			95% Confidence	
			Interval (CI)	
α	β	**Indirect effect (α·β)**	Lower	Upper
20	4.6	94.363	22.578	191.3
		Direct effect (τ)	Lower	Upper
		48.372	-35.584	109.96

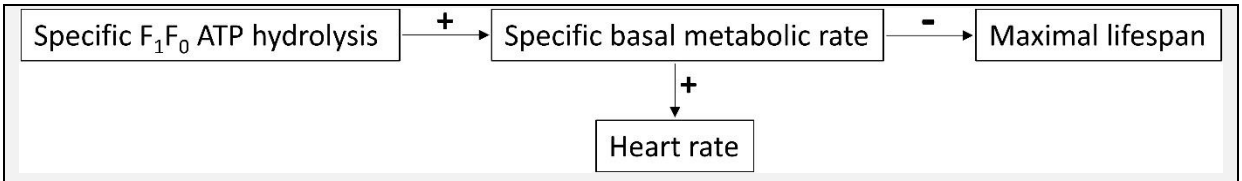

Figure 10 - Mediation model. Supported by the mediation analysis herein. In this model, specific F_1F_0 ATP hydrolysis sets heart rate, and maximal lifespan, via setting specific basal metabolic rate.

The mediation analysis, when instead using "Standardized estimates", is presented in the table below. In this case, the specific basal metabolic rate values are *not* multiplied by 10,000. For each arm of the mediation model (afore-presented in Figure 10): as before, there is no zero (0) within the 95% confidence interval for the indirect effect. But there is for the direct effect. Indicating that, for each arm, there *is* an indirect effect (via the Mediator variable [specific basal metabolic rate]), and *no* direct effect. This corresponds with the mediation analysis results presented earlier. Further supporting the mediation model of Figure 10.

			95% Confidence				
			Interval (CI)				
Specific F1F0 ATP hydrolysis → Specific basal metabolic rate → Maximal lifespan							
α	β	Indirect effect (α·β)	Lower	Upper			
0.66	-0.61	-0.402	-1.096	-0.137			
		Direct effect (τ)	Lower	Upper			
		-0.297	-0.759	0.485			
Specific F1F0 ATP hydrolysis → Specific basal metabolic rate → Heart rate							
α	β	Indirect effect (α·β)	Lower	Upper			
0.66	0.76	0.506	0.12	1.007			
		Direct effect (τ)	Lower	Upper			
		0.259	-0.186	0.589			

Interventional evidence for causality in the mediation model

Mediation analysis in the previous section showed that the data is consistent with a model in which specific F_1F_0 ATP hydrolysis dictates maximal lifespan, via dictating specific basal metabolic rate. Specific F_1F_0 ATP hydrolysis → specific basal metabolic rate → maximal lifespan. Where the first arrow denotes a positive relation, and the second a negative relation.

Evidence for causality between specific F_1F_0 ATP hydrolysis and specific basal metabolic rate is that an interventional decrease in F_1F_0 ATP hydrolysis causes a decrease in metabolic rate (O_2 consumption). As presented herein, in the earlier Results section components titled "Local inhibition of F_1F_0 ATP hydrolysis" and "Inhibiting F_1F_0 ATP hydrolysis decreases [ROS]". For example, to quote therefrom: "extra IF1 protein decreased F_1F_0 ATP hydrolysis by 40% and decreased State 3 respiration rate by 44%". Moreover, in the "New experimental results" section earlier herein, drug inhibiting F_1F_0 ATP hydrolysis decreased metabolic heat generation (i.e. decreased metabolic rate), causing body temperature drop in mice (*when* body > ambient temperature). In Figure 2.

Evidence for causality between less specific basal metabolic rate and longer maximum lifespan is that an interventional decrease in metabolic rate can extend lifespan. As shown in the work of [75-76]. Where mice with less metabolic heat generation (consuming less O_2/kg/hour than control mice), and lower mean body temperature (average of 0.3°C and 0.34°C less in males and females respectively), had an increased median lifespan (by 12% and 20% in males and females respectively). Wherein females had greater mean body temperature drop, and greater median lifespan extension. This lower metabolic rate was conferred by overexpressing uncoupling protein UCP2 in hypocretin neurons of the

hypothalamus. Selectively making this brain region hotter, so that the nearby preoptic area (POA) was also hotter, fooling it into thinking the rest of the body was warmer than it was, so that it directed less metabolic heat generation.

To summarize this section, drug inhibiting F_1F_0 ATP hydrolysis (*without inhibiting F_1F_0 ATP synthesis*) decreases metabolic heat generation (lower specific metabolic rate) and decrease of metabolic heat generation (lower specific metabolic rate) increases lifespan. The former is shown in Figure 2 herein, and the latter is shown in [75-76]. In both cases, the ambient temperature was such that the decreased metabolic heat generation resulted in lower body temperature. So, to restate, with this aspect included: drug inhibiting F_1F_0 ATP hydrolysis (*without inhibiting F_1F_0 ATP synthesis*) decreases metabolic heat generation (lower specific metabolic rate, lower body temperature) and decrease of metabolic heat generation (lower specific metabolic rate, lower body temperature) increases lifespan. Thus there is an ambiguity because the lifespan increase could be due to the decreased metabolic heat generation (lower specific metabolic rate) and/or the lower body temperature caused thereby. I suggest it is due to both. As explained by the Discussion section.

Future experiment

However, although there is the aforementioned interventional evidence for causality between (*i*) specific F_1F_0 ATP hydrolysis and specific metabolic rate, and (*ii*) between specific metabolic rate and lifespan. Plain, rather than interpolated, interventional evidence for causality between specific F_1F_0 ATP hydrolysis and lifespan is absent to date. A future aim is a mouse lifespan (or surrogate endpoint/biomarker [77]) study. With the mice administered a selective F_1F_0 ATP hydrolysis inhibiting drug (*that doesn't inhibit F_1F_0 ATP synthesis*), e.g. from my US patent application [16]. Predicted to lengthen lifespan. First ensuring the drug dose used can decrease ROS generation in the body (expected on the basis of Figure 5 herein). Assayed by less exhalation of ethane and/or pentane (lipid peroxidation products [78-91]). And/or assayed, probably more accurately, by less of one or more F2-Isoprostane species (lipid peroxidation products [55, 92-97]) in one or more bodily fluids, such as plasma or urine. The production of all these lipid peroxidation species increases with age, wherein the drug is expected to shallow their gradient of increase. Optionally starting with already aged mice. Or using a shorter living species, e.g. the forest shrew (*Myosorex varius*), which has a maximal lifespan of 2.1 years [1].

I hypothesize that the reason for the lower metabolic heat generation, and lower body temperature thereby, of the transgenic mice in [75] is their brain instructing cells of their body to upregulate activity of their natural, selective F_1F_0 ATP hydrolysis inhibitor (*that doesn't inhibit F_1F_0 ATP synthesis*): IF1 protein. If so, this would be a direct interventional connection already shown between less F_1F_0 ATP hydrolysis and longer lifespan. The first author of [75] says (in personal communication) that he still has cryopreserved sperm for this transgenic mouse line, and so (at least for now) it is still possible to explore this. IF1 protein, in mouse and human, has a phosphorylation control switch serine: S14 in the mature (without mitochondrial import sequence) IF1 protein sequence. IF1 protein is inactivated by said phosphorylation, thereby increasing F_1F_0 ATP hydrolysis. Phosphorylated by cyclic AMP (cAMP)-dependent Protein Kinase A (PKA) [98]. My hypothesis is that the transgenic and control mice differ in what fraction of their IF1 protein is phosphorylated at this S14 position and/or differ in IF1 protein amount, conferring less specific F_1F_0 ATP hydrolysis in the transgenic mice.

<u>Does F_1F_0 ATP hydrolysis (at least partially) turn the hands of the epigenetic clock?</u>

Epigenetic clocks are reviewed in [99]. Below is a series of equations, implicit from "Clock 1" in [100] (note that the "log" in Clock 1 of [100] refers to the natural logarithm, ln). Which relates *DNAmAge* (DNA methylation age, also known as epigenetic clock age) to chronological age. For eutherian species.

$$M = \ln(Age + 2)$$

$$DNAmAge = e^{M}$$

$$\therefore DNAmAge = e^{\ln(Age+2)}$$

Where *Age* is chronological age, *DNAmAge* is predicted age, *M* is a linear combination of DNAm (=β) values for selected DNA cytosines, and the +2 offset is to avoid negative numbers with any prenatal data. The natural logarithm (ln) is required because *M* changes ("ticks") slower in eutherian species with a higher maximal lifespan. Indeed, [101] reports the rate of epigenetic ticking is inversely proportional to maximal lifespan across 26 bat species. [102] reports the rate of epigenetic ticking is inversely proportional to maximal lifespan across 3 species (mouse, monkey, human). Moreover, [103] reports (using a 6 mammal species set) slower epigenetic ticking in longer-lived species. And (using a transchromosomic mouse strain, *Tc1*, that harbours a largely intact functional human chromosome 21) shows much faster epigenetic ticking upon a human chromosome when it is in mice (instead of

human) cells. Why this slower ticking of the epigenetic clock in longer-living mammals? What even causes the ticking of the epigenetic clock? I hypothesize that Reactive Oxygen Species (ROS) cause (partially or completely) the ticking of the epigenetic clock. And, as shown herein, shorter-living mammals have greater specific F_1F_0 ATP hydrolysis, higher specific basal metabolic rate [so faster heart rate], greater ROS generation rate, and greater intracellular [ROS].

In support, if cells *in vitro* are cultured in lower O_2 concentration, their epigenetic clock ticks slower [104] ([ROS] in cells inherently being a function of [O_2] in cells). Calorie restriction, which can reduce ROS [105], slows the epigenetic clock in mice [102]. Men have a greater specific basal/resting metabolic rate than women [106-110] and their epigenetic clock ticks faster [111]. Metabolism slows, and the epigenetic clock ticks slower, during hibernation [112]. ROS cause DNA methylation changes by a variety of mechanisms, reviewed in [113-114]. For example, 5-methyl-cytosine (5mC) can be oxidized by the hydroxyl radical (a ROS) to 5-hydroxymethyl-cytosine (5hmC), which when repaired results in demethylation [115-116]. At least mechanistically, it has been reported how superoxide (a ROS) could promote DNA and histone methylation [117].

The degree to which a length of DNA is wound up in chromatin presumably dictates ROS access to it. Different cell-types, as a function of different patterns of gene expression, tend to have different parts of the genome unwound to different extents. Possibly (at least partially) explaining why some epigenetic clocks (which use a subset of DNA cytosines) are tissue specific. Whilst pan-tissue (e.g. [118]; and/or pan-species, e.g. [100]) epigenetic clocks (which use different subsets of DNA cytosines) might be solely/predominantly using DNA stretches that tend to be reasonably unwound across multiple cell-types (and/or species).

ΔM is the average change in (aforementioned variable) M per year in a eutherian species:

$$\Delta M = \frac{\ln(MaxAge + 2)}{MaxAge}$$

Where *MaxAge* is the maximal lifespan (in years) of the species. What this new equation does, in its numerator, is calculate the maximal value of M in this species, i.e. at its maximal lifespan. And then divide that by the number of years to get to that point (the maximal lifespan), to get the average change in M per year in that particular species. As earlier, a +2 offset is used. For eutherian species probed by the mammalian methylation array [119] (used

by [100]), those 116 species thereof whose maximal lifespan is reported in the AnAge database [1], including human, the Pearson correlation coefficient (R) between *ΔM* (calculated) and maximal lifespan (values sourced from AnAge [1]) is -0.74. With a (one-tailed, because the alternative hypothesis is directional) p-value of 1.15814E-21 (N.B., if human is omitted: R = -0.7784, one-tailed p-value = 6.77223E-25). So, the greater the maximal lifespan of a eutherian species, the slower its epigenetic clock ticks. Shown (including human data) in Figure 11. With the caveat that these values of *ΔM* are inferred from a fitted function to experimental data ("Clock 1" in [100]), rather than directly from experimental data. The primary (methylation) data of [100] isn't (at least presently) publically available.

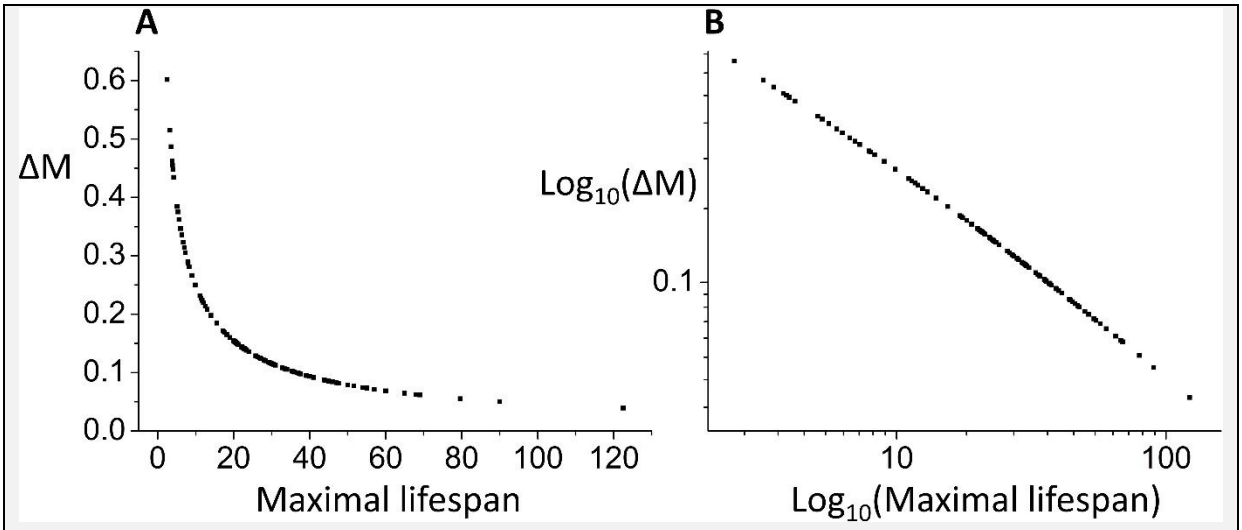

Figure 11 – **(A)** Across 116 eutherian species (different points are for different species): average epigenetic change per year (*ΔM*) is inversely proportional to maximal lifespan. **(B)** Log-log plot (base 10) of the data of panel A. Both these plots show calculated rather than experimental data.

The following table correlates the variables listed along its top (their data is presented in a table in the Methods section: but in this specific case omitting the birds {chicken and pigeon}, restricting to eutherians because the *ΔM* equation was derived solely from eutherian data, and completely omitting human by rationale given in the Methods section, relevant here because *ΔM* calculation uses maximal lifespan) to *ΔM* (p-values are one-tailed, because each

alternative hypothesis is directional):

		Specific F1F0 ATP hydrolysis	Specific basal metabolic rate	Heart rate	Maximal lifespan	log10(body mass)
R	ΔM	0.8476	0.8908	0.944	-0.943	-0.8876
p		0.0019535	0.0006355	0.000065	0.000069	0.000701

Using the same data as used to produce the table immediately above: Results of mediation analysis between specific F_1F_0 ATP hydrolysis and *ΔM*, with the Mediator variable being specific basal metabolic rate, are in the table below. On its first line of data. On its second line of data, are results of mediation analysis between specific basal metabolic rate and maximal lifespan, with the Mediator variable being *ΔM*. Note that when inputting data into the JASP software, I multiplied all the specific basal metabolic rate values (W/g) by 10,000, and the values of *ΔM* by 100 (rescaled these variables), to prevent "numerical underflow" in the underlying computations performed. Bootstrap method (called "Percentile" in JASP) was used with 10,000 replications.

			95% Confidence Interval (CI)			95% Confidence Interval (CI)	
α	β	**Indirect effect (α·β)**	Lower	Upper	**Direct effect (τ)**	Lower	Upper
23	0.26	5.86	3.156	18.95	5.572	-7.466	11.663
0.39	-0.61	-0.238	-0.799	-0.006	0.002	-0.396	0.403

In both cases mediation is shown. Because, for both, there is no zero (0) within the 95% confidence interval for an indirect effect. And thence this data is consistent with the following mediation cascade:
Specific F_1F_0 ATP hydrolysis → Specific basal metabolic rate → *ΔM* → Maximal lifespan. Where all arrows signify positive effect, except the last, which signifies negative effect. This result is consistent with the ticking of the epigenetic clock as a drive, rather than merely a reporter, of aging. It curtailing maximal lifespan. Incidentally, mediation is also observed as per: Specific F_1F_0 ATP hydrolysis → *ΔM* → Maximal lifespan (data not shown).

Using the data used to produce Figure 11, using data from those 55 species thereof that have a specific basal metabolic rate value in the AnAge database [1], mediation analysis (using the "Percentile" option in JASP, with 10,000 replications) was performed. Assaying mediation between specific basal metabolic rate (multiplied by 10,000) and maximal lifespan, via variable *ΔM* (multiplied by 100). Which is observed (N.B., mediation also observed if human is excluded, data not shown):

			95% Confidence Interval (CI)			95% Confidence Interval (CI)	
α	β	**Indirect effect (α·β)**	Lower	Upper	**Direct effect (τ)**	Lower	Upper
0.13	-1.2	-0.156	-0.374	-0.091	0.03	-0.1	0.093

The data analysis of this section is consistent with the aforementioned hypothesis that specific F_1F_0 ATP hydrolysis is a drive (via its setting of specific basal metabolic rate and thence ROS generation) to the ticking of the epigenetic clock. A future experiment is to assay whether a selective F_1F_0 ATP hydrolysis inhibiting drug (*that doesn't inhibit F_1F_0 ATP synthesis*), e.g. of my US patent application [16], can slow the ticking of the epigenetic clock of human cells *in vitro*. In the assay used in [120-121].

New experimental results

Anti-cancer

I've discovered that cancers disproportionally use F_1F_0 ATP hydrolysis. Indeed, distinctively from normal cells, they absolutely require it. Not for heat generation (which isn't an absolute need because exogenous heat {i.e., the ambient temperature} can substitute for its absence). But for operating their distinctive, abnormal, heavily glycolytic ("Warburg effect") metabolism (some literature upon this metabolism: [122-127]). Indeed, I show that drugs, which inhibit F_1F_0 ATP hydrolysis, each exert potent anticancer activity (against 60 different cancers from 9 tissues) *in vitro*, in testing at the National Cancer Institute (USA): Figures 12 and 13. With analysis proving that this anticancer action is by inhibiting F_1F_0 ATP hydrolysis. These cancer drugs might (unlike present cancer drugs) help rather than harm normal cells. Indeed, by making their metabolism more efficient (less chemical energy of food dissipated as heat), each of these drugs may combat cachexia (wasting/weight loss). Cachexia is prevalent in advanced cancer patients and is often the cause of death [128]. In support, transgenic mice with less metabolic heat generation have greater body weight (and longer lifespan) [75-76].

Figures 12 and 13 show results from the NCI-60 one-dose *in vitro* assay. Performed by the National Cancer Institute (NCI, USA). With compounds I submitted. This protocol tests the effect, if any, of a single test compound (10 μM) on the growth/survivability of 60 different cancer cell lines, originated from 9 different tissues, as compared to the no compound control [129]. A tested compound's activity can range from negative % (cancer growth promotion),

to 0% (no activity), to 100% (complete cancer growth inhibition), to 200% (all starting cancer cells are dead). NCI-60 tests are performed at a controlled temperature of 37°C. For 48 hours.

More specifically, Figures 12 and 13 show that compounds which potently inhibit F_1F_0 ATP hydrolysis exert potent anti-cancer activity. Figure 12 shows the *in vitro* anti-cancer activity of separated stereoisomers 6a and 6b. Figure 12A shows their structure. 6a is the *R* stereoisomer in high enantiomeric excess (>97% ee). 6b is the *S* stereoisomer in high enantiomeric excess (>97% ee; administered to mice in Figure 2). Figure 12B shows the anti-cancer activity of 6a (10 μM). Figure 12C shows the anti-cancer activity of 6b (10 μM). As specified in Figure 12A, 6b potently inhibits F_1F_0 ATP hydrolysis (EC_{50} F_1F_0 ATP hydrolysis = 0.018 μM [=18 nM] in a Sub-Mitochondrial Particle {SMP} assay {in which *no* inhibition of F_1F_0 ATP synthesis by this drug was observed} [28-29]). Whilst 6a does not (EC_{50} F_1F_0 ATP hydrolysis > 100 μM in the SMP assay {in which *no* inhibition of F_1F_0 ATP synthesis by this drug was observed} [28-29]). In other words, the *S* stereoisomer potently inhibits F_1F_0 ATP hydrolysis, and the *R* stereoisomer does not. But the anti-cancer activity of 6a and 6b is similar in Figures 12B and 12C. Because, to interpret, they both undergo racemization in a biological system. Which erodes their enantiomeric excess during the 48 hours duration of the NCI-60 anti-cancer tests. So, they both converge towards/upon being the racemate, 19a (EC_{50} F_1F_0 ATP hydrolysis = 0.033 μM in the SMP assay [28-29], Figure 12A). Such that both samples ultimately contain a substantial proportion of *S* stereoisomer. And so both exert anti-cancer activity by inhibiting F_1F_0 ATP hydrolysis. But racemization is not instantaneous, and so the 6b sample confers greater *S* stereoisomer exposure ("area under the curve") to the cancer cells than the 6a sample. And thence confers greater anti-cancer activity: 66% vs. 57% mean (67% vs. 59% median) cancer growth inhibition, across all 60 cancer cell lines.

Observable in aforementioned Figure 12a, opposite stereoisomers, 6a and 6b, have hydrogen on their chiral carbon. Figure 13 discloses the anti-cancer activity of stereoisomers 7a and 7b. These have the same structure as 6a and 6b, except that they have deuterium (enrichment) instead of hydrogen on their chiral carbon (>99% molar percent deuterium incorporation at their chiral carbon). Their structure is shown in Figure 13A. 7a is the *R* stereoisomer in high enantiomeric excess (>97% ee). 7b is the *S* stereoisomer in high enantiomeric excess (>97% ee). Figure 13B shows the anti-cancer activity of 7a (10 μM). Figure 13C shows the anti-cancer activity of 7b (10 μM). This anti-cancer data is also from the National Cancer Institute's standardized NCI-60 testing protocol. So, directly comparable to the

aforementioned anti-cancer data for 6a and 6b. To summarize all the NCI-60 data, the mean and median % cancer growth inhibition conferred (by 10 μM) is shown in the table below:

	6a	6b	(6b-6a)	7a	7b	(7b-7a)	(7b-7a)/(6b-6a)
Mean	57.3	66.15	8.85	52.35	72.81	20.46	2.3
Median	58.62	66.9	8.28	52.09	74.51	22.42	2.7

7b exerts greater anti-cancer activity than 6b. 7a exerts less anti-cancer activity than 6a. Thence the difference between the anti-cancer activity of 7b and 7a is greater than that between 6b and 6a. To interpret, this is because, whereas 6a and 6b have hydrogen (H) attached to the chiral carbon, 7a and 7b have deuterium (D, ^{2}H) attached to the chiral carbon. Deuterium slows the racemization rate by a Kinetic Isotope Effect (KIE [130]; C-^{2}H bond is stronger than a C-H bond). So, because of a slower racemization rate, 7b maintains its enantiomeric excess (of *S*) better than 6b. Conferring 7b greater anti-cancer activity than 6b. Because of a slower racemization rate, 7a maintains its enantiomeric excess (of *R*) better than 6a. Conferring 7a less anti-cancer activity than 6a. The disparity in anti-cancer activity between 7b and 7a is 2-3 times greater than that between 6b and 6a. Which is the correct order of magnitude for a KIE (>1 and ≤10 [131], greater if tunnelling is very mechanistically relevant [132]).

If the *S* stereoisomer has anti-cancer activity, and the *R* stereoisomer does not, hypothesizing their enantiomerization in a biological system, the mean of 6a and 6b anti-cancer activity should equal the anti-cancer activity of the 6a/6b racemate. If this racemate was tested. Similarly, the mean of 7a and 7b anti-cancer activity should equal the anti-cancer activity of the 7a/7b racemate. If this racemate was tested. Supportively, the mean of 6a and 6b median anti-cancer activity is equal to the mean of 7a and 7b median anti-cancer activity: numbers below are drawn from the earlier table:

{(58.62+66.9)/2} = 62.76 = 63%, ≈ {(52.09+74.51)/2} = 63.3 = 63%

(*The mean of 6a and 6b mean anti-cancer activity is nearly equal to the mean of 7a and*

7b mean anti-cancer activity: {(57.3+66.15)/2} = 61.73 = 62%, ≈ {(52.35+72.81)/2} = 62.58 = 63%).

The following features of the data have already been herein addressed/explained, wherein each following sample name refers to the median of its anti-cancer activity (sourced from earlier table): (7a+7b)/2=(6a+6b)/2, 7b>7a, 6b>6a, 7b>6b, 7a<6a. In NCI-60 compound testing, anti-cancer activity can range from 0% (no activity) to 100% (complete cancer growth inhibition) to 200% (all starting cancer cells are dead). So, the possible range is 0-200% (*if* the assumption is made that no administered compound will promote cancer growth, and so *if* the possibility of increased cancer growth upon compound administration is dismissed). To do some supporting theoretical analysis, using A, B, C, D, wherein each of these letters can independently be any integer in the range 0-200, the chance, by chance, of all of the following being true at the same time: (A+B)/2=(C+D)/2 (equivalently A+B=C+D), A>B, C>D, A>C, B<D, is 0.04% (125 times smaller than 5%, the most common significance threshold used by those of the art; its corresponding decimal p-value is 0.0004, which is <0.05). If A, B, C, D can be fractional also, and not only integers, the chance is even smaller, much smaller (not shown). The chance, by chance, of all of the following being true at the same time (delimited to integers): (A+B)/2=(C+D)/2=63, A>B, C>D, A>C, B<D, is 0.00025% (corresponding decimal p-value is 0.0000025, which is <0.05).

The anti-cancer activity of 6a, 6b, 7a, 7b are all highly correlated (in the table below, p-values are one-tailed because each alternative hypothesis is directional). Because they tend to have greater, or lesser, anti-cancer activity against the same of the 60 cancer cell lines. This, by the rationale/basis of [133], indicates that they are exerting anti-cancer activity by the same molecular mechanism. Indeed, to interpret the data herein, by selectively inhibiting F_1F_0 ATP hydrolysis (*without inhibition of F_1F_0 ATP synthesis*).

Pearson Correlation Coefficient (R):					
	6a	6b	7a	7b	
6a	1				
6b	0.7991	1			
7a	0.7693	0.5205	1		
7b	0.6614	0.6451	0.8049	1	
N=60 for all samples; P-value (one-tailed):					
	6a	6b	7a	7b	
6a	/				
6b	9.85E-15	/			
7a	3.48E-13	1.01E-05	/		
7b	4.39E-09	1.32E-08	4.60E-15	/	
Fisher's combined probability test					
Using p-values for [6a vs. 7a] and [6b vs. 7b]					
			3.48E-13	1.32E-08	
p-value = **2.20E-19** = 0.0000000000000000002					

So, Figures 12 and 13 show that compounds which potently inhibit F_1F_0 ATP hydrolysis exert potent anti-cancer activity. I predicted this result before it was observed. By rational design. Because I reasoned that the abnormally glycolytic metabolism of cancers (Warburg effect [122]), especially used by the most dangerous thereof [123-127], hinges upon abnormally high rates of F_1F_0 ATP hydrolysis. Consuming glycolytic ATP (imported into mitochondria by the Adenine Nucleotide Transporter, driven by higher [ATP], and lower [ADP], in the cytoplasm than in the mitochondrial matrix). Releasing glycolysis from ATP negative feedback inhibition (ATP allosterically exerts negative feedback inhibition upon the glycolytic enzymes phosphofructokinase and pyruvate kinase [134]). Yielding higher glycolytic rate. Thence more glycolytic intermediates are available to be shunted into biosynthesis (enabling faster cancer cell proliferation). And conferring more NADPH produced by the pentose phosphate pathway, enabling more Reactive Oxygen Species (ROS) mitigation. By the NADPH dependent glutathione, and NADPH dependent thioredoxin, ROS mitigation systems. And less ROS are produced because oxidative phosphorylation {OXPHOS} is disfavoured by the high proton motive force (pmf, comprising high {more hyperpolarized} Ψ_{IM} [135]) across the mitochondrial inner membrane created by F_1F_0 ATP hydrolysis. So, [ROS] is lower. Freeing them from aging, thereby conferring "limitless replicative potential" (i.e. immortality, which is distinctive trait of cancer [136], which normal somatic cells don't share; {I propose} mutational load of cancer primarily acquired before, on the path to, cancer). A selective F_1F_0 ATP hydrolysis inhibiting drug (*that doesn't*

inhibit F_1F_0 ATP synthesis) inhibits this cancer metabolic program, conferring anti-cancer activity. Whilst (prospectively) helping, instead of harming, normal cells *in vivo*. Increasing their metabolic efficiency, so less chemical energy of food is dissipated as heat (Figure 2). Thereby (*if* the ambient temperature, and/or bodily insulation, substitutes for lower metabolic heat production) possibly combating cachexia/wasting. Which is observed in many advanced/terminal cancer patients, and is often the cause of their death [128]. Moreover, *in vivo*, to hypothesize, cachexia/wasting might be additionally combated by the compound conferred decrease in glycolytic rate of cancer cells. Decreasing their glucose influx and lactate efflux. Thence decreasing the energetically expensive conversion of lactate to glucose by the Cori cycle of the liver. Which costs 6 ATP for every lactate to glucose converted [134]. Elevated blood [lactate] correlates with worse cancer prognosis [137]. In this way, the anti-cancer benefit *in vivo* is expected to be greater than that shown herein *in vitro*. Especially in the case of cancer cells in a solid (hypoxic/anoxic) tumour, which might singly rely upon F_1F_0 ATP hydrolysis to maintain pmf (Ψ_{IM}). Where loss of Ψ_{IM} is a well-known trigger for apoptosis [138]. The *in vitro* studies herein cannot report this (hypothesized) effect because they are conducted at atmospheric pO_2 (at the elevation of the National Cancer Institute in Maryland, USA). Tumour hypoxia correlates with poor patient prognosis [139-144]. Tumour hypoxia is associated with radio- [145-146] and chemo- [147-148] resistant cancer.

In further supporting data, I've shown anti-cancer activity, in NCI-60 testing, by other compounds, of completely different scaffolds, which also selectively inhibit F_1F_0 ATP hydrolysis (*that don't inhibit F_1F_0 ATP synthesis*). For example, please see the 45 pages of experimental data in my US patent application [16] (following my earlier application [17]). My work, predominantly in the patent (rather than scholarly) literature, reports a new molecular target for exerting anti-cancer activity. F_1F_0 ATP hydrolysis. And novel drugs acting upon that target.

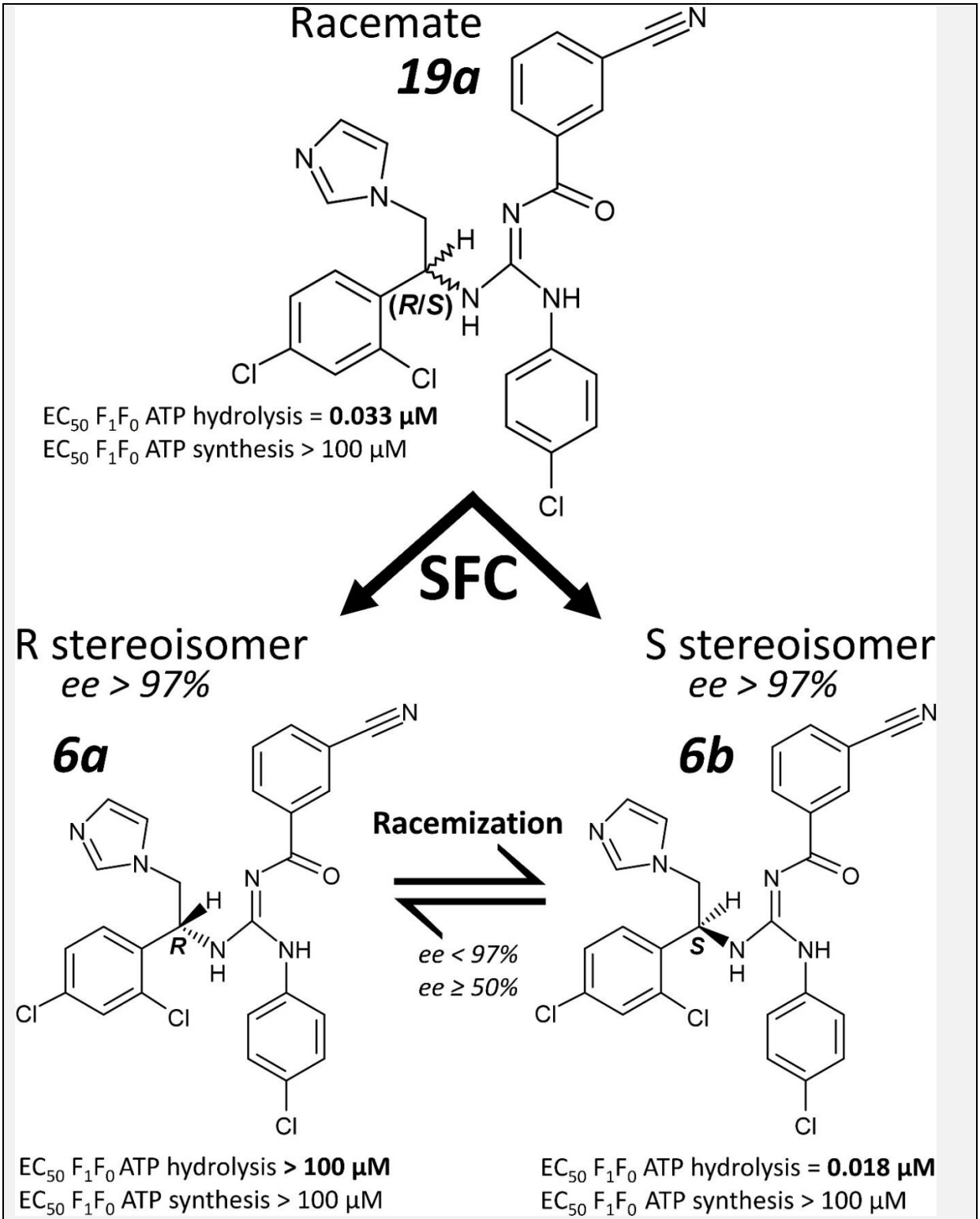

Figure 12A - Structure of racemate, 19a, and its separated stereoisomers (separated stereoisomer fractions) 6a and 6b. SFC is chiral supercritical fluid chromatography, ee is enantiomeric excess. EC_{50} values are from a Sub-Mitochondrial Particle (SMP) assay.

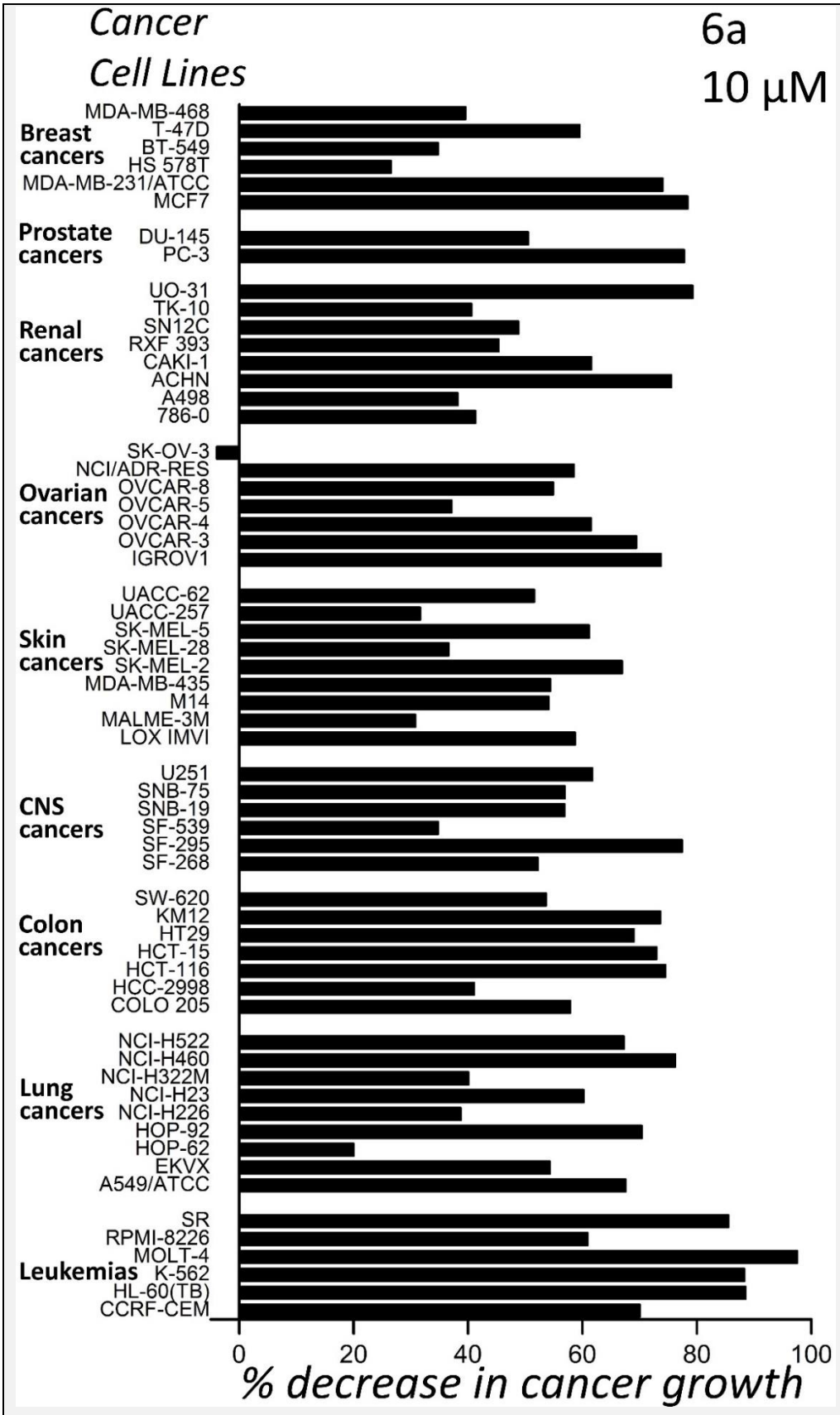

Figure 12B - Anti-cancer activity of compound 6a (10 µM) in NCI-60 testing.

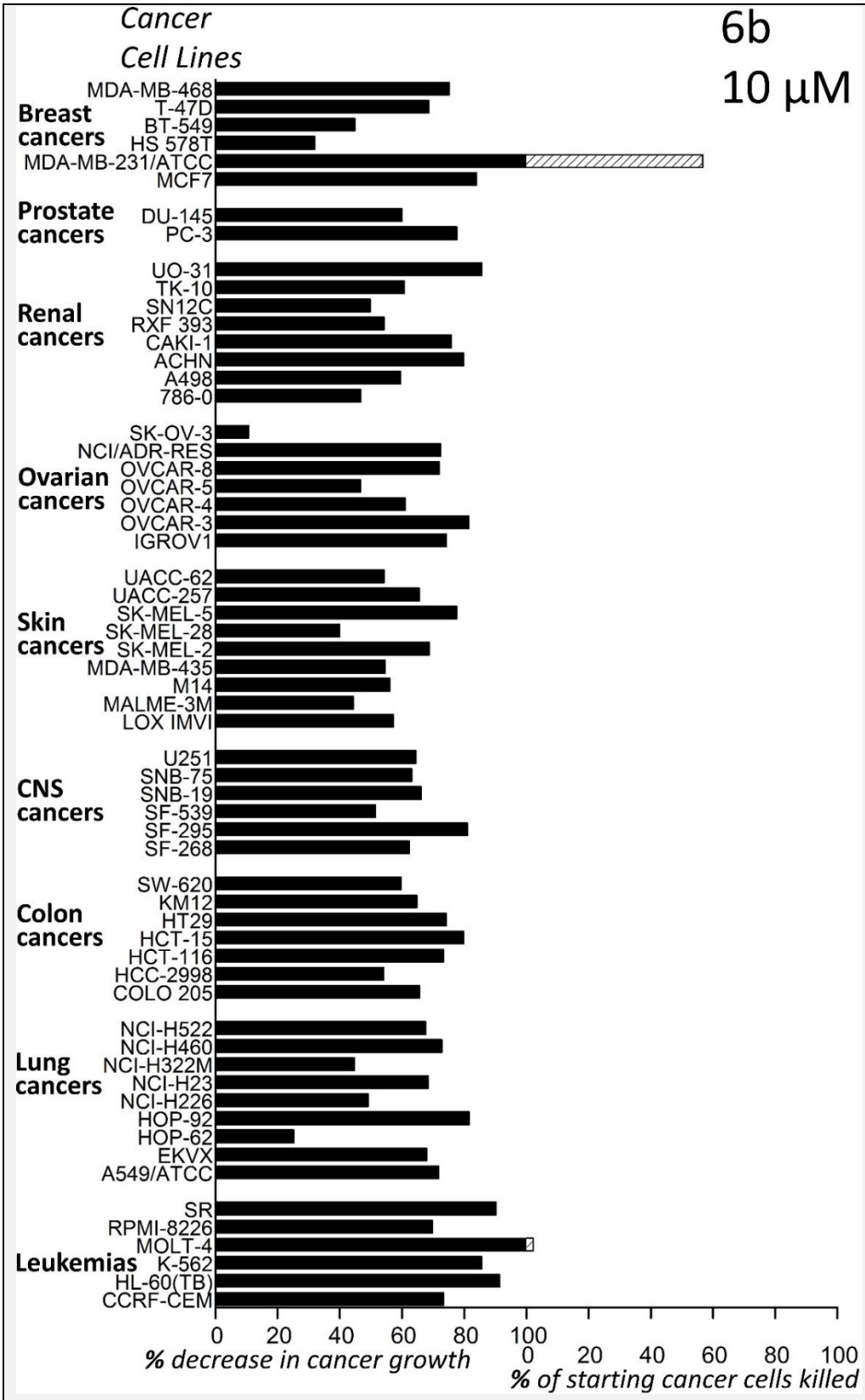

Figure 12C - Anti-cancer activity of compound 6b (10 µM) in NCI-60 testing.

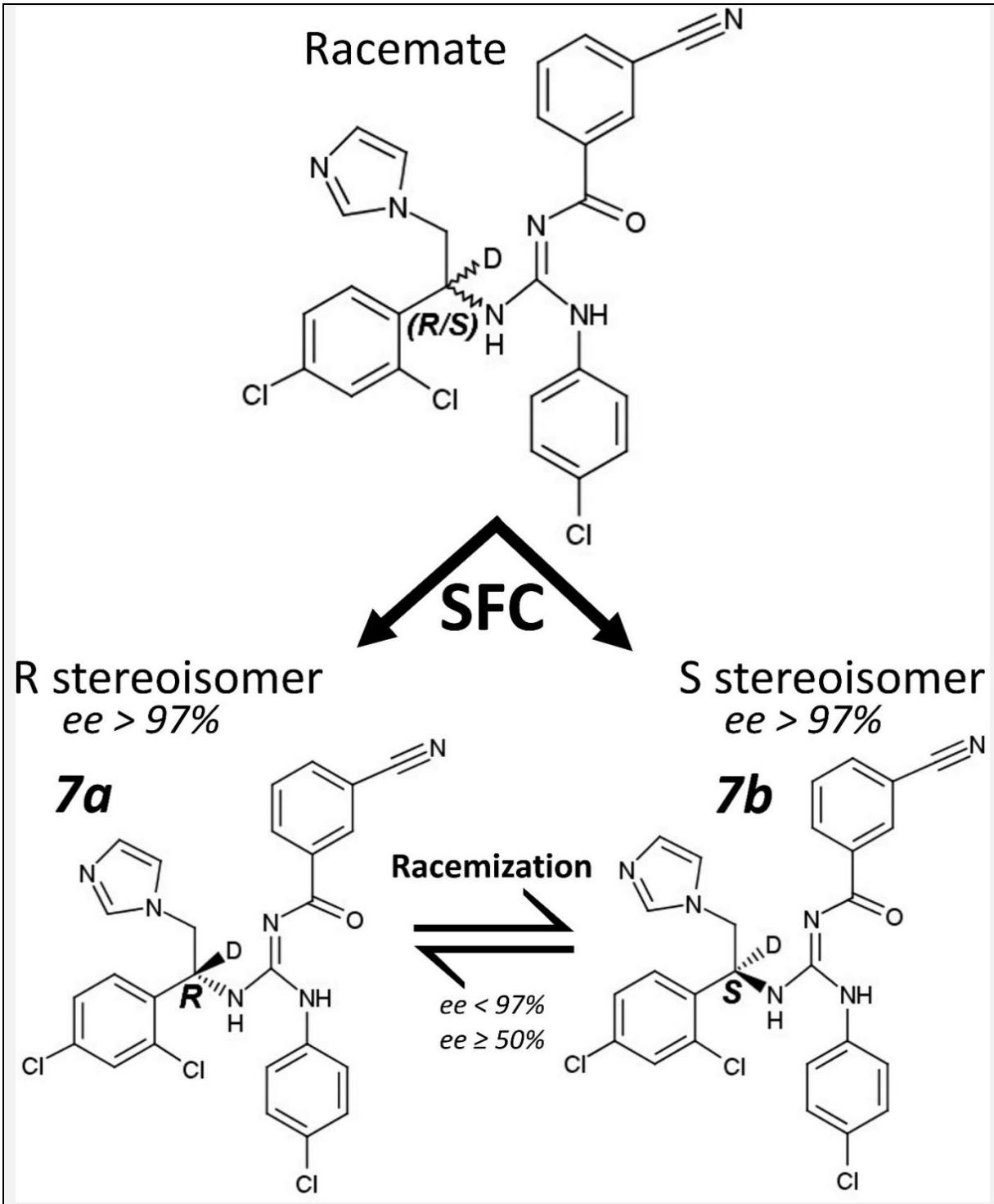

Figure 13A - Structure of separated stereoisomers (separated stereoisomer fractions) 7a and 7b. SFC is chiral supercritical fluid chromatography, ee is enantiomeric excess. D is deuterium (^{2}H).

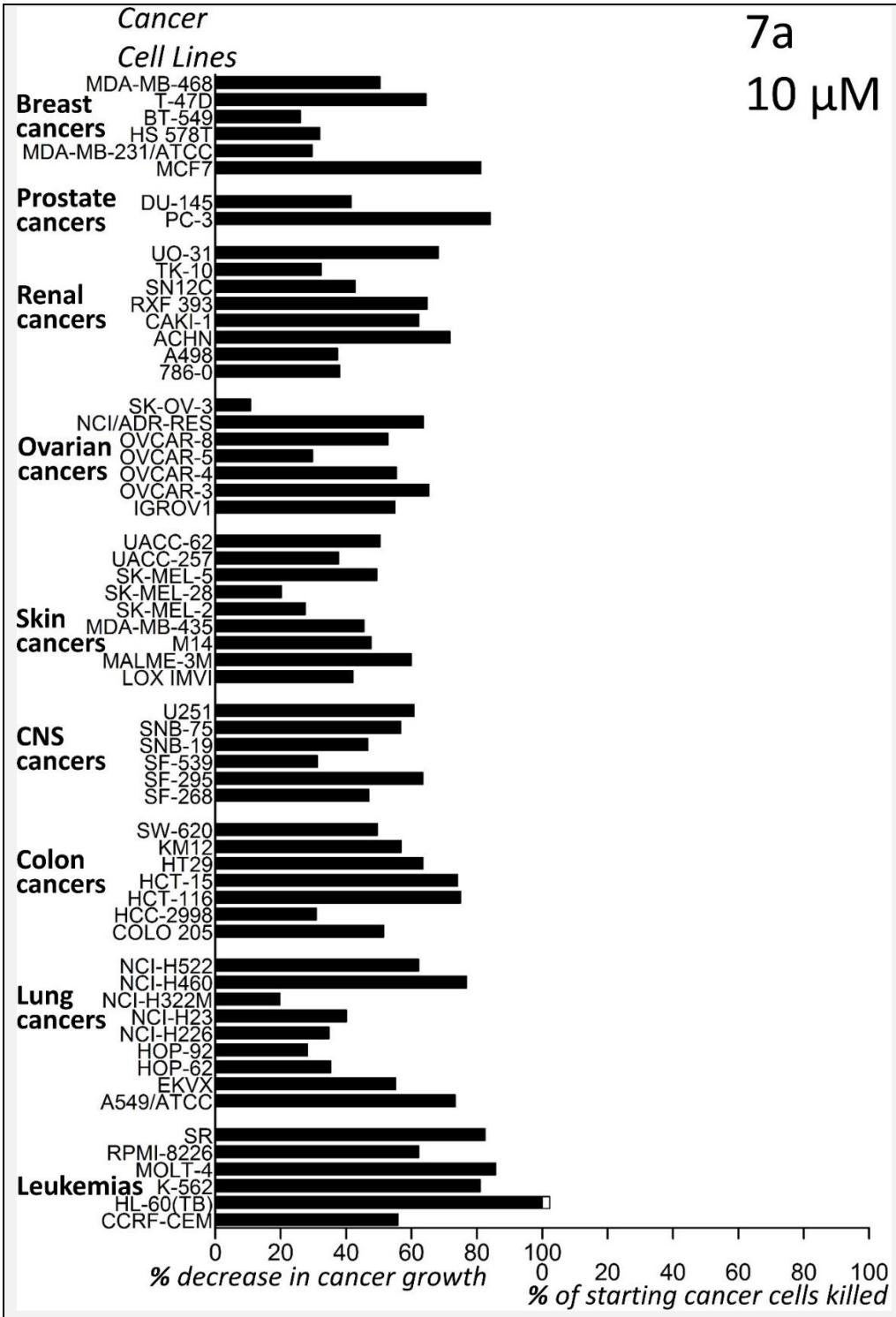

Figure 13B - Anti-cancer activity of compound 7a (10 µM) in NCI-60 testing.

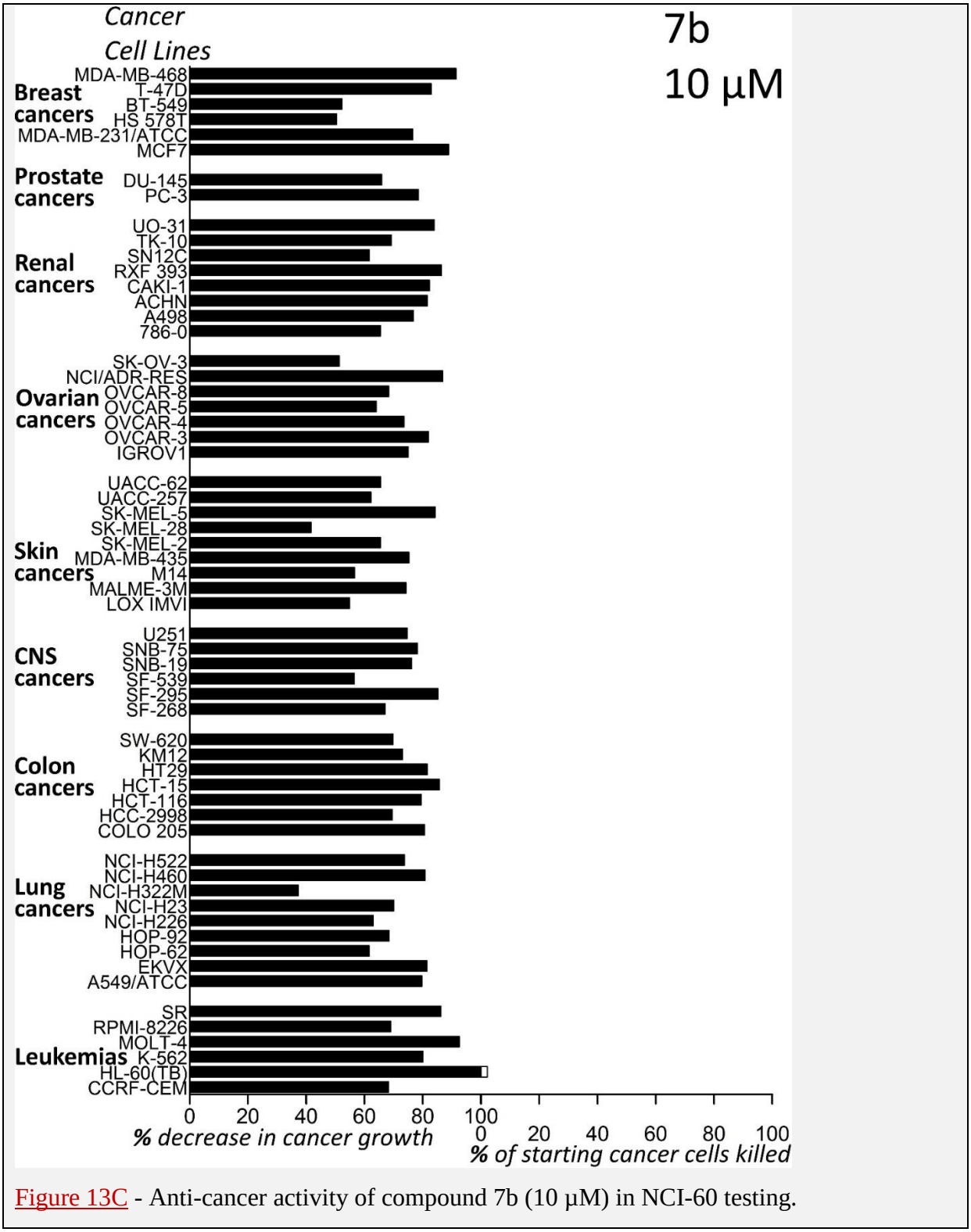

Figure 13C - Anti-cancer activity of compound 7b (10 µM) in NCI-60 testing.

It is notable that selective F_1F_0 ATP hydrolysis inhibiting compounds (*that don't inhibit F_1F_0 ATP synthesis*), hypothesized to slow aging herein (Discussion section), have anti-cancer activity (Figures 12 and 13). Because a worry/critique of trying to slow aging is the argument that, because cancer is immortal [136], conferring slower aging/immortality upon a normal

cell is making it closer to being cancer. Such that even if an anti-aging approach could be found, because of it inextricably increasing the cancer risk, lifespan wouldn't be very much extended, if at all. Conferring a practical block/limit to appreciable lifespan extension. For example, this is a concern, in at least some people's minds, with expression of telomerase (in normal somatic cells) approaches [149-151]. However, by contrast, selectively inhibiting F_1F_0 ATP hydrolysis (*without inhibiting F_1F_0 ATP synthesis*) actively exerts potent anti-cancer activity (Figures 12 and 13). So, distinctively, it is a drive against, and not to, cancer. Arguably, anti-cancer activity is a highly desirable, if not a mandatory, trait of a longevity drug. Indeed, rapamycin (also known as sirolimus), an mTOR inhibiting drug, which can slow aging and extend lifespan in mice, has anti-cancer activity also [152]. In NCI-60 one-dose (10 μM) testing, it confers mean and median % cancer growth inhibition of 56.22% and 55.45% respectively (NSC 226080 in [153]). Temsirolimus, a prodrug of rapamycin (metabolized to rapamycin in the body), is approved by the U.S. Food and Drug Administration (FDA), and the European Medicines Agency (EMA), for the treatment of Renal Cell Carcinoma (RCC) [154].

At least some present cancer treatments, e.g. radiotherapy, (probably because their Mechanism of Action {MOA} is, at least in part, to increase Reactive Oxygen Species, ROS [145-148]) accelerate aging in normal cells. Thence (presumably because aging/age is a major risk factor for cancer [155]) increasing subsequent cancer risk [156-157]. I propose selective F_1F_0 ATP hydrolysis inhibitor compounds do the inverse. Still conferring anti-cancer therapy (Figures 12 and 13. Partly, by aforementioned rationale, via increasing [ROS] in cancer cells). But whilst slowing aging in normal cells (by reducing their intracellular [ROS], Figure 5), which reduces the subsequent/secondary cancer risk.

To theorize, inhibiting F_1F_0 ATP hydrolysis slows both heavily glycolytic (cancer) and predominantly oxidative (normal cell) metabolisms. The former *increases* intracellular [ROS] in cancer cells. The latter *decreases* intracellular [ROS] in normal cells.

Note that cancer can increase body temperature [158]. Indeed, cancers can cause fever [159]. Especially some types thereof, such as Hodgkin's and non-Hodgkin's lymphoma, renal cell carcinoma, hepatocellular carcinoma, Acute Myeloid Leukaemia (AML), hairy cell leukaemia, glioblastoma multiforme, blast crisis of Chronic Myelogenous Leukemia (CML), and ovarian cancer. At low/moderate ambient temperature, this higher body temperature

confers margin/benefit for a greater dose of a selective F_1F_0 ATP hydrolysis inhibiting drug (*that doesn't inhibit F_1F_0 ATP synthesis*).

Compound 7b has the best anticancer activity. Conceivably, its anticancer utility confers margin to follow a *relatively* fast regulatory path to its clinical approval in humans. Afterward used/trialled as a treatment/preventative for other diseases of aging. Those many varied diseases whose incidence increases exponentially with age/aging. Such as Age-related Macular Degeneration (AMD) and Alzheimer's disease. If aging is causal to age-related diseases, (conceivably) a single drug, which slows aging (predicted of compound 7b), can confer therapy for all these (many and varied) diseases.

Supplementary data

Supplementary information, data and analysis can be found in this paper's Methods section, interwoven with its methods. Of particular note, data is presented there showing that in a set of species, maximal lifespan positively correlates with specific IF1 protein activity. IF1 protein is an endogenous inhibitor of F_1F_0 ATP hydrolysis (*that doesn't inhibit F_1F_0 ATP synthesis*) [7-13].

DISCUSSION

Discovery of a keystone of homeothermy

A contribution of this paper (*and my corresponding patent applications, e.g. [16-17]*) is the new finding, from new experimental data, that F_1F_0 ATP hydrolysis is prevalent *in vivo*, it conferring metabolic heat generation. Evidenced by Figure 2 herein.

Slightly lower body temperature corresponds with a much longer lifespan

As aforementioned, mice made (by experimental intervention) to have a slightly lower mean body temperature have a much increased lifespan (0.34°C lower increases median lifespan by 20% in females, 0.3°C lower increases median lifespan by 12% in males) [75]. Moreover, Ames dwarf mice have a 1.6°C lower mean body temperature than normal sized mice [160], with a mean lifespan ≥68% longer in females, and 49% longer in males [161]. Lower body temperature extends the lifespan of *D. melanogaster* (fruit fly) [162-163], *Calliphora stygia* (a blowfly) [164], *C. elegans* (a nematode worm) [165], *Trichogramma platneri* (a wasp) [166], and *Cynolebias adloffi* (a fish) [167]. For example, the median lifespan of *D.*

melanogaster is 86% longer when their body temperature is 5°C less [162]. In a set of humans, mean body temperature ranged (2.2°C) from 35.2 to 37.4°C in [168]. And (2.4°C) from 35.3 to 37.7°C, across 35,488 human subjects, in [158]. And human rectal temperature data ranged (3.4°C) from 34.4 to 37.8°C in [169] (this paper consolidates data from multiple studies). In humans, in the Baltimore Longitudinal Study of Aging, people with a body temperature (at study entry) in the bottom half of the observed body temperatures (at study entry) had lower mortality over the subsequent 25 years of monitoring [170]. Analysis of 677,423 human body temperature measurements, spanning 157 years (1860–2017), showed that mean body temperature has decreased 0.03°C per birth decade (men born in the early 19th century had a body temperature 0.59°C higher than men today), alongside an increase in median lifespan over the same time period [171]. In a 18,630 people cohort (ages in the range of 20-98 years old): >60 years old, the proportion of people with a mean body temperature <35.56°C was more, whilst the proportion of people with a mean body temperature >36.67°C was less, possibly reflecting increased survival of individuals with lower mean body temperature (and/or a decrease of mean body temperature with age) [172]. In a large cohort of (35,488) humans, higher mean body temperature was linked to higher one year mortality [158]. In humans, lower early morning body temperature correlates with better physical (e.g. faster walking speed) functioning in aged individuals [173]. And lower body temperature correlates with better mental functioning in aged humans [174].

Calorie restriction slows aging and extends lifespan in model organisms, such as rodents and primates [175-176]. It causes a lower body temperature [177], by as much as 5°C in some mouse strains [178]. Calorie restriction decreases body temperature in humans [179-181]. Calorie restriction is the best intervention for life extension that we have found to date, e.g. increasing the mean and maximal lifespans of mice by 65% and 51% respectively [175]. Rapamycin drug, which can slow aging and extend lifespan in mice [152], can decrease the body temperature of mice [182].

To interpret the preceding paragraphs of this section, lower body temperature can extend longevity (at least partly) because chemical reactions run slower at lower temperature (*the exponential dependence of chemical reaction rate upon temperature can be seen in the Arrhenius [183] and Eyring [184] equations {the latter having an additional pre-exponential temperature term}*). And so ROS generation and ROS-caused molecular damage occurs more slowly. Repair thereof also runs more slowly. But since there is net damage over repair

(damage outruns repair), there is a net benefit to lower temperature. Also, in homeotherms, if the lower body temperature is because of less metabolic heat generation, there is much less Reactive Oxygen Species (ROS) generation per unit time.

The transgenic mice of [75-76] have a lower mean body temperature because of less metabolic heat generation, and have a longer lifespan accordingly. As shown in Figure 2 herein, a selective F_1F_0 ATP hydrolysis inhibiting drug (*that doesn't inhibit F_1F_0 ATP synthesis*) can reduce body temperature of mice (dose-dependently; *if* the ambient temperature is permissively low). By reducing metabolic heat generation.

Difference in human life expectancy between higher and lower body temperature groups

Using data from the Baltimore Longitudinal Study of Aging, Fig. 1D in [170] plots cumulative survival vs. time (over 25 years; corrected for initial subject age). With two plots: one for men with a body temperature below, and the other for men with a body temperature above, the median body temperature of men in the study (recorded upon entry into the study; there was no significant difference in subject age between the two groups at the start of the study; subject ages ranged from 18 to 91 upon study entry; 324 men died over the 25 years of observation). I used the aforementioned WebPlotDigitizer to pull representative data points from one of the plots. And then did the same for the other plot. I then opened the data for the lower body temperature group in OriginPro 8 software (OriginLab Corporation, Northampton, MA, USA), plotted it as a scatter plot, and then fitted a polynomial curve to it. Using this fitted polynomial equation {$y=0.99534+(0.00101*x)+(-5.12587E\text{-}4*x^2)$} I generated further data points to extrapolate this plot to y = 0 (all subjects dead). Making the assumption that the curve follows the same trajectory until all subjects die. I then integrated this plot. Its mathematical area (under the curve) was 29.765031340107, which I then divided by the y-axis value at the beginning of the time period (1), which returned 29.765031340107. Which is the life expectancy of that group in years (from the start of the study period, not from birth). A notional life expectancy because the x-axis isn't subject age but time since start of observation. [185] guided this technique I used, to get (notional) life expectancy from a survival plot (dimensionally correct because the y-axis has the dimension of persons, the x-axis has the dimension of years, so the area under the curve has the dimension of person years, and when divided by the number of persons alive at the beginning, the dimension is years). I then repeated this methodology for the other plot. That for the higher body temperature group. Which returned {its polynomial plot: y=0.99673+(4.39509E-4*x)+(-

$5.87422E\text{-}4*x^2)\}$ a notional life expectancy of 27.394083088806 years. So, a difference in life expectancy of 2.3709482513 (=2.4) years, i.e. men with a lower body temperature have a greater life expectancy. A significant difference (to at least $p < 0.05$), inheriting significance from that shown for this data by [170]. Although acknowledging that my calculation is assumptive and abstractive.

Hereafter I tentatively extrapolate this data (from a sample of the US population) to the entire US population. If the half of men with higher than mean body temperature, and 2.4 years less life expectancy, were to maintain an effective amount of a selective F_1F_0 ATP hydrolysis inhibiting drug (*that doesn't inhibit F_1F_0 ATP synthesis*) in their system, by regular oral administration, such that their body temperature was lower than the original mean body temperature (with the same distribution of values below it than the other half of men), then the overall life expectancy of all men would be increased by 1.2 years. Assuming this effect could be replicated for woman also, the overall life expectancy for both genders would be increased by 1.2 years. Economists calculate that a slowdown in aging, which increases US life expectancy by 1 year, is worth $38 trillion US dollars [186].

To extrapolate further, an even greater increase in life expectancy might be conferred if everyone's resting body temperature was bought down to, not just below the original mean resting body temperature, but to the lowest values naturally observed within the human population. Or possibly even lower. As aforementioned, mice with 0.34°C lower mean body temperature have 20% greater median lifespan [75]. Wherein the body temperature of many people could be reduced by at least 0.34°C and their body temperature would still be within the range of resting mean body temperature observed within the human population (which is 35.2 to 37.7°C, i.e. a 2.5°C range [158, 168]).

A drug-conferred body temperature difference of 0.34°C is anticipated to be imperceptible to a human because our body temperature imperceptibly varies by more than that (0.7 to 1.6°C) during the course of a day (following the circadian rhythm) [187]. And more than that over the course of a month in women, whose body temperature varies with their menstrual cycle (0.3 to 0.7°C body temperature difference between the luteal and follicular phases) [188]. Human body temperature can vary with season, being around 0.2°C cooler in winter [189]. Human body temperature is imperceptibly lower during calorie restriction. For example, mean human body temperature is 0.2°C lower during calorie restriction (0.3°C lower in a

calorie restriction and exercise group) in [179-180], and 0.5-0.8°C lower during semi-starvation in [181]. Conceivably, administration of a F_1F_0 ATP hydrolysis inhibiting drug (*that doesn't inhibit F_1F_0 ATP synthesis*) allows one to have the cooler body temperature of calorie restriction, which might be componentry to how calorie restriction extends lifespan [190]. Thereby acting as a calorie restriction mimetic.

The prior calculated difference in life expectancy (2.4 years) between the two groups might be an underestimate because (according to personal communication with the first author of [170]) the subjects of this study didn't each have their body temperature recorded at the same time of day. But instead at varying times of day (disproportionally within typical working hours within the USA). Given that body temperature can vary with time of day [187], this is a confounding factor, which I speculate attenuated the magnitude of the calculated disparity in life expectancy between the two groups.

To put such increased life expectancy in perspective: curing/eliminating all cancers would increase US life expectancy (from birth) by 3.2 years [191].

In humans, the variation in resting body temperature [158, 168-174], which correlates with the variation in life expectancy [158, 170-172], might be due (at least in part) to variation in F_1F_0 ATP hydrolysis (due to variation in IF1 protein activity, per the amount of ATP synthase). The lower body temperature of humans undergoing calorie restriction [179-181] might be due (at least in part) to less F_1F_0 ATP hydrolysis (due to greater IF1 protein activity, per the amount of ATP synthase).

<u>Alzheimer's disease increases body temperature, which accelerates/exacerbates its pathology</u>

In a mouse model of Alzheimer's disease (AD), raising body temperature (by 0.50–0.79°C) results in enhanced BACE1 expression, more amyloid beta (Aβ) generation, greater Aβ plaque area, greater amount and hyperphosphorylation of tau, and worse memory (in a maze task. "Our study highlights an impact of high body temperature on the progression of AD pathologies, providing a mechanistic insight for its prevention") [192]. From early in disease progression, mice of a mouse model of Alzheimer's have greater mean body temperature than control mice (0.2-0.4°C more, statistically significant), which cannot be lowered by ibuprofen (an antipyretic) administration [193]. Body temperature is increased (at statistical significance), by around 0.1°C, in people with Alzheimer's disease (from a meta-analysis,

summarizing six independent studies, with a total of 90 Alzheimer's patients and 78 healthy controls [194]). Perhaps (at least in part) because of thermogenesis by Aβ aggregation [195]. Where, *in vitro*, greater temperature promotes greater Aβ production [196] and greater Aβ aggregation [195, 197-200]. Thence positive feedback is possible: Aβ aggregation generates heat, driving more Aβ aggregation, which generates more heat, in a runaway loop. Systemic administration of a selective F_1F_0 ATP hydrolysis inhibiting drug (*that doesn't inhibit F_1F_0 ATP synthesis*), which (*if ambient temperature is sufficiently low, e.g. at typical room temperature: ~20°C [201]*) dose-dependently lowers body temperature, might interdict this runaway pathology (e.g., the drug of Figure 2 herein). Returning body temperature to within the normal range, optionally to the low end of this range, or even lower. This should reduce Aβ production and aggregation. Conferring the benefit that it is likely to simultaneously slow all the steps up to Aβ plaque formation, for all the different lengths of Aβ peptides, inside and outside cells.

Particularly, this drug should reduce ROS generation, as per the teaching of Figure 5 herein. Note that Aβ monomers are antioxidants and might be produced in such pathological, aggregating quantities in response to high [ROS] [202-211]. Their amount dictated by the amount of BACE1 [212-217], whose gene promoter senses [ROS] [212]. But when the Aβ concentration gets too high, Aβ aggregates and thereby some report [203] it becomes pro-oxidising. ROS might be the cause of Alzheimer's disease [213, 218-246]. Which might be why drugs operating to the "amyloid hypothesis" [247-249] have underwhelmed to date, because they are merely acting upon a response to the cause, which may even be attenuating to the cause, at least at lower response levels. [ROS] in the body increases with age [53-55]. Much data suggests that oxidative damage could be an early, arguably the earliest, event in Alzheimer's disease [250-271]. In mice models of Alzheimer's disease, interventional decrease of oxidative stress decreases BACE1 expression and activity, decreases the amount of Aβ and plaques thereof, decreases tau amount and phosphorylation, decreases neurofibrillary tangles, improves memory, and increases lifespan [272-275]. Whereas interventional increase of oxidative stress increases the amount of Aβ and plaques thereof, increases tau phosphorylation, and accelerates the behavioural pathology [272, 276-282]. Two different antioxidants, one of them being Vitamin E (locates to cell membranes), were each separately shown to modestly slow the decline in performance of activities of daily living and the need for care, but not the decline in cognitive test scoring, in human Alzheimer's patients in a double-blind, placebo controlled, randomized, multicentre clinical

trial [282]. Mice studies indicate that the result might have been better if this clinical trial had utilized patients earlier in the course of the disease [281]. Human epidemiological studies show dietary and/or supplemental antioxidants decrease the risk of Alzheimer's disease [282-284]. The flawed approach of ROS mitigation (antioxidants) was contrasted with the merit of decreasing ROS generation (by selective F_1F_0 ATP hydrolysis inhibition, Figure 5) earlier herein.

A selective F_1F_0 ATP hydrolysis inhibiting drug (*that doesn't inhibit F_1F_0 ATP synthesis*) is anticipated to slow aging, as it can (*if ambient temperature is sufficiently low, e.g. at typical room temperature: ~20°C [201]*) dose-dependently lower body temperature (Figure 2) and slightly lower body temperature corresponds with a much longer lifespan in mice [75] and humans [158, 170-172] (and a much longer healthspan in humans [173-174]). Which is relevant here if Alzheimer's disease correlates with age/aging because aging is a causal drive of it. For clinical trialling, a simple, quick clinical endpoint can be used. Assaying whether this drug can reduce the pathologically high body temperature of Alzheimer's disease [194] to normality. If it can, this should be sufficient for clinical approval, for helping patients with Alzheimer's disease (especially because data suggests that higher body temperature accelerates Alzheimer's disease progression [192]). Optionally screening a population of Alzheimer's patients and (by setting the inclusion/exclusion criteria as such) only admitting those with the highest body temperatures into the clinical trial.

Aducanumab is a human monoclonal antibody drug that binds aggregated Aβ. Weekly, intraperitoneal (i.p.) administration of (a murinized analogue of) aducanumab to Tg2576 mice (a mouse model of Alzheimer's), starting at 9.5 months old, assessed at 15.5 months old, at the highest dose tested (30 mg/kg), reduced Aβ plaque amount in the cortex and hippocampus by up to 63% (Figure 4c-d in [286]. When instead starting drug administration at 18 months old, assessed at 24 months old, there was failure to reduce Aβ plaque amount [287]). To contrast, in mice of the same mouse model of Alzheimer's (Tg2576, starting at 4 months old, assessed at 17 months old), those with a body temperature of 0.50–0.79°C (*middle of this range is 0.65°C, which is less than the variation in resting body temperature across different humans [158, 168]*) lower had up to 50% less Aβ plaque amount in their cortex and hippocampus (Figure 3a in [192]). Distinctly, whilst there is no published data showing that aducanumab can improve cognition in a mouse model of Alzheimer's disease, there is such data for a slightly lower body temperature, showing that it confers better memory [192]. So,

at least in mice, slightly lower body temperature nearly decreases Aβ plaque amount by as much as 30 mg/kg i.p. aducanumab. Less Aβ plaque amount (measured by PET imaging) is a surrogate endpoint for "accelerated approval" for Alzheimer's disease by the United States Food and Drug Administration (FDA) [288]. As conferred upon aducanumab, which is now on the US market, with the caveat that a further "post-marketing" (Phase IV) trial be conducted to get further data for it, especially pertaining to efficacy against cognitive decline [289-291]. If this isn't positive, its clinical approval will be rescinded. In two Phase III trials to date, restricting entry to patients early in the course of the disease (but that do have Aβ plaque burden observed by PET imaging), although aducanumab certainly reduced Aβ plaque amount, whether it slowed cognitive decline (assayed by Clinical Dementia Rating scale Sum of Boxes, CDR-SB, scoring at 18 months) was equivocal in one of these trials.

Given the aforementioned implication of ROS in Alzheimer's disease, a good surrogate endpoint (that could be proposed to the FDA for their "accelerated approval" pathway) would be to test if a candidate drug can decrease ROS generation in the body. Assayed by less exhalation of ethane and/or pentane (lipid peroxidation products [78-91]). And/or assayed, probably more accurately, by less of one or more F2-Isoprostane species (lipid peroxidation products [55, 92-97]) in one or more bodily fluids, such as plasma, urine, or cerebrospinal fluid (CSF). These molecular species are actually elevated in Alzheimer's disease patients as compared to control subjects [292-293], correlating with disease severity [294]. They're also elevated in patients with Mild Cognitive Impairment (MCI), which is prodromal to Alzheimer's disease, as compared to control subjects [271]. My interpretation (of the data in hand to date) is that decreasing Aβ plaque area, as aducanumab does, is acting upon a downstream effect, whilst reducing ROS is to intervene at the upstream cause of the disease. Where Alzheimer's is caused, as aging is caused, by ROS. Indeed, arguably Alzheimer's *is* aging. Subclinical in many elderly people, who ultimately succumb to another facet of an aging body.

In two different mouse models of Alzheimer's disease, calorie restriction reduces Aβ plaque number and size [295]. Perhaps (at least in part) because calorie restriction can decrease body temperature [177-181]. However, calorie restriction is arguably dangerous in Alzheimer's patients because of the following. Some Alzheimer's disease patients, despite such patients tending to have equivalent or more/hyperphagic food intake [296-300], tend to lose body weight [296-298, 301-311] (*incidentally, such weight loss was first reported by Alois*

Alzheimer himself), an increasing amount as their disease progresses, wherein those Alzheimer's patients that instead maintain or gain body weight have lower mortality [310-311] (perhaps relatedly, multiple mouse models of Alzheimer's disease exibit hypermetabolism [312-315] and at least one of these models has an elevated body temperature [193]). Transgenic mice with less metabolic heat generation, and so slightly lower body temperature, have higher body weight (with the same food consumption as control mice) [75]. Presumably because of greater metabolic efficiency, with less of the chemical energy of food dissipated as heat. A selective F_1F_0 ATP hydrolysis inhibiting drug (*that doesn't inhibit F_1F_0 ATP synthesis*) increases metabolic efficiency, decreasing the fraction of food energy dissipated as heat (Figure 2), which is expected to counteract weight loss. Counteracting (e.g. slowing of) weight loss is a very objective, tractable clinical trial endpoint/surrogate endpoint.

There is presently no proven treatment for Alzheimer's disease ("for disease-modifying therapies (DMTs), the failure rate has been 100%" [316]). A huge unmet medical need. The number of people with the disease is increasing every year as populations age [317]. Its financial burden to the USA alone, which was $259 billion per year in 2019, is projected to exceed $1 trillion per year by 2050 [316] ($9.1 trillion per year worldwide [318]). "Alzheimer's disease poses a grave and growing challenge to our Nation" [319]. An efficacious drug for Alzheimer's could become the best-selling drug (by sales revenue) on the market. Exceeding the present leader, Humira (for rheumatoid arthritis), which had $20.4B of sales in 2020 alone [320]. Because, for one reason, the market size for Alzheimer's disease is a multiple of that for rheumatoid arthritis, probably a double-digit multiple [319, 321].

To summarize: Alzheimer's patients can have higher body temperature [194], where higher body temperature has been shown to accelerate/exacerbate the disease in a mouse model of Alzheimer's (e.g., causing greater Aβ plaque area and worse memory) [192]. A selective F_1F_0 ATP hydrolysis inhibiting drug (*that doesn't inhibit F_1F_0 ATP synthesis*) can (*if ambient temperature is sufficiently low, e.g. at typical room temperature: ~20°C [201]*) dose-dependently lower body temperature (shown in mice, Figure 2) and thereby is expected to delay/slow/combat Alzheimer's disease. Moreover, Alzheimer's disease correlates with age/aging, probably because aging is causal to it, and slightly lower body temperature corresponds with much slower aging in mice and humans [75, 158, 170-174]. Furthermore, many papers, and much data, suggests that ROS are causal to Alzheimer's disease [52-54,

202-246, 250-270, 272-285]. And selective inhibition of F_1F_0 ATP hydrolysis (*without F_1F_0 ATP synthesis inhibition*) decreases ROS generation (Figure 5).

Interim summary: Possibly a single drug for many diseases

Resting body temperature varies across different people in a 2.5°C range, from 35.2 to 37.7°C [158, 168]. Wherein people with lower resting body temperature have a longer healthspan [173-174] and lifespan [158, 170-172]. Making the mean body temperature of mice 0.34°C less increases their median lifespan by 20% [75]. People with Alzheimer's have a higher body temperature [194], which accelerates/exacerbates the disease [192]. A selective F_1F_0 ATP hydrolysis inhibitor drug (*that doesn't inhibit F_1F_0 ATP synthesis*) can (*if ambient temperature is sufficiently low, e.g. at typical room temperature: ~20°C [201]*) dose-dependently lower body temperature (in mice in Figure 2). Therefore this drug might slow aging. And thereby simultaneously delay/slow/avert/ameliorate/treat ***all*** age-related diseases (assuming they correlate with age/aging because aging is causal to them). Such as Alzheimer's disease. Economists calculate that slowing aging is worth $38T for each year of increased US life expectancy [186]. Slight decrease of body temperature is known to be safe because it occurs during calorie restriction [177-181] (which extends lifespan [175-176]). Moreover, as shown and explained herein, selective F_1F_0 ATP hydrolysis inhibiting drugs (*that don't inhibit F_1F_0 ATP synthesis*) have anticancer activity. Rectifying the body temperature of Alzheimer's patients to normality could be the endpoint, or the surrogate endpoint (for the "accelerated approval" pathway [288]), of such a drug's clinical trial(s) for FDA approval. If approved, this drug might generate more revenue than any before. For example, more than Humira (a drug for rheumatoid arthritis), which has revenue of >$20B per year [320].

Lower specific metabolic rate extends the lifespan of mice

The longer median lifespan of the transgenic mice of [75-76] could be because of their lower metabolic heat generation (lower specific metabolic rate) and/or their lower mean body temperature. I suggest it is because of both. And I try to delineate their relative contributions now. Using the transgenic female mice data (*sourced from the supplementary information of [75]. Assuming the wild-type mean body temperature is 37°C [1]*), the Q_{10} temperature coefficient [322-323] for their lower mean body temperature (0.34°C lower) and longer median lifespan (+20%) is $(R_2/R_1)^{(10/\{T_2-T_1\})} = (550/662)^{(10/(37-(37-0.34)))} = 0.00429033474$. A fraction because higher temperature decreases (rather than increases) the temperature-

dependent variable, median lifespan. If the Q_{10} equation is modified to instead make Q_{10} >1 in this case: $(662/550)^{(10/(37-(37-0.34)))} = 233.08204613$ (for a temperature range of 36.66-37°C). For ectotherms (which don't have metabolic heat generation), the Q_{10} value for ambient temperature (which sets their body temperature) and mean lifespan is, using the afore-used modification of the Q_{10} equation, 2 (for fruit fly *Drosophila melanogaster*, for a temperature range of 9-34°C) [163], or 2.25 (for blowfly *Calliphora stygia*, for a temperature range of 12-34°C) [164]: mean = 2.125. I *assume* what is observed in ectotherms teaches us the order of magnitude of a lifespan effect due to modified temperature alone. And so the remainder (overwhelming majority. 100-((2.125/233.08204613)*100) = 99.09%. *Actually more because of the different temperature ranges of the Q_{10} values, wherein Q_{10} is less with higher temperature ranges*) of the lifespan extension with the transgenic mice in [75] is due to less metabolic heat generation (lower specific metabolic rate). And so is not conditional upon any body temperature drop. It can cause lower body temperature, but presumably only if the ambient temperature is conducive to that. To remind, a selective F_1F_0 ATP hydrolysis inhibitor drug (*that doesn't inhibit F_1F_0 ATP synthesis*) decreases specific metabolic rate in mice (Figure 2).

Humans with lower specific basal metabolic rate have a longer lifespan

In the Baltimore Longitudinal Study of Aging, people with lower specific basal metabolic rate at entry to the study had *significantly* lower mortality over the subsequent >40 years of monitoring [106]. Above a specific basal metabolic rate (BMR) of 36.4 kcal/m^2/h at study entry, "the risk of death increased significantly as a squared function of BMR" [106]. The transform of [324] can convert a standardized mortality ratio difference into a corresponding difference in life expectancy ("a 1% decrease (or increase) in the standardized mortality ratio (SMR) will result in 0.1373 years increased (or decreased) life expectancy based on white male data for the US population"). Using this transform with data (already adjusted/controlled for age and various other risk factors) from Figure 2 of [106], humans with a specific basal metabolic rate in the range of 31.3-33.9 kcal/m^2/h have 3.90 and >7.32 years (e.g., 13.28 years) greater life expectancies than those with higher specific basal metabolic rates in the range of 33.9-36.4 kcal/m^2/h (*i.e. 7.82% more*) and >36.4 kcal/m^2/h (*i.e. >11.66% more*) respectively.

Consistent with this intra-species (human) data, there is inter-species data: across species studied, there is a *significant* correlation between lower specific basal metabolic rate and

greater maximal lifespan (Figure 3. And next Discussion section). Interventional evidence, that lifespan is inversely proportional to specific basal metabolic rate, is that calorie restriction slows metabolic rate (beyond the effect of weight loss. Decreasing oxidative damage) in humans [325-326], wherein calorie restriction can extend lifespan in rodents and primates [175-176] (*no study has yet explored the effect, if any, of calorie restriction upon human lifespan*).

Why do different species age at different rates, and have different maximal lifespans?

Mammals (and birds) are endothermic and metabolically generate heat to maintain their body temperature. In Euclidean geometry, smaller objects have a larger surface-area (A) to volume (V) ratio than larger objects. Because, where L is length, $A \propto L^2$ and $V \propto L^3$ ("square-cube law"). So, smaller mammal species have a larger surface-area-to-volume ratio. And so, they lose a greater fraction of their metabolically generated heat. Thus they must produce more heat per unit mass, requiring them to have a greater metabolic rate per unit mass (serviced by a greater heart rate). Therefore, generating more ROS per unit mass, per unit time. Accumulating (ROS caused) molecular damage faster. (*Possibly*) explaining why smaller mammal species tend to age faster, and have shorter maximal lifespans.

How is the metabolic rate per unit mass of different sized mammal species set differently (which {*possibly*} in turn sets their different aging rates)? By the 2nd law of thermodynamics, whenever energy converts from one form to another, some of this energy must be dissipated as heat (no energy conversion can be 100% efficient). I've discovered that mammals cyclically synthesize and hydrolyse ATP (F_1F_0 ATP synthesis and F_1F_0 ATP hydrolysis respectively). Conditional upon passing, and pumping, protons along their concentration gradient across the inner mitochondrial membrane, respectively. So, cyclically interconverting between chemical and potential energies. Which (by the inefficiency of energy conversions) generates heat to maintain body temperature. Energy from food sustains this cycle. F_1F_0 ATP synthesis exceeds F_1F_0 ATP hydrolysis, conferring net ATP production. Because ATP is consumed by cellular ATP demand (denying it to F_1F_0 ATP hydrolysis), and because IF1 protein only inhibits F_1F_0 ATP hydrolysis. Wherein the amount of F_1F_0 ATP hydrolysis (amount of heat generated) is constrained by the amount of IF1 protein activity. Per unit mass, smaller (shorter lifespan) species run this "futile" (merely heat-generating) cycle more than large (longer lifespan) species (Figure 3). Because they have less specific IF1

protein activity (data in the Methods section). Suggesting that IF1 protein activity is a molecular determinant of lifespan.

This futile cycle also generates heat by its increase of proton leak across the inner mitochondrial membrane. By it pumping protons into the mitochondrial intermembrane space. Increasing the chance that protons cross the inner mitochondrial membrane, into the mitochondrial matrix, outside of ATP synthase. Dissipating their potential energy as heat.

Evidence for this novel account is the mouse data of Figure 2. Showing that F_1F_0 ATP hydrolysis is a causal input into metabolic heat generation and so metabolic rate (less F_1F_0 ATP hydrolysis, lower metabolic rate). Further mouse data shows that F_1F_0 ATP hydrolysis is a causal input into Reactive Oxygen Species (ROS) generation (less F_1F_0 ATP hydrolysis, lower ROS generation, Figure 5). And other data herein shows a *significant* correlation, across species studied, between less specific F_1F_0 ATP hydrolysis *in vitro* and lower specific basal metabolic rate *in vivo*. Moreover, across species studied, a *significant* correlation is shown between less specific F_1F_0 ATP hydrolysis *in vitro* and less mitochondrial ROS detected *in vitro*. And to less damage. To nuclear DNA, mitochondrial DNA (mtDNA), proteins (by inference), epigenetic information, and to cellular/membrane lipids. Furthermore, there is a *significant* correlation shown, across species studied, between less specific F_1F_0 ATP hydrolysis *in vitro* and greater maximal lifespan. Wherein performed mediation analysis suggests that less specific F_1F_0 ATP hydrolysis dictates longer maximal lifespan, via dictating lower specific basal metabolic rate. Interventional (mouse) experiments indicate causality between less F_1F_0 ATP hydrolysis and less metabolic heat generation (lower metabolic rate), and causality between less metabolic heat generation (lower metabolic rate) and longer lifespan. Across species studied, specific F_1F_0 ATP hydrolysis *in vitro* is shown to be inversely correlated with specific IF1 protein activity *in vitro,* where the latter positively correlates with maximal lifespan.

Hereby possibly explaining (at least partially) why different mammal species have different maximal lifespans. Thereby potentially teaching a mechanism, and compounds, to slow aging.

<u>In essence</u>

My interpretation of the data herein is that (at least partially) the basis to different maximal lifespans, in different mammal species, is different specific F_1F_0 ATP hydrolysis rates. Set by different specific IF1 protein activities. So, IF1 protein activity is a molecular determinant of maximum lifespan.

This interpretation makes experimentally testable predictions.

Predicted

Depending on the dose and ambient temperature, a systemically administered selective F_1F_0 ATP hydrolysis inhibitor drug (*that doesn't inhibit F_1F_0 ATP synthesis*) can slow aging in a subject in two possible ways: (*a*) by decreasing F_1F_0 ATP hydrolysis (and thereby decreasing specific basal metabolic rate and ROS generation), (*b*) by slightly decreasing body temperature (and thereby decreasing the rate of ROS generation and ROS-conferred damage [which, as chemical reactions, are temperature dependent]). (*a*) can occur in the absence of (*b*) (Figure 14). Or they can occur together, with (*a*) causing (*b*). That (*a*) can occur without (*b*) means a very high drug dose (conferring *much* slower aging) can be safely administered. Where higher ambient temperature permits more of (*a*) without (*b*). When ambient ≥ body temperature, (a) can be maximal and (*b*) cannot occur. An ambient temperature slightly below normal body temperature enables the maximum of (*a*), yet still with (*b*). If ambient is at typical room temperature (~20°C [201]) then only a relatively small drug dose is permissible, sub-optimally slowing aging by a relatively small amount of (*a*), and by (*b*) atop. Although, to *speculate*, if a high drug dose is used at typical room temperature it might actually be safe, just the large body temperature drop (to not much above room temperature) will put the subject into a torpor/hibernation (until enough of the drug clears from the body), which has applications. Continual, intravenous infusion of drug could maintain the subject in this state for an extended period. During which there would be *considerably* slower aging. And even slower aging if the ambient temperature was lower (although, given that mammals are mostly water, its freezing temperature of 0°C might be a lower limit). Indeed, hibernating species tend to have longer maximal lifespans [327-331]. This torpor/hibernation might be terminated by gradually raising the ambient temperature (and then re-entered by gradually lowering it again if enough drug is still in the body, toggled between states by ambient temperature, which might be useful for spaceflight [332]). To *speculate* further, this same mechanism may actually be a drive to torpor and/or hibernation in species that do one or both, they entering

such a state by (at least in part) upregulating activity of the aforementioned natural selective F_1F_0 ATP hydrolysis inhibitor: IF1 protein.

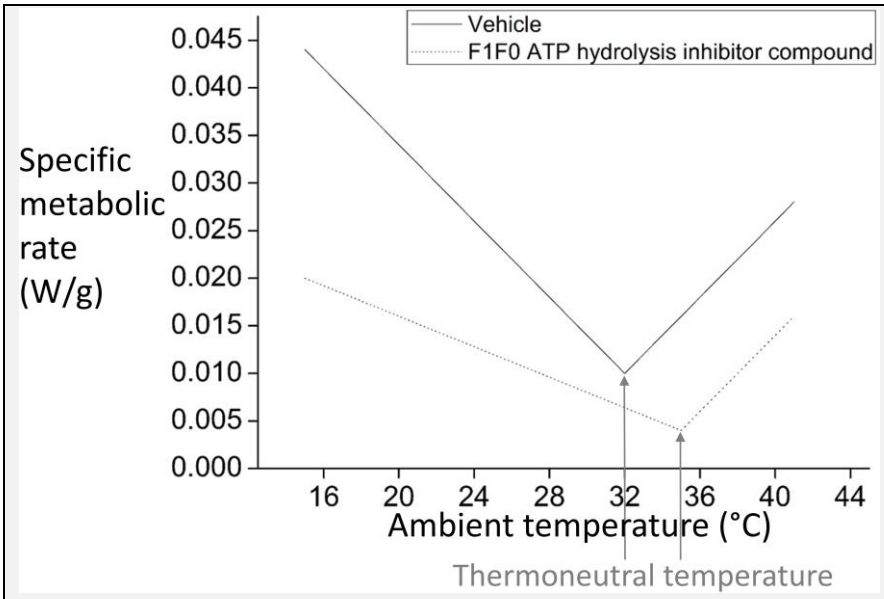

Figure 14 – Diagram: Why systemic administration of a selective F_1F_0 ATP hydrolysis inhibitor drug (*that doesn't inhibit F_1F_0 ATP synthesis*) doesn't necessarily reduce body temperature. This diagram relates to a mouse. Mice have a natural body temperature of 37°C [1]. "Thermoneutral temperature" is the ambient temperature that the body is most comfortable at (*at which specific metabolic rate is the "specific basal metabolic rate"*). Above and below which, greater metabolic rate is required to maintain the body at 37°C [333]. At the mouse's natural thermoneutral temperature of 32°C, its specific basal metabolic rate is 0.0092125 W/g [334] (*N.B. human thermoneutral temperature is less because humans are bigger, and moreover wear clothes. Thermoneutral temperature of a human in typical clothes is 20.3°C [335]*). Systemic administration of a selective F_1F_0 ATP hydrolysis inhibitor drug (*that doesn't inhibit F_1F_0 ATP synthesis*) reduces the mouse's specific basal metabolic rate and shifts its thermoneutral temperature higher. Illustratively to 35°C in this figure. Which makes the mouse more comfortable (lower metabolic rate) at equal or higher ambient temperatures. Furthermore, this figure anticipates that F_1F_0 ATP hydrolysis is integral to thermogenic metabolic rate, in addition to basal metabolic rate. And so the gradient of the thermogenic metabolic rate increase is shallower, because of reduced F_1F_0 ATP hydrolysis. The specific basal metabolic rate at thermoneutral temperature = 35°C was selected by drawing a line from the specific basal metabolic rate at thermoneutral temperature = 32°C, =

0.0092125 W/g, which is an experimental data point from [334], to 37°C on the x-axis (thermoneutral temperature = 37°C, specific basal metabolic rate = 0 W/g) and selecting the corresponding specific basal metabolic rate for 35°C on this line (the equation of this line is y=a+bx=0.06817+-0.00184*x). Accordingly, the specific basal metabolic rate was 60% lower. And, in concordance, the gradient of the thermogenic plot was reduced by 60% also. Anticipating that F_1F_0 ATP hydrolysis contributes equally to basal and thermogenic metabolic rates. Although it probably contributes more to the thermogenic than basal metabolic rate, in which case the ascending thermogenic metabolic gradient should be shallower. Regardless, this diagram is here to show that decreased metabolic heat generation, by drug-conferred selective F_1F_0 ATP hydrolysis inhibition, increases the thermoneutral temperature. Which does *not* cause body temperature drop unless the drug dose and ambient temperature are such that the updated thermoneutral temperature exceeds the ambient temperature. In which case, because of the shallower thermogenic gradient, mouse body temperature falls towards (but never less than) the ambient temperature. So, if for example the ambient temperature is 36°C, if the administered drug dose increases the thermoneutral temperature (from 32°C) to 35°C then there is ***no*** body temperature drop and the mouse is made more thermocomfortable at this ambient temperature. But if the ambient temperature is still 36°C, and a greater drug dose increases the thermoneutral temperature to 36.5°C then there *is* a body temperature drop. Its magnitude being a function of thermoneutral minus ambient temperature. No matter the drug dose, thermoneutral temperature can never be made equal or greater than 37°C (because equal and greater would mean a specific basal metabolic rate of zero and negative respectively). Remember that body temperature drop can only occur when the thermoneutral exceeds the ambient temperature, wherein the thermoneutral temperature can't be equal or greater than 37°C, and so if the ambient temperature is equal or greater than 37°C, no body temperature drop can occur, no matter how great the administered drug dose.

Metabolism gives life but causes damage/aging that ultimately takes it away. A lower metabolic rate confers a longer lifespan (*maximal lifespan is inversely proportional to specific basal metabolic rate, across a set of species, in data herein. Humans with greater specific basal metabolic rate have increased mortality [106]*). In humans, much of the metabolic rate is to keep body temperature at around 37°C. F_1F_0 ATP hydrolysis is the principal reaction for metabolic heat generation. It makes a human (in typical clothes) most comfortable at an ambient temperature of around 20.3°C. But in a hot climate/season, not as

much metabolic heat generation is needed (none if the ambient temperature is ≥37°C). And the excess makes the person feel hot and uncomfortable. Solvable by taking a selective F_1F_0 ATP hydrolysis inhibiting drug (*which doesn't inhibit F_1F_0 ATP synthesis*). That reduces metabolic heat generation (*how much scales with drug dose; shown in mice, Figure 2*). And that slows aging (*prediction*).

Reduced metabolic heat production is desirable in many hotter parts of the world. Because it increases the ambient temperature that the body is most comfortable at. Its "thermoneutral temperature". Above and below which, greater metabolic rate is required to maintain the body at 37°C (Figure 14). An awake, typically clothed human is most comfortable at an ambient temperature of around 20.3°C [335] (this is their thermoneutral temperature). But much of the world is hotter than that (for at least part of the year). Administering a selective F_1F_0 ATP hydrolysis inhibitor drug (*that doesn't inhibit F_1F_0 ATP synthesis*), by decreasing metabolic heat generation, increases their thermoneutral temperature, the dose dictating by how much more (and the drug pharmacokinetics dictating for how long). For example, a drug dose can increase the thermoneutral temperature (of someone in typical clothes) to 23°C, a higher dose to 27°C, an even higher dose to 32°C, etc. Thereby it can increase thermal comfort in hot climates/seasons/rooms (i.e. upon much of the globe. Whilst simultaneously slowing aging). For example, anywhere (at not too high altitude) near to the equator, which is hot all year round (43% of the world's population [3.8 billion people] live in the tropics [336]). Or in seasonally hot climates, e.g. in summer the temperature in Riyadh (Saudi Arabia) is in the thirties and forties of °C.

The ambient temperature to the subject, and/or their bodily insulation (e.g. clothing), only needs to be conducive to the drug dose when they have an effective amount of drug in their system. Which, optionally, can be timed to be only/predominantly at night, whilst they sleep (while sheltered in a, optionally heated, building/room, and/or under a blanket{s}). Taking the drug before sleep and, if its pharmacokinetics permits, it totally or fractionally clearing from the body by morning.

The drug's dose can be modified/paused depending on the subject's location (and its season/weather), shelter and clothing. A subject from a cold place may relocate to a hotter place (e.g. to a different country), to live or just for a period(s), to enable them to regularly take a higher dose of this drug. Perhaps in retirement. Perhaps when suffering from cancer

and/or another age-related disease(s), favouring relocation rather than a heated home/hospital ward.

Two predicted applications

[1] ***Systemically*** administer a selective F_1F_0 ATP hydrolysis inhibitor compound (*that doesn't inhibit F_1F_0 ATP synthesis*), to slow aging in the entirety of the body, wherein the subject's ambient temperature and/or bodily insulation (e.g. more clothing) offsets their decrease in metabolic heat generation (the decrease of which scales with the drug dose). If this offset/compensation is incomplete or absent, and so there is a slight/safe body temperature drop, this is permissible and perhaps even desirable (slightly lower body temperature corresponds with a much longer lifespan in mice [75] and humans [158, 170-172], and a much longer healthspan in humans [173-174]).

[2] ***Locally*** administer a F_1F_0 ATP hydrolysis inhibitor compound (*that doesn't inhibit F_1F_0 ATP synthesis*), to slow aging in just part(s) of the body, but wherein there are no thermoregulatory issues to be concerned with. Because of heat transfer, especially via blood flow, from other body regions. That maintains this body part(s) at ~37°C. Local inhibition of F_1F_0 ATP hydrolysis has proven safe in mice (refer to Results section titled "Local inhibition of F_1F_0 ATP hydrolysis").

For example, *local* administration to skin of the human face (e.g. around the eyes; e.g. via a cosmetic cream). For example, of a functional human IF1 protein fragment (e.g. its residues 42-58 [337-340]). Concatenated, to its N-terminal end, is a Mitochondrial Import Sequence (MIS), as used by the complete IF1 protein. And concatenated, to its N-terminal end, is a Cell Penetrating Peptide (CPP) sequence. Once inside the cell, endogenous protein machinery in the mitochondrial matrix cleaves off the MIS (and inherently the {more N-terminal} CPP sequence with it). A string of seven arginine residues is a very effective CPP sequence [341]. Wherein this is an amino acid sequence that occurs naturally within the human body. In a number of different proteins findable by a BLAST [342] search. So, this candidate cosmetic agent, taught by my international (PCT) patent application [343], is a concatenation of amino acid sequences that naturally occur within the human body. Many cosmetics, especially the premium brands, contain amino acid sequences (peptides) these days.

A model

The rate of damage caused by Reactive Oxygen Species (ROS) is a linear function of [ROS]. Whilst the repair/replacement of ROS damage is done by enzymes and so its rate is a Michaelis–Menten function of [ROS] [344-345]. So, with less [ROS] there is less damage *and* repair/replacement. But given their different gradients, there is a *net* reduction in damage. If [ROS] is decreased enough, and the amount of repair/replacement enzyme(s) is sufficient, then the rate of repair/replacement of ROS damage can exceed the rate of ROS damage, which means prior ROS damage (*assuming* it can still be recognized as damage) can get repaired/replaced. In this case, the rate of ROS damage doesn't just slow, but is reversed. Illustrated, for the case of DNA damage in Figure 15. But equally applicable to other forms of ROS damage. Such as (hypothesized herein) ROS-driven "ticking" of the epigenetic clock. In experiment, selectively inhibiting F_1F_0 ATP hydrolysis (*without inhibition of F_1F_0 ATP synthesis*) very substantially decreases [ROS] (Figure 5). A drug that reverses, rather than just slows, damage only has to be administered intermittently.

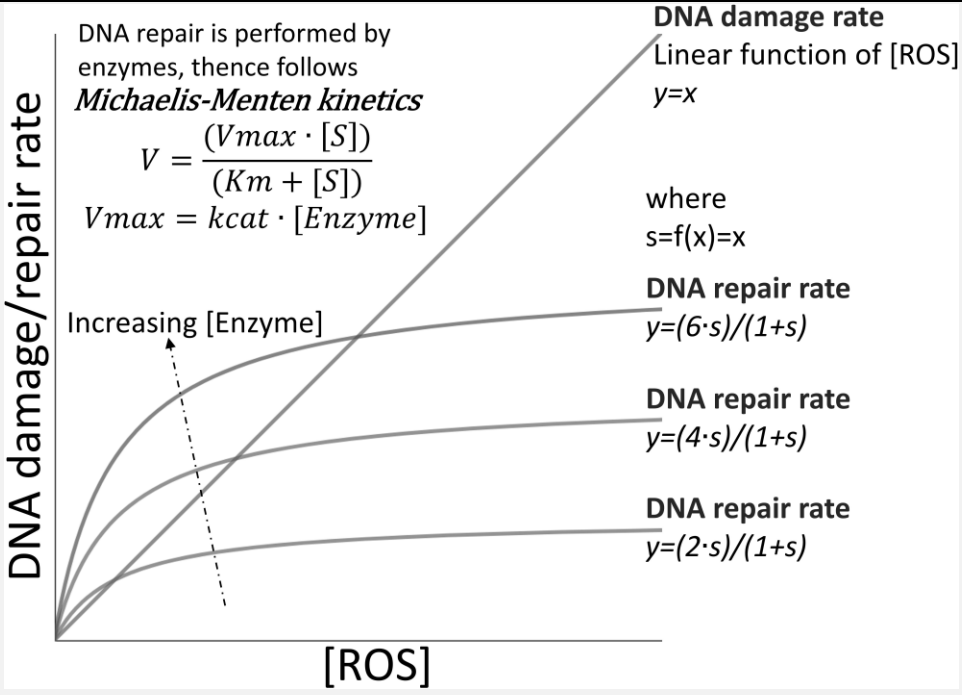

Figure 15 - Diagram: With less [ROS], there is less DNA damage *and* repair, but given their different gradients, there is a *net* reduction in DNA damage. If [ROS] falls further, DNA repair can exceed DNA damage, *if* there is excess DNA damage from a prior time when DNA damage exceeded DNA repair (*if* this DNA damage can still be recognized as damage by the DNA repair system), and *if* [Enzyme] is sufficient.

In the figure's definition of s, f(x) is approximated to x, such that s=x. But a more faithful simulacrum is provided in the Methods section. Where s=x+z, wherein x is [ROS] (=DNA damage it causes, because plot of DNA damage, y, is y=x) and z is any accumulated DNA damage due to the balance of past DNA damage and repair due to any past [ROS].

"Increasing [Enzyme]" in the figure, at least alone, is a constrained approach because (typically) when something is being repaired its use is prevented/impaired. A better approach is less [ROS], and so less ROS damage in the first place. In this DNA case, more repair would require more repair enzymes "sliding" (1D instead of 3D diffusion [346-347]) along the DNA looking for damage, further disrupting gene transcription. More repair requires more ATP energy, which can mean (via more oxidative phosphorylation) more ROS generation and damage, requiring more repair.

Conceivably, slight body temperature drop can assist repair/replacement vs. damage. Because repair/replacement is, and damage isn't, enzyme catalysed. Wherein enzymes follow macromolecular rate theory (MMRT), which can have (near their optimum temperature, T_{opt}) a shallower gradient of reaction rate decline with declining temperature [348-351], e.g. refer to Figure 1B in [351].

If possible, leveraging the body's own breadth of repair/replacement mechanisms, as hypothesized above, is probably easier than us trying to execute repair/replacement, for all the many different types of molecular damage (that characterize/are aging), in parallel, *de novo*.

Historical odds of progressing into clinical trials

The compound used to produce Figure 2 has therein shown efficacy in mice. For seeking FDA approval, its next step is testing in "Non-clinical toxicology" studies (also called "IND-enabling studies") in two mammalian species, one of which must be a non-rodent. For example, rat and dog. If passing those it can proceed into human clinical trials. It is interesting to look at historical data to see how often drug candidates succeed in passing this Non-clinical toxicology step, to make it into human clinic trialling. Analysing the pooled small-molecule pipelines of four pharmaceutical companies, over ten years, looking at pre-clinical compounds nominated for further pursuit [352]: for 386 compounds that made it into the clinic, 211 compounds failed Non-clinical toxicology (legend of Figure 6 in [352]): 100-

((211/(211+386))*100) = 64.66% penetrance for this Non-clinical toxicology step. Some or all of the other 145 compounds that were dismissed pre-clinically, for a reason unrelated to Non-clinical toxicology (Figure 2c of [352]. *For example, 75 compounds were dismissed because of "rationalization of company portfolio", and 26 compounds were dismissed because of "commercial" reason*), might have passed Non-clinical toxicology beforehand. If we assume all of them did, then the success rate is instead: 100-((211/(211+386+145))*100) = 71.56%. 60 pre-clinical compounds are labelled "progressing" in Figure 1 of [352], which might mean that all these compounds had already passed Non-clinical toxicology, and so were ready to progress into the clinic, or that was only the case for zero or more and one or more others were still undergoing (or yet to undergo) Non-clinical toxicology. If we assume the former, then the success rate is instead: 100-((211/(211+386+145+60))*100) = 73.69%. Alternatively, more conservatively, these "progressing" pre-clinical compounds are dismissed (by assuming they have the same proportional outcomes as the other pre-clinical compounds). In which case the historical penetrance for Non-clinical toxicology (IND-enabling studies) into the clinic is somewhere in the range 64.66-71.56%. Splitting the difference = 68.11% = 68%. The probability can be projected as higher still for this present compound (>68%) because if it is found to be only systemically toxic its use can be restricted to local administration, as Unity Biotechnology did with its "senolytic" drugs [353]. Such local administration is still anticipated to have much utility.

Clinical utility of local administration

There is a thesis that neurodegenerative diseases, such as Alzheimer's (which can cause dementia) and Parkinson's disease, correlate with aging because they are caused by aging. Indeed, caused by the oxidative stress of aging [213, 218-246]. "Mitochondrial dysfunction and oxidative stress occur early in all major neurodegenerative diseases, and there is strong evidence that this dysfunction has a causal role in disease pathogenesis" [229]. More broadly, many further diseases have an exponentially increased risk of incidence with age. And can be said to be diseases of aging. Many, if not all, diseases of aging might be caused by a body part(s) aging, and declining in function, faster than the rest of the body. So, such diseases might be prevented/ameliorated by locally slowing the aging of that body part(s). So that it better matches the aging rate of the rest of the body. Or is even slower. This can better match healthspan to lifespan. For example, dopamine neurons in the pars compacta, in the substantia nigra, decline in number by 5-10% per decade, presumably by dying, which is a predisposing drive to Parkinson's disease [354-356]. Extrapolating from (predicting upon) the data herein:

specifically reducing F_1F_0 ATP hydrolysis (*without reducing F_1F_0 ATP synthesis*) in these neurons will slow their aging rate. Where their resulting reduction in metabolic heat production will be offset by heat transfer from other cell types and body regions, especially via blood flow. Another postulated use case is topical administration of a selective F_1F_0 ATP hydrolysis inhibitor drug (*that doesn't inhibit F_1F_0 ATP synthesis*) to the eye(s), to avert/slow/combat Age-related Macular Degeneration (AMD). Wherein there is presently no treatment for dry AMD, which more than 150 million people have now. Its incidence is projected to increase to nearly 300 million people by 2040 [357].

Some further medical applications?

As taught herein (e.g., refer to the Results section titled "New experimental results", which encompasses Figure 2), a systemically administered selective F_1F_0 ATP hydrolysis inhibitor drug (*that doesn't inhibit F_1F_0 ATP synthesis*) can reduce body temperature to a value controlled by the intersection of drug dosage and ambient temperature. Even at maximum possible effect, the drug cannot make body temperature fall below, only towards/to, ambient temperature. So, at high (systemically administered) drug dose, body temperature can be controlled by controlling ambient temperature.

This might have many medical applications. For example, emergency grade hyp*er*thermia is an extremely dangerous aspect to many Emergency Room (ER) admissions, e.g. in some trauma patients. And there are many medical conditions in which the body can get too (dangerously) hot: e.g., fever, sepsis, malignant hyperthermia, neuroleptic malignant syndrome, hypermetabolism, etc. It may also enable controlled hyp*o*thermia for a medical/surgical/protective purpose (called "Targeted Temperature Management, TTM", "therapeutic hypothermia", or "protective hypothermia"), for which there are many applications: e.g., neuroprotection after a stroke, cardioprotection after a heart attack, deep hypothermic circulatory arrest for surgery (e.g. brain surgery, e.g. brain tumour removal), slowing adverse chemical reactions/bleeding/bacterial growth in the body after poisoning/injury (e.g. gun-shot wound), conferring longer than the "golden hour" to get an injured soldier to a field hospital, etc.

Addressing an anticipated objection: "But what about bats?"

At least some bat species have a much greater maximal lifespan than expected for their adult body mass [358]. For example, *Myotis brandtii* has a maximal lifespan of 41 years, despite only having a typical adult body mass of 7 g [1]. By contrast, using the applicable best fit line

equation of Figure 3 herein, an inputted body mass of 7 g predicts a maximal lifespan of 3.6 years. This discrepancy might be explained by the following. Bats, probably because they can fly and so can sleep in very safe places (e.g., hanging from the roof of caves), lower their metabolism to an atypically large extent during sleep. So much that their body temperature can fall to just above ambient temperature. Indeed, when the ambient temperature is low, at least some bat species cannot fly when they first wake up, having to metabolically generate heat to raise their body temperature first, which takes time (0.63°C per minute in greater, and slower than this in lesser, horseshoe bats) [359]. Quotes from [360]: "Bats tend to hibernate whenever they fall asleep, even in the middle of a summer night", "body temperature of bats drops considerably during this period of torporific sleep", "poikilothermic sleep", "in bats the daytime drop in metabolism was as much as 90 per cent" (bats sleep during the day, and for much of the night). When awake, which is just for 4 hours per 24 hours in some bat species [361], they are typically flying and inherently generating heat thereby. So bats are anomalous amongst mammals in that metabolic heat generation isn't as significant a component of their metabolic rate. A lower body temperature for most of the time, just above ambient temperature, doesn't require as great a specific metabolic rate to maintain, even with a small body mass. This feature then confers geography (e.g. latitude and altitude), setting the ambient temperature, as a determinant of what the bat's metabolic rate is for most of its lifespan, thence (I would argue) is a determinant of its lifespan. Some bat species hibernate (living longer thereby) [362], e.g. for up to 8 months of a year [363], tending to hibernate for longer in places with longer (typically inherently colder) winters [364]. Greater latitude is a predictor of longer maximal lifespan in both non-hibernating and, to a greater extent, in hibernating bat species (table 2 of [327]). The *Myotis brandtii* individual that died at 41 years old lived in Siberia [364]. Some tropical bat species, or only some individuals within such species, are poikilothermic [365], but are often mischaracterised in the literature as universally homeothermic. Moreover, as compared to *Blarina brevicauda* (short-tailed shrew) and *Peromyscus leucopus* (white-footed mouse), the respiratory chain of *Myotis lucifugus* (little brown bat) fumbles a lower percentage of the electrons it passages, producing fewer Reactive Oxygen Species (ROS) per unit of O_2 consumed [366].

<u>Addressing an anticipated objection: "But what about naked mole rats?"</u>

Naked mole rats have a much greater maximal lifespan (31 years) than expected for their typical adult body mass (35 g) [1]. Naked mole rats are anomalous amongst mammals in that metabolic heat generation isn't as significant a component of their metabolic rate. Firstly,

because their body temperature is atypically low for a mammal, at around 32°C [1]. Secondly, because they generate very little metabolic heat [367-369] and rely on the ambient temperature to maintain their body temperature. Which they can do because their ambient temperature (~30°C) is *stably* close to their body temperature (~32°C). Because they live underground in sealed burrows, hardly ever leaving these, eating underground tubers, in a hot equatorial East African climate. Underground is buffered from short colder periods above ground. For example, during storms. Moreover, it protects against rain, where getting wet is a thermoregulatory challenge, especially when combined with wind. So, to theorize, naked mole rats produce less metabolic heat, with a lower specific basal metabolic rate thereby, and live longer accordingly. And even longer still because of their low body temperature.

Their specific basal metabolic rate (*for mean body mass of 42.8 g, ambient temperature was in their thermoneutral zone {31-34°C}, O_2 consumption of 1 ml/g/h [367] = 0.00558333333 W/g using 1 ml O_2 = 20.1 Joules [333, 370]*) is atypically low for a mammal of their size. Much lower than the value predicted (*0.0083558914 W/g*) for an animal of 42.8 g body weight from the best fit line for specific basal metabolic rate vs. body mass of Figure 3 herein. *Data of [369] reports a specific metabolic rate value of 0.00307083333 W/g. But this isn't a basal value, because it was sourced at an ambient temperature of 30°C, and the lower temperature of the naked mole rat's thermoneutral zone is 31°C. The corresponding specific basal metabolic rate value, sourced at thermoneutrality, would be even lower.*

An interesting parallel is that systemic administration of a selective F_1F_0 ATP hydrolysis inhibiting drug (*that doesn't inhibit F_1F_0 ATP synthesis*), at high dose, confers the aforementioned naked mole rat profile: low endogenous heat generation, conferring reliance on exogenous heat (ambient temperature) to maintain body temperature. With lower specific basal metabolic rate, and (*predicted*) slower aging thereby. Unlike naked mole rats, humans don't live in *stably* hot burrows in equatorial East Africa, buffered from cold spells above. But humans have an option that naked mole rats don't: to increase their bodily insulation with clothes, which can be waterproof, where the capability of clothing shouldn't be underestimated (e.g., it permits people to live in Siberia, which is *extremely* cold in winter). Furthermore, humans in the tropics can pause their use of the drug (or reduce its dose) when a big/multiday, much colder temperature conferring, storm is predicted. And/or take shelter in a building(s).

Addressing an anticipated objection: "But what about marsupials?"

Some (especially smaller bodied) marsupial species seem to opt for life on a budget, with a lower body temperature [371] (e.g., 35°C in the North American opossum, *Didelphis virginiana* [1]), reducing their food demand and risk of starvation, but presumably increasing their risk of predation. As their nerve conduction (and so action/reaction) must then be slower than predators with a body temperature of 37°C (action potential characteristics, such as conduction velocity, are temperature dependent [372-377]). Indeed, the North American opossum is renowned for feigning death, "playing possum", rather than running away. So, perhaps because predation constrains their lifespan to short anyhow, and doubling down on their "life on a budget" ecological niche, these marsupial species tend not to allocate as much (NADPH) energy to antioxidant defences. Possibly, I suggest, explaining the longstanding mystery [358] of why these marsupial species tend to have short (for their adult body size) maximal lifespans. Indeed, such a marsupial species, the Brazilian gracile opossum (*Gracilinanus microtarsus*), of similar size to a mouse, has a "poor NADPH dependent antioxidant capacity", "both content and state of reduction (mainly of NADPH) were lower in the marsupial mitochondria than in mice mitochondria", "a more oxidized state of the mitochondrial NADP was demonstrated by HPLC analysis which strongly supports the idea that the mitochondrial NADPH dependent antioxidant systems glutathione and thioredoxin peroxidases/reductases are less effective in the marsupial due to a lower reducing power provided by NADPH", isolated liver mitochondria from *Gracilinanus microtarsus*, compared to isolated liver mitochondria from mice, "have a much lower constitutive antioxidant capacity represented by the NADPH/$NADP^+$ content and redox potential" [378]. Where predation is less, the mean and maximal lifespan of the North American opossum population can be selected (in evolutionary senescence theory) to be more [379].

Addressing an anticipated objection: "But women are smaller, and yet live longer, than men".

On average, women live longer than men [380] (life expectancy at birth {2020} was 6.8% and 6.3% higher in women than men in Japan and USA respectively [381]). Perhaps because, on average, women have a lower specific (per unit mass) resting/basal metabolic rate than men [106-107, 110], e.g. 22% less in [108], 11% less in [109], 8% less in [106]. Possibly because, on average, a greater proportion of a woman's body composition is fat [107], conferring greater thermal insulation, and so less metabolic heat generation is required to maintain their body temperature. Any difference in body temperature between men and women is very small to non-existent depending upon the study [382].

Addressing an anticipated objection: "But why do antioxidants only extend life modestly or not at all?"

To be expected. As explained earlier in the Results section (keyword search for "antioxidant" to find quickly).

To add to that here, even an endogenous antioxidant enzyme can be pro-oxidizing. SOD mitigates superoxide ($O_2^{\bullet-}$). But it can also perform a side-reaction, generating the hydroxyl radical ($^{\bullet}OH$, arguably the most damaging ROS, e.g. can cause DNA double-strand breaks) from H_2O_2 [383-388]. Which must become increasingly prevalent as intracellular H_2O_2 increases with age [53-56]. So, SOD is essential (mice without SOD2 die within 10 days of birth [389]) but more SOD isn't necessarily beneficial. This is especially noted with SOD2, which has manganese (Mn) in its active site. As ROS damage releases iron (Fe) from ferritin [390] and from iron-sulfur (e.g. Fe-S, Fe_2-S_2 etc.) centres of proteins [391-394], increasing intracellular [Fe], Fe increasingly outcompetes Mn to be in the active site of SOD2. Forming FeSOD2 instead of MnSOD2 [395], which produces $^{\bullet}OH$ from H_2O_2 by the Fenton reaction.

Moreover, it should be remembered that (varied) exogenous and endogenous antioxidants, at least at some dosage(s), *can* extend lifespan, e.g. [49-51, 396-404]. For which, a parsimonious interpretation is that ROS *are* a drive of aging. Indeed, to my knowledge, no one has been able to explain this lifespan data otherwise.

Postscript

Much herein has already published, via (some of) my patent applications already publishing (e.g., variants of Figures 2 and 12 published [as Figures 15 and 8 respectively] in my patent application [16], variants of Figures 3 and 13 published [as Figures 24 and 10 respectively] in my patent applications [405-406]). But this present paper is its first report in the scholarly literature. A recent paper has further confirmed one of the assertions of this present paper, and its patent application predecessors (e.g. [405-406]), that (to quote it) "IF1 is required to prevent the onset of ATP hydrolysis under OXPHOS conditions", "IF1 is essential under OXPHOS conditions to prevent reverse ATP synthase activity", "our data clearly show that IF1 is necessary to block ATP hydrolysis under OXPHOS conditions", "to prevent futile ATP synthesis/hydrolysis cycles by reverse ATP synthase activity and ATP hydrolysis, IF1 is essential even and especially under OXPHOS conditions", "IF1 is beneficial for ATP production even under OXPHOS conditions", "ATP levels were lower in IF1-KO cells under

OXPHOS conditions", "clearly, this data demonstrates the importance of IF1 to block futile ATP hydrolysis under OXPHOS conditions" [407].

METHODS (*with supplementary information, data & analysis*)

Some definitions: "specific" (by convention) can refer to "per unit mass", which is a convention used often herein. "Maximal lifespan" of a species is the longest lifespan ever recorded for a member of that species.

6b drug administered to mice (*generating Figure 2*)

Four female C57BL/6 strain mice (*Mus Musculus*) were sourced from Shanghai Lingchang Bio-Technology Co. Ltd. They were 12-14 weeks old on the day of the rectal temperature recording experiment. Their care and use was in strict accordance with the regulations of the Association for Assessment and Accreditation of Laboratory Animal Care (AAALAC). Some details of their care: *ad libitum* Co^{60} irradiation sterilized dry granule food, reverse osmosis autoclaved drinking water, corn cob bedding, polysulfone individually ventilated cage (IVC, containing up to 5 animals): 325 mm*210 mm*180 mm, 12 hour light/dark cycle, 40-70% humidity, 20-26°C room temperature.

StudyDirector™ software (Studylog Systems, Inc. CA, USA) was used to allocate/randomize control/treatment groups. Mice were marked by ear coding (notch).

When recording rectal temperature, care was taken to ensure constant depth of probe insertion across different recordings. Time was afforded for rectal probe temperature to equilibrate with rectal temperature. And time was afforded between recordings for probe temperature to reset. The rectal temperature recording experiment was started between 8 and 9 am.

Intravenous (IV) administration (tail vein): dosing volume per weight of drug = 10 µl/g, solution (not suspension). Sterilised (0.22 µm filter), vortexed vehicle = 12.5% solutol, 12.5% ethanol, 75% water (admittedly, it was unwise to include a drug, ethanol, in the vehicle. All be it is commonly used for this purpose). IV solutions freshly prepared before injection.

The two mice intravenously injected with 20 and 40 mg/kg drug doses both exhibited hypoactivity and tachypnea. Which are both signs of hypothermia [408], coinciding with their rectal temperature drop to below 30°C. 210 minutes (3.5 hours) after the intravenous injection of 20 mg/kg, that mouse died ("choked when drinking water" was the reported observation by the experimenter. Reason/how is unknown). The mouse injected with 40

mg/kg was found dead the next day. The mouse injected with 2 mg/kg survived, and was sacrificed 54 days later. 24 hours post the IV injection, its rectal temperature was 39.99°C, compared to 39.48°C in the control (vehicle administered) mouse. So, the (intravenous) Maximal Tolerated Dose (MTD) in mice is definitely greater than 2 mg/kg, and possibly less than 20 mg/kg. Demonstrated, it is an active, potent drug *in vivo*. A prediction is that the MTD would be greater if the ambient temperature was safely higher. For example, it would be higher if the ambient temperature was instead 30°C. Even higher if it was 34°C, and higher still if 37°C. *Incidentally, it is widely unknown/underappreciated that, for any mouse experiment, laboratory mice should be kept at a higher than typical room temperature. Typical room temperature (~20°C [201]) is thermoneutral for us humans (in clothes [335]) but it isn't for mice, whose thermoneutral temperature is instead ~32°C [333, 409-411]*.

A possibility is that either or both of the ≥20 mg/kg drug administered mice were mischaracterized as dead (if the 40 mg/kg drug administered mouse was mischaracterized, then the drug's MTD is ≥40 mg/kg). And instead of dead, one or both were merely hypothermic due to the drug action. With reduced body temperature (at slightly above ambient temperature, which was ~22°C), as a function of reduced metabolic rate. And unresponsive to external stimuli upon cursory inspection (rodent unresponsiveness during hypothermia was observed by [412]: "it did not arouse even when repeatedly disturbed"). Because of the drug's action, unable to generate heat to arouse themselves. Unfortunately, the experimenter wasn't forewarned to be vigilant to this possibility (e.g. not told to check for a heartbeat, all be it likely slowed). Rendering an inconclusive MTD. Because one or both of these mice might have survived if given the opportunity. Returning to normal/normothermia as the drug cleared from the body. Which might have taken some time given that reaction rates are temperature dependent, and these mice had a lower than normal body temperature. Data of [412] suggests that rodents can recover from hypothermia, once the hypothermic drive is removed.

In this case the effect size is large (the drug-conferred changes in mouse body temperature are large, e.g. dropping body temperature to below 30°C). When an effect size is large it can be detected at statistical significance by a small sample size (observable by playing with the Excel spreadsheet of [413] or statistical power calculators such as [414]). For animal studies, an overpowered sample size (more subjects than required to hit statistical significance) is anathema to the 3Rs (Replacement, Reduction, Refinement) [415].

A (unfortunate, but mice sparing) confounding issue is that in the 43 days preceding the rectal temperature recording experiment (which was conducted on day 44) the mice were used in a different experiment. A dose escalation study of a different chemical entity. Of the same chemical formula, but the opposite stereoisomer thereof (*R*), in enantiomeric excess (≥97%): compound 6a in Figure 12A. Which, unlike compound 6b, does *not* inhibit F_1F_0 ATP hydrolysis (6b EC_{50} F_1F_0 ATP hydrolysis = 0.018 μM, 6a EC_{50} F_1F_0 ATP hydrolysis > 100 μM [28-29]). This experiment sought the Maximal Tolerated Dose (MTD) in mice of compound 6a. Wherein the control mouse was always administered vehicle, and the three test mice were administered an escalating 6a dose amount every 3 days, ultimately reaching 40 mg/kg. The final dose of 6a was on day 39, wherein the highest dose given then was 2 mg/kg (ran out of 6a and so doses were low on that last day). So, the MTD was not successfully found for 6a.

More details of these experiments can be found in my US patent application [16].

To give some data for comparison: in mice, the intravenous LD_{50} (dose that kills 50% of the cohort) values for the FDA approved anti-depressants, clomipramine HCl and imipramine HCl, are 22 and 27 mg/kg respectively (Register of Toxic Effects of Chemical Substances, RTECS). Some human patients take these drugs daily, safely, for years.

Generating Figure 3

For each species, the F_1F_0 ATP hydrolysis data herein is from Sub-Mitochondrial Particles (SMPs). Produced by sonicating mitochondria, which were isolated from ischemic heart tissue. Ischemia, by collapsing the proton motive force (pmf), causing a lower pH in the mitochondrial matrix, increases the active fraction of IF1 protein. Which comprises IF1 protein monomers and dimers, which *can* bind ATP synthase [13]. As opposed to IF1 protein tetramers, and higher oligomers, which cannot. Ischemia ensures that a large proportion of IF1 protein complexes with the membrane bound ATP synthase. Which means that more IF1 protein is retained/available after the subsequent SMP generation protocol. SMPs are inside-out (inverted). With the mitochondrial matrix side of the membrane, and so the ATP hydrolysing and IF1 binding modules of ATP synthase, on their outer face. So, IF1 protein is wanted on the outside, not on the inside, of the SMPs. Prior ischemia, which combines IF1 protein with the mitochondrial matrix side of ATP synthase, assists this. Moreover, (at least some of) this activated IF1 protein fraction carries over into the start of the subsequent F_1F_0 ATP hydrolysis assay (conducted at pH 7.8, for 5 minutes). So best showcasing differences in IF1 protein activity between different species. Rendering them detectable by the resolution of

this experiment. Where (to hypothesize) the differences in IF1 protein activity, driving differences in F_1F_0 ATP hydrolysis, comprise differences in IF1 protein amount (versus ATP synthase amount), IF1 protein inhibitory potency for F_1F_0 ATP hydrolysis, and IF1 protein tendency/self-affinity for tetramerization and higher oligomerization (self-sequesteration) at non-acidic pH. This F_1F_0 ATP hydrolysis data was sourced from [58] (column titled "Ischemic" in its Table 1), along with its heart rate and body mass data therein. Maximum lifespan data was sourced from the AnAge database [1]. Specific basal metabolic rate data herein, for each cited species, is the mean of values for that species sourced from AnAge [1] and the landmark papers by Max Kleiber in 1932 and 1947 [67-68], which set out Kleiber's Law. But the specific basal metabolic rate of rat value from [68] was omitted from this mean, because its value is not from an adult. Further incorporated into the mean of mouse is the value of 0.0092125 W/g (sourced at ambient [thermoneutral] temperature of 32°C, for C57 mouse strain) from [334]. Further incorporated into the mean of rat is the value of 0.005695 W/g (sourced at ambient [thermoneutral] temperature of 28°C) from [370]. For converting O_2 consumption into energy I used [1 ml O_2 = 20.1 Joules], which is a well-known conversion factor, e.g. as used by [333, 370].

Best fit lines were calculated by OriginPro 8 software (OriginLab Corporation, Northampton, MA, USA), using its "Fit Linear" functionality. Which uses linear regression, with least squares estimation.

Marrying data

In Figure 3, body mass data and data in the 1st (top) and 3rd panels is from [58], data in the 2nd and 4th panels is from the AnAge database [1] (*the 2nd panel incorporates further data from other sources, as specified above*). This data combination, and its interpretation here, is novel. There was some (enduring) margin for error in marrying these data sets because [58] uses imprecise terms such as sheep, hamster etc., wherein there are a number of different species in [1] that can fall into these categories. But a common sense alignment was applied in each case, by estimating which species [58] likely had easiest access to, so most likely used, and so most likely refers to. So, utilizing this estimation, the 12 species that Figure 3 herein refers to are: cow (domestic cattle, *Bos taurus*), mouse (house mouse, *Mus musculus*), rat (brown rat, *Rattus norvegicus*), hamster (golden hamster, *Mesocricetus auratus*), guinea pig (*Cavia porcellus*), pigeon (common wood-pigeon, *Columba palumbus*), chicken (*Gallus gallus*), rabbit (European rabbit, *Oryctolagus cuniculus*), sheep (domestic sheep, *Ovis aries*),

pig (*Sus scrofa domesticus*), dog (*Canis lupus familiaris*) and human (*Homo sapiens*). Although an acknowledged, reasonable possibility is that the pigeon species that [58] used was instead the rock pigeon (*Columba livia*). Which I discuss later on, in the section titled "Birds".

Data from [1] was sourced primarily in August 2018. Which is when the kernel (e.g. Figure 3) of this work was done.

Omitting human maximal lifespan

Herein, the maximum lifespan of human from [1] (122.5 years) isn't shown in any of the figures. Nor utilized in any of the calculations, e.g. not used in any of the Pearson (or Spearman's rank) correlation coefficient calculations to maximal lifespan. Because (arguably) this value isn't fairly comparable to the maximal lifespan values used. Because (*a*) modern medicine is disproportionally applied to humans, (*b*) many modern humans live in shelter and comfort (*and* with complete freedom and stimulation, unlike an animal in a zoo for example, whose optimal husbandry might not even be known/performed), and (*c*) the verifiable lifespan data set for humans is very much larger, with so many countries recording births and deaths (the bigger the data set, the greater the chance a higher maximum lifespan will be found). So, compared to the human number, which is drawn from a huge sample size, the other numbers, drawn from small sample sizes, are likely to be an underestimate of species maximal lifespan. Human could perhaps be more comparably incorporated by using a maximum lifespan record from a smaller human data set. To mirror the small data sets for the other species. Preferably wherein this data set comes from humans living in the past, e.g. from 1881 Germany, where life expectancy of men and women was 35.6 and 38.5 years respectively (Statistisches Bundesamt Deutschland, www.destatis.de). However, omission was chosen instead.

Chicken maximum lifespan

The AnAge database [1] states 30 years for the maximal lifespan of chicken (red junglefowl, *Gallus gallus*). *But* in the "Observations" section of this database entry, AnAge says that this "remains unproven. For comparative analyses the use of a more conservative value for maximum longevity, such as 15 or 20 years, is recommended". I split the difference, between 15 and 20, and use 17.5 years.

Raw (unlogged) data used to produce Figure 3

	Body mass	Specific F1F0 ATP hydrolysis	Specific basal metabolic rate	Heart rate	Maximum lifespan
Cow	500	1.32	0.000798458	50	20
Pig	100	0.81	0.000771	73	27
Human	90	1.31	0.001164574	69	Unused
Sheep	60	1.49	0.001319925	75	22.8
Dog	25	1	0.001804232	85	24
Rabbit	2	1.12	0.002887816	213	9
Chicken	2	2.89	0.002418352	318	17.5
Pigeon	0.6	2.66	0.004975053	305	17.7
Guinea Pig	0.4	2.71	0.003740752	265	12
Rat	0.2	3.02	0.00601463	481	3.8
Hamster	0.1	3.9	0.006377	400	3.9
Mouse	0.025	2.73	0.010858546	618	4

Specific F_1F_0 ATP hydrolysis (μmol/min/mg) data is from [58] (column titled "Ischemic" in its Table 1). Body mass (kg) and heart rate (bpm) data is also from [58] (Table 3 therein). Maximal lifespan (years) data is from [1]. Specific basal metabolic rate (W/g) data is the mean of data from [1], [67-68], [334, 370]: a compilation of sources because no single source has data for all the investigated species. The mean specific basal metabolic rate data in the table above is calculated from its source papers as shown in the subsequent table, where [α] is [1], [β] is [67], [γ] is [68], [δ] is [334], and [ε] is [370]. The specific basal metabolic rate of rat value from [68] is omitted, because its value is not from an adult. With data from [334] and [370], for converting O_2 consumption into energy I used [1 ml O_2 = 20.1 Joules], which is a well-known conversion factor, e.g. as used by [333, 370].

	[α]	[β]	[γ]	[δ]	[ε]	Mean
Cow	0.000884	0.000759568	0.000751805			0.000798458
Pig	0.000771					0.000771
Human	0.001183	0.001195378	0.001115345			0.001164574
Sheep		0.001296472	0.001343377			0.001319925
Dog		0.001745968	0.001862497			0.001804232
Rabbit	0.003411		0.002364633			0.002887816
Chicken	0.002216	0.002620705				0.002418352
Pigeon		0.004975053				0.004975053
Guinea Pig	0.003333		0.004148504			0.003740752
Rat	0.006786	0.00556289	Omitted		0.005695	0.00601463
Hamster	0.006377					0.006377
Mouse	0.015056		0.008307139	0.0092125		0.010858546

Figures 4 and 8 use the same raw data as Figure 3, except without the body mass data.

My workings to get to the 0.0092125 W/g figure from [δ] [334]: from its Table 3, ignoring error bars, for the C57 mouse strain, at an ambient temperature of 32°C (which is the ambient temperature with the lowest O_2 consumption on this line of table. And so, out of the ambient temperatures tested at, this one is most likely closest to, or possibly even at, the C57 mouse's thermoneutral temperature. The thermoneutral temperature of mice is known to be at/around 32°C, e.g. refer Fig. 5 in [333]), O_2 consumption = 1.65 cc/g/hour, where "cc" is cubic centimetre (cm^3), (*to get into kg, which is the SI unit of mass*) *1,000 = 1,650 cm^3/kg/hour = (*because 1 cm^3 = 1 ml, and 1 ml O_2 consumption = 20.1 Joules* [333]) 33,165 J/kg/hour = (*because power = energy/time = J/s; 60*60 seconds in 1 hour*) 33,165/(60*60) = 9.2125 W/kg = 0.0092125 W/g.

My workings to get to the 0.005695 W/g figure from [ε] [370]: from the first line of its Table 1, which refers to BMR (=Basal Metabolic Rate), sourced at an ambient temperature of 28°C (at/around the thermoneutral temperature of a rat [370]), for the Simonsen (Sprague-Dawley derived) rat strain, O_2 consumption = 17 ml/kg/minute = (*because 1 ml O_2 consumption = 20.1 Joules* [333, 370]) 341.7 J/kg/minute = (*because power = energy/time = J/s; 60 seconds in 1 minute*) 341.7/60 = 5.695 W/kg = 0.005695 W/g. Which actually corresponds well with the value given for specific metabolic rate on the same line of the same table = 5.7 W/kg.

The conversion algorithm I used for data from [67] and [68]: starting with metabolic rate per day (Kcal) and body weight (kg): converted kcal to calories, converted calories to Joules, divided this by body weight (kg) to get in J/kg/day, (*because power = J/s*) divided by number of seconds in a day (24*60*60) to get in W/kg, then /1000 to get in W/g.

Data was drawn from Table 1 of Kleiber's 1932 paper [67]: from its "W Average weight, kilo-grams" and "Cals. per 24 hrs. per animal" columns. In my calculations, an error in this paper was corrected: the table actually reports kilocalories (kcal), not calories as it purports. This error is evident, for example, when comparing the data (e.g. for woman) of Kleiber's 1932 [67] and 1947 [68] papers (which report independent data sets: "No data were used that were already incorporated in the earlier study (1932)" [68]). The latter's Table 2, where the unit of its "Metabol. rate per day" column is correctly labelled kcal. The unit error is identified to be with the 1932, rather than the 1947 paper, because I know the order of magnitude of calories that a person needs per day, even if inactive, is thousands of kilocalories. For example, from the National Health Service (NHS) website: "As a guide, an

average man needs around 2,500 kcal (10,500 kJ) a day to maintain a healthy body weight. For an average woman, that figure is around 2,000 kcal (8,400 kJ) a day" [416].

Note, to relay a possibly confounding issue in the data sourced from [67]: quoting [67]: "The relatively low value of the hen may be in connection with the fact that the determinations had been made in darkness".

Note that, in at least some cases, a specific basal metabolic rate value sourced from [1] is a mean of values sourced from a number of different sources ("if more than one pair of values was available, the logarithmic average was used. If discrepancies were noticed between two or more pairs of values, then only the most recent pair was used" [417]). But none of these sources include any of [67], [68], [334], [370]. So, these are all independent data sources. At least for now. But these paper values may well get incorporated into the means of the [1] database, called the AnAge (Animal Ageing and Longevity) database, in the future.

Normality of data

Kolmogorov-Smirnov Test of Normality (D)		p-value	Verdict		
Specific F1F0 ATP hydrolysis	0.22906	0.48489	Normal		
Specific basal metabolic rate	0.17987	0.77037	Normal		
Heart rate	0.23315	0.46279	Normal		
Maximal lifespan	0.17922	0.81215	Normal		
Normal = data does not differ significantly from that which is normally distributed					

Spearman

Correlations were assessed using the Pearson correlation coefficient (R), which assays for a *linear* correlation (change in *x* associated with a *proportional* change in *y*). By contrast, Spearman's rank correlation coefficient (ρ) assays for a *monotonic* correlation (change in *x* associated with a proportional, *or non-proportional*, change in *y*). It using the ranked values for each variable rather than the raw data. For comparison, for the data used to produce Figure 4, the following table presents Spearman's rank correlation coefficients, and associated p-values (one-tailed, because each alternative hypothesis is directional), for its inter-relations:

Spearman's rank correlation coefficient (ρ)				
	Specific basal metabolic rate	Heart rate	Maximal lifespan	
Specific F1F0 ATP hydrolysis	0.75525	0.78322	-0.80909	
	Specific basal metabolic rate	0.93007	-0.86364	
		Heart rate	-0.82727	
p-value (one-tailed)				
	Specific basal metabolic rate	Heart rate	Maximal lifespan	
Specific F1F0 ATP hydrolysis	0.002254	0.001293	0.0012795	
	Specific basal metabolic rate	0.000006	0.000306	
		Heart rate	0.0008385	
Asymptotically exact harmonic mean p-value for combining independent/dependent tests				
Of all the p-values above (in this present table) = 0.00003467136 = **0.00003**				
Fisher's combined probability test				
Using p-values for [Specific F1F0 ATP hydrolysis vs. Maximal lifespan] (=0.0012795) &				
[Heart rate vs. Specific basal metabolic rate] (=0.000006) = 0.0000002				

Heart rate

Heart rate values were sourced from [58]. For species with a range of values disclosed therein, the middle value of the range was taken. This heart rate data comes from conscious animals, *except* for hamster: its values are from anesthetized animals. This disparity was ignored. But if instead it isn't, this can increase at least some of the correlations to heart rate, and their statistical significance. The anesthetized heart rate range for hamster in [58] is 375-425. And the value drawn was 400. But if the upper bound value is taken instead, 425, then at least some of the investigated Pearson correlation coefficient (R) values relating to heart rate are increased. And their associated (one-tailed) p-values decreased, i.e. increased statistical significance:

		Specific F1F0 ATP hydrolysis	Specific basal metabolic rate	Maximal lifespan	log10(Body mass)
Heart rate	R	0.8139	0.9476	-0.8648	-0.9439
	p	0.000637	0.0000015	0.000295	0.000002

Birds

Conceptually, a different way to decrease ROS generation is, instead of (or in addition to) reducing metabolic rate and O_2 consumption rate, modifying the respiratory chain such that it fumbles a lower percentage of the electrons it passages (i.e. increased efficiency) [418]. Some species, possibly at least some bird species, may have availed themselves of such increased efficiency. For example, there is data suggesting that the particularly long-lived (for its size) pigeon species, *Columba livia*, has such increased efficiency [419]. An observed strategy, for increased efficiency, is to reduce the amount of Complex I [420-423].

Moreover, long-lived (for their size) bird species' membranes (e.g. the mitochondrial inner membrane) tend to have less propensity to amplify ROS damage (wherein lipid peroxidation PUFA products are themselves ROS, which can attack further PUFA molecules, a chain reaction, which can go on to damage other cellular components, e.g. membrane proteins, mtDNA, etc.) because their polyunsaturated fatty acids (PUFAs) tend to have less double bonds [424-429].

To generate the principal correlative Results of this paper I used data from [58], which was published 34 years ago. Including its data from pigeon. But [58] doesn't specify which particular pigeon species it used. I made the estimation that [58] used the common wood pigeon (*Columba palumbus*), which has a maximal lifespan of 17.7 years [1]. Although I concede that [58] may instead have used the rock pigeon (*Columba livia*), which has a very different maximal lifespan. Of 35 years [1]. So, nearly twice as long. Given this uncertainty, I reason that a maximal lifespan of 17.7 years (that for *Columba palumbus*) is the best value to use for pigeon, by the balance of probabilities, as I explain later. And so this is the maximal lifespan that I allocated to pigeon. Which is of the order of the maximal lifespan (in brackets after each name) of most other pigeon and dove {Columbidae family} species in [1]: *Leucosarcia melanoleuca* (16.3), *Patagioenas leucocephala* (14.4), *Columba oenas* (12.6), *Cepphus Columba* (15.2), *Caloenas nicobarica* (20.5), *Patagioenas fasciata* (18.5), *Streptopelia decaocto* (17.9), *Streptopelia risoria* (12), *Streptopelia turtur* (13.2), *Columbina passerina* (7.2), *Streptopelia chinensis* (9.8), *Geopelia striata* (14), *Leptotila verreauxi* (8.6), *Columbina inca* (13.3). *But* there are three longer-lived, outlier species: *Columba livia* (35), *Zenaida macroura* (31.3), *Zenaida asiatica* (25) [1]. The particularly long-lived *Columba livia* (*particular breed thereof unspecified*) has been shown to have low Complex I content, in the aforementioned [420]. And a low number of double bonds in its PUFAs, in the aforementioned [425-426]. If [58] used *Columba livia*, which is more of an outlier species, living longer (maximal lifespan of 35 years) for its size, instead of *Columba palumbus*, then the Pearson correlation coefficients (R, and their p-values, one-tailed because each alternative hypothesis is directional) are as follows: wherein the second line of R shown is if pigeon is omitted from the data set, and the third line of R shown is if the other bird species (chicken) is omitted also, such that all the remaining species are mammals (N.B., [1] didn't, and presently {*July 2021*} doesn't, have metabolic data for any pigeon, so the specific basal metabolic rate value of pigeon [particular species unknown] is singly from [67]):

		Specific F1F0 ATP hydrolysis	Specific basal metabolic rate	Heart rate	log10(Body mass)
Maximal lifespan	R	-0.5041	-0.6008	-0.66	0.6221
	p	0.0569265	0.025307	0.013556	0.0204885
Maximal lifespan	R	-0.7535	-0.8413	-0.8744	0.8915
	p	0.005924	0.0011405	0.000467	0.0002655
Maximal lifespan	R	-0.8189	-0.8387	-0.8993	0.9042
	p	0.0034685	0.002361	0.000483	0.0004075

A complication of *Columba livia* is that there are many (hundreds of) different breeds thereof. Different "fancy pigeons". Which can be very morphologically diverse. And which, at least in some cases, have had very different maximal lifespans reported, which *may* reflect true differences in maximal lifespan. Perhaps reflecting, deliberate and/or inadvertent, artificial selection for longer lifespan in at least some breeds. For example, discussing different breeds of *Columba livia*, a Cropper pigeon reportedly lived to 35 years old, but (from the *same* source paper) the "limit of the age of the Pouter Pigeon is only 10 to 12 years, the "great proportion dying in less than half that time"" [430] (*incidentally, [430] is the {once removed} upstream source of the 35 year maximal lifespan reported for Columba livia in [1], for which [430] cites a further upstream source, dating from 1911*). Whilst as regards the original/ancestor *Columba livia*, without any breeding/selecting by man: in captivity, in Egypt, at the Giza zoo, "two Rock-Pigeons [*Columba livia*] from the Dongola Province of the Sudan lived certainly for 8 years and possibly for 12 years 10 months" [430]. In captivity, at the same location, a hybrid cross pigeon, of *Columba livia* x *Columba lumbus*, lived for 5 years, 7 months, 17 days [430]. So, it *might* be that *some* breeds of *Columba livia* have a maximal lifespan that is less than, or comparable to, that of *Columba palumbus*. Given that we don't truly know which species of pigeon [58] used, nor which breed thereof (*if* it used *Columba livia*), nor definitively how different breeds of *Columba livia* map to maximal lifespan, moreover wherein at least some bird species tend to live much/anomalously longer than similarly sized mammal species, where mammals are my primary focus, there is a case for omitting pigeon from the data/investigation. But in the Results section of this present paper, wherever a pigeon maximal lifespan is utilized/presented, a relatively conservative maximal lifespan value (17.7 years), that of a very common pigeon species (*Columba lumbus*) [1], of the order of the maximal lifespan of most other pigeon species [1], and *possibly* of *some* breeds of *Columba livia*, is used. Instead of omission.

If omission is selected instead, as shown below, the Pearson correlation coefficients (R) between maximal lifespan and the presented variables are *greater*, and some of the (one-tailed) p-values are accordingly lower (despite the smaller value of *n*):

		Specific F1F0 ATP hydrolysis	Specific basal metabolic rate	Heart rate	log10(Body mass)
WITH pigeon					
Maximal lifespan	R	-0.7192	-0.8144	-0.8572	0.8573
	p	0.0063065	0.001136	0.000373	0.000761
WithOUT pigeon					
Maximal lifespan	R	-0.7535	-0.8413	-0.8744	0.8915
	p	0.005924	0.0011405	0.000467	0.0002655

Wherein "WITH pigeon" data is that presented in the Results section herein. And "WithOUT pigeon" is the same as presented in the preceding table, in this present section.

Replication of the specific F_1F_0 ATP hydrolysis data (utilized herein) by other studies

In the table below, Paper [α] is [58] (whose data is used in the Results section of this present paper), Paper [β] is [431], Paper [γ] is [432], Paper [δ] is [433], Paper [ε] is [434], and Paper [ψ] is [435]. All these papers are from the same laboratory. But with varied authorship. Probably (at least partly) because their publication dates span 9 years. Notably, the co-author of Paper [γ] is Maynard E. Pullman, who co-discovered the IF1 protein in 1963 [7]. There are some differences in protocol between at least some of the papers. For (non-exhaustive) example, to prepare Sub-Mitochondrial Particles (SMPs), Paper [α] uses sonication only. But Papers [γ] and [ψ] use sonication *and* at least one subsequent centrifugation step. Centrifugation is for mitochondrial debris clearing, e.g. of large mitochondrial remnants and membrane fragments. But it must be implemented judiciously, lest it remove some of the IF1 protein. Confusingly, at least some of these papers use an idiosyncratic terminology. Where they refer to mitochondrial preparations that have undergone both sonication and centrifugation as Sub-Mitochondrial Particles (SMPs). Whilst referring to those that have only undergone sonication as "sonicated mitochondria". This terminology is somewhat misleading because *both* these preparations contain SMPs (it is the sonication step that breaks up the mitochondria into SMPs). A constant for the data in the table below is that the mitochondria, broken up to form SMPs, were sourced from ischemic heart tissue. If body mass is reported as a range in a source paper, I report its middle value in the table below. An uncontrolled aspect is body mass differences, in some cases large, between the different

(paper's) studies.

	Paper [α]		**Paper [β]**		**Paper [γ]**		**Paper [δ]**		**Paper [ε]**		**Paper [ψ]**	
	[A]	[B]	[A]	[B]	[A]	[B]	[A]	[B]	[A]	[B]	[A]	[B]
Cow	500	1.32										
Pig	100	0.81	17.01	1.33 (±0.15)								
Human	90	1.31										
Sheep	60	1.49										
Dog	25	1			NS	0.87 (±0.11)	30	1.12 (±0.12)	10	1.75 (±0.08)		
Rabbit	2	1.12	1	1.32 (±0.18)							1	1.18 (±0.08)
Chicken	2	2.89										
Pigeon	0.6	2.66	0.4	2.99 (±0.12)							0.6	3.35 (±0.16)
Guinea Pig	0.4	2.71	0.4	3.04 (±0.06)								
Rat	0.2	3.02	0.3	3.27 (±0.11)			0.25	2.91 (±0.24)	0.5	2.66 (±0.17)		
Hamster	0.1	3.9										
Mouse	0.03	2.73	0.025	3.31 (±0.07)								
	[A] **= Body mass (*kg*),** [B] **= F1F0 ATP hydrolysis (*μmol/min/mg*)**; NS= Not Specified											

Firstly, to compare just Paper [α] and Paper [β]. Their source papers, [58] and [431] respectively, were published 7 years apart, in different peer-reviewed journals, by the same laboratory, wherein the latter paper has two additional authors. Paper [β] specifies its tested species more precisely: *Sus scrofa* ("farm pig"), *Oryctolagus cuniculus* (rabbit), *Columba livia* (rock pigeon, Indian Fantail breed), *Cavia porcellus* (guinea pig), *Rattus norvegicus* (brown rat), *Mus musculus* (mouse). Note the large difference in pig body mass between the two studies. Where Paper [β] presumably reports upon piglets/adolescents rather than adults (I took the middle value of its weight range: "thirty-five to 40-lb. farm pigs" = 17.01 kg). Which *might* be why it reports a greater specific F_1F_0 ATP hydrolysis for pig. Because, to speculate, piglets/adolescents are smaller than adult pigs, so have a higher surface-area to volume ratio, thence require greater heat generation per unit mass, and so a higher specific basal metabolic rate, driven by greater specific F_1F_0 ATP hydrolysis.

From the table above, only using data from the lines that present data from both studies: The Pearson correlation coefficient (R) between the specific F_1F_0 ATP hydrolysis data of Paper [α] and Paper [β] is 0.98751 (one-tailed, because the alternative hypothesis is directional, p-value = 0.0001165). This is without applying the error bars. If these are instead applied, R is instead 0.97423. Ignoring the error bars, comparing the specific F_1F_0 ATP hydrolysis data of Paper [α] and Paper [β]: they are *not* significantly different from each other: independent (two-tailed) t-test statistic = -0.6706, p-value = 0.517661; Mann-Whitney U test (two-tailed): U-value = 9, z-score = -1.36109, p-value = 0.17384; Kruskal-Wallis test: H statistic = 2.0769, p-value = 0.14954; Levene's test of homogeneity of variance: f-ratio = 0.00078, p-value = 0.978277. If the error bar is added or subtracted (operation independently selected in each

case) from each datum of Paper [β], whichever manipulation makes each value further from the corresponding value from Paper [α], again the data sets are *not* significantly different from each other: independent (two-tailed) t-test statistic = -0.89801, p-value = 0.390289; Mann-Whitney U test (two-tailed): U-value = 8, z-score = -1.52122, p-value = 0.12852; Kruskal-Wallis test: H statistic = 2.5641, p-value = 0.10931; Levene's test of homogeneity of variance: f-ratio = 0.02019, p-value = 0.889822.

Now to compare, as regards specific F_1F_0 ATP hydrolysis, for their shared species/genera, Paper [α] with the mean of Papers [β], [γ], [δ], [ε], [ψ]. Ignoring error bars. The Pearson correlation coefficient (R) = 0.9708 (one-tailed, because the alternative hypothesis is directional, p-value = 0.0001375). These two data sets are *not* significantly different from each other: independent (two-tailed) t-test statistic = -0.60998, p-value = 0.553253; Mann-Whitney U test (two-tailed): U-value = 13, z-score = -1.40553, p-value = 0.15854; Kruskal-Wallis test: H statistic = 2.1592, p-value = 0.14172; Levene's test of homogeneity of variance: f-ratio = 0.03268, p-value = 0.859571. Incidentally, the pigeon species used by Paper [ψ] is *Columba livia* (White Carneaux breed).

IF1 protein content

Under normal conditions *in vivo*, the inhibitory capability of a species' IF1 protein population is at least a function of (*a*) how much IF1 protein it has per ATP synthase molecule, (*b*) how potently (how much inhibition, per unit amount) its IF1 protein can inhibit *its* F_1F_0 ATP hydrolysis, and (*c*) it's IF1 protein's tendency/self-affinity for tetramerization and higher oligomerization (self-sequesteration) at the alkaline pH of the mitochondrial matrix. Assaying, at pH 7.8, for 5 minutes, F_1F_0 ATP hydrolysis in Sub-Mitochondrial Particles (SMPs), which are derived (by sonication) from mitochondria that have been isolated from an ischemic tissue of the species, reflects upon (*a*), (*b*) and (*c*). Their combination. Enabling species comparisons. Such data has been utilized up until this point (e.g. utilized in Figure 3). By contrast, this present section uses a more limited assay, which doesn't as fully reflect upon (*a*) and (*b*), and doesn't reflect upon (*c*) at all. Only capturing the IF1 protein quantity (and not its ratio to ATP synthase) aspect of (*a*). And (aside from for rat) not capturing the "*its* F_1F_0 ATP hydrolysis" aspect to (*b*). This present assay reports the combination of (*i*) IF1 protein amount, with (*ii*) IF1 protein potency against rat F_1F_0 ATP hydrolysis. Although in the literature, the latter potency element is overlooked/discounted, and this assay is considered to

simply report upon "IF1 protein amount" or "IF1 protein content". Hereafter I align with this terminology, with the caveat of what has been said (in the main text this data is referred to as specific IF1 protein activity). For different species, the table below utilizes "IF1 protein content", which is the amount of mitochondrial extract {measured as mg of mitochondrial protein} from a species that can decrease F_1F_0 ATP hydrolysis of rat Sub-Mitochondrial Particles (SMPs) by 1 μmol/min. Assay performed at pH 6.2. This assay works because rat has very little endogenous IF1 protein, and so a high rate of F_1F_0 ATP hydrolysis. Moreover, because IF1 protein sequences, and ATP synthase protein sequences, are incredibly conserved across species. Such that IF1 proteins are typically interoperable between species, e.g. yeast IF1 protein can inhibit bovine F_1F_0 ATP hydrolysis [436]. In the table below, IF1 protein content data, for 12 different species, is used from Paper [α] [58] (*from column titled "ATPase Inhibitor Content, IU/mg" in its Table 1*). And from 6 different species from Paper [β] [431] (*from column titled "IF1 content (I.U./mg)" in its Table III*; those species of same genera as found in Paper [α], comprising the 5 species it {most probably} shares with Paper [α], and the specified pigeon species in Paper [β], *Columba livia* {Indian Fantail breed}, which I allocated a maximal lifespan of 35 years [1]). Pearson correlation coefficients are reported, and one-tailed (because each alternative hypothesis is directional) p-values.

			Specific basal metabolic rate	Heart rate	Maximal lifespan	log10(Body mass)
Paper [α]	IF1 protein content	R	-0.6669	-0.6051	0.6261	0.486
		p	0.0089225	0.018549	0.019661	0.054583
Paper [β]	IF1 protein content	R	-0.8211	-0.9285	0.6677	0.7488
		p	0.0225725	0.003743	0.073644	0.0433635

Comparing corresponding species/genus data (*i.e. comparing corresponding pig, rabbit, guinea pig, rat, mouse, and pigeon data*), the Pearson correlation coefficient (R) between the IF1 protein content data from Papers [α] and [β] is 0.8971. For which the one-tailed (because the alternative hypothesis is directional) p-value is 0.007669. Comparing corresponding species/genus data, the IF1 protein content data from Papers [α] and [β] is *not* significantly different from each other: independent (two-tailed) t-test statistic = -0.42674, p-value = 0 .677802; Mann-Whitney U test (two-tailed): U-value = 14, z-score = 0.56045, p-value = 0.57548; Kruskal-Wallis test: H statistic = 0.4103, p-value = 0.52184; Levene's test of homogeneity of variance: f-ratio = 0.29322, p-value = 0.600018. The IF1 protein content data of Paper [α] doesn't have error bars. But that of Paper [β] does. If the error bar is added or subtracted (operation independently selected in each case) from each datum of Paper [β], whichever manipulation makes each value further from the corresponding value from Paper

[α], again these IF1 protein content data sets are *not* significantly different from each other: independent (two-tailed) t-test statistic = 0.35084, p-value = 0.73299; Mann-Whitney U test (two-tailed): U-value = 14, z-score = 0.56045, p-value = 0.57548; Kruskal-Wallis test: H statistic = 0.4103, p-value = 0.52184; Levene's test of homogeneity of variance: f-ratio = 0.32067, p-value = 0.58369.

The IF1 protein content data, as used to produce the table (most immediately) above, aligns with the other data herein, supporting the conclusions drawn therefrom.

Incidentally, relating to what was discussed in the earlier section titled "Birds", if the pigeon of Paper [β] is considered to have a maximal lifespan of 17.7 (instead of 35) years, its R (between IF1 protein content and maximal lifespan) is much greater than presented in the table above, being 0.8023 (one-tailed p-value = 0.027382). If the pigeon of Paper [α] is considered to have a maximal lifespan of 35 (instead of 17.7) years, its R (between IF1 protein content and maximal lifespan) is greater than presented in the table above, being 0.6444 (one-tailed p-value = 0.0161685).

Combining specific F_1F_0 ATP hydrolysis and IF1 protein content data

The Pearson correlation coefficient between the afore-used specific F_1F_0 ATP hydrolysis and IF1 protein content data, of [58], is -0.5292. With a one-tailed (because the alternative hypothesis is directional) p-value of 0.038426. So, the greater the IF1 protein content, the less the specific F_1F_0 ATP hydrolysis. In earlier sections, both these entities have been independently correlated, by Pearson correlation coefficient, to specific basal metabolic rate, heart rate, and maximal lifespan. As shown below, Fisher's combined probability test was used to combine their p-values for each of these correlations. The independence requirement of Fisher's method is met here, because specific F_1F_0 ATP hydrolysis and IF1 protein content are different measures, assayed by different experimental protocols. These combined p-values are presented in the table below, on the row labelled "*Combined*". Along with, on lower rows, some afore-presented correlations. Lower down in the table below, all these p-values are combined by two different methods: the asymptotically exact harmonic mean p-value for combining independent/dependent tests [41] (*its post-published corrected method, as corrected on 7 October 2019*), and using Fisher's combined probability test.

p-value (one-tailed)						
	Specific basal metabolic rate	Heart rate	Maximal lifespan			
Combined	0.00053569	0.0001955	0.00123938			
	Specific basal metabolic rate	0.0000015	0.001136			
		Heart rate	0.0003725			
Asymptotically exact harmonic mean p-value for combining independent/dependent tests						
Of all the p-values above (in this present table) = 0.000008850359 = **0.000009**						
Fisher's combined probability test						
Using p-values for [*Combined* vs. Maximal lifespan] (=0.00123938) &						
[Heart rate vs. Specific basal metabolic rate] (=0.0000015) = 0.00000004						

Bradford Hill criteria

Historically, the Bradford Hill criteria (also known as Hill's criteria for causation) [437] were used to persuade that lung cancer *correlates* with smoking in epidemiological data, because smoking *causes* lung cancer. The present work reports a correlation between more IF1 protein activity (less F_1F_0 ATP hydrolysis) and longer maximal lifespan. This correlation, although not epidemiological, satisfies (at least the spirit of) at least most of the Bradford Hill criteria.

Confirmatory

The multi-pronged hypothesis, that IF1 protein activity (by curtailing F_1F_0 ATP hydrolysis, setting specific basal metabolic rate [which sets heart rate]) is a molecular determinant of maximal lifespan, was set before the consistent/supporting data above was in hand. So, in statistical terminology, this study is “confirmatory” (hypothesis before data, and the data is consistent with {supports} the hypothesis). Rather than “exploratory” (data before hypothesis: hypothesis sourced from data).

Which (if any) of damage to DNA, lipids or proteins constrains maximal lifespan?

Mediation analysis, at least with the JASP software used (version 0.14.1), selecting its bootstrap method called “Percentile”, run with 10,000 replications, requires a reasonable number of *n* (data entries) for it to converge, and return a result. Species, for which I have data for *both* specific F_1F_0 ATP hydrolysis, and one or more of DNA, lipid or protein damage data, were too few to perform mediation analysis. But I did have sufficient data, across species, to assay mediation between specific basal metabolic rate and maximal lifespan, via each of DNA, lipid and protein damage (data used is in the next table). Whilst

(foundationally) mediation analysis, in the main text, suggests that specific F_1F_0 ATP hydrolysis dictates maximal lifespan, via its setting of specific basal metabolic rate.

	Max. lifespan	Specific basal metabolic rate	[A]	[B]	[C]	[D]	[E]	[F]	[G]	[H]	[I]
Cow	20	0.000798458	0.17475		200.4802816	0.018668124	13.13718182	2.503762542	50.06451613	0.227811078	0.154552
Human	Unused	0.001164574		6.566666667	45.91443356	0.011279331	2.338496425			0.246004629	Unused
Dog	24	0.001804232		21.24	251.2699028	0.036982	38.72766273				0.135754
Rabbit	9	0.002887816	0.51825	26.58333333	217.9789987	0.019998982	22.81770176	3.432274247	39.61290323		0.266433
Rat	3.8	0.00601463	0.97	40.26333333	680.1305899	0.102512004	122.7983042	5.580267559	76.48387097	0.363310031	0.462594
Mouse	4	0.010858546	1.35175	62.34666667	791.1805121	0.140225608	158.995934	7.009336678	98.83870968	0.353242119	0.44794
Cat	30	0.00245358			287.6516	0.018642484	31.94855444				0.115525
Ferret	11.1	Not known			496.39948	0.06148557	60.883646				0.231767
Giraffe	39.5	Not known			99.11235523	Not known	7.12118775				0.094321
Horse	57	Not known			132.4468849	0.015638082	7.801665875	2.72212932			0.071536
Lion	28	0.000965			159.8665767	0.020623782	26.4114425				0.121471
Naked mole rat	31	0.003626			90.05321882	0.025561911	10.29925018			0.253644265	0.112791
Ring-tailed lemur	37.3	Not known			103.5027907	0.017708289	6.27145075				0.098424
Black-and-white colobus	35	0.001604			80.36053079	0.017166283	9.5643306				0.103169
Tiger	26.3	0.000971			225.673621	0.062244437	47.87444714				0.127105
Pig	27	0.000771	0.36325	8.616666667				4.536231884	25.67741935		0.124715
Sheep	22.8	0.001319925						4.043478261	42.80645161		0.140826
Guinea Pig	12	0.003740752	1.05263					4.545150502	66.32258065	0.305584721	0.219921
Hamster	3.9	0.006377	1.615							0.376919182	0.455116
Chinchilla	17.2	0.003								0.233197897	0.171797
Blind mole rat	20.2	0.004372								0.268021261	0.15347
Beaver	23.4	Not known								0.219434529	0.138237
Humpback whale	95	Not known								0.220605353	0.048155
Bowhead whale	211	Not known								0.169924411	0.025409

The binomial/Latin names of the species in the table above: Cow (*Bos taurus*), Human (*Homo sapiens*), Dog (*Canis lupus familiaris*), Rabbit (*Oryctolagus cuniculus*), Rat (*Rattus norvegicus*), Mouse (*Mus musculus*), Cat (*Felis catus*), Ferret (*Mustela furo*), Giraffe (*Giraffa camelopardalis*), Horse (*Equus ferus caballus*), Lion (*Panthera leo*), Naked mole rat (*Heterocephalus glaber*), Ring-tailed lemur (*Lemur catta*), Black-and-white colobus (*Colobus guereza*), Tiger (*Panthera tigris*), Pig (*Sus scrofa domesticus*), Sheep (*Ovis aries*), Guinea Pig (*Cavia porcellus*), Hamster (*Mesocricetus auratus*), Chinchilla (*Chincilla lanigera*), Blind mole rat (*Nannospalax ehrenbergi*), Beaver (*Castor canadensis*), Humpback whale (*Megaptera novaeangliae*), Bowhead whale (*Balaena mysticetus*). Maximal lifespan (years) values are from [1]. For cow, human, dog, rabbit, rat, mouse, pig, sheep, guinea pig, and hamster: specific basal metabolic rate (W/g) values are as reported in an earlier table, with references and calculations given at that point. The specific basal metabolic rate (W/g) values for naked mole rat, blind mole rat, chinchilla, lion, tiger, and black-and-white colobus are from [1]. The specific basal metabolic rate (W/g) value for cat is from [68]. In the table, [A] is mitochondrial ROS detected data (mean of superoxide and hydrogen peroxide data, that used to produce columns F and K in the main text's table that reports correlations to mitochondrial ROS detected); data from [57]. Incidentally, the Pearson correlation coefficient between this superoxide and hydrogen peroxide data is 0.6579 (one-tailed, because the alternative hypothesis is directional, p-value is 0.0540995). To remind, these ROS data sets are from reduced systems: Sub-Mitochondrial Particles (SMPs) and isolated mitochondria

respectively. Reporting ROS detected (not ROS generated), after the interdicting action of any antioxidant enzyme(s) present in the experimental preparation (e.g. in the mitochondrial matrix in the case of isolated mitochondria). [B] is mean urinary excretion of (probable) repair products of oxidative DNA damage: 8-oxoGua, 8-oxodG, and 5-HMUra; data from [60]. [C] is DNA substitution (mean of SBS1, SBSB, and SBSC types) rate per year; data from [64]. [D] is mtDNA mutations per mtDNA copy per year; data from [64]. [E] is DNA indel (somatic insertions and deletions) rate per year; data from [64]. [F] is mean (in heart and brain, calculated as specified before in the main text) amount of ROS damage product, 8-oxodG, in mtDNA; data from [63]. [G] is amount of lipid peroxidation product MDA; data from [65]. [H] is median protein degradation rate constant (median K_{deg}), which I *assume* to indirectly report upon (be a function of) the rate of ROS damage of proteins (*hypothesizing* that greater rate of ROS damage to proteins requires/means a greater protein degradation rate); data from [66] (median K_{deg} for bowhead whale herein is mean of that for two bowhead whale individuals in [66]). [I] is *calculated* (from experimental data, not experimental data itself) average epigenetic change per year, ΔM (defined in the main text); included here for comparison to the other variables. Correlations of some variables to the data of [A], [B], [C], [D], [E], [F], [G], [H], [I] have been reported in the main text. Their correlations to each other are in the table below (Pearson correlation coefficients; p-values, in the lower table section, are one-tailed because each alternative hypothesis is directional). It is noteworthy that they are all significant (at $p < 0.05$; even despite some variables being amount of a damage, and others being the rate of a damage). Moreover that they each correlate with the calculated rate of epigenetic change, [I], such that monitoring epigenetic change (e.g. by an epigenetic clock) is likely a good surrogate/proxy for monitoring them all. The high degree of correlation here is consistent with ROS, abstracted by variable [A], driving (at least in part) each of the other variables: [B], [C], [D], [E], [F], [G], [H], [I].

Pearson correlation coefficient (R):									
	[A]	[B]	[C]	[D]	[E]	[F]	[G]	[H]	[I]
[A]	1								
[B]	ID	1							
[C]	ID	0.9517	1						
[D]	ID	0.9449	0.9322	1					
[E]	ID	0.9498	0.9707	0.98	1				
[F]	0.8745	ID	0.9789	0.9864	0.9896	1			
[G]	0.8722	ID	ID	ID	ID	0.7495	1		
[H]	0.9069	ID	0.9422	0.9482	0.9579	ID	ID	1	
[I]	0.8267	0.8876	0.9204	0.8663	0.9121	0.8016	0.8421	0.951	1
p-value (one-tailed):									
	[A]	[B]	[C]	[D]	[E]	[F]	[G]	[H]	[I]
[A]	1								
[B]	ID	1							
[C]	ID	0.0063	1						
[D]	ID	0.0077	5.00E-07	1					
[E]	ID	0.0067	9.92E-10	4E-10	1				
[F]	0.0113	ID	0.001834	0.001	0.0006	1			
[G]	0.0117	ID	ID	ID	ID	0.0262	1		
[H]	0.0168	ID	0.008268	0.007	0.0052	ID	ID	1	
[I]	0.0109	0.0222	1.5E-06	6E-05	3E-06	0.0084	0.0087	4E-06	1
ID = Insufficent Data to calculate									

The asymptotically exact harmonic mean p-value [41] (*its post-published corrected method, as corrected on 7 October 2019*) for all the p-values in the table above = 6.835006e-09 = 0.000000007. Very significant.

Results of mediation analysis between specific basal metabolic rate and maximal lifespan, where the Mediator variable is selected from one of [A], [C], [D], [E], [F], [G], [H], [I] is in the table below (*[B] data (n=5) was too few to perform mediation analysis, and so is absent*). Note that when inputting data into JASP, I multiplied all the specific basal metabolic rate values (W/g) by 10,000, and the values of [H] and [I] each by 100 (rescaled these variables). To prevent "numerical underflow" in the underlying computations performed. Human data was not used by rationale given elsewhere herein. *n* is the number of species used

(constrained by which species I had data for, for each variable).

				95% Confidence			95% Confidence		
Mediator				Interval (CI)			Interval (CI)		
variable	α	β	**Indirect effect (α·β)**	Lower	Upper	**Direct effect (τ)**	Lower	Upper	n
[A]	0.01	-6.1	-0.076	-0.2	0.644	-0.131	-1.028	-0.016	7
[C]	6.8	-0.04	-0.282	-0.55	0.423	0.021	-0.78	0.302	10
[D]	1.4	-0.15	-0.218	-0.556	0.301	-0.044	-0.681	0.296	10
[E]	0.001	-119	-0.142	-0.672	0.189	-0.119	-0.604	0.389	10
[F]	0.04	4.3	0.151	-0.268	0.316	-0.361	-0.644	0.114	7
[G]	0.63	-0.11	-0.071	-0.46	0.296	-0.139	-0.723	0.235	7
[H]	0.16	-1.4	-0.224	-1.137	-0.083	0.002	-0.121	0.73	8
[I]	0.4	-0.8	-0.323	-0.583	-0.204	0.042	-0.116	0.226	16

The only demonstrated Mediator variables here, between specific basal metabolic rate and maximal lifespan, are variables [H] and [I]. Because these are the only assayed variables without zero (0) within their 95% confidence interval for an indirect effect. Mediation is also observed between specific basal metabolic rate and maximal lifespan, via the variable that is the product of variables [H] and [I] multiplied together (data not shown). Maximum lifespan might not be mediated by mitochondrial ROS detected, the variable [A], because of sparse data and/or because the ROS detection experiments were too reduced/artificial (using SMPs and isolated mitochondria) and/or because maximal lifespan isn't a direct function of [ROS], but of ROS damage instead, which is a function of [ROS] *and* repair and/or replacement of ROS damage. For example, in the case of ROS-damaged DNA there is repair. And in the case of ROS-damaged proteins there is repair (e.g. methionine sulfoxide reductases converting {ROS caused} methionine sulfoxide back to methionine [438]) and replacement by protein turnover. Incidentally, mediation analysis with ΔM of variable [I], using larger data sets, is presented in the main text (which observes mediation also).

To interpret all the correlative and mediation analysis up to this point, in both this present section and in the main text (in its combined entirety): it suggests greater specific F_1F_0 ATP hydrolysis drives greater specific basal metabolic rate, which drives greater ROS damage of proteins and epigenetic information, and thereby shorter maximal lifespan. Where specific F_1F_0 ATP hydrolysis also drives greater ROS damage of DNA and lipids, but this isn't a constraint on maximal lifespan. Because ROS damage of proteins and epigenetic information becomes lethal first. In this model, upstream of all these damage variables (of DNA, lipids, proteins, epigenetics) is ROS, and further upstream is F_1F_0 ATP hydrolysis. So, to theorize,

inhibiting F_1F_0 ATP hydrolysis, e.g. by a selective F_1F_0 ATP hydrolysis inhibiting drug (*that doesn't inhibit F_1F_0 ATP synthesis*) of my US patent application [16], slows aging. Perhaps even reverses it, because of extant repair and degradation/turnover processes (e.g. protein turnover). Where decreasing ROS generation (by selectively inhibiting F_1F_0 ATP hydrolysis) is a better strategy than increasing repair/replacement processes. Because the latter requires ATP energy, which inherently generates more ROS (if this ATP is made aerobically), thence actually requiring greater repair/turnover, which subtracts from (and possibly even detrimentally exceeds) any benefit from the increased repair/turnover.

Alternatively, ROS damage of DNA and/or lipids *is* a constraint on maximal lifespan along with one, both or none of ROS damage of proteins and epigenetic information. And just the rather sparse data, and/or perhaps the method, used is insufficient to report this. Indeed, the analysis of the next headed section indicates that ROS damage of DNA and lipids *is* relevant. Unexplored here, ROS damage to other biological macromolecules, e.g. to carbohydrates and/or RNA (e.g., tRNA and mRNA), may be relevant in addition or instead.

There weren't enough species of overlap to get correlations to the data of [439], or to perform mediation analysis therewith. [439] reports that telomere shortening rate inversely correlates with maximal lifespan. ROS are a known drive to telomere shortening [440-444] (and senescence [445-454]). So, selectively inhibiting F_1F_0 ATP hydrolysis, e.g. by a drug in my US patent application [16], is predicted to slow telomere shortening (and delay senescence).

<u>Relative detriment of the different types of molecular damage</u>

I hypothesize that variables [B], [C], [D], [E], [F], [G], [H] and [I] are (at least partially; directly/indirectly) ROS damage (N.B., ROS can cause DNA deletions and insertions [455-458]; ROS damage may increase other forms of damage by being damage of, and/or taking resource(s) {e.g., energy} away from, their repair/replacement/mitigation processes). And that they each correlate with each of specific F_1F_0 ATP hydrolysis, specific basal metabolic rate, and variable [A] (≈intracellular [ROS]) because they are all (at least partially) driven by these three variables. With specific F_1F_0 ATP hydrolysis being a drive of specific basal metabolic rate, which in turn drives variable [A] (≈intracellular [ROS]), which then (at least partially) drives variables: [B], [C], [D], [E], [F], [G], [H], [I]. So F_1F_0 ATP hydrolysis is the most upstream. A drive of all of these other variables. Such that they might all be reduced by

a selective F_1F_0 ATP hydrolysis inhibitor drug (*that doesn't inhibit F_1F_0 ATP synthesis*; e.g. a drug of my US patent application [16]).

Which of these ROS damage variables is most detrimental to maximal lifespan? This was investigated by populating secondary/derived variables (each being the difference between one primary variable and another primary variable) and assaying each of their correlations to maximal lifespan. For example, making a secondary/derived variable consisting of [C]-[D], and finding the Pearson correlation coefficient (R) of this secondary/derived variable with maximal lifespan. A (statistically significant) negative value of R in this case suggests that when [C] is greater relative to [D], maximal lifespan is shorter. Suggesting that [C] is more detrimental to maximal lifespan than [D]. For different example, making a secondary/derived variable consisting of [D]-[E], and finding the Pearson correlation coefficient (R) of this secondary/derived variable with maximal lifespan. A (statistically significant) positive value of R in this case suggests that when [D] is greater relative to [E], maximal lifespan is longer. Suggesting that [D] is less detrimental to maximal lifespan than [E]. The results of this method are in the table below. Columns on the right are the values when human data is included in the analysis. P-values are two-tailed. ID denotes there was insufficient data to calculate ($n<5$).

			With human data	
	R	*p-value*	**R**	*p-value*
[B]-[C]	ID		0.6911	0.196262
[B]-[D]	ID		-0.739	0.153644
[B]-[E]	ID		0.5677	0.318142
[B]-[F]	ID		ID	
[B]-[G]	ID		ID	
[B]-[H]	ID		ID	
[B]-[I]	-0.8437	0.072413	-0.638	0.172758
[C]-[D]	-0.7579	0.002685	-0.597	0.014706
[C]-[E]	-0.7739	0.001162	-0.606	0.016663
[C]-[F]	-0.6808	0.205804	ID	
[C]-[G]	ID		ID	
[C]-[H]	ID		-0.686	0.200878
[C]-[I]	-0.7714	0.000288	-0.598	0.018614
[D]-[E]	0.7191	0.005602	0.541	0.045748
[D]-[F]	0.6451	0.239829	ID	
[D]-[G]	ID		ID	
[D]-[H]	ID		-0.075	0.904978
[D]-[I]	0.8434	0.000292	0.6625	0.00983
[E]-[F]	-0.6481	0.236915	ID	
[E]-[G]	ID		ID	
[E]-[H]	ID		-0.629	0.256125
[E]-[I]	-0.7327	0.002876	-0.543	0.03638
[F]-[G]	0.8089	0.027582	ID	
[F]-[H]	ID		ID	
[F]-[I]	-0.5918	0.122234	ID	
[G]-[H]	ID		ID	
[G]-[I]	-0.8061	0.028558	ID	
[H]-[I]	0.5474	0.081342	0.6174	0.032437
ID = Insufficient Data to calculate				

The relative order of detriment (to maximal lifespan), from worst to least:

[C] > [E] > [B] > [G] > [F] > [I] > [H] = [D].

The equal placing between [H] and [D] is solely from the data set that includes human data. Since it is set by less data, it has less basis. The relative placing of [B] is very unconstrained by the data and so might be wrong. But where [B] and [F] are redundant anyhow, each being better represented by [C] and [D] respectively, because of their greater number of data points. The relative order, with [B] and [F] omitted:

[C] > [E] > [G] > [I] > [H] = [D].

To interpret, the most detrimental (to maximal lifespan) form of damage appears to be to genomic DNA (in the nucleus), which both [C] and [E] relate to. Then it is damage of lipids,

[G]. Next (calculated) epigenetic damage, [I]. Then (inferred) damage of proteins, [H], and damage to mtDNA, [D], as equally deleterious. But this ordering should be considered provisional. Because of the unequal number of data points in each variable. And the low number of data points in each variable. But it is sufficient to hint at a strategy that nature may use to get a slightly higher maximal lifespan in some species. To concede more of one type(s) of ROS damage in order to have less of another (more deleterious) type(s) of ROS damage. Because not all types of ROS damage are equally deleterious (to maximal lifespan). But since they are all deleterious (hypothesized: a multifactorial drive of aging), all be it unequally so, the margin for extending maximal lifespan using this strategy is likely very constrained. A better strategy is just to have less ROS generated. Which may also be a strategy nature uses. Achieving it by bigger mammal body size (e.g. 100,000 kg of adult bowhead whale), permitting a lower specific basal metabolic rate (less ROS generated) to keep body temperature at ~37°C, enabling a longer maximal lifespan.

Damage to genomic DNA is probably most deleterious because a single damage there has the potential to deleteriously change the sequence of many copies of a protein, or to reduce/stop/increase the expression of one or more protein types. Single damage to a lipid can be very deleterious because some products of lipid peroxidation are themselves ROS, which can attack further lipid molecules [459]. So, lipid peroxidation can be an autocatalytic, self-propagating process (a peroxidative chain reaction; positive feedback loop; amplifying ROS damage). Which can in turn damage, corrupting the operation of, other cellular components (e.g. peroxidized cardiolipin, in the inner mitochondrial membrane, can inactivate Complex IV [460]). Single damage to epigenetic information may have the potential to reduce/stop/increase the expression of one or more protein types. Single damage to a single protein copy is, by contrast to the aforementioned, likely to be relatively inconsequential. Single damage to a single mtDNA copy has the potential to deleteriously change the sequence of many copies of a protein, or to reduce/stop/increase the expression of one or more protein types. But this isn't as problematic as with genomic DNA because there are multiple mtDNA copies, in a single mitochondrion, and across mitochondria. To remind, the detriment equivalence between [H] and [D] is very unconstrained by data, and is especially provisional.

It is interesting that variables [H] and [I] are low down in the afore-presented ordering. When these were the only of this set of variables reported mediatory between specific basal

metabolic rate and maximal lifespan in the prior section herein. Perhaps because these variables tend to have less repair and/or replacement (indeed, because their damage is less deleterious). And so their damage is a much more direct function of (ROS generation by) specific basal metabolic rate.

My interpretation: total ROS damage is divided unequally across a number of different types of ROS damage. To different types of biological macromolecules/information. Wherein different species may differ in how their total ROS damage is fractionated amongst different ROS damage types. Some species electing for less ROS damage of one type(s), perhaps because that type(s) confers greater detriment (e.g. to maximal lifespan) per unit of damage, inherently conferring more ROS damage of another type(s). But the margin that this can extend maximal lifespan is limited. Because all/much ROS damage is detrimental, and I hypothesize is a multifactorial (possibly synergistic) drive to aging. Some species may elect to have greater repair and/or replacement as regards some type(s) of ROS damage, but the margin in this is limited because it requires ATP energy (so more food), which inherently (if this ATP is made aerobically) generates ROS, creating more ROS damage (moreover, when something is being repaired its use is typically impaired/prevented). And so maximal lifespan is still very much just a function specific basal metabolic rate (which sets ROS generation rate). Examples of strategies (correlating with maximal lifespan) used to decrease ROS damage of one type (presumably increasing ROS damage of other type[s]) include less cysteine [461] and methionine [462] usage in mitochondrial encoded proteins, decreasing their susceptibility to oxidation damage. Or a lower degree of membrane fatty acid unsaturation (less double bonds), which decreases their susceptibility to peroxidation [459]. Or greater GC (thence lower AT) content of mtDNA, conferring more negative free energy of mtDNA (strands more tightly bound to each other and so less regions of separation/single-stranded mtDNA over time), making it less susceptible to oxidative damage [463]. Or more "junk DNA", which I hypothesize (by being sacrificially ROS damaged and repaired) reduces the probability of ROS damage to non-junk DNA, wherein more (seemingly) junk DNA in mtDNA correlates with longer maximal lifespan [464-465]. Species differ in their investment in antioxidant defences (shorter-living mammal species, with greater ROS generation, have greater amounts of antioxidant enzymes [466-467]) which, depending upon their cellular location(s), presumably interdict some forms of ROS damage more than others. But antioxidant molecules can only do so much because they must be outnumbered by other working molecules of the cell, in order for the cell to work properly. And so an ROS, in bulk

cytoplasm (or even in bulk mitochondrial matrix), is always more likely to cause damage than be mitigated. Better than ROS mitigation (and better than letting ROS damage occur, and then trying to repair it) is less ROS generation (*especially because both the ROS mitigation and ROS damage repair systems use energy, requiring more food intake*). Herein, in the main text, selective F_1F_0 ATP hydrolysis inhibition is shown to substantially decrease ROS generation (Figure 5).

Scaling with adult body mass

A log-log plot (base 10) of variable (one of [A], [B], [C], [D], [E], [F], [G], [H], [I]) vs. adult body mass (kg; data sourced from [1]; mass of ferret, *Mustela furo*, taken as that of *Mustela putorius*, which is likely its wild form) has a best fit line $\log_{10}(y) = \log_{10}(a) + b \cdot \log_{10}(x)$, where *b* is gradient. This gradient value (with error bar) is shown for each variable below (n is number of species):

	Gradient	Error	n
[A]	-0.20096	0.02811	7
[B]	-0.23092	0.0501	6
[C]	-0.10649	0.05859	15
[D]	-0.12647	0.05655	14
[E]	-0.16437	0.08396	15
[F]	-0.07578	0.02089	8
[G]	-0.09078	0.03472	7
[H]	-0.03782	0.00784	13
[I]	-0.12987	0.02217	22

Too few data points can lead to a misleading gradient, which (at least partially) explains the discrepancy between [B] and [C] (which relate to amount and rate of damage respectively). To illustrate, when a subset of [C] is used, with just 5 species (those species overlapping with variable [B]), the gradient is instead -0.28, i.e. very different. Both variables [D] and [F] relate to mtDNA (rate and amount of damage respectively), but they have very different gradients. Where that of [D] is given precedence because [D] has more data points (and because [F] comprises data of individuals, in different species, of very different "biological ages" {chronological age as % of maximal lifespan}, as mentioned in the main text, and so arguably its data isn't as controlled). It might be argued that there are too few data points (too low value of n) for all the variables here to draw any conclusions as to their gradients.

Variable [I] is ΔM for a species set. Using a larger species set: those eutherian species probed by the mammalian methylation array [119] (used by [100]), the subset thereof which have their maximal lifespan and adult body mass reported in [1] (n=115): the gradient is -0.10631 (±0.01007). So, somewhat close to the gradient value for [I] here, but still 18% different. Generally speaking, more species in the set makes the gradient value more accurate.

For the full number of species (n=24), which each of the variables [A] through to [I] has data for a subset of, the gradient of a log-log (base 10) plot of maximal lifespan (data from [1]; excluding human, so n=23) vs. adult body mass is +0.18125 (Error = ±0.03169). Which has +20 within its margin of gradient error, which corresponds to the exponent value reported for a set of eutherian species in [468]. Variable [A] (which is the mean of superoxide output from Sub-Mitochondrial Particles {SMPs} and hydrogen peroxide output from isolated mitochondria) has a gradient of -0.20. Why don't the variables (hypothesized to be) of ROS damage, variables [B] through to [I], simply inherit this gradient of -0.20? Perhaps because of the protective action of antioxidant enzymes (some of which are extra-mitochondrial), whose activities have a steeper negative gradient with adult body mass (as shown later), which shallows the gradients of these ROS damage variables. Whose gradients aren't equal because they are different functions of [ROS]. Presumably because of different cellular locations, different susceptibilities to ROS damage, and different repair and replacement capacities. Maximal lifespan vs. adult body mass may have a steeper gradient (of opposite sign) than any single kind of ROS damage because it is a (possibly synergistic) function of their combination. An aggregate function with closer fidelity to the amount of ROS generation by specific basal metabolic rate.

To define some further variables, populated with antioxidant activity data across different species: variable [J] is catalase enzyme activity (units/gram) in liver, variable [K] is selenium-dependent GSH-peroxidase enzyme activity (μmol NADPH/min.g) in liver. Data sourced from [466]. Somewhat non-intuitively, smaller (shorter-living) species have *more* (per unit mass) of these antioxidant enzymes. Presumably because they have greater ROS generation, and so a greater need for them. For a log-log (base 10) plot of [J] or [K] vs. adult body mass (kg; data from [1]; *assuming* that pig-tailed macaque and baboon in [466] were *Macaca nemestrina* and *Papio hamadryas* respectively), where *n* is number of species:

	Gradient	Error	n
[J]	-0.6954	0.15772	5
[K]	-0.35914	0.07373	5

To interpret the data of this section, the negative gradient of [J] and [K], relating to antioxidant enzymes, being steeper than the negative gradient of [A], makes the negative gradient of the ROS damage variables shallower than that of [A]. Where the salient ROS damage variables here are [C], [D], [E], [G], [H], [I]. Dismissing variables [B] and [F] because they are inferior (less data) and redundant to variables [C] and [D].

Incidentally, the gradient in the case of using telomere shortening rate data (bp/year; from [439]; adult body mass data sourced from [1]) is -0.25621 (±0.11533). With the caveat that it is drawn from only 9 data points.

Supplementary content for the Results section titled "Numerical prediction observed"

The table below shows correlations (R is the Pearson correlation coefficient, and p-values are one-tailed, because each alternative hypothesis is directional) to the *absolute* value of the resting mitochondrial membrane potential, $|\Psi_{IM}|$. Ψ_{IM} data (mV) is from [469], from isolated hepatocytes. For correlations to (s/v) and l, $n = 6$, because the number of overlapping species was 6. For the other correlations shown, $n = 5$. There weren't enough overlapping species to calculate correlations to g and w. At least across species, for these species, the greater the proton leak, l, the smaller the value of $|\Psi_{IM}|$, i.e. the less hyperpolarised the mitochondrial membrane potential. Proton leak is attenuating to the proton motive force (pmf), and its Ψ_{IM} component. As is futile cycling of F_1F_0 ATP synthesis (pmf dissipation) and F_1F_0 ATP hydrolysis (pmf creation), because no energy conversion can be 100% efficient (2nd Law of Thermodynamics). At least across species, for these species, the less hyperpolarised the mitochondrial membrane potential (i.e. the smaller the value of $|\Psi_{IM}|$), the shorter the maximal lifespan.

		(s/v)	l	h	Specific basal metabolic rate	Heart rate	Maximum lifespan
|ΨIM|	R	-0.6482	-0.7588	-0.7818	-0.8956	-0.899	0.8712
	p	0.081938	0.0401	0.05913	0.0199265	0.018971	0.027202

Proton leak is not only an (attenuating) input into Ψ_{IM}, but also a function of it. Wherein greater Ψ_{IM} is an Ohmic, or supra-Ohmic, drive to greater proton leak. The proton leak

variable used herein, *l*, is the proton leak when Ψ_{IM} is fixed at a value of -170 mV (and when ATP synthase is blocked by oligomycin). But, as referred to earlier, the different species don't have the same (resting) value of Ψ_{IM}. And so then there is a question mark over the fidelity of *l* to the actual proton leaks of these species. So use of *l* herein is with this caveat.

A new variable, *l* divided by resting Ψ_{IM}, would be interesting to explore. But there weren't enough shared species to calculate Pearson correlation coefficients for it.

Caveat

For expediency of explanation, at some points in the paper I write as though all homeothermic species maintain a body temperature of (around) 37°C. Although this is true for many (possibly most) homeothermic mammals (e.g. mice and humans [1]), it certainly isn't true for all. For example, the naked mole rat (*Heterocephalus glaber*) maintains a body temperature of (around) 32°C instead [1].

Synthesis of 6a and 6b (*6b administered to mice in Figure 2; anti-cancer data in Figure 12*)

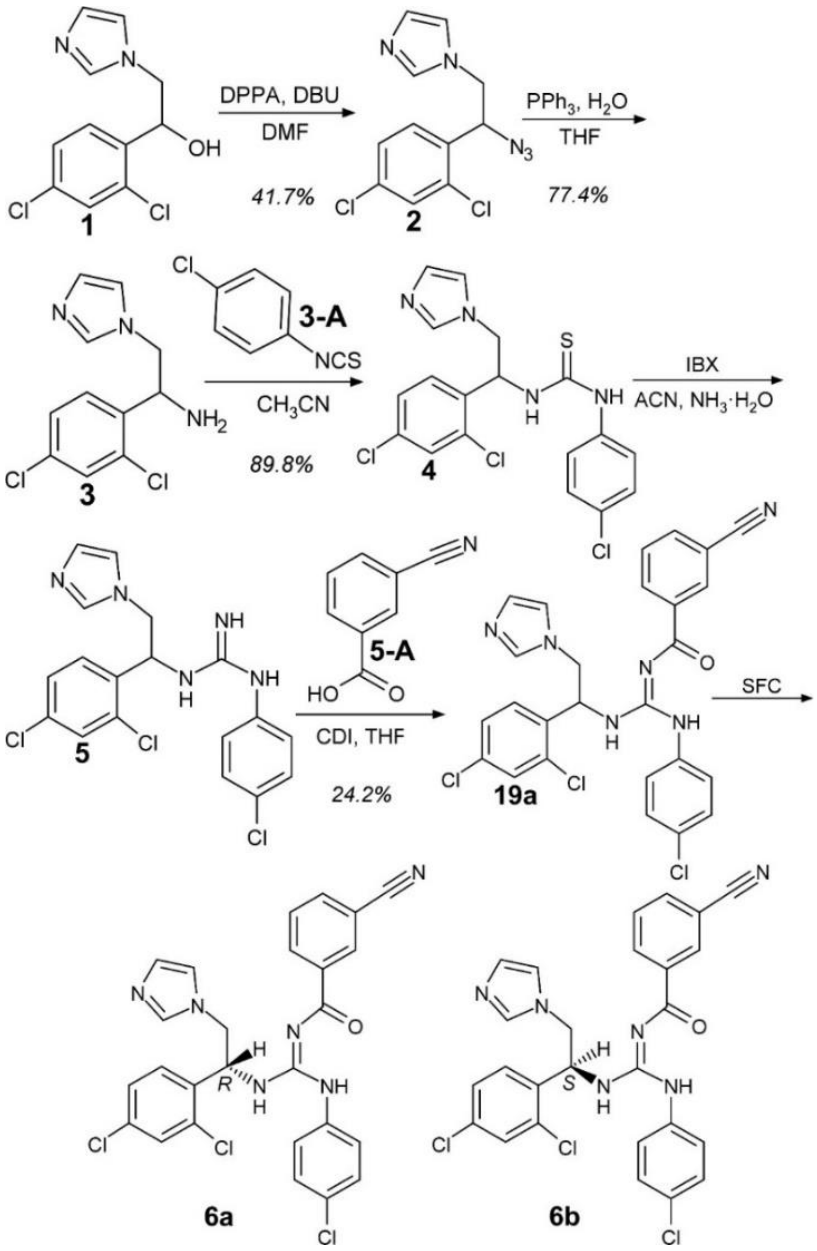

6a {enantiomeric excess (ee) ≥97%}: Liquid Chromatography-Mass Spectrometry (LC-MS): Liquid Chromatography (LC) Retention Time (RT) = 2.516 minutes, Mass spectrometry (MS; electrospray ionization, positive mode): *m/z* 537.1 $[M+H]^+$, 559.1 $[M+Na]^+$, 269.1 $[M+2H]^{2+}$.

^{1}H NMR (400 MHz, DMSO-*d6*) δ (ppm) 11.43 (s, 1H), 8.30 (s, 1H), 8.21 (d, J = 7.9 Hz, 1H), 7.93 (d, J = 7.8 Hz, 2H), 7.67 – 7.56 (m, 3H), 7.50 (t, J = 6.5 Hz, 4H), 7.20 (s, 1H), 7.09 (d, J = 8.2 Hz, 2H), 6.97 (s, 1H), 5.96 (s, 1H), 4.34 (s, 1H), 4.19 (s, 1H). {*NMR probe temperature = 298.15 K*}.

6b {enantiomeric excess (ee) ≥97%}: Liquid Chromatography-Mass Spectrometry (LC-MS): Liquid Chromatography (LC) Retention Time (RT) = 2.516 minutes, Mass Spectrometry

(MS; electrospray ionization, positive mode): *m/z* 537.1 $[M+H]^+$, 559.1 $[M+Na]^+$, 269.1 $[M+2H]^{2+}$.

^{1}H NMR (400 MHz, DMSO-*d6*) δ (ppm) 11.43 (s, 1H), 8.30 (s, 1H), 8.21 (d, J = 7.9 Hz, 1H), 7.93 (d, J = 7.8 Hz, 2H), 7.68 – 7.56 (m, 3H), 7.56 – 7.46 (m, 4H), 7.20 (s, 1H), 7.09 (d, J = 8.1 Hz, 2H), 6.97 (s, 1H), 5.96 (s, 1H), 4.33 (s, 1H), 4.19 (s, 1H). {*NMR probe temperature = 298.15 K*}.

The presented Nuclear Magnetic Resonance (NMR) peaks are from using the "Auto Assignment" algorithm in MestReNova version 12 software (Mestrelab Research, Santiago de Compostela, Spain). Which picks peaks in an inputted NMR spectrum, influenced by an inputted structure, which was structure 19a in the reaction scheme above.

<u>Performed synthesis of 6a and 6b in detail</u>

In this section, numbers in square brackets are CAS numbers.

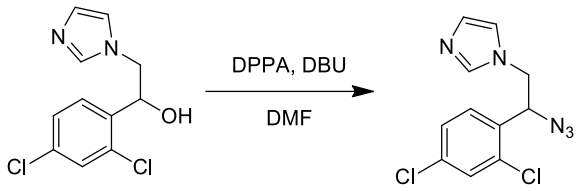

1 **2**

1. Charged Compound 1 [24155-42-8] (10.0 g, 1.00 X by weight) and DPPA [26386-88-9] (10.7 g, 1.07 X by weight) in DMF [68-12-2] (50 mL, 5.00 X by volume).
2. Charged DBU [6674-22-2] (5.90 g, 0.59 X by weight) into the mixture, under nitrogen atmosphere at 0°C, then stirred for about 15 minutes.
3. After that, took the reaction mixture to 20-30°C and stirred for 24 hours.
4. Thin-Layer Chromatography (TLC; DCM/MeOH = 10/1, R_f = 0.6) showed raw material remained, LC-MS (Starting Material [SM]: RT = 0.729 minutes, Product: RT = 0.822 minutes) indicated reaction mixture had desired product.
5. The reaction mixture was extracted with EtOAc (100 mL x 3).
6. The combined organic phase was washed with aq.NaCl (100 mL), dried with Na_2SO_4, filtered and concentrated in vacuum to get the residue.
7. The residue was purified by column chromatography (DCM/MeOH = 1/0 to 100/1).
8. Compound 2 (4.82 g, 41.7%, 95% purity) was obtained as a yellow oil, which was confirmed by ^{H}NMR and HPLC (Retention Time (RT) = 1.919 minutes).

Compound 2: ^{1}H NMR ($CDCl_3$, 400 MHz) δ (ppm) 7.47 (d, J = 2.2 Hz, 1H), 7.41 (s, 1H), 7.33 - 7.28 (m, 1H), 7.26 - 7.23 (m, 1H), 7.06 (s, 1H), 6.92 (s, 1H), 5.26 (m,1H), 4.23 (m, 1H), 4.02 (m, 1H).

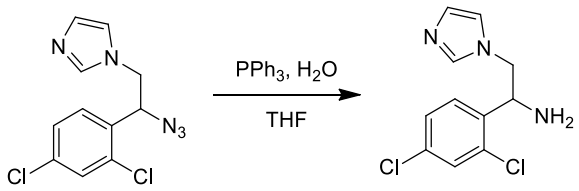

2 **3**

1. Charged Compound 2 (3.00 g, 1.00 X by weight) and PPh_3 [603-35-0] (8.40 g, 2.80 X by weight) in H_2O (1 mL, 0.33 X by volume) and THF [109-99-9] (10 mL, 3.33 X by volume).
2. Stirred at 70°C for 24 hours.
3. Checked the reaction by LC-MS (SM: RT = 0.822 minutes, Product: RT = 0.299 minutes), it showed that Compound 2 was consumed completely, and that the desired mass was detected.
4. The reaction mixture was concentrated under reduced pressure to remove THF.
5. The reaction mixture was added with H_2O (30 mL), adjusted pH to 3 with con.HCl and washed with EtOAc (30 mL).
6. After that, collected water phase, adjusted pH to 13 with 1N aq.NaOH, then exacted with EtOAc (30 mL x 2).
7. The combined organic phase was washed with aq.NaCl (30 mL), dried with Na_2SO_4, filtered, and concentrated in vacuum to obtain the product.
8. Compound 3 (2.23 g, 77.4%, 94.5% purity) was obtained as a yellow liquid, which was confirmed by ^{H}NMR and HPLC (Retention Time = 0.658 minutes).

Compound 3: ^{1}H NMR ($CDCl_3$, 400 MHz) δ (ppm) 7.48 - 7.37 (m, 3H), 7.30 - 7.26 (m, 1H), 7.06 (s, 1H), 6.91 (s, 1H), 4.72 (m, 1H), 4.21 (m, 1H), 3.91 (m, 1H).

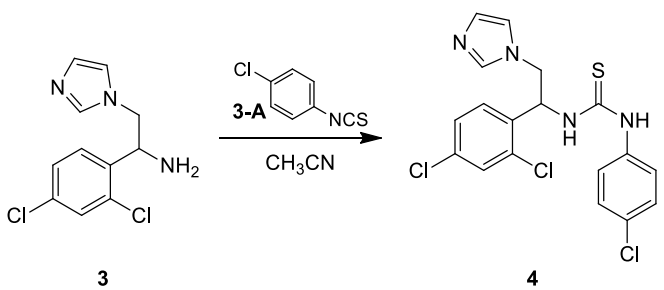

3 **4**

1. Charged Compound 3 (2.00 g, 1.00 X by weight) and Compound 3-A [2131-55-7] (1.30 g, 0.65 X by weight) in CH_3CN [75-05-8] (30 mL, 15.00 X by volume).
2. Stirred at 20-30°C for 12 hours.
3. Checked the reaction by TLC (DCM/MeOH = 10/1, R_f = 0.7) and LC-MS (SM: RT = 0.299 minutes, Product: RT = 0.949 minutes), desired product was detected, TLC indicated Compound 3 was consumed completely.
4. The reaction mixture was concentrated under reduced pressure to remove CH_3CN to obtain the residue.
5. The residue was purified by column chromatography (DCM/MeOH = 1/0 to 50/1).
6. Compound 4 (2.95 g, 89.8%, 99.7% purity) was obtained as a white solid, which was confirmed by ^{H}NMR and HPLC (Retention Time = 2.521 minutes).

Compound 4: ^{1}H NMR (DMSO-*d6*, 400 MHz) δ (ppm) 9.81 (s, 1H), 8.54 (d, J = 7.5 Hz, 1H), 7.64 (s, 1H), 7.55 (s, 1H), 7.53 - 7.48 (m, 1H), 7.45 - 7.41 (m, 1H), 7.38 (d, J = 8.6 Hz, 2H), 7.28 (d, J=8.4 Hz, 2H), 7.11 (s, 1H), 6.94 (s, 1H), 6.03 (s, 1H), 4.46 - 4.34 (m, 1H), 4.31 - 4.22 (m, 1H).

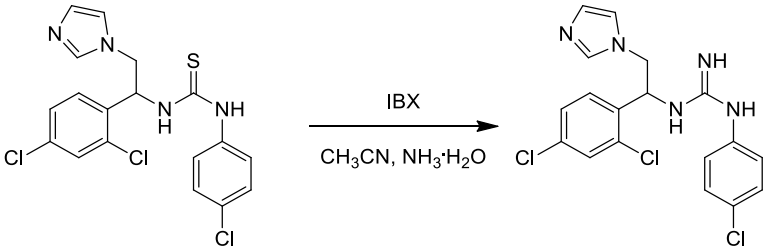

4 **5**

1. Charged Compound 4 (1.63 g, 1.00 X by weight) and IBX [61717-82-6] (1.18 g, 0.75 X by weight) in CH_3CN [75-05-8] (16 mL, 10.00 X by volume) and $NH_3.H_2O$ [1336-21-6] (8 mL, 5.00 X by volume).
2. Stirred at 20-30°C for 18 hours.
3. Checked the reaction by LC-MS (SM: RT = 0.949 minutes, Product: RT = 1.050 minutes) and HPLC (SM: RT = 2.535 minutes, Product: RT = 1.757 minutes), desired product was detected.
4. The reaction mixture was extracted with EtOAc (20 mL x 3).
5. The combined organic phase was washed with aq.NaCl (20 mL), dried with Na_2SO_4, filtered and concentrated *in vacuo* to obtain the crude product (1.0 g, white solid), which was used into next step directly.

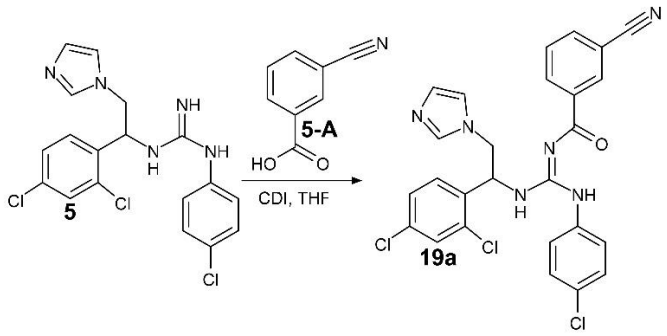

1. Charged Compound 5-A [1877-72-1] (0.36 g, 0.36 X by weight) and CDI [530-62-1] (0.40 g, 0.36 X by weight) in THF [109-99-9] (20 mL, 20.00 X by volume), stirred at 20-30°C for 3 hours.
2. Charged Compound 5 into the reaction mixture, stirred at 20-30°C for 14 hours.
3. Checked the reaction by LC-MS (SM: RT = 1.050 minutes, Product: RT = 1.347 minutes) and TLC (DCM/MeOH = 10/1, R_f = 0.75), desired mass was detected. TLC indicated the raw material was consumed completely.
4. The reaction mixture was concentrated under reduced pressure to remove THF.
5. The reaction mixture was extracted with EtOAc (20 mL x 3)
6. The combined organic phase was washed with aq.NaCl (20 mL), dried with Na_2SO_4, filtered and concentrated *in vacuo* to obtain the residue.
7. The residue was purified by column chromatography (DCM/MeOH = 1/0 to 100/1) and chiral SFC {column: AD (250 mm*50 mm, 10 μm); mobile phase: [0.1%NH_3H_2O IPA]; B%: 28%-28%, 3.5 minutes} separating the stereoisomers of Compound 19a: 6b (0.17 g, SFC RT = 2.35 minutes) was obtained as a white solid, 6a (0.15 g, SFC RT = 2.69 minutes) was obtained as a white solid.

Abbreviations used: Ph=phenyl, MeOH=methanol, CDI=1,1'-carbonyldiimidazole, DCM=dichloromethane, DBU=1,8-diazabicyclo[5,4,0]undec-7-ene, DMF=N,N-dimethylformamide, DPPA=diphenylphosphoryl azide, EtOAc=ethyl acetate, IBX=2-iodoxybenzoic acid, IPA=isopropanol, R_f=retention value, RT=retention time, THF=tetrahydrofuran, TLC=thin-layer chromatography, SM=starting material, SFC=chiral supercritical fluid chromatography, LC-MS=Liquid Chromatography Mass Spectrometry, HPLC=High-performance liquid chromatography, NMR=Nuclear magnetic resonance, aq.=aqueous, con.=concentrated, MeCN=methyl cyanide (acetonitrile), DMSO=dimethyl sulfoxide.

Spectral data for 6b

Its expected/calculated *m/z*, from its structure (Figure 2), using the "exact molecular weight" calculator in MarvinSketch software (Chemaxon, Budapest, Hungary), which uses the mass of the *most prevalent* isotope of each element in the molecule:
537.08 $[M+H]^+$, 559.06 $[M+Na]^+$, 269.04 $[M+2H]^{2+}$, 575.03 $[M+K]^+$).

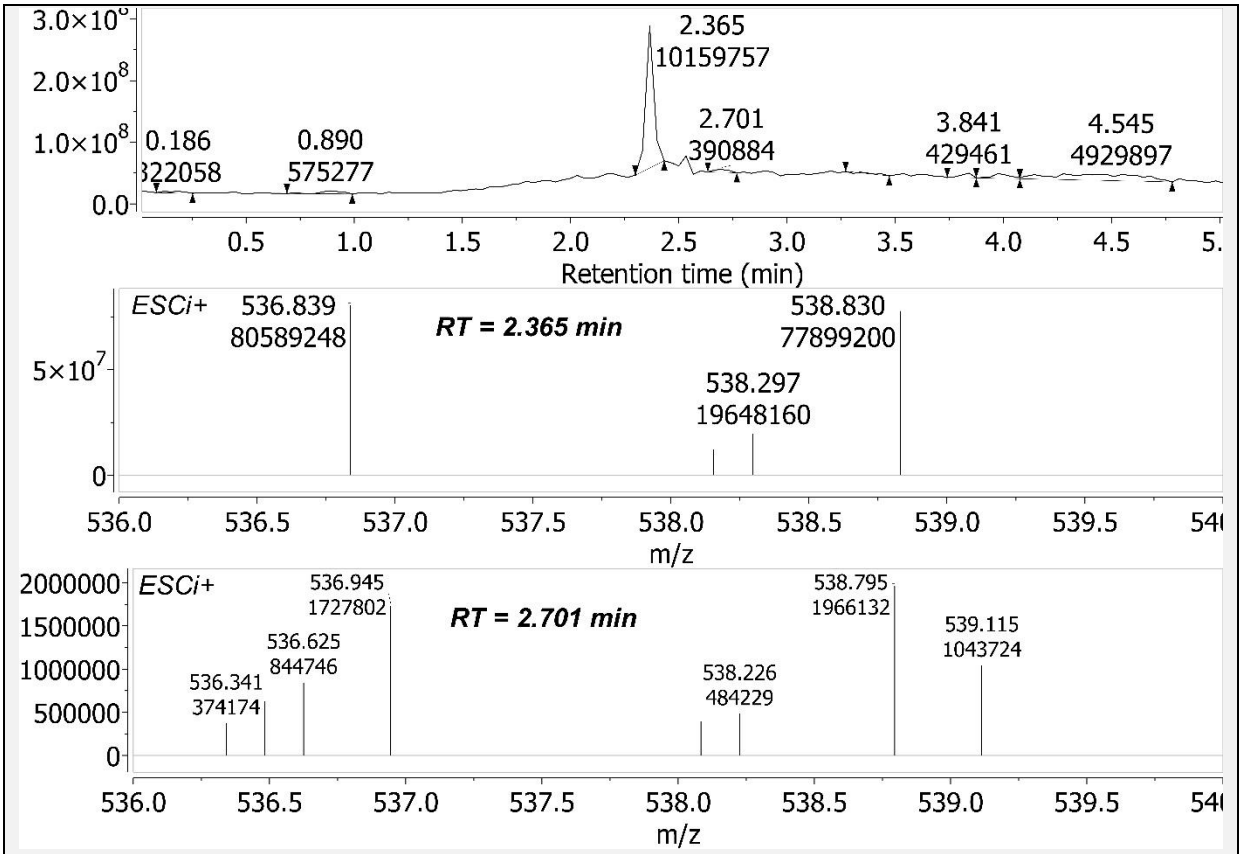

Figure 16 - Chiral Supercritical Fluid Chromotography Mass Spectrum (chiral SFC-MS) of 6b sample. *Upper panel*: Chiral-SFC annotated with Retention Time (RT, minutes), and area under peak. *S* stereoisomer is found in the [RT=2.365] peak. *Middle panel*: Component of the Mass Spectrum (MS) of the [RT=2.365] peak. Therein is *m/z* 536.839 $[M+H]^+$ (*0.19 removed from Expected. Better concordance in subsequent spectra*). Y-axis presents intensity. ESCi™ is multi-mode ionization (PCT/US03/16892), which switches at very high speed between Electrospray Ionization (ESI) and Atmospheric Pressure Chemical Ionization (APCI) ionization methods. ESCi+ refers to using ESCi in its positive ionization mode. Polarity positive. *Bottom panel*: Component of the Mass Spectrum (MS) of the [RT=2.701] peak.

Using this present figure, *S* stereoisomer excess (%) in this sample = (80589248/(80589248+1727802))*100 = 97.9%; enantiomeric excess (ee, %) = (97.9-50)*2 = 95.8%. Calculating the ee directly, rather than via the stereoisomer excess, ee =

((80589248-1727802)/(80589248+1727802))*100 = 95.8%. Working back from this ee to the stereoisomer excess: (95.8/2)+50 = 97.9%.

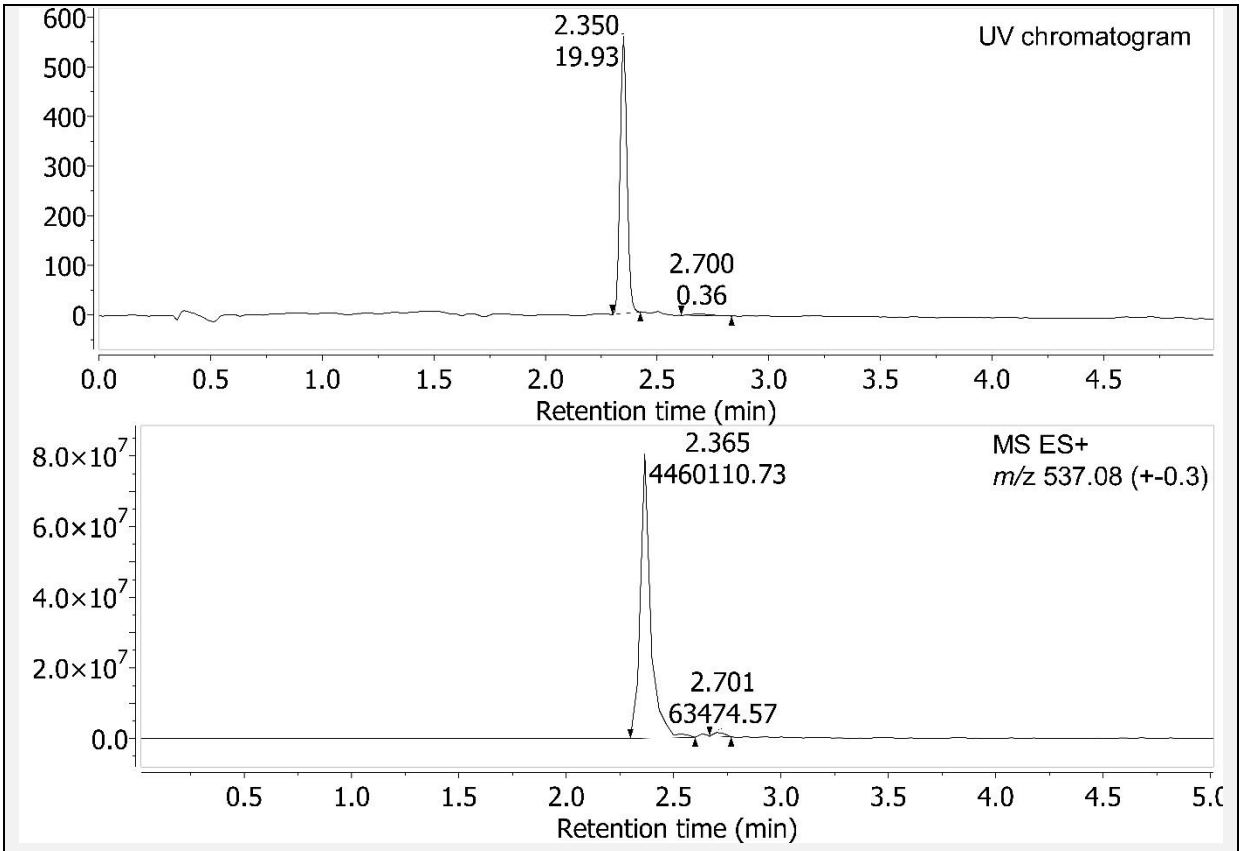

Figure 17 – Chiral Supercritical Fluid Chromotography (chiral-SFC) of 6b sample. Using the UV Chromatogram component, *S* stereoisomer excess (%) in this 6b sample = (19.93/(19.93+0.36))*100 = 98.23%; enantiomeric excess (ee) = (98.23-50)*2 = 96.46%.

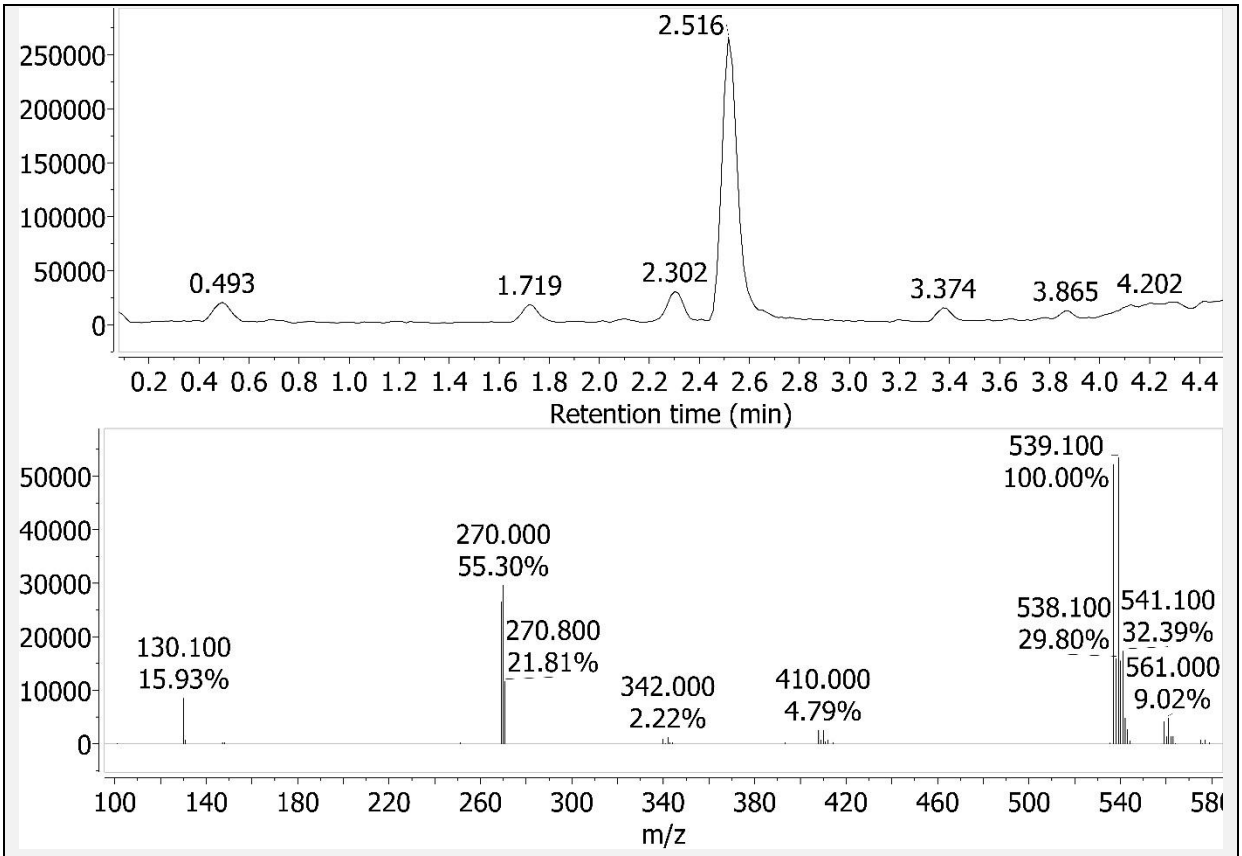

Figure 18 - Liquid Chromatography–Mass Spectrometry (LC-MS) spectrum for 6b sample. *Upper panel*: Liquid Chromatography (LC) Retention Time (RT) = 2.516 minutes. *Lower panel*: Mass Spectrum (MS) of the [RT peak=2.516]. Shows positively charged species: "Ionization mode = API-ES" and "Polarity = Positive". Wherein API is "Atmospheric Pressure Ionization". And ES is Electrospray. Percentages are relative abundance.

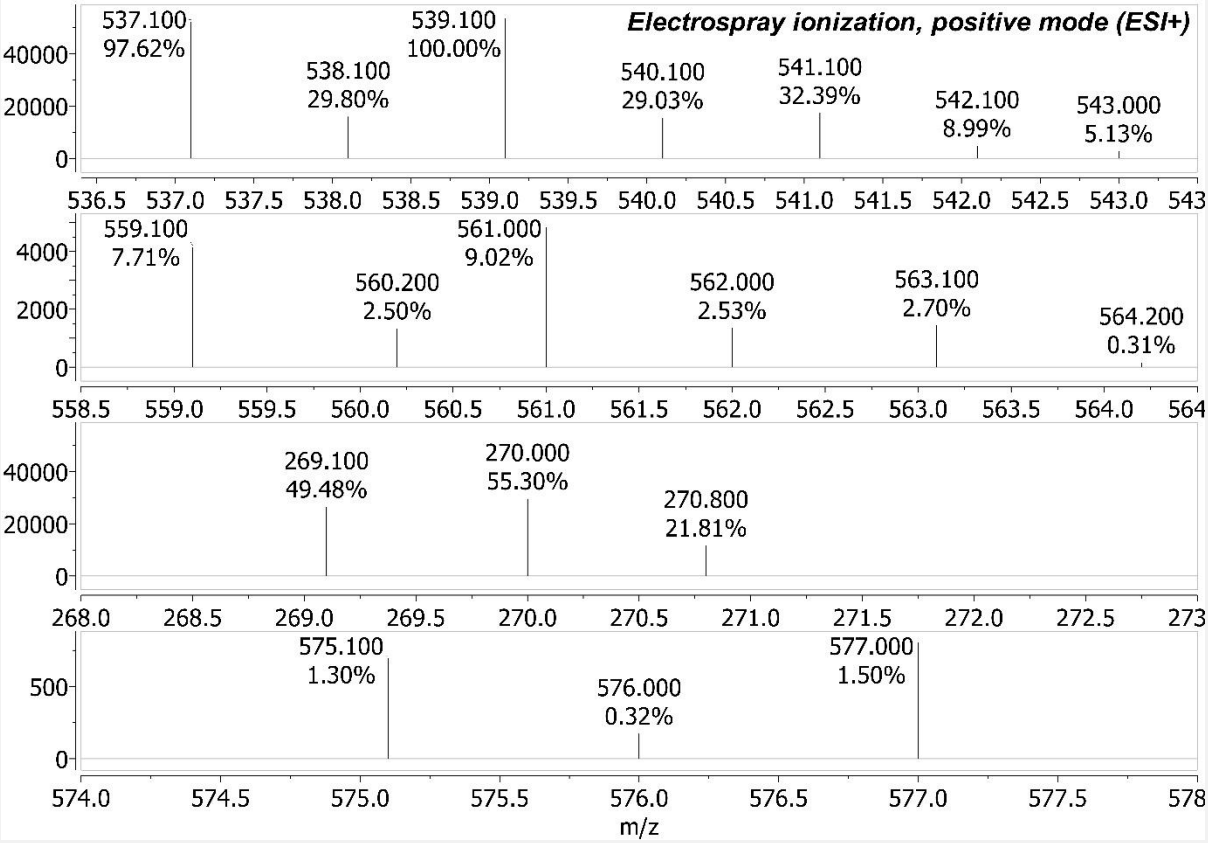

Figure 19 – Some Mass Spectrum (MS) components of Figure 18. *Upper panel*: *m/z* 537.1 $[M+H]^+$. *2nd panel*: *m/z* 559.1 $[M+Na]^+$. *3rd panel*: *m/z* 269.1 $[M+2H]^{2+}$. *Bottom panel*: *m/z* 575.1 $[M+K]^+$. All these Observed *m/z* are within 0.07 of Expected.

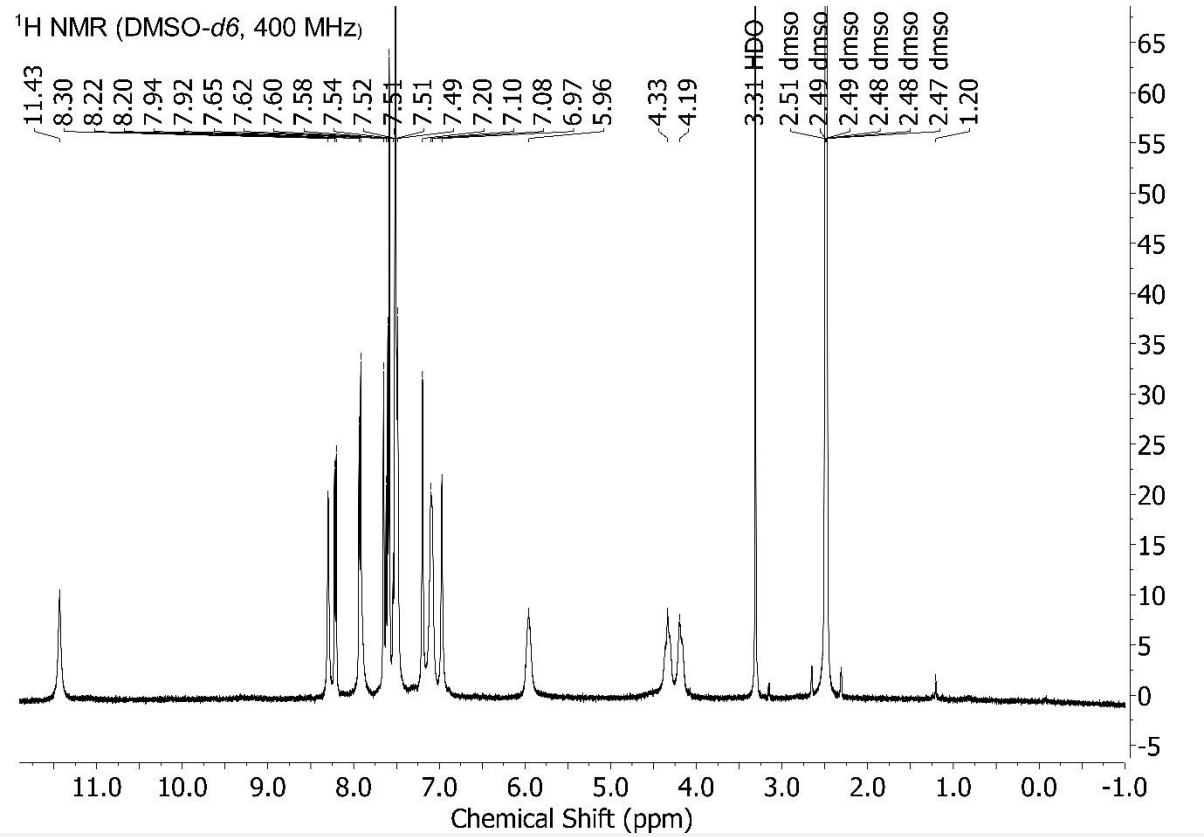

Figure 20 - ^{1}H NMR {*NMR probe temperature = 298.15 K*} for 6b sample. Scaled to the highest compound peak. Peaks identified by the "Auto peak picking" algorithm (based on Global Spectral Deconvolution, GSD) of MestReNova version 12 software. With default program settings used. And no chemical structure used/inputted to guide/constrain this peak picking.

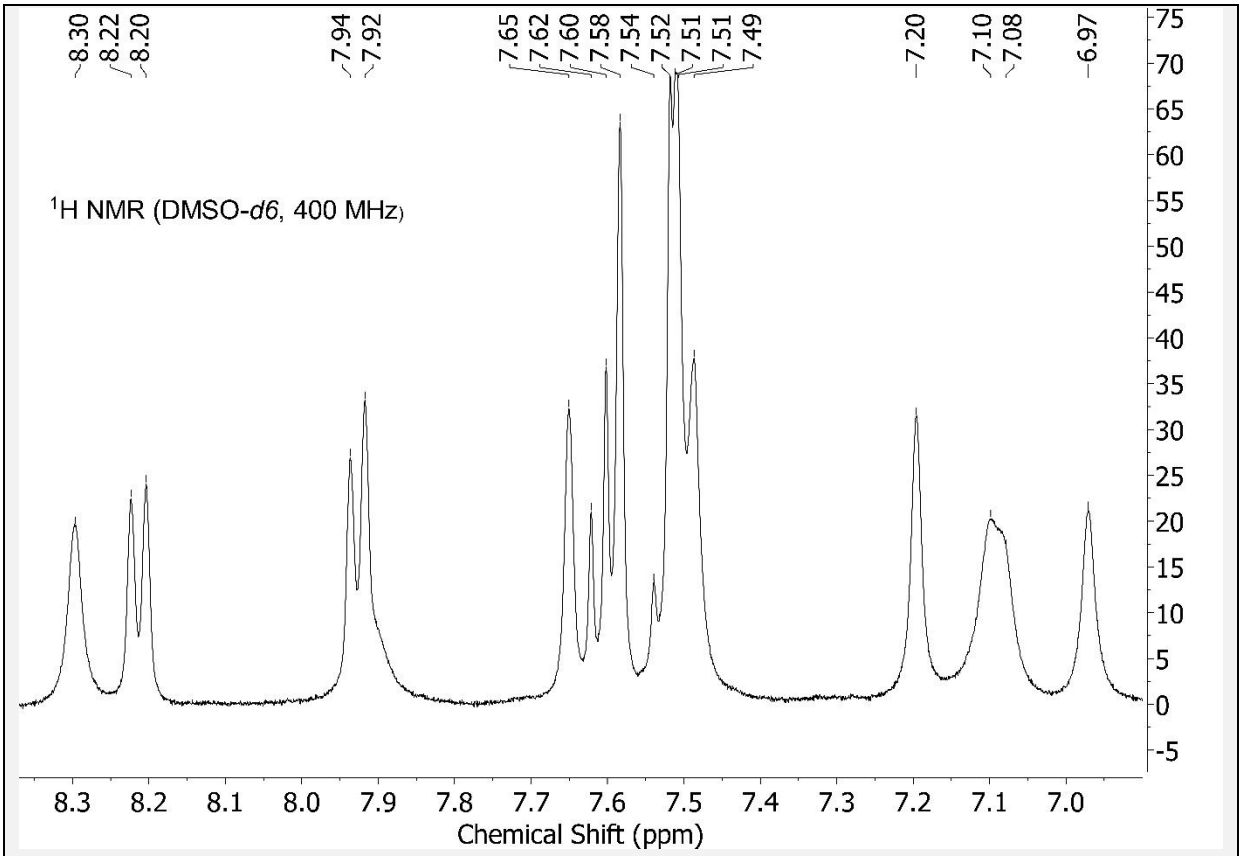

Figure 21 - Aromatic region of Figure 20 expanded.

Spectral data for 6a

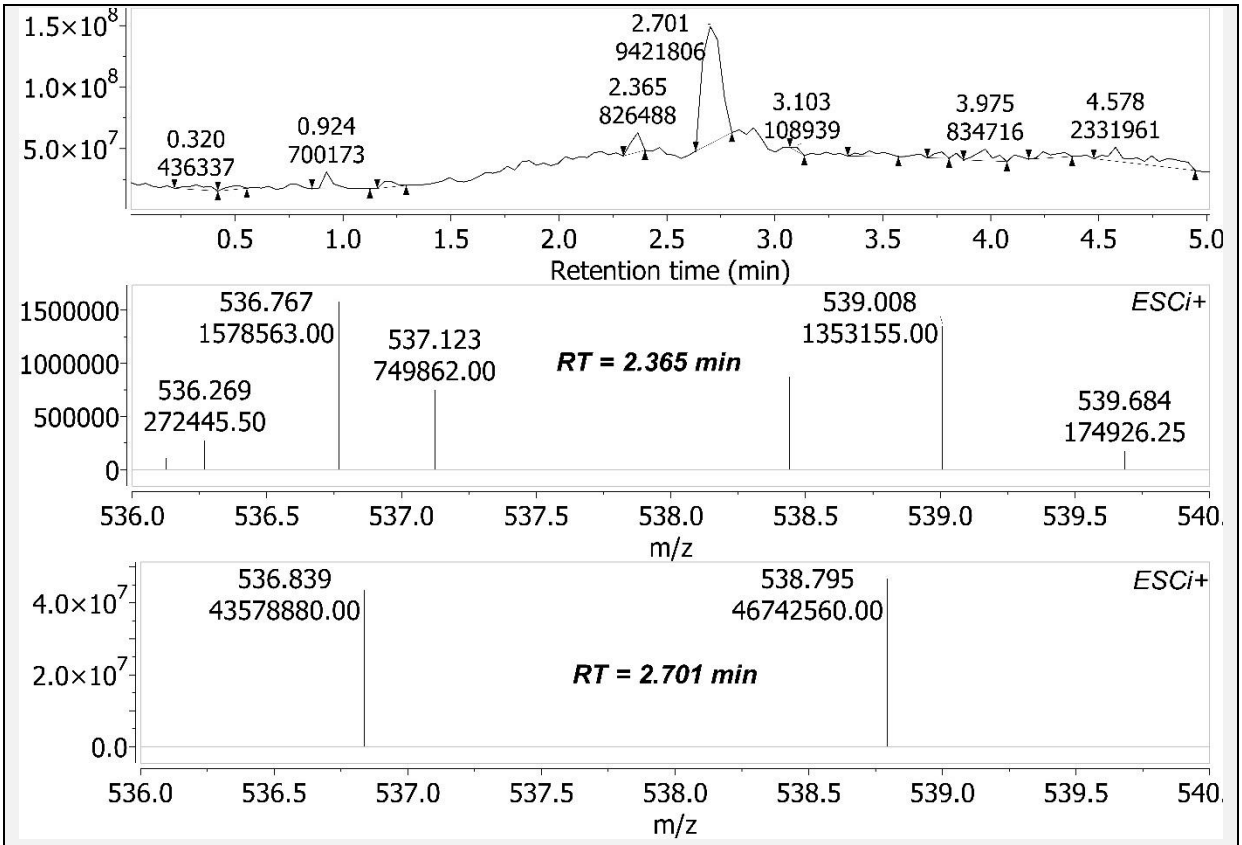

Figure 22 - Chiral SFC-MS of 6a sample. *Upper panel*: Chiral-SFC annotated with Retention Time (RT, minutes), and area under peak. *R* stereoisomer is found in the [RT=2.701] peak. *Middle panel*: Component of the Mass Spectrum (MS) of the [RT=2.365] peak. *Bottom panel*: Component of the Mass Spectrum (MS) of the [RT=2.701] peak. Therein is *m/z* 536.839 $[M+H]^+$ (*0.19 removed from Expected. Better concordance in subsequent spectra*). Using this present figure, *R* stereoisomer excess (%) in this sample = (435788880/(435788880+1578563))*100 = 99.64%; enantiomeric excess (ee) = (99.64-50)*2 = 99.28%.

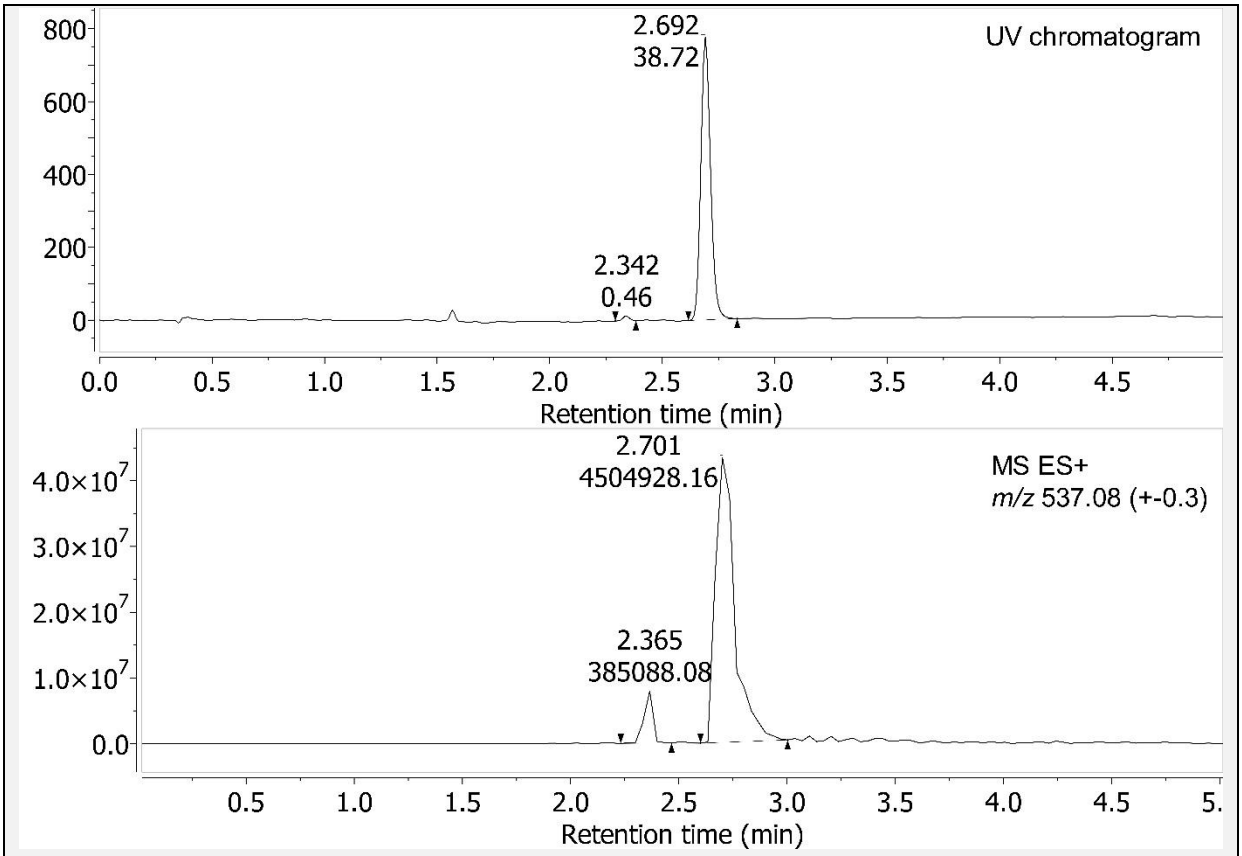

Figure 23 – Chiral-SFC of 6a sample. Using the UV Chromatogram component, *R* stereoisomer excess (%) in this 6a sample = (38.72/(38.72+0.46))*100 = 98.83%; enantiomeric excess (ee) = (98.83-50)*2 = 97.66%.

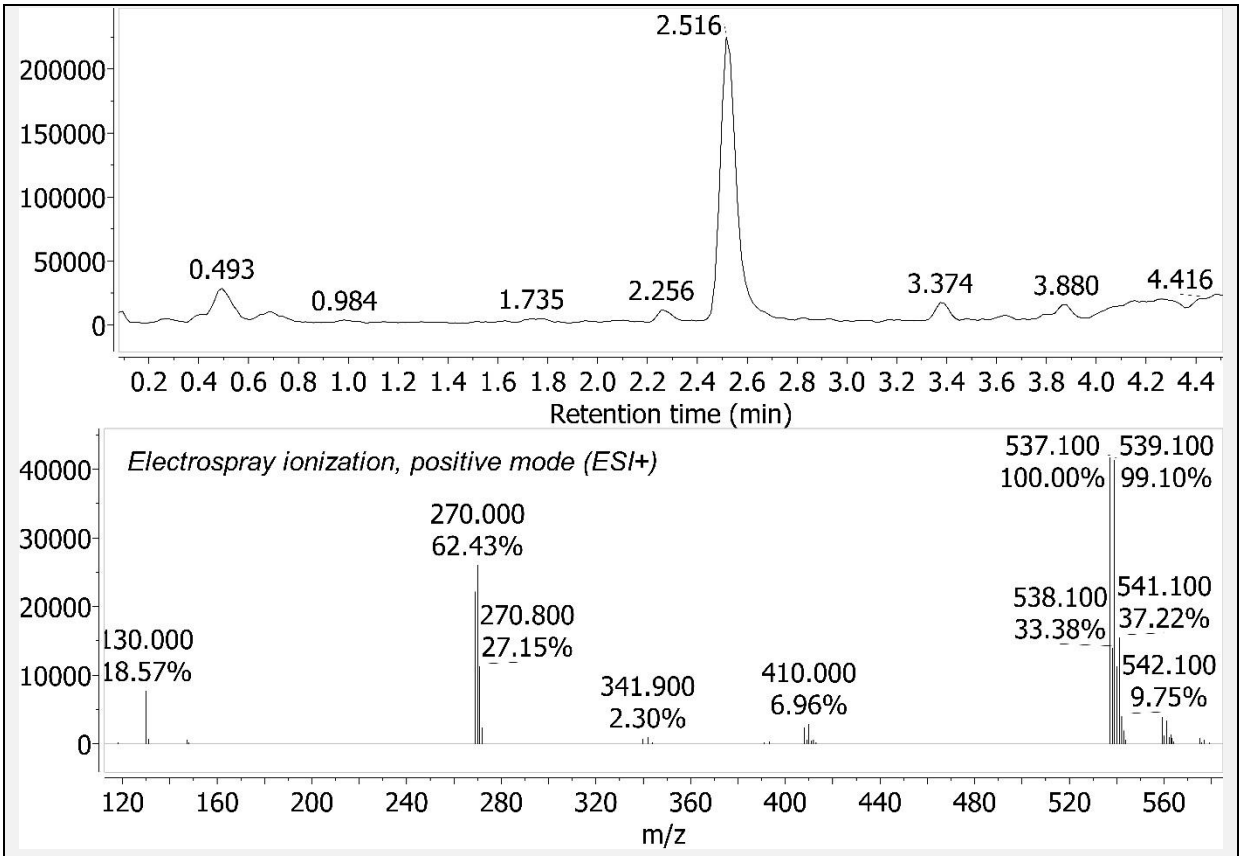

Figure 24 – LC-MS spectrum for 6a sample. *Upper panel*: Liquid Chromatography (LC) Retention Time (RT) = 2.516 minutes. *Lower panel*: Mass Spectrum (MS) of the [RT peak=2.516].

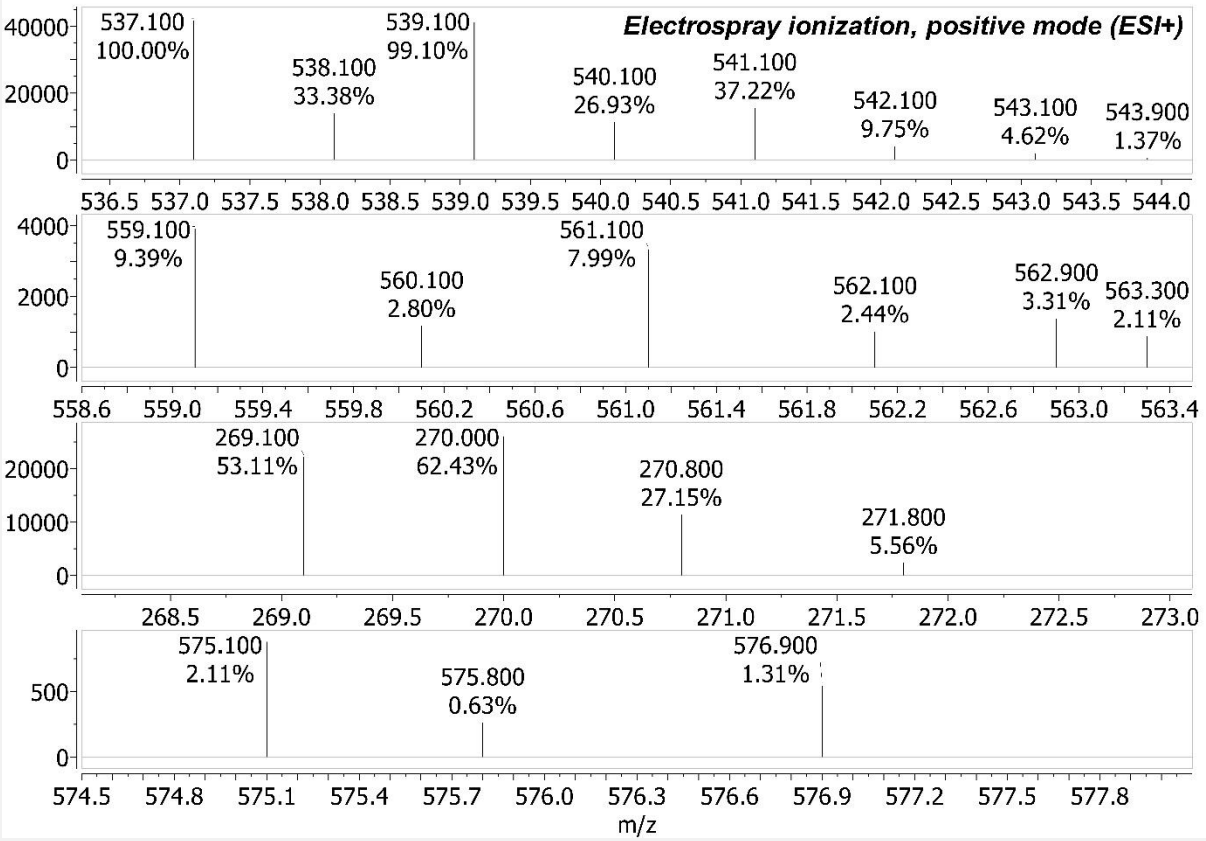

Figure 25 – Some Mass Spectrum (MS) components of Figure 24. *Upper panel*: *m/z* 537.1 $[M+H]^+$. *2nd panel*: *m/z* 559.1 $[M+Na]^+$. *3rd panel*: *m/z* 269.1 $[M+2H]^{2+}$. *Bottom panel*: *m/z* 575.1 $[M+K]^+$. All these Observed *m/z* are within 0.07 of Expected.

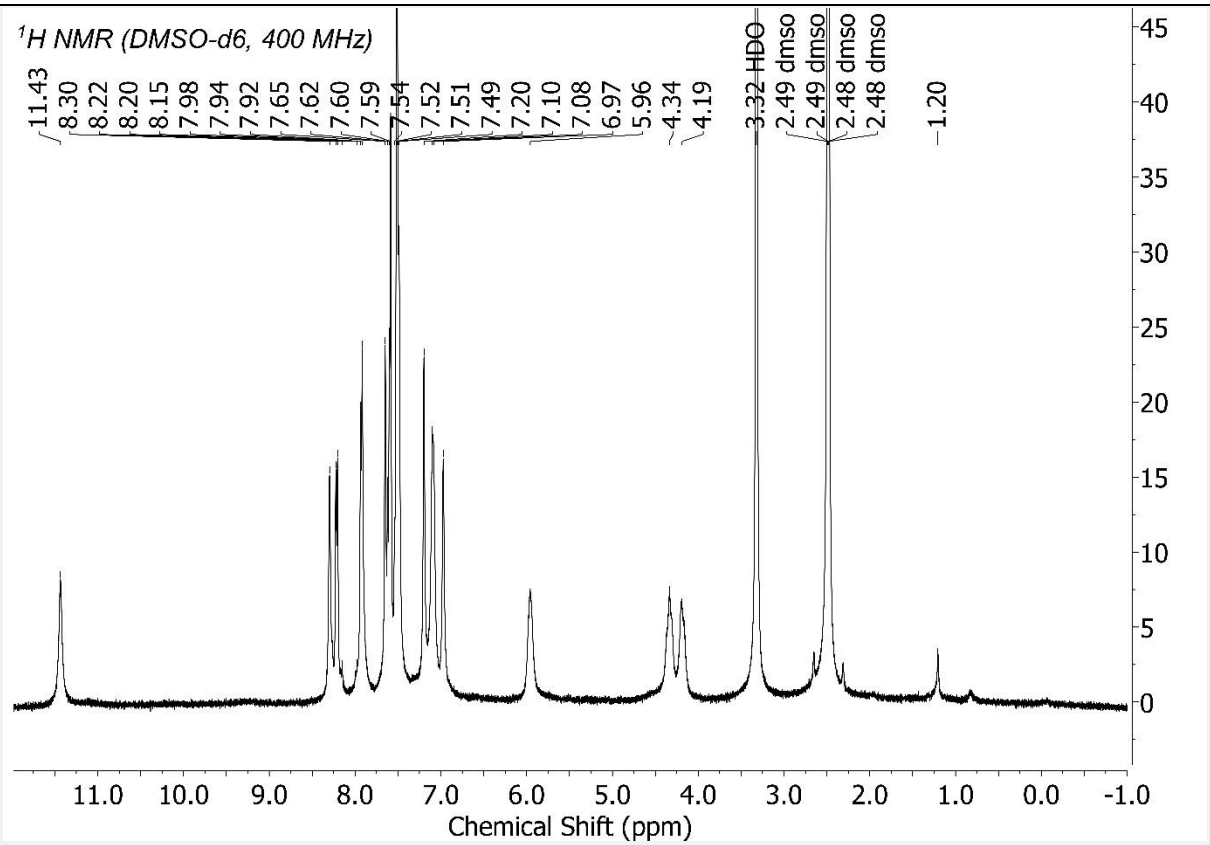

Figure 26 – ^{1}H NMR {*NMR probe temperature = 298.15 K*} for 6a sample. Scaled to the highest compound peak. Peaks identified by the "Auto peak picking" algorithm (based on Global Spectral Deconvolution, GSD) of MestReNova version 12 software. With default program settings used. And no chemical structure used/inputted to guide/constrain this peak picking.

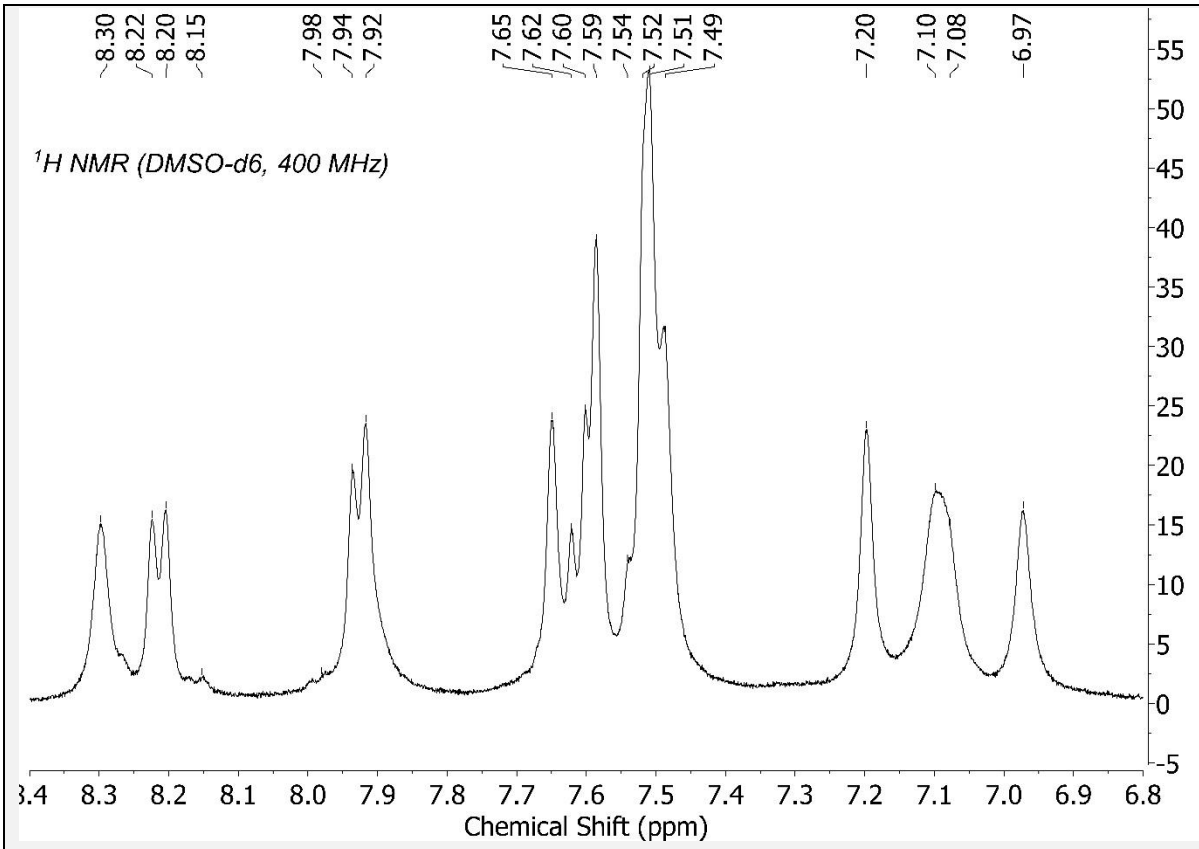

Figure 27 - Aromatic region of Figure 26 expanded.

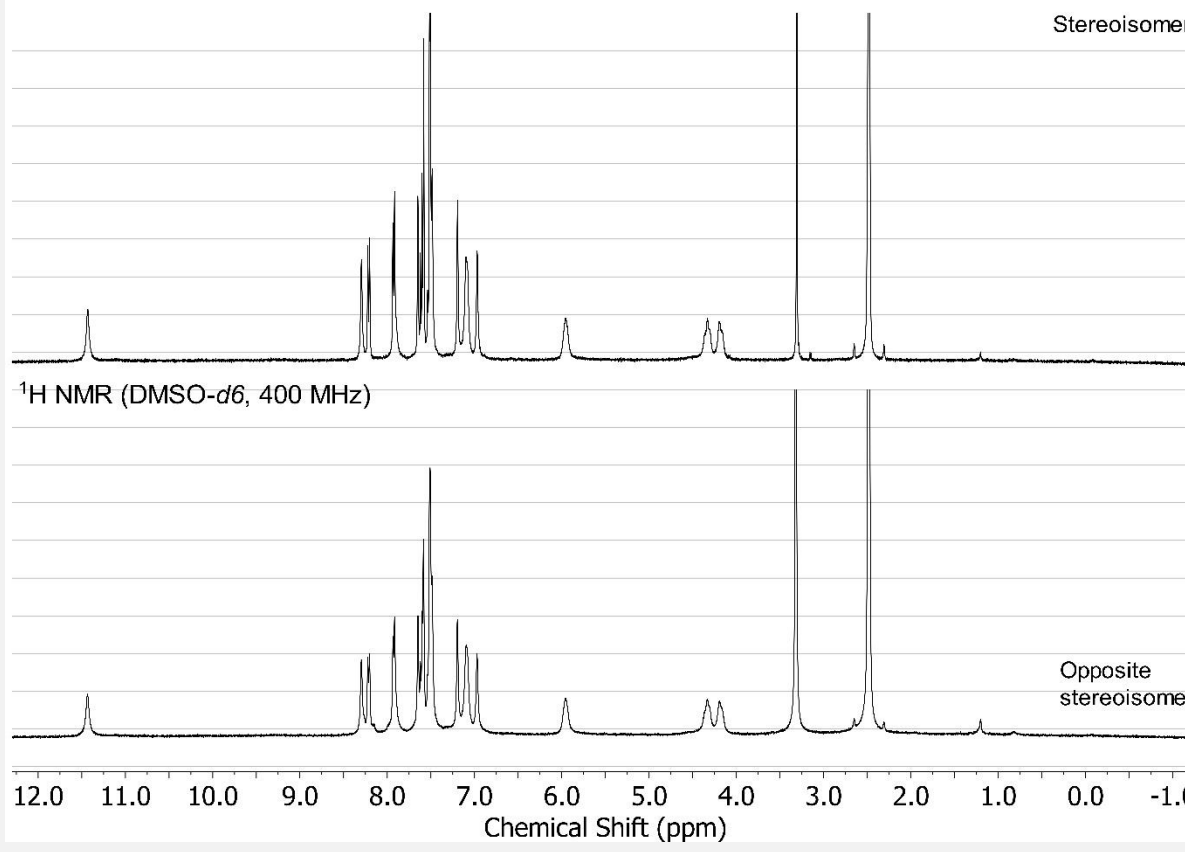

Figure 28 - 6b data in upper panel, 6a data in lower panel.

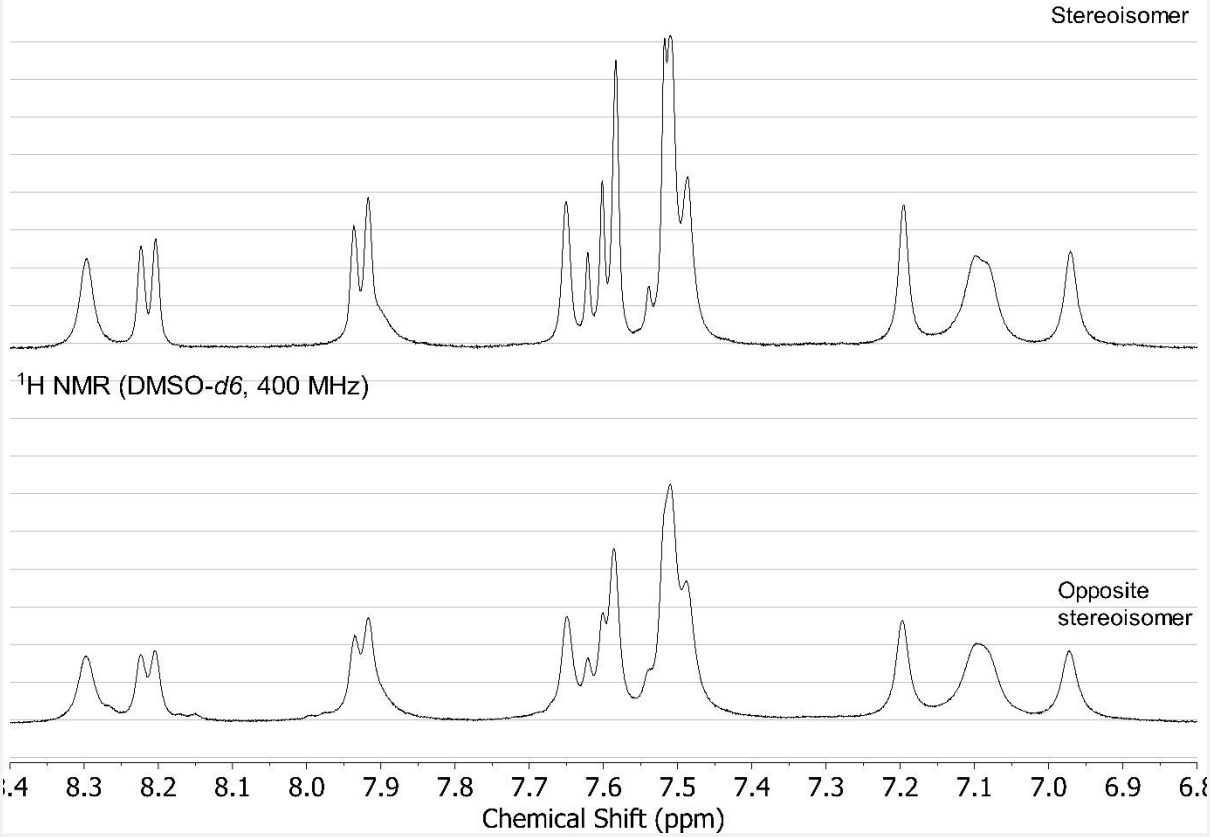

Figure 29 - Aromatic region: 6b data in upper panel, 6a data in lower panel.

Synthesis of 7a and 7b (*anti-cancer activity in Figure 13*)

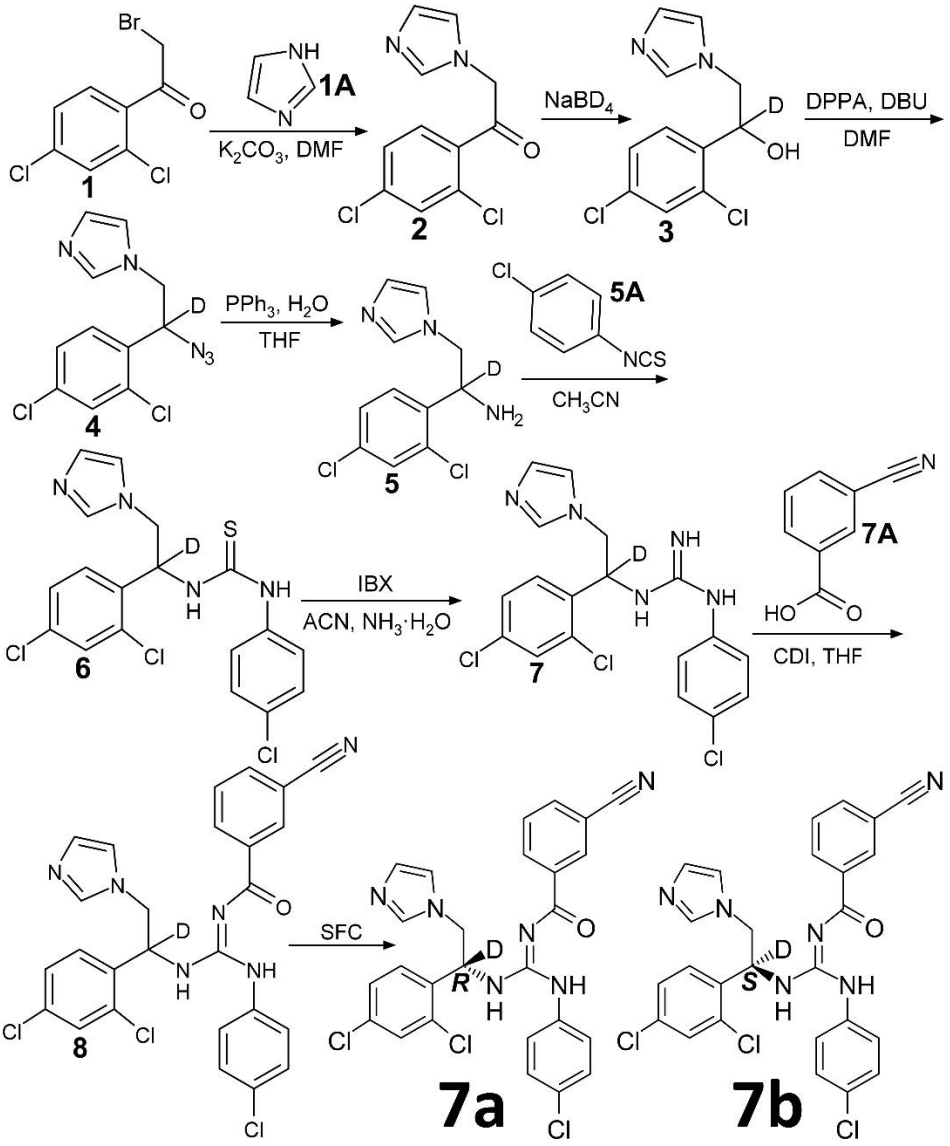

7a (enantiomeric excess (ee) ≥97%): Liquid Chromatography-Mass Spectrometry (LC-MS): LC Retention Time (RT) = 2.685 minutes, MS (electrospray ionization, positive mode): *m/z* 538.1 $[M+H]^+$, 560.1 $[M+Na]^+$, 269.6 $[M+2H]^{2+}$. High Resolution Mass Spectrometry (HRMS): Liquid Chromatography-Time of Flight (LC-TOF) MS (electrospray ionization, positive mode): LC Retention Time (RT) = 0.163 minutes, *m/z* 538.0727757864 $[M+H]^+$, *m/z* 560.0513502753 $[M+Na]^+$, *m/z* 576.0327248583 $[M+K]^+$, molar percent deuterium incorporation at chiral carbon = 99.14%.

^{1}H NMR (400 MHz, DMSO-*d6*) δ 11.46 (s, 1H), 8.32 (s, 1H), 8.24 (d, J = 7.9 Hz, 1H), 7.95 (d, J = 7.7 Hz, 2H), 7.70 – 7.59 (m, 3H), 7.59 – 7.49 (m, 4H), 7.21 (s, 1H), 7.12 (d, J = 7.9 Hz, 2H), 6.99 (s, 1H), 4.36 (d, J = 13.9 Hz, 1H), 4.22 (s, 1H). {*NMR probe temperature = 300.7 K*}.

7b (enantiomeric excess (ee) ≥97%): LC-MS: LC Retention Time (RT) = 2.685 minutes, MS (electrospray ionization, positive mode): *m/z* 538.1 $[M+H]^+$, 560.1 $[M+Na]^+$, 269.6 $[M+2H]^{2+}$. HRMS: LC-TOF MS (electrospray ionization, positive mode): LC RT = 0.166 minutes, *m/z* 538.0745928061 $[M+H]^+$, *m/z* 560.0600137508 $[M+Na]^+$, *m/z* 576.0250917093 $[M+K]^+$, molar percent deuterium incorporation at chiral carbon = 99.13%.
^{1}H NMR (400 MHz, DMSO-*d6*) δ 11.48 (s, 1H), 8.33 (s, 1H), 8.25 (dt, J = 7.8, 1.5 Hz, 1H), 7.96 (dt, J = 7.7, 1.5 Hz, 1H), 7.92 (s, 1H), 7.71 – 7.60 (m, 3H), 7.60 – 7.49 (m, 4H), 7.23 (s, 1H), 7.14 (s, 2H), 7.00 (s, 1H), 4.38 (d, J = 14.1 Hz, 1H), 4.23 (s, 1H). {*NMR probe temperature = 301 K*}.

Presented NMR peaks are from using the "Auto Assignment" algorithm in MestReNova version 12 software (Mestrelab Research, Santiago de Compostela, Spain). Which picks peaks in an inputted NMR spectrum, influenced by an inputted structure, which was structure 8 in the reaction scheme above. However, after automatic assignment, I manually made a single change for 7a: I changed the number of hydrogens at 7.95 ppm from 1H to 2H. I executed this change by manually extending the integration line (this manipulation automatically changes the MestReNova program's integration calculation method from "peak" to "sum") in this 7.95 ppm region for 7a, making it the same length as the integration line in the same region for 7b. Which then rendered/integrated this region with 2H as compared to 1H. The same as for 7b in this region (by "Auto Assignment" algorithm: 7b has peaks at 7.96 [1H] and 7.92 [1H] = 2H in 7.95 ppm region). This change in integration increases the nuclide count to the correct number for the structure (18H). This manipulation is best explained in pictures and so please refer to Figures 43 and 44. Which both show 7b data in the upper panel, 7a data in the lower panel. Wherein Figure 43 shows how this region was automatically integrated. And Figure 44 shows how I manually extended the integration line for 7a, to match the length of that for 7b. Such that both integrated to 2H in this region.

<u>Performed synthesis of 7a and 7b in detail</u>

In this section, numbers in square brackets are CAS numbers.

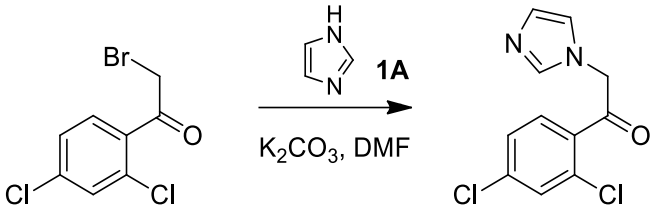

1 2

1. Charged Compound 1 [170894-53-8] (15.0 g, 55.9 mmol) and DMF [68-12-2] (150 mL) into the reactor at 25°C under N_2.
2. Charged K_2CO_3 [584-08-7] (23.2 g, 167 mmol) into the reactor at 25°C.
3. Charged imidazole [288-32-4] (11.4 g, 167 mmol) into the reactor at 25°C.
4. The mixture was stirred at 25°C for 3 hours.
5. TLC (petroleum ether:ethyl acetate = 5:1, R_f = 0.0) showed raw material was consumed.
6. The mixture was quenched with water (100 mL).
7. The aqueous phase was extracted with ethyl acetate (100 mL x 2). The combined organic phase was washed with brine (50 mL), dried with anhydrous Na_2SO_4, filtered and concentrated in vacuum.
8. The residue was purified by silica gel chromatography (column height: 250 mm, diameter: 100 mm, 100-200 mesh silica gel, petroleum ether/ethyl acetate=20/1, 3/1) to give Compound 2 (13.0 g, 38.8 mmol, 69.3% yield, 76.1% purity) as yellow solid.

Compound 2: ^{1}H NMR ($CDCl_3$, 400 MHz) δ (ppm) 7.55 (d, J = 8.0 Hz, 1H), 7.50 (s, 1H), 7.35-7.37 (dd, J = 8.0 Hz, 8.0 Hz, 1H), 7.09 (d, J = 8.0 Hz, 1H), 6.93 (s, 1H), 5.32 (s, 2H).

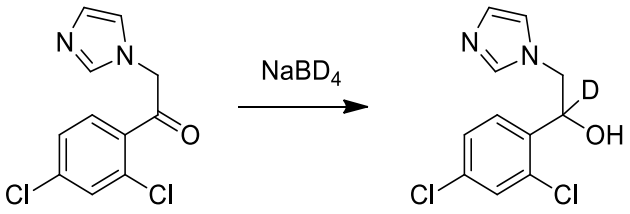

2 3

1. Charged Compound 2 (8.00 g, 31.3 mmol) and MeOH (40 mL) into the reactor at 25°C under N_2.
2. Charged $NaBD_4$ [15681-89-7] (1.31 g, 34.5 mmol) to the solution.
3. The mixture was stirred at 50°C for 3 hours.
4. LC-MS (product: RT= 0.914 min) showed raw material was consumed.
5. The reaction was quenched with water (100 mL).

6. The aqueous phase was extracted with ethyl acetate (50 mL x 2). The combined organic phase was washed with brine (50 mL), dried with anhydrous Na_2SO_4, filtered and concentrated in vacuum.

7. The residue was purified by silica gel chromatography (column height: 250 mm, diameter: 100 mm, 100-200 mesh silica gel, petroleum ether/ethyl acetate=10/1, 0/1) to give Compound 3 (5.50 g, 21.3 mmol, 67.9% yield) as white solid.

Compound 3: ^{1}H NMR ($CDCl_3$, 400 MHz) δ (ppm) 7.57 (d, J = 8.0 Hz, 1H), 7.39 (m, 1H), 7.28-7.30 (dd, J = 8.0 Hz, 8.0 Hz, 1H), 6.88 (d, J = 8.0 Hz, 2H), 4.20 (d, J = 12 Hz, 1H), 3.84-3.88 (d, J = 16 Hz, 1H).

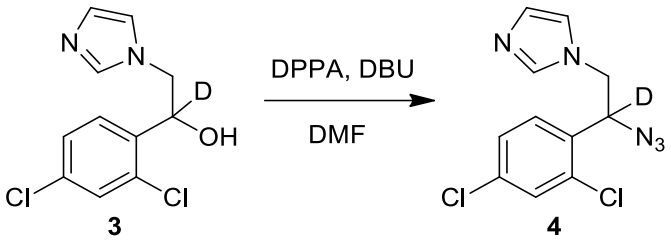

3 4

1. Set up a reactor R-1. (Note: R-1 is a 100 mL three-necked bottle)

2. Charged Compound 3 (4.50 g, 17.4 mmol) and DPPA [26386-88-9] (4.80 g, 17.4 mmol, 3.78 mL), DMF (22.5 mL) into the reactor R-1 at 25-30°C.

3. Charged DBU [6674-22-2] (2.65 g, 17.4 mmol, 2.63 mL) into the mixture under nitrogen atmosphere at 0-5°C, then the mixture was stirred for about 15 minutes.

4. After that, the reaction mixture was stirred for 24 hours at 20-30°C.

5. TLC (DCM/MeOH = 10/1, SM R_f = 0.55, product R_f = 0.72) showed raw material was consumed, LC-MS (product: RT = 0.764 min) and HPLC (product: RT = 1.893 min) indicated reaction mixture has desired product.

6. The reaction mixture was extracted with EtOAc (40 mL x 3).

7. The combined organic phase was washed with brine (40 mL), dried with Na_2SO_4, filtered and concentrated in vacuum to get the residue.

8. The residue was purified by column chromatography (SiO_2, dichloromethane: methanol = 1/0 to 100/1) to give Compound 4 (3.80 g, crude) as yellow oil.

Compound 4: ^{1}H NMR ($CDCl_3$, 400 MHz) δ (ppm) 7.50 (s, 1H), 7.44 (s, 1H), 7.35 (d, J = 2.0 Hz, 1H), 7.33 (d, J = 2.0 Hz, 1H), 7.29-7.30 (m, 1H), 6.94-7.10 (m, 1H), 4.25 (d, J = 14.4 Hz, 1H), 4.04 (d, J = 14.4 Hz, 1H).

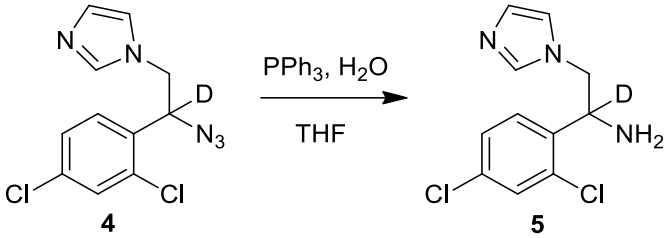

1. Set up a reactor R-1. (Note: R-1 is a 100 mL three-necked bottle)

2. Charged Compound 4 (3.80 g, 13.4 mmol), PPh_3 [603-35-0] (10.5 g, 40.2 mmol), THF [109-99-9] (12.6 mL) and H_2O (1.26 mL) into the reactor R-1 at 25-30°C.

3. Stirred at 65-70°C for 16 hours.

4. Checked the reaction mixture by TLC (dichloromethane: methanol=10:1, SM: R_f = 0.54, product: R_f = 0.45) and LC-MS (product: RT = 1.253min) showed that reactant was consumed completed.

5. The reaction mixture was concentrated under reduced pressure to remove THF.

6. The reaction mixture was added with H_2O (38 mL), adjusted pH to 3 with con. HCl and washed with EtOAc (38 mL).

7. The water phase was adjusted pH to 13 with 1N aq. NaOH, then exacted with EtOAc (38 mL x 2).

8. The combined organic phase was washed with brine (38 mL), dried with Na_2SO_4, filtered and concentrated in vacuum to give Compound 5 (2.60 g, crude) as a yellow liquid.

Compound 5: ^{1}H NMR ($CDCl_3$, 400 MHz) δ (ppm) 7.44 (d, J = 14 Hz, 1H), 7.41 (s, 1H), 7.29 (d, J = 2.0 Hz, 1H), 7.27 (d, J = 1.2 Hz, 1H), 7.07 (s, 1H), 6.92 (s, 1H), 4.21 (d, J = 14 Hz, 1H), 3.92 (d, J = 14 Hz, 1H).

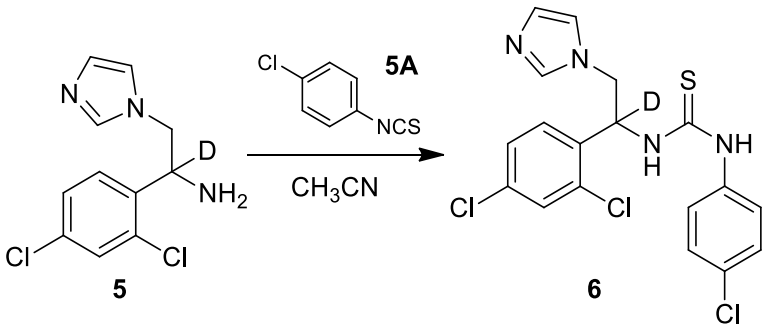

1. Charged Compound 5 (2.50 g, 9.72 mmol), Compound 5A [2131-55-7] (1.65 g, 9.72 mmol) and MeCN (37.5 mL) into the reactor at 25°C.

2. The mixture was stirred at 25°C for 12 hours.

3. TLC (dichloromethane: methanol=10:1, SM: R_f = 0.5, product: R_f = 0.2) showed raw material was consumed completed.

4. The mixture was concentrated in vacuum.

5. The residue was purified by silica gel chromatography (column height: 250 mm, diameter: 100 mm, 100-200 mesh silica gel, petroleum ether/ethyl acetate=3/1, 0/1) to give Compound 6 (3.60 g, 8.44 mmol, 86.7% yield) as white solid.

Compound 6: ^{1}H NMR ($CDCl_3$, 400 MHz) δ (ppm) 9.08 (s, 1H), 7.48 (d, J = 2.0 Hz, 1H), 7.33 (d, J = 8.0 Hz, 1H), 7.25-7.28 (m, 1H), 7.16 (d, J = 2.0 Hz, 1H), 7.00 (s, 1H), 6.88 (d, J = 8.0 Hz, 1H), 6.72 (s, 1H), 4.46 (dd, J = 14.4 Hz, 14 Hz, 1H), 1.84 (s, 1H).

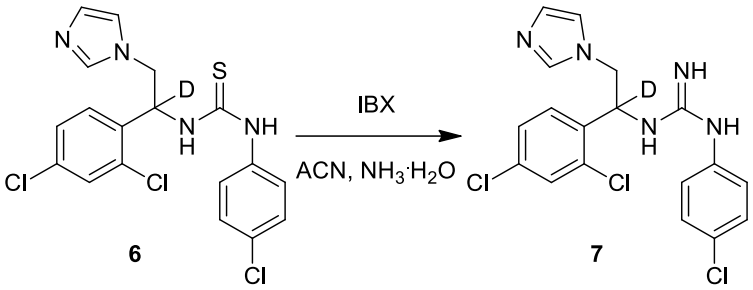

1. Charged Compound 6 (3.00 g, 7.03 mmol) and MeCN (30 mL) into the reactor at 25°C.

2. Charged IBX [61717-82-6] (2.17 g, 7.73 mmol) into the reactor at 25°C.

3. Charged $NH_3.H_2O$ [1336-21-6] (13.6 g, 116 mmol, 15 mL, 30% purity) into the reactor at 25°C.

4. The mixture was stirred at 25°C for 12 hours.

5. LC-MS (product: RT = 0.717 min) showed raw material was consumed completed.

6. The mixture was filtered and the filter cake was concentrated in vacuum to give Compound 7 (2.50 g, 6.10 mmol, 86.8% yield) as white solid.

Compound 7: ^{1}H NMR ($CDCl_3$, 400 MHz) δ (ppm) 7.87 (d, J = 8.0 Hz, 1H), 7.67 (s, 1H), 7.55-7.60 (m, 2H), 7.37-7.41 (m, 2H), 7.23 (s, 1H), 7.07-7.09 (m, 1H), 6.92 (s, 1H), 4.33 (dd, J = 14.4 Hz, 14 Hz, 1H).

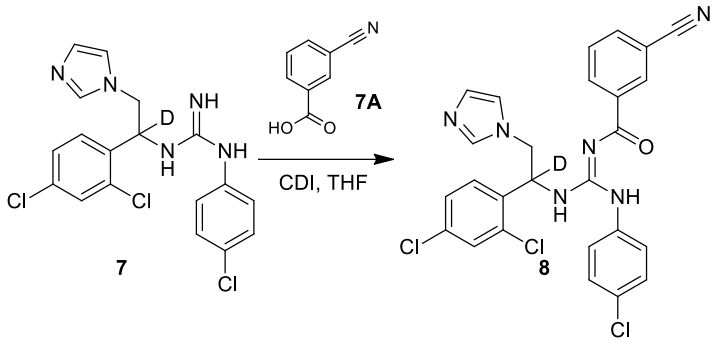

1. Charged Compound 7 (538 mg, 3.66 mmol), CDI [530-62-1] (593 mg, 3.66 mmol) and THF [109-99-9] (30 mL) into the reactor at 25°C.

2. The solution was stirred at 25°C for 3 hours.

3. Charged compound 7A [1877-72-1] (1.50 g, 3.66 mmol) into the reactor at 25°C.

4. The mixture was stirred at 25°C for 12 hours.

5. LC-MS (SM: RT = 0.730 min, product: RT = 1.030 min) showed the raw material was consumed/completed.

6. The mixture was concentrated in vacuum.

7. Separating stereoisomers of Compound 8: the residue was purified with Prep-HPLC (column: DAICEL CHIRALPAKAD-H (250 mm*30 mm, 5 µm); mobile phase: [0.1% NH_3H_2O IPA]; B%: 44%-44%, 6.45 min) to give 7b (0.025 g, 45.8 µmol, 1.25% yield, 98.8% purity) as white solid and 7a (0.025 g, 45.5 µmol, 1.24% yield, 98.1% purity) as white solid.

Spectral data for 7b

Its expected/calculated *m/z*, from its structure (Figure 13A), using the "exact molecular weight" calculator in MarvinSketch software (Chemaxon, Budapest, Hungary), which uses the mass of the *most prevalent* isotope of each element in the molecule:
538.08 $[M+H]^+$, 560.06 $[M+Na]^+$, 269.54 $[M+2H]^{2+}$, 576.04 $[M+K]^+$).

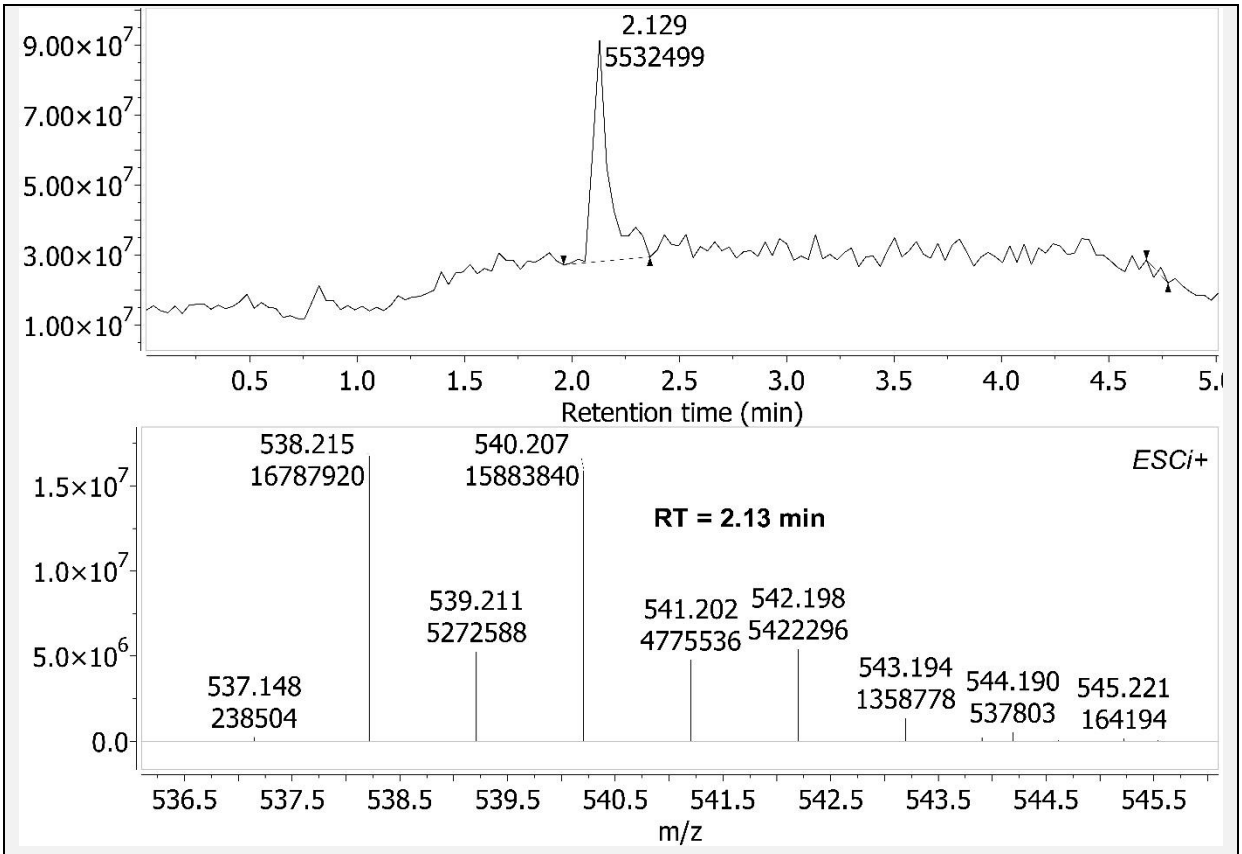

Figure 30 – Chiral SFC-MS for 7b sample. *Upper panel*: Chiral-SFC annotated with Retention Time (RT, minutes) and area under peak. *S* stereoisomer is found in [RT=2.13] peak. *Lower panel*: component of mass spectrum of [RT=2.13] peak. And therein is *m/z* 538.215 $[M+H]^+$ (*0.135 removed from Expected. Better concordance in subsequent spectra*).

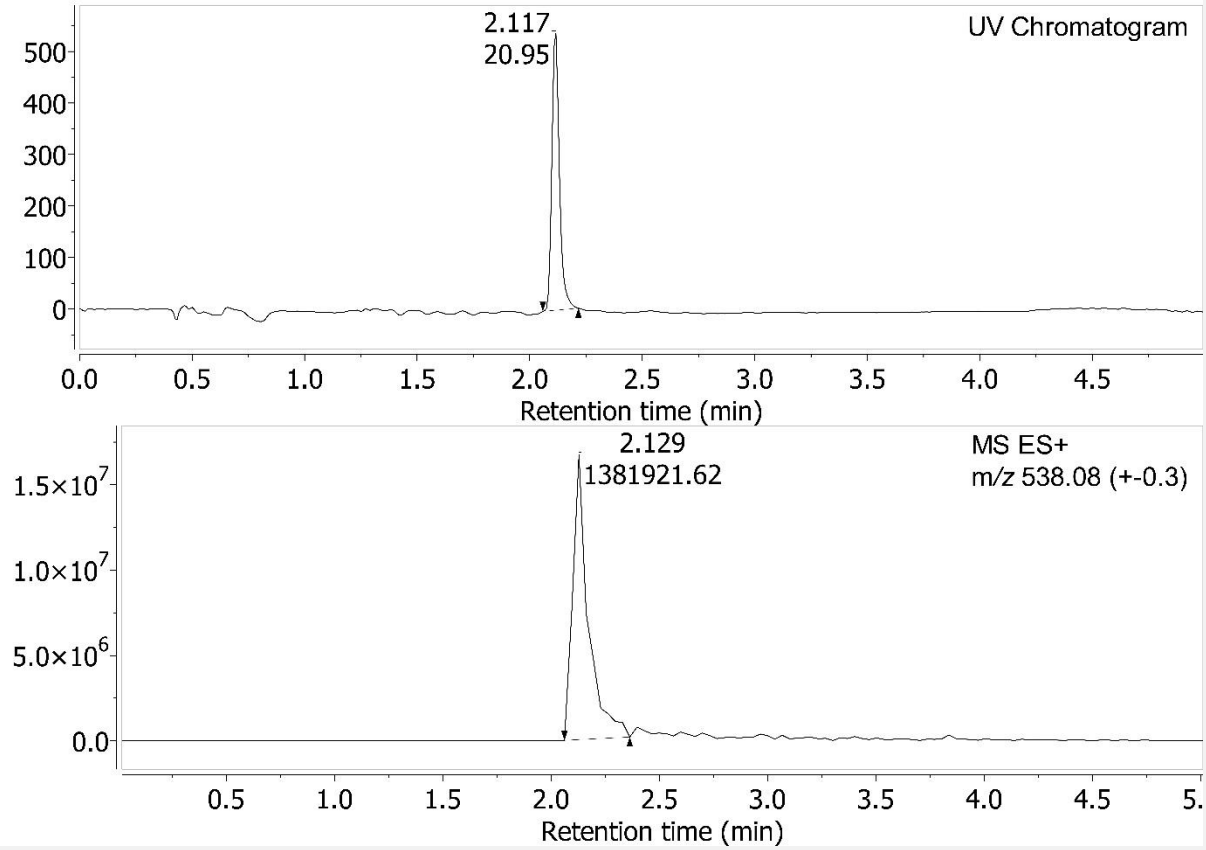

Figure 31 – Chiral-SFC of 7b sample. *S* stereoisomer excess = 100% (no other peak in the UV chromatogram). Enantiomeric excess (ee) = (100-50)*2 = 100%.

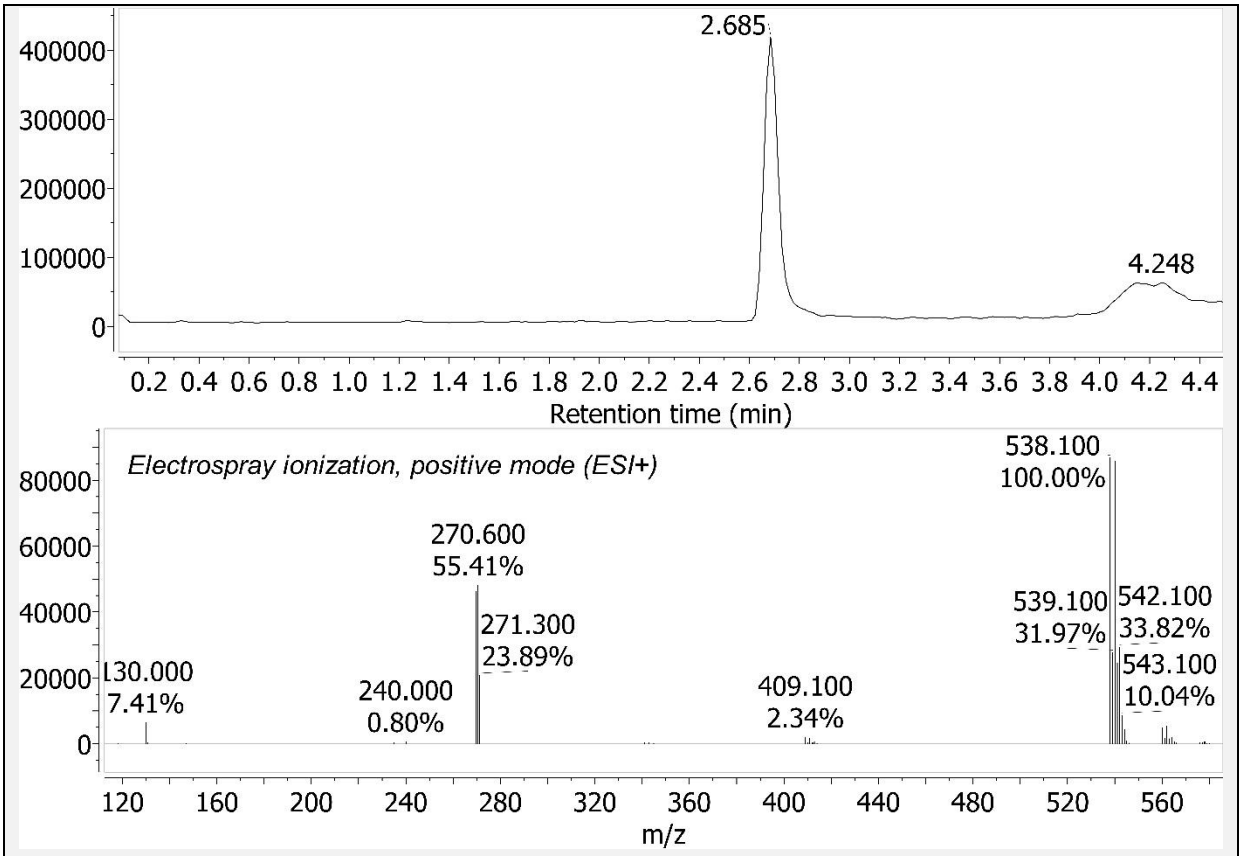

Figure 32 – LC-MS spectrum for 7b sample. *Upper panel*: Liquid Chromatography (LC) Retention Time (RT) = 2.685 minutes. *Bottom panel*: Mass Spectrum (MS) of [RT=2.685 peak]. Shows positively charged species (API-ES positive). Percentages are relative abundance.

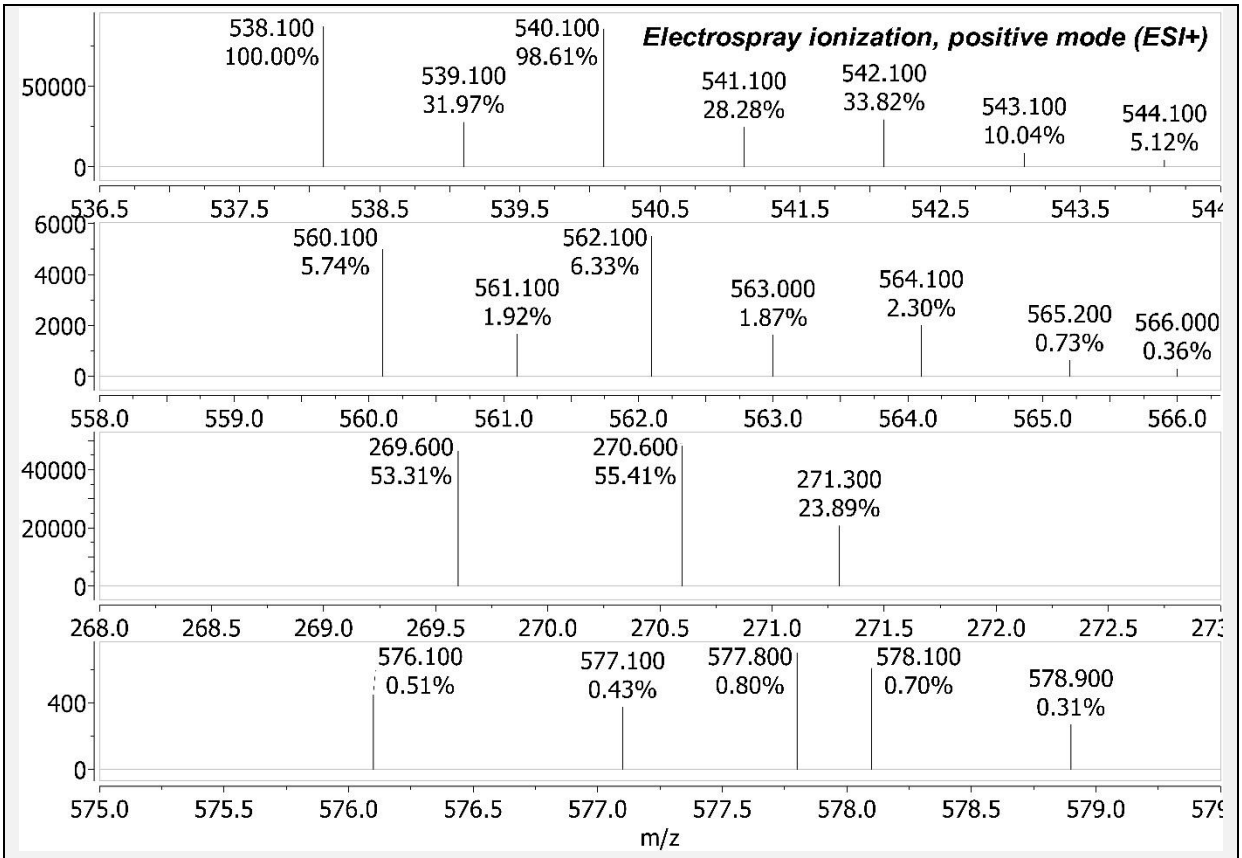

Figure 33 – Some Mass Spectrum (MS) components of Figure 32. *Upper panel*: *m/z* 538.1 $[M+H]^+$. *2nd panel*: *m/z* 560.1 $[M+Na]^+$. *3rd panel*: *m/z* 269.6 $[M+2H]^{2+}$. *Bottom panel*: *m/z* 576.1 $[M+K]^+$. All these Observed *m/z* are within 0.06 of Expected.

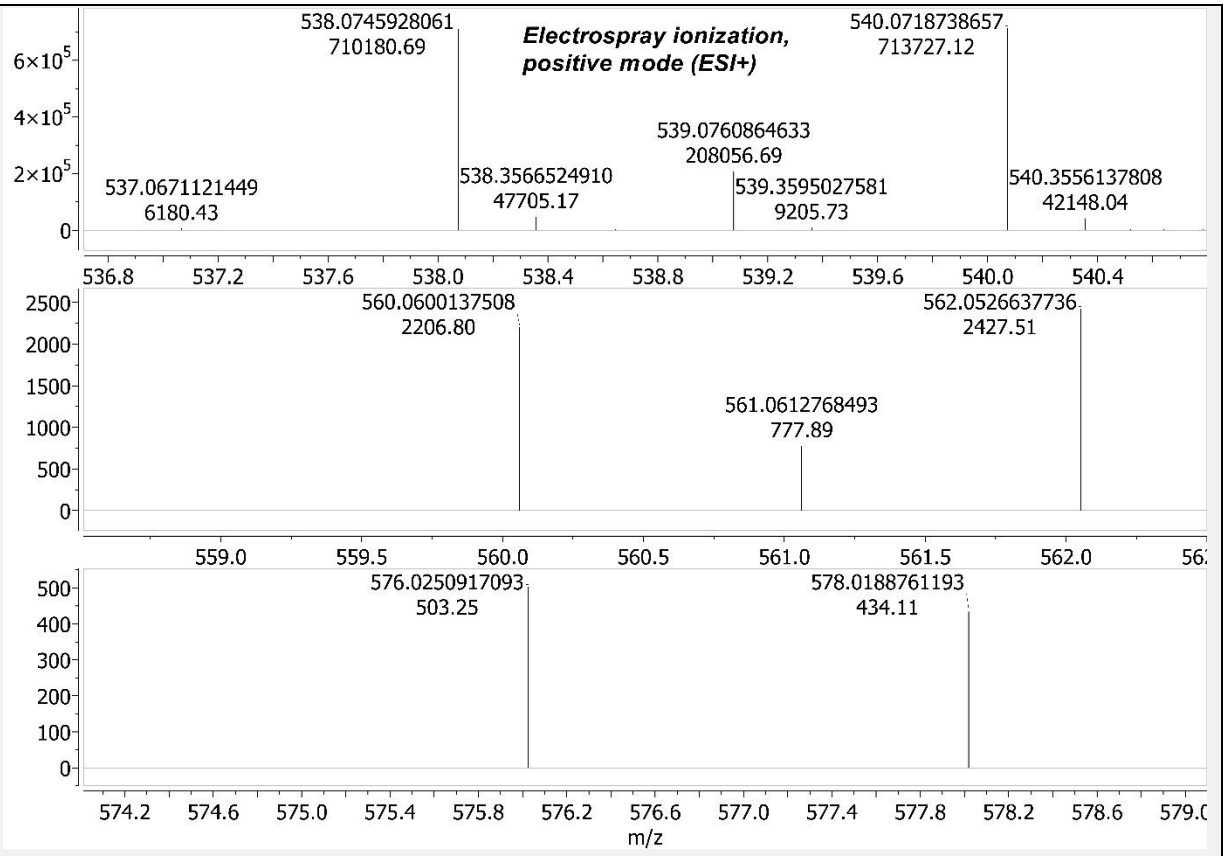

Figure 34 – High Resolution Mass Spectrometry (HRMS): Liquid Chromatography-Time of Flight (LC-TOF) Mass Spectrometry (MS) for 7b sample. LC Retention Time (RT) = 0.166 minutes (LC data not shown). *Upper panel*: OBSERVED *m/z* 538.0745928061 $[M+H]^+$. CALCULATED from structure *m/z* 538.0821456 $[M+H]^+$. So, Observed mass is only 0.0075527939 Daltons (0.7% the mass of a proton) removed from calculation. The species with *m/z* 537.0671121449 $[M+H]^+$ has hydrogen instead of deuterium on the chiral carbon. And indeed is the mass of a neutron (1.008664 Daltons) lighter: (538.0745928061-537.0671121449) = 1.0074806612 Daltons mass difference (0.12% removed from being the exact mass of a neutron difference). Absolute abundance is shown on the y-axis. And the molar percent deuterium incorporation for 7b sample at the chiral carbon is 100% - ((6180.43/710180.69)*100=0.87%) = 99.13%. *2nd panel*: OBSERVED *m/z* 560.0600137508 $[M+Na]^+$. CALCULATED from structure *m/z* 560.0640898 $[M+Na]^+$. So, Observed mass is only 0.0040760492 Daltons (0.4% the mass of a proton) removed from calculation. The species with hydrogen instead of deuterium on chiral carbon is too low abundance to be observed here. *Bottom panel*: OBSERVED *m/z* 576.0250917093 $[M+K]^+$. CALCULATED from structure *m/z* 576.0380270 $[M+K]^+$. So, Observed mass is only 0.0129352907 Daltons (1.3% the mass of a proton) removed from calculation. The species with hydrogen instead of deuterium on chiral carbon is too low abundance to be observed here.

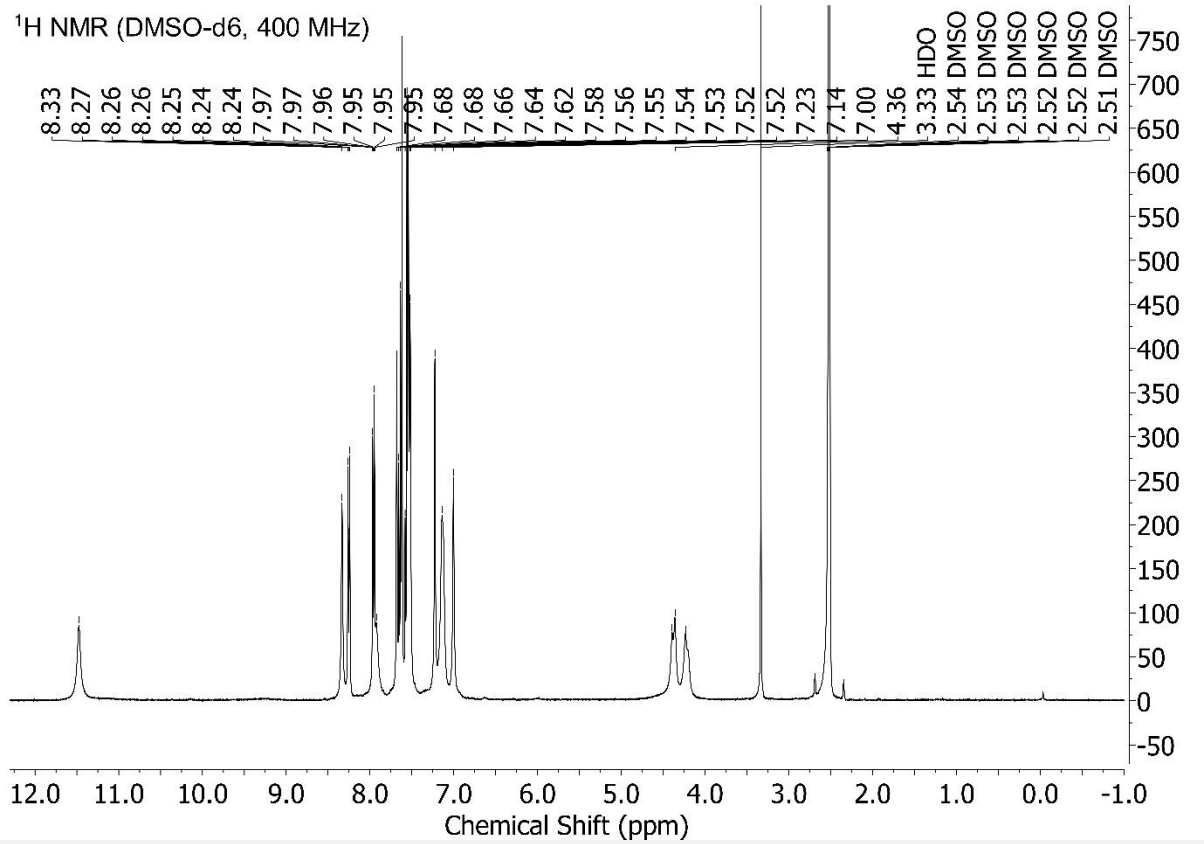

Figure 35 – ^{1}H NMR {*NMR probe temperature = 301 K*} for 7b sample. Scaled to highest compound peak. Peaks identified by "Auto peak picking" algorithm of MestReNova v12 software. With default program settings used. And no chemical structure used/inputted to guide/constrain this peak picking.

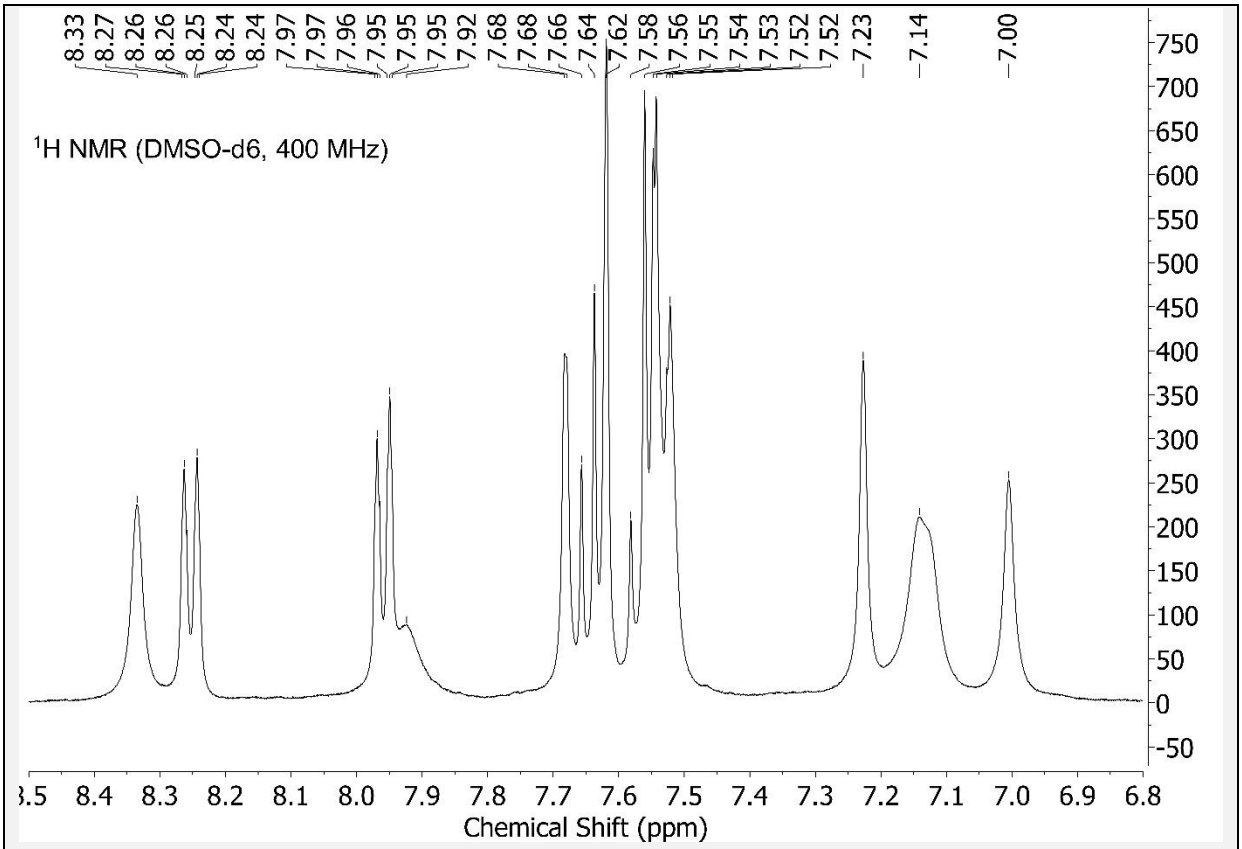

Figure 36 – Aromatic region of Figure 35 expanded.

Spectral data for 7a

Note that for 7a, its LC-MS, HRMS and NMR data are not all correspondent. To explain, LC-MS, HRMS and ^{1}H NMR were performed for 7a. And its ^{1}H NMR showed a high amount of impurities (spectrum not shown). Further mass based purification steps were taken as a result. And the ^{1}H NMR was repeated (spectrum shown herein). And ^{13}C NMR performed. All showing a much lower, acceptable level of impurity. And it is this purer form that was entered into anti-cancer testing at the National Cancer Institute (Figure 13B). However, LC-MS and HRMS were not repeated. But the LC-MS and HRMS are clear enough to identify the [M+ion] species needed. All be it with some additional species/impurities also observed, which aren't in the LC-MS and HRMS spectra for 7b (e.g. compare Figures 34 and 40).

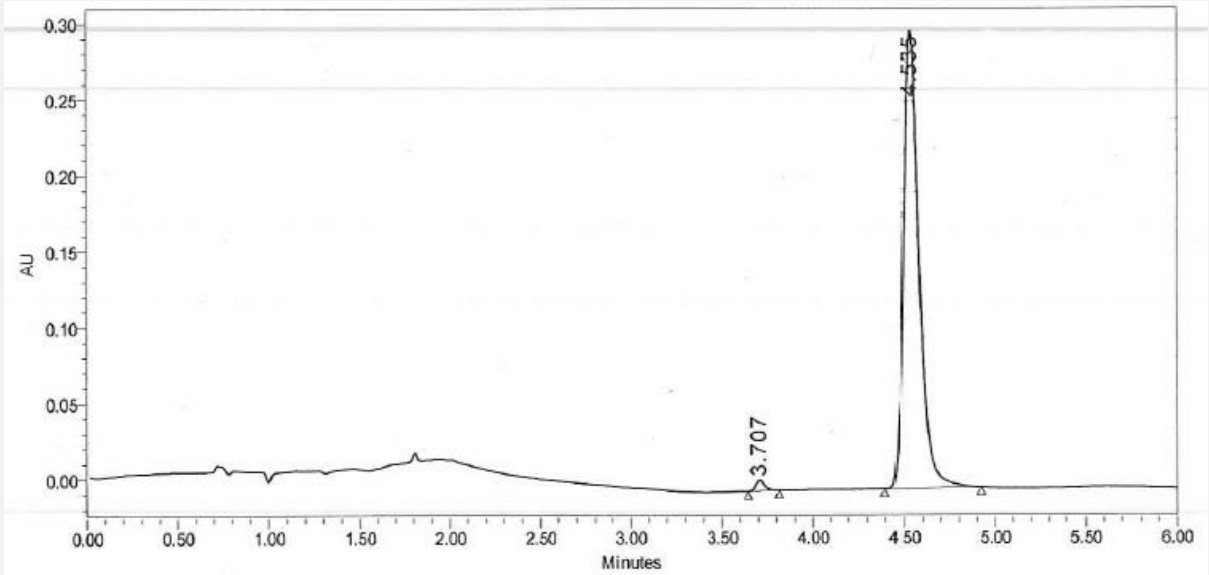

	RT	Area	% Area	Height
1	3.707	23021	1.29	6747
2	4.535	1765686	98.71	301165

Figure 37 – The chiral SFC-MS machine broke down. And so a different machine, with only chiral-SFC capability, had to be used. So, only chiral-SFC was performed for the 7a sample. Retention Time (RT) = 4.535 min.

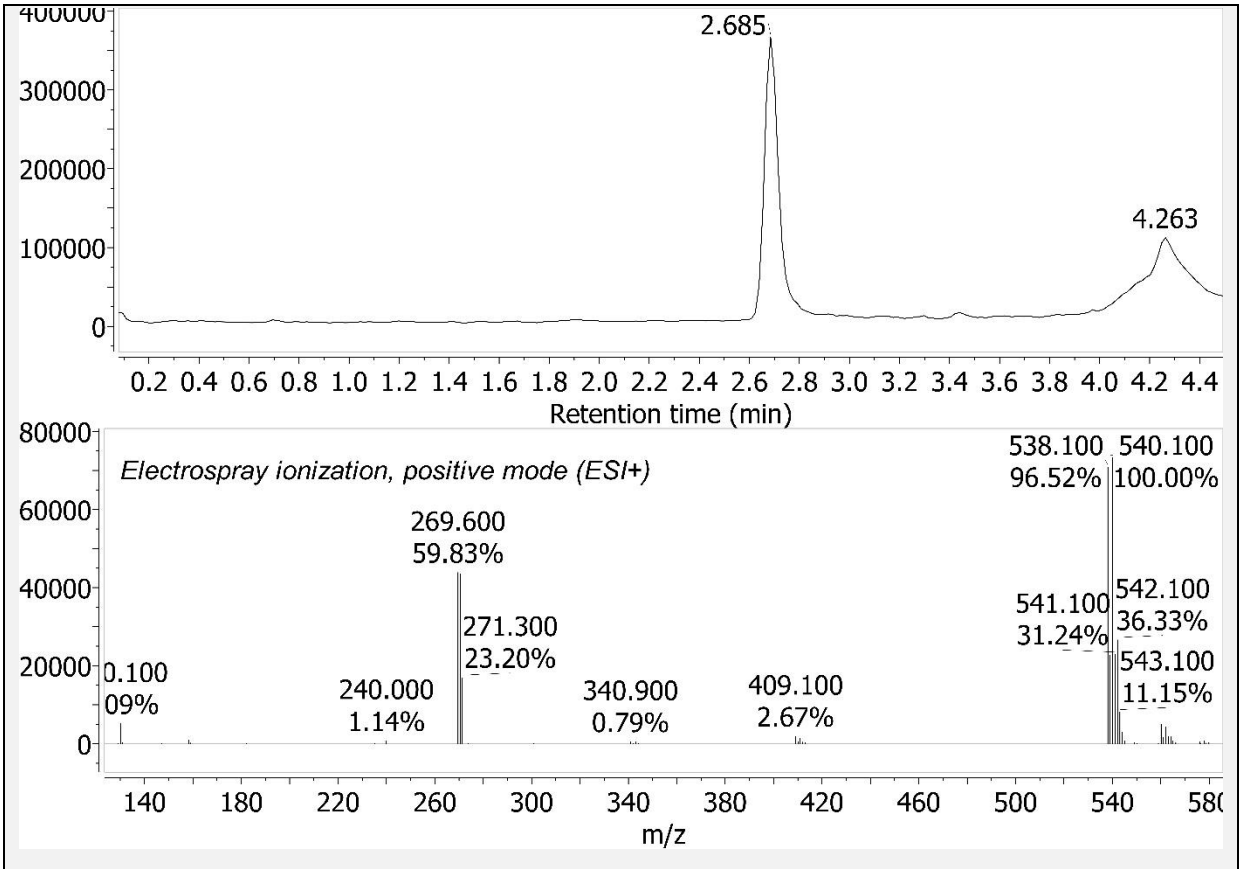

Figure 38 – LC-MS spectrum for 7a sample. Retention Time (RT) = 2.685 minutes.

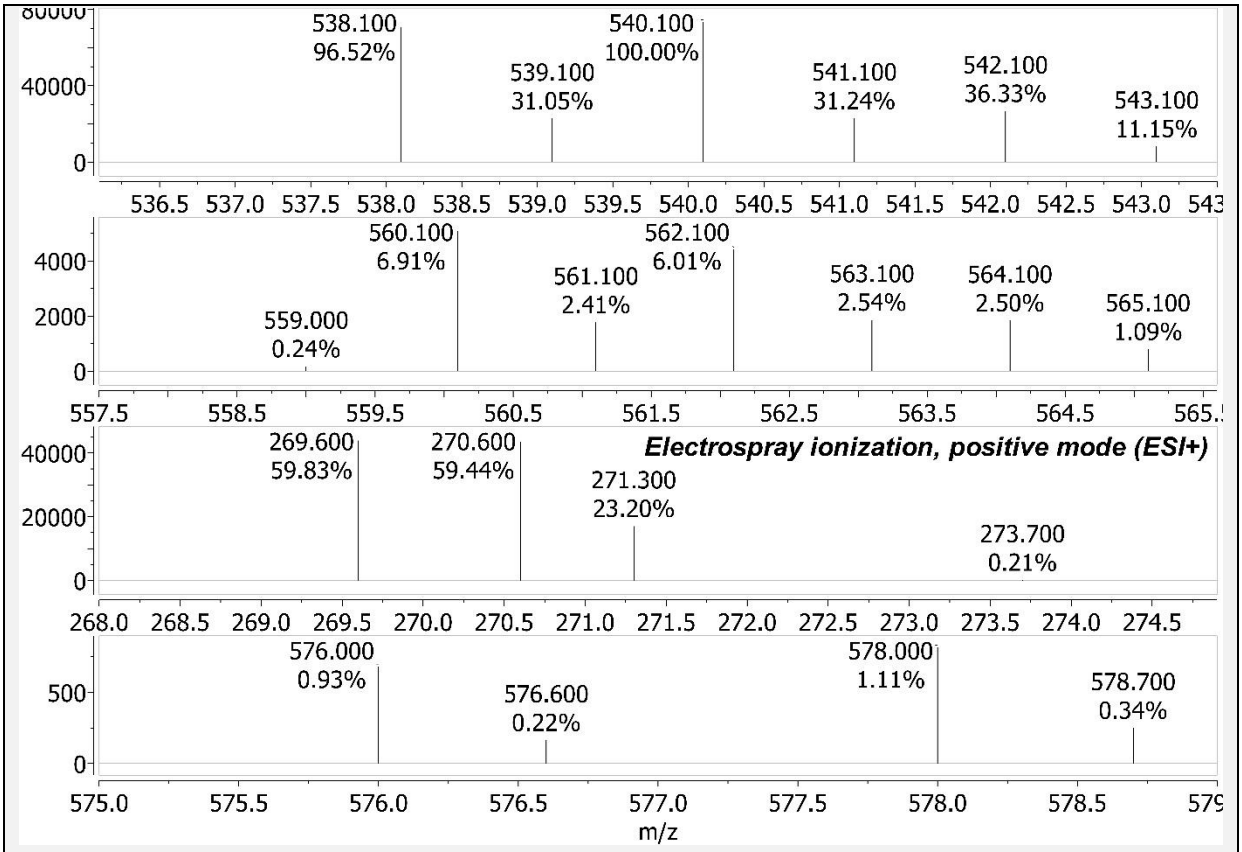

Figure 39 – Some Mass Spectrum (MS) components of Figure 38. *Upper panel*: *m/z* 538.1 $[M+H]^+$. *2nd panel*: *m/z* 560.1 $[M+Na]^+$. *3rd panel*: *m/z* 269.6 $[M+2H]^{2+}$. *Bottom panel*: *m/z* 576.0 $[M+K]^+$. All these Observed *m/z* are within 0.06 of Expected.

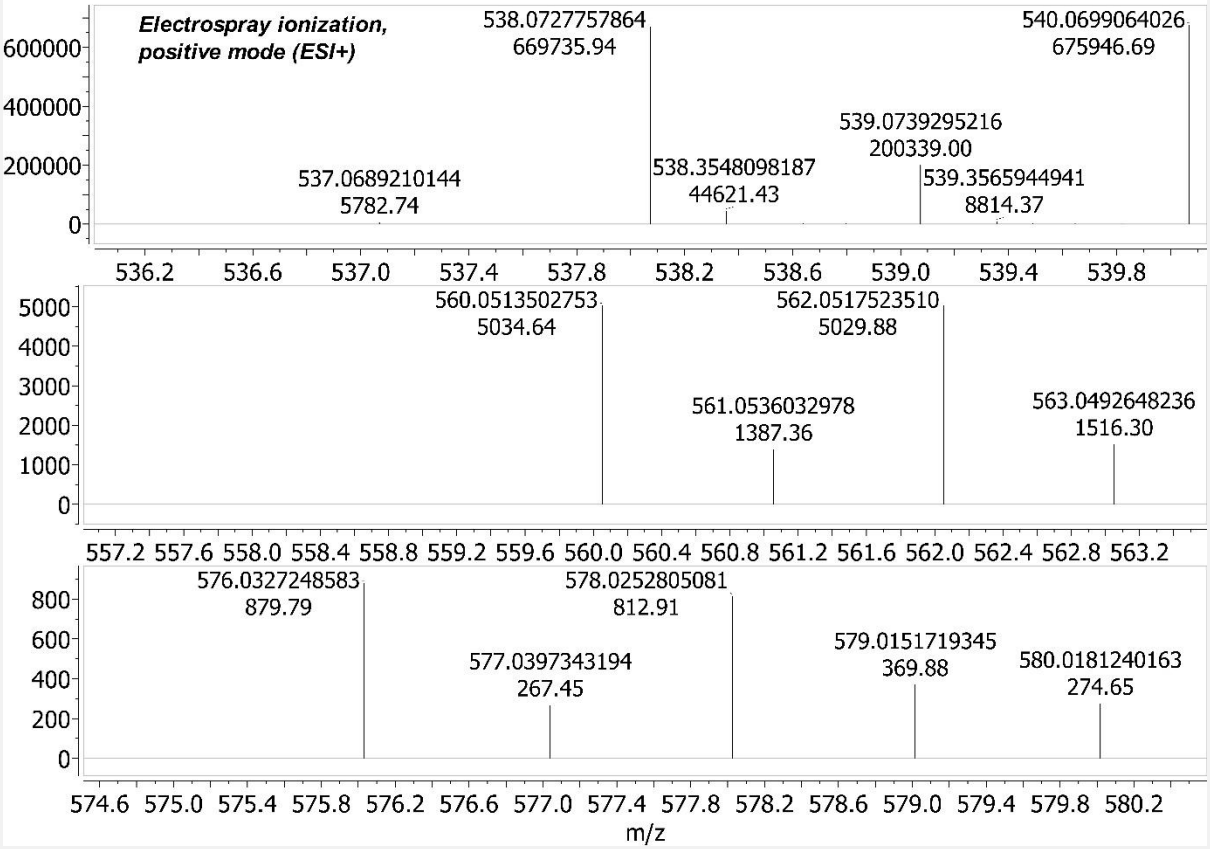

Figure 40 – HRMS: LC-TOF MS for 7a sample. LC Retention Time (RT) = 0.163 minutes (LC data not shown). *Upper panel*: *m/z* 538.0727757864 $[M+H]^+$. The species with *m/z* 537.0689210144 $[M+H]^+$ has hydrogen instead of deuterium on the chiral carbon. Absolute abundance is shown on the y-axis. And the molar percent deuterium incorporation for 7a at the chiral carbon is 100% - ((5782.74/669735.94)*100=0.86%) = 99.14%. *2nd panel*: *m/z* 560.0513502753 $[M+Na]^+$. *Bottom panel*: *m/z* 576.0327248583 $[M+K]^+$.

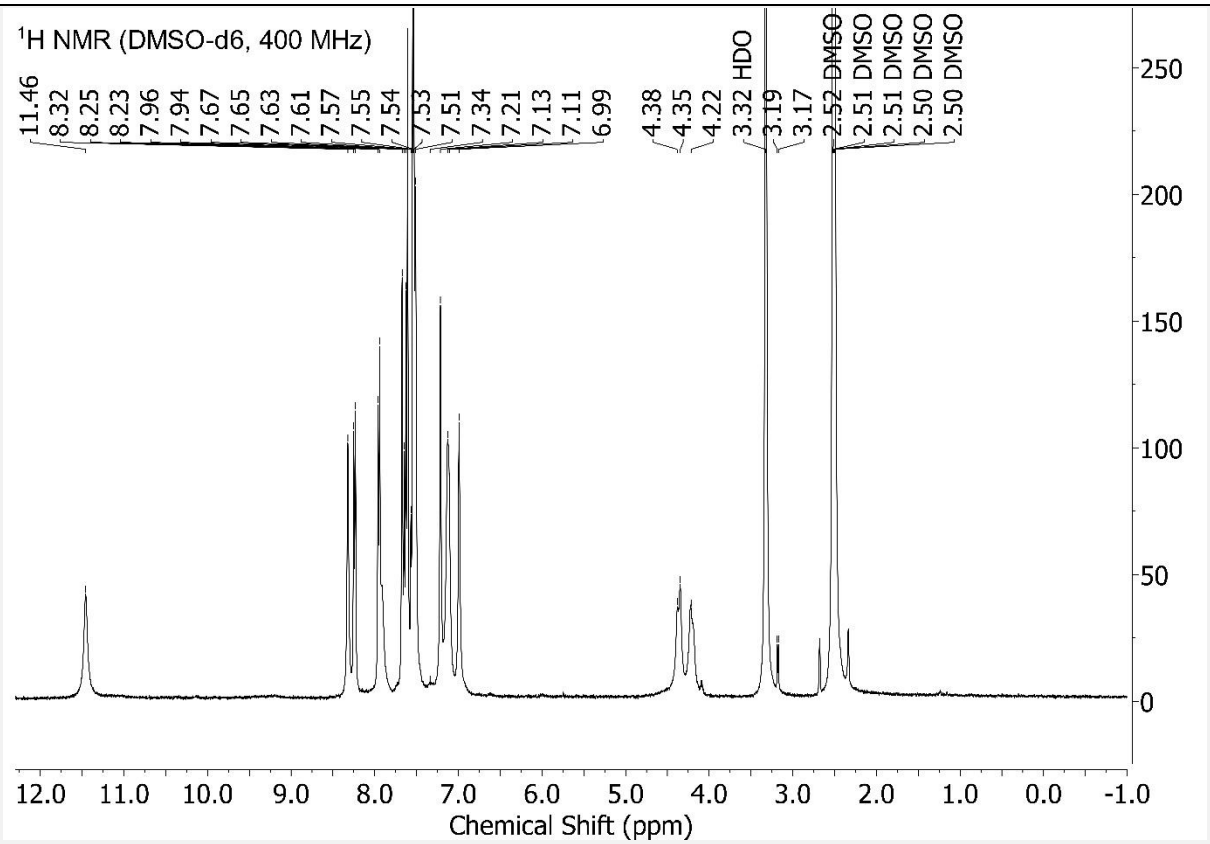

Figure 41 – ^{1}H NMR {*NMR probe temperature = 300.7 K*} for 7a sample. Scaled to highest compound peak. "Auto peak picking" algorithm in MestReNova v12 used to pick peaks shown. With default program settings used. And no chemical structure used/inputted to guide/constrain this peak picking.

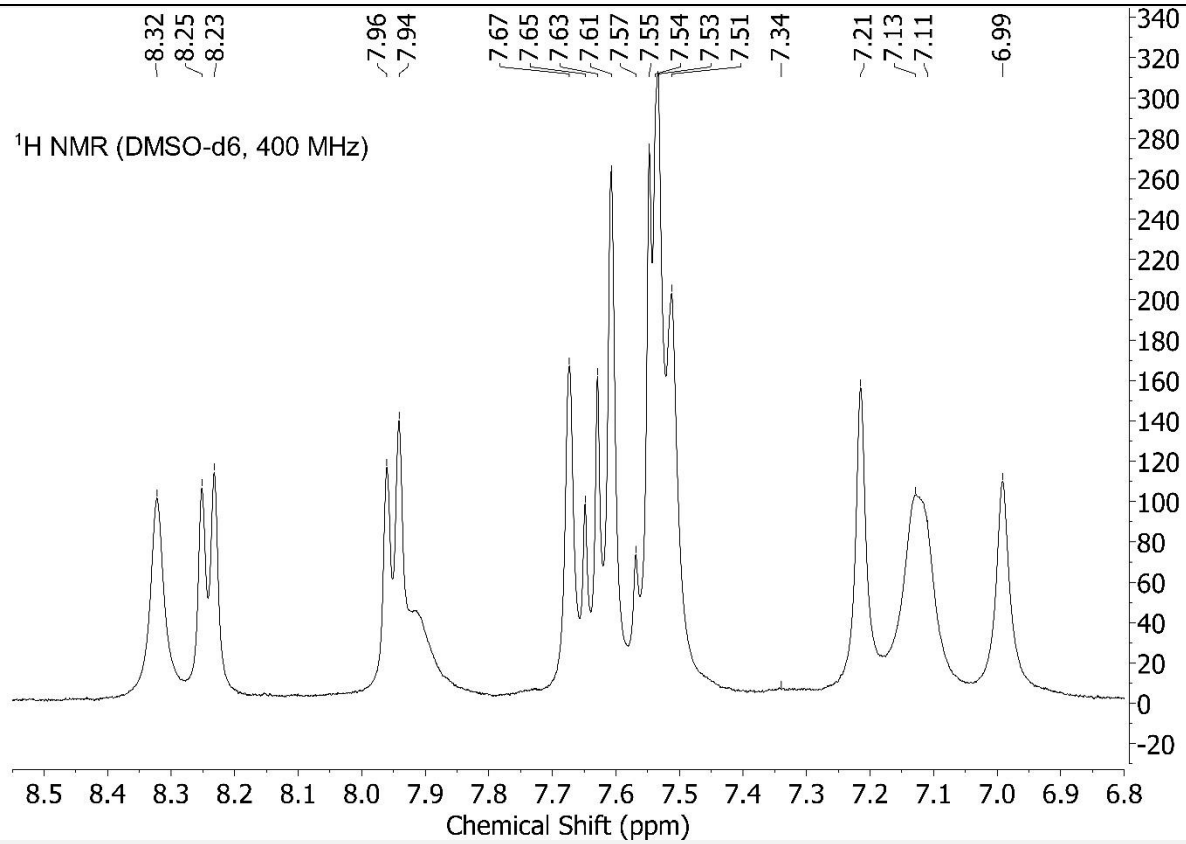

Figure 42 – Aromatic region of Figure 41 expanded.

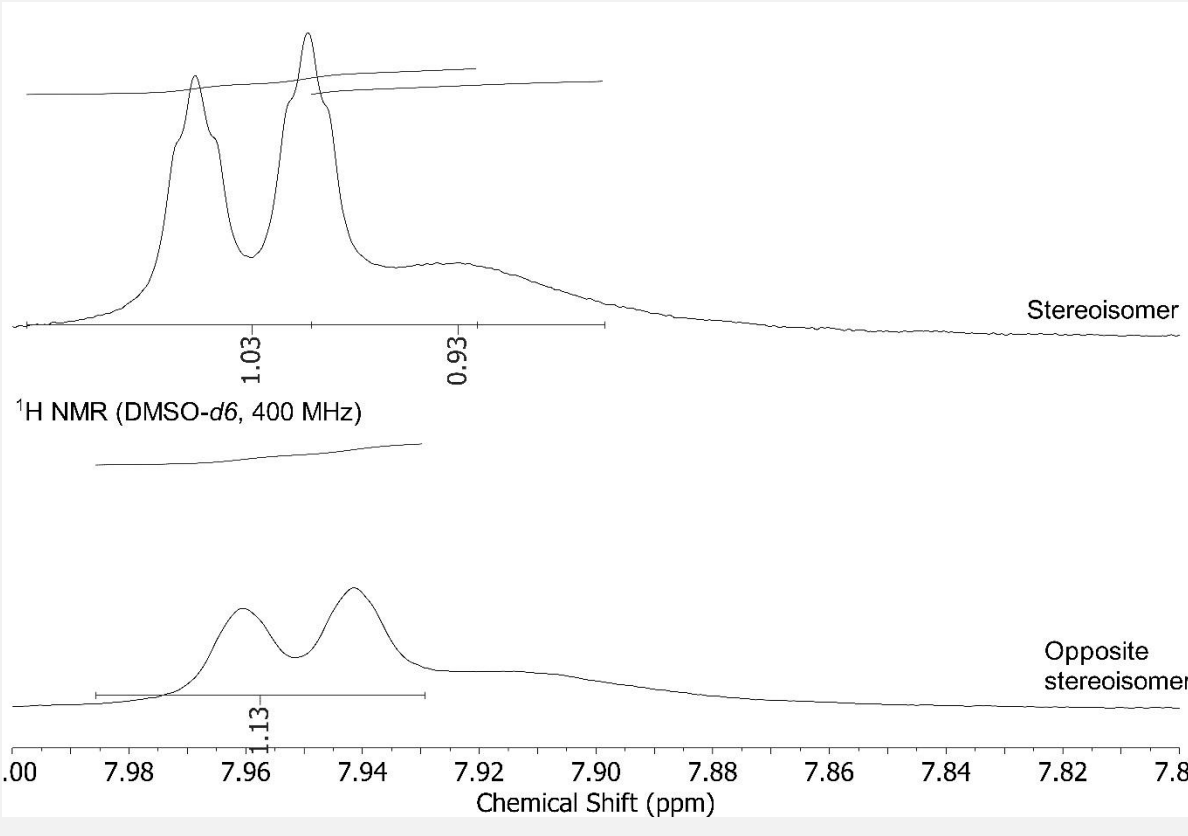

Figure 43 – 7b data in upper panel, 7a data in lower panel. Figure shows integration values in this ppm region as automatically assigned by the MestReNova v12 software used. 7b has 2H assigned (1.03+0.93=1.96, rounds to 2), whilst 7a has 1H assigned (1.13, rounds to 1), in this ppm region.

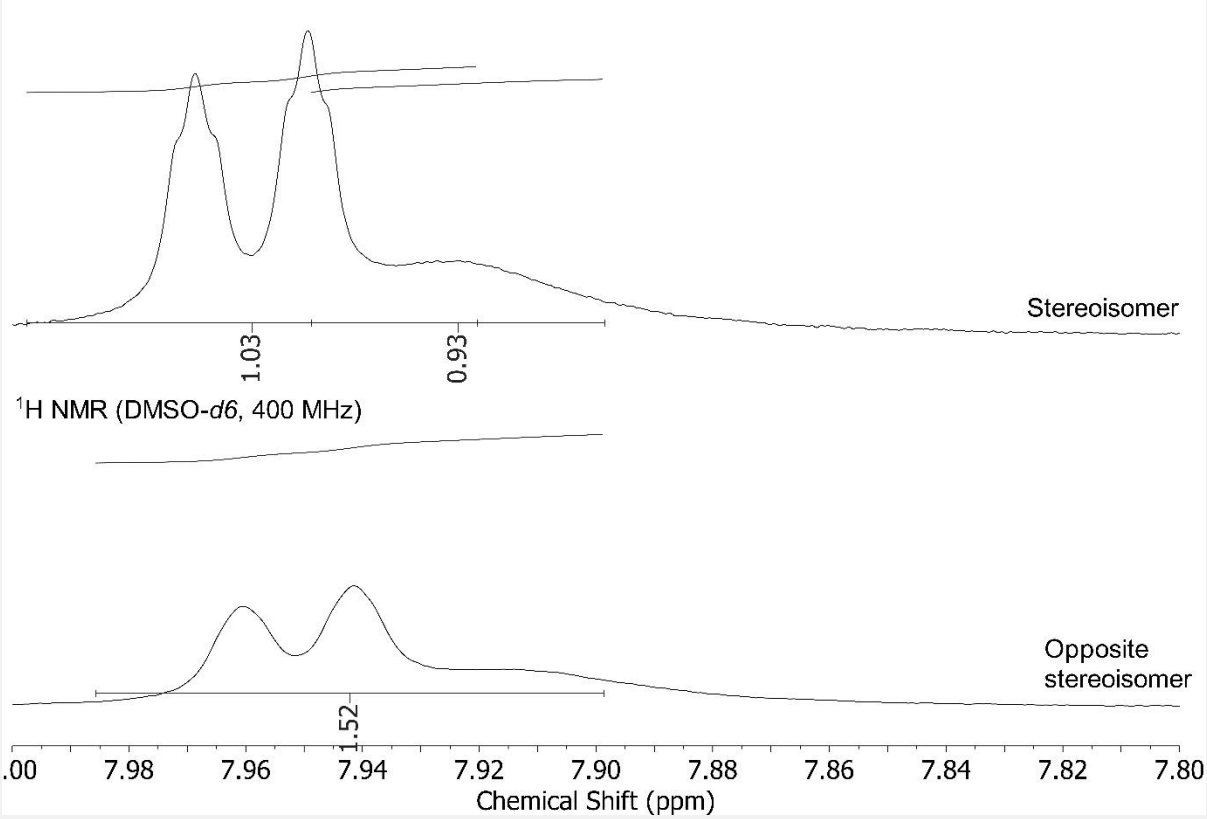

Figure 44 – Shown here, I manually extended the integration line (N.B., this automatically changes the MestReNova v12 integration calculation method from "peak" to "sum") for 7a to be the same length as that for 7b. Which changes its integration value from 1.13 (prior) to 1.52, which rounds to 2H. This improves the 7a assignment because now it has the correct number of hydrogen nuclides (18H), whereas before it had (incorrectly) 17H. It is true that 1.52 only narrowly crosses the threshold for 2H. But interestingly, the integration value is also very low in this ppm region for the hydrogen on chiral carbon stereoisomers (integration value at 7.93 ppm = 1.51 for 6b, 1.57 for 6a. As assigned by "Auto Assignment" algorithm of MestReNova v12).

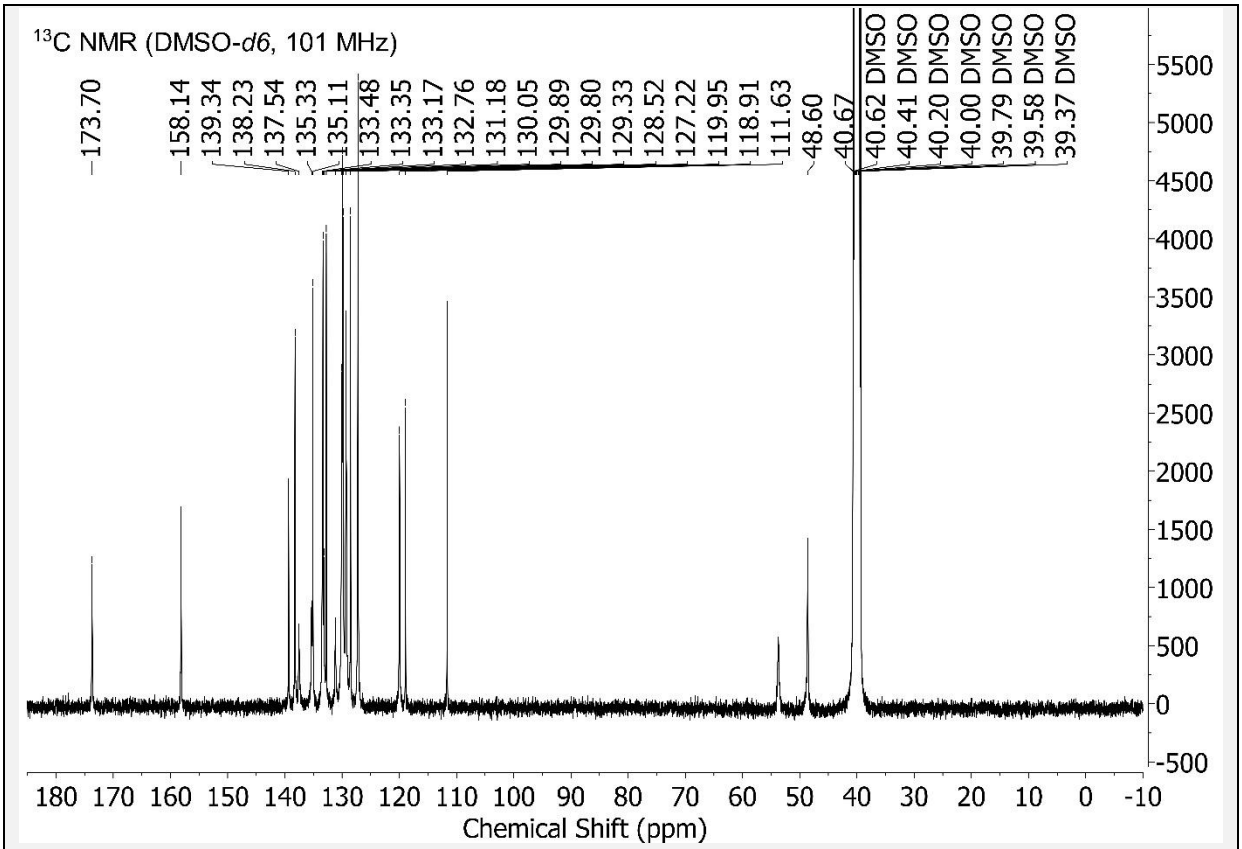

Figure 45 – ^{13}C NMR {*NMR probe temperature = 311.9 K*} for 7a. Scaled to highest compound peak. "Auto peak picking" algorithm in MestReNova v12 used to pick peaks shown. With default program settings used. And no chemical structure used/inputted to guide/constrain this peak picking.

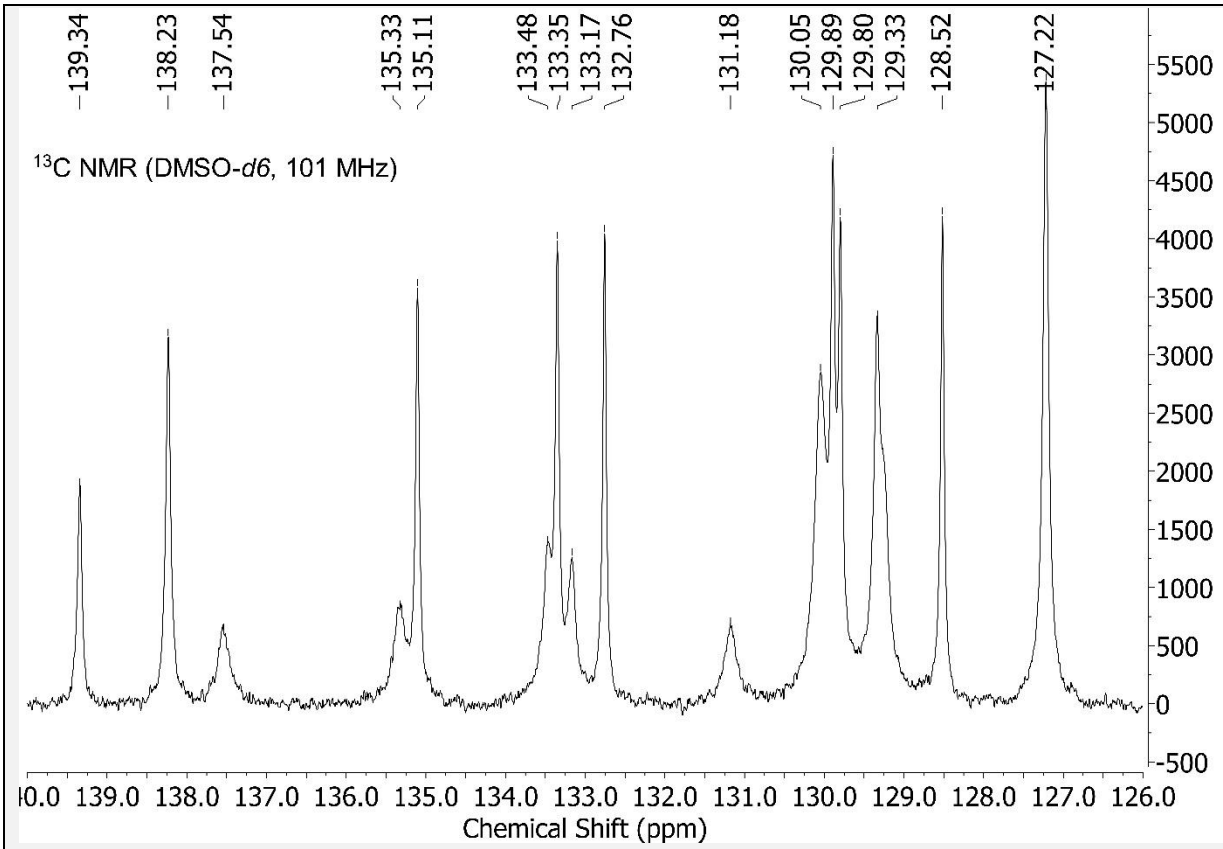

Figure 46 – Region of Figure 45 expanded.

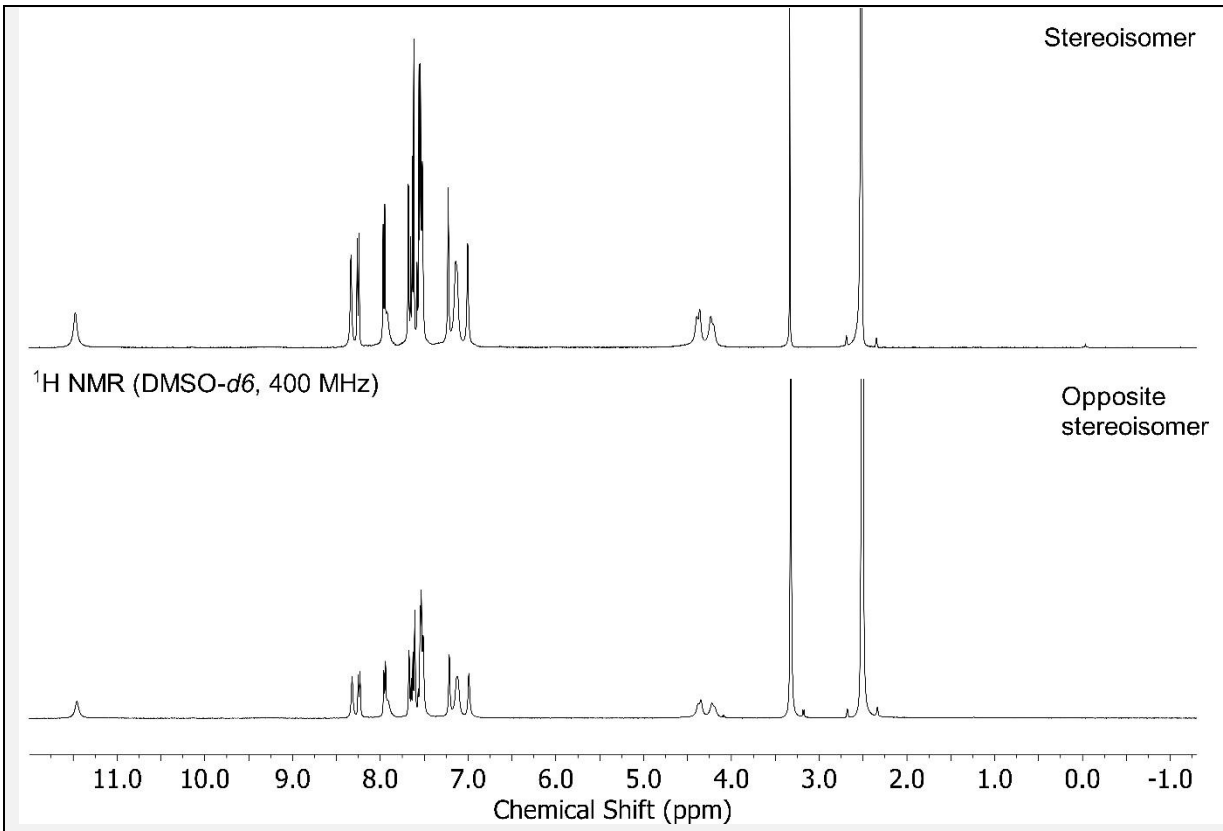

Figure 47 – 7b data in upper panel, 7a data in lower panel.

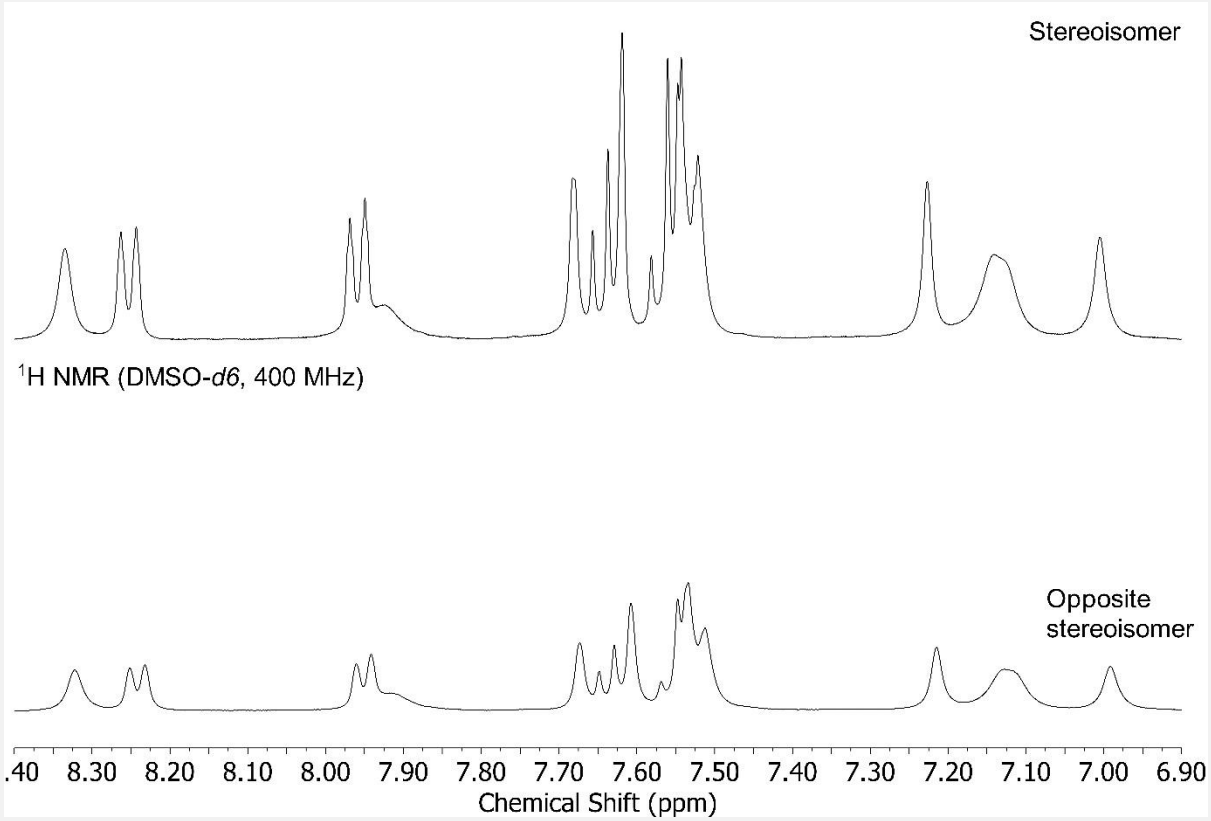

Figure 48 – Aromatic region. 7b data in upper panel, 7a data in lower panel.

Hydrogen vs. deuterium on chiral carbon

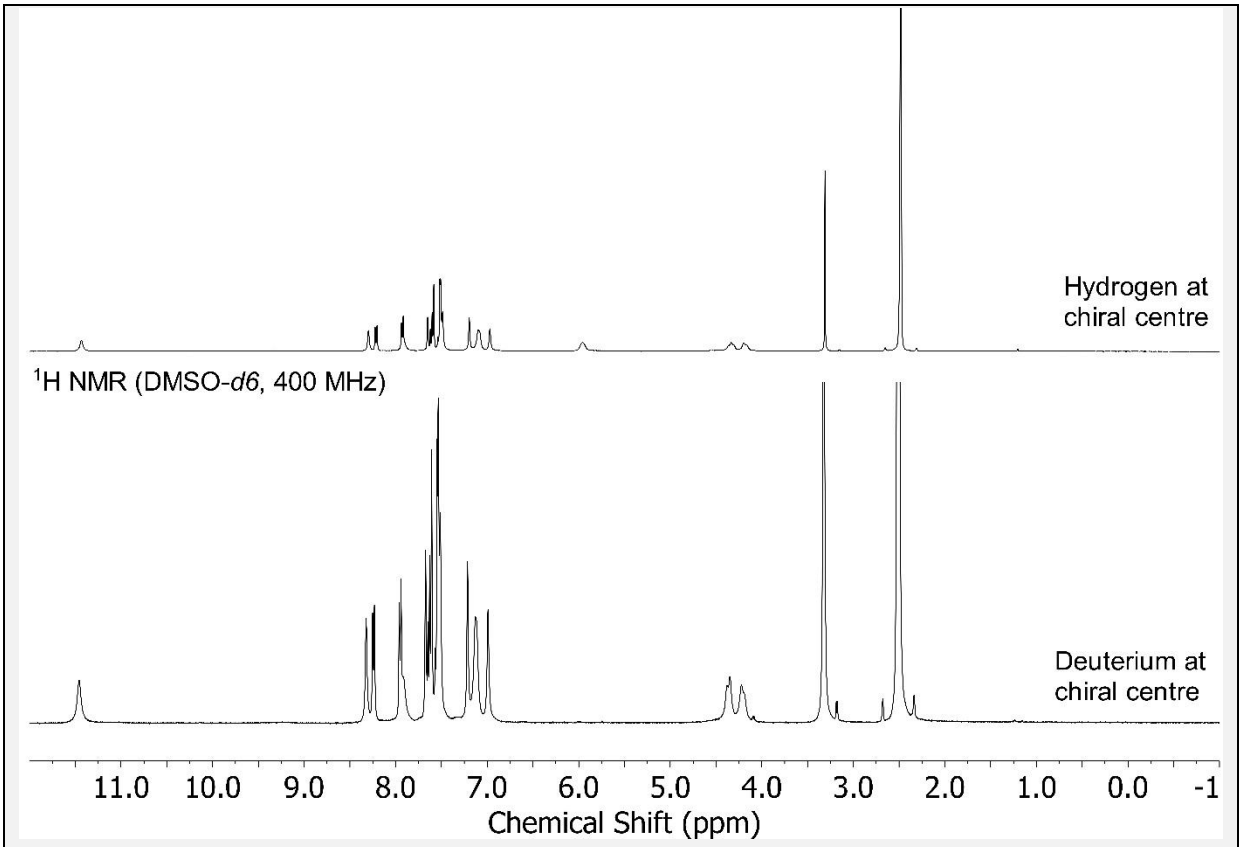

Figure 49 – *Upper panel*: ^{1}H NMR spectrum for 6b. *Lower panel*: ^{1}H NMR spectrum for 7a. The upper has a peak at 5.96 ppm from the hydrogen attached to its chiral carbon. The lower has this hydrogen replaced with a deuterium, and thence this 5.96 ppm peak is absent in its ^{1}H NMR spectrum.

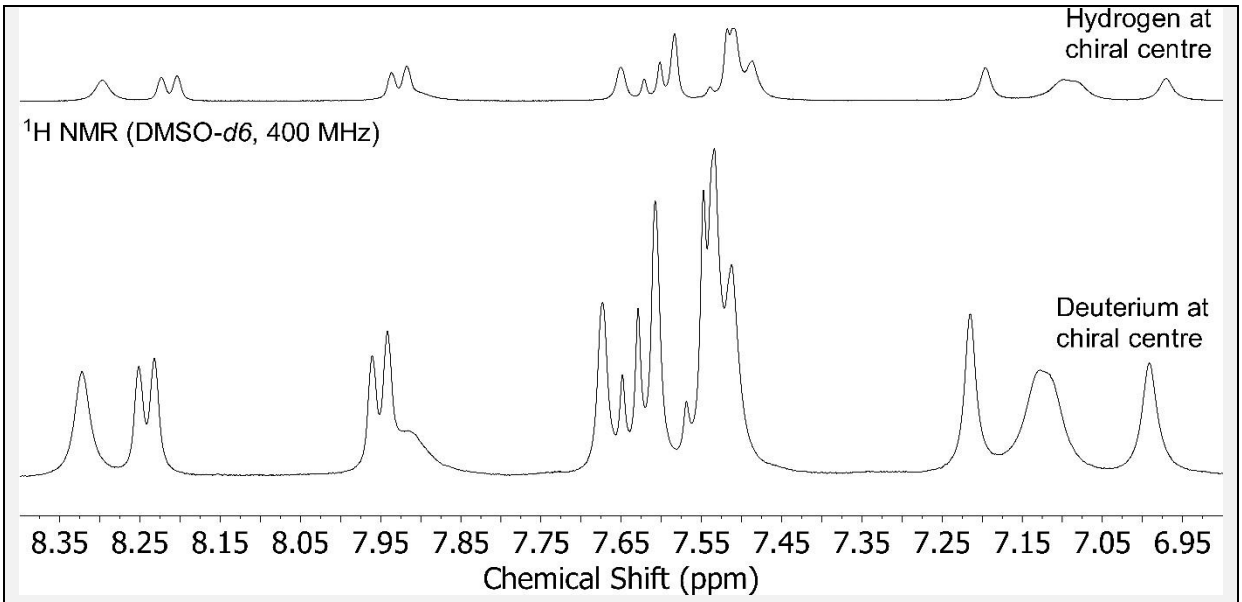

Figure 50 – Aromatic region. *Upper panel*: ^{1}H NMR spectrum for 6b. *Lower panel*: ^{1}H NMR spectrum for 7a.

Supplementary content for the Results section titled "Anti-cancer"

Consolidated absolute excess, and enantiomeric excess, data:

[From MassLynx 4.1 software on the Chiral SFC-MS machine used]			[***SAME data in different software: Mestrelab***]				
	Chiral SFC (UV chromatogram)		**Chiral SFC (UV chromatogram)**		***Chiral SFC-MS***		
	Absolute(%)	ee(%)	Absolute(%)	ee(%)	Absolute(%)	ee(%)	
6a	98.79	97.58	98.83	97.66	99.64	99.28	
6b	99.02	98.04	98.23	96.46	97.9	95.8	
7a	98.71	97.42	*Done on a different machine (other broke) **				
7b	100	100	100	100	*Can't calculate #*		
		Enantiomeric excess (ee) = (Absolute excess-50)*2					
Wavelength (λ) for UV chromatogram = 220 nm							
* This other machine *only* has Chiral SFC capability. It is *not* a Chiral SFC-MS machine.							
Its shown data is *not* from MassLynx 4.1, but from Empower 3 software instead.							
This data won't open in Mestrelab (incompatibility).							
Chiral SFC-MS machine used = Thar analytical SFC with UV & mass detectors.							
Chiral SFC machine used = Waters Acquity UPC2 with PDA detector.							
# Without equivalent Chiral-SFC data for 7a, it isn't possible to calculate from the Chiral SFC-MS data of 7b. Because the Retention Time (RT) of 7a on this machine is unknown.							

As shown earlier, the mean of 7a and 7b median anti-cancer activity (63.30) is slightly greater (0.54) than the mean of 6a and 6b median anti-cancer activity (62.76). Similarly, the mean of 7a and 7b mean anti-cancer activity (62.58) is slightly greater (0.85) than the mean of 6a and 6b mean anti-cancer activity (61.73). These differences are small enough (<1) to be within a margin of experimental error. This is their most likely explanation. But, alternatively, perhaps, they might actually reflect features of the data. Because (*i*) 7b has slightly greater enantiomeric excess than 6b, (*ii*) 7a has slightly less enantiomeric excess than 6a. Meaning, for absolute excess values, (7b-7a) is 1.06 greater than (6b-6a). Wherein values 0.54, 0.85, and 1.06 all round to 1.

A better plot of DNA repair rate for substitution into Figure 15

This section should be read with Figure 15 and its legend. It contributes a more faithful simulacrum of DNA repair rate, y. In the DNA repair rate equation below, the s variable is DNA damage concentration, [DNA damage], which is a function of not only present [ROS], x, shown on the x-axis of Figure 15, but *also* any past [ROS]. For example, where t is present time, (t-Δt) is a very short time (Δt) before the present time (t), t=0 is time at the start of this DNA, with surrounding [ROS], system, Δt is the step-size in time to use in the calculation,

wherein a smaller value of Δt confers more accuracy, t_i is the latest interim time in the calculation of z, x is [ROS] (=DNA damage it causes, because plot of DNA damage, y, is y=x), wherein this equation system has a Michaelis-Menten form at various points within it, wherein its selected values are merely illustrative, and not restricting:

plot of DNA repair rate, y, wherein z is any accumulated DNA damage due to the balance of past DNA damage and repair due to past [ROS], in the past time period (t=0)→(t-Δt):

$$y = \left(\frac{2 \cdot s}{1+s}\right)$$

$$s = f(x) = x + z$$

$$z = \begin{cases} \sum\limits_{(t=0)\to(t-\Delta t)} \begin{cases} \left(x - \left(\frac{2 \cdot x}{1+x}\right)\right) & if\ x > \left(\frac{2 \cdot x}{1+x}\right) \\ 0 & if\ x = \left(\frac{2 \cdot x}{1+x}\right) \\ 0 & \begin{cases} if\ x < \left(\frac{2 \cdot x}{1+x}\right) \\ and\ if \left(\sum\limits_{(t=0)\to t_i} x\right) \le \left(\sum\limits_{(t=0)\to t_i} \left(\frac{2 \cdot x}{1+x}\right)\right) \end{cases} \\ \left(x - \left(\frac{2 \cdot x}{1+x}\right)\right) = v & \begin{cases} if\ x < \left(\frac{2 \cdot x}{1+x}\right) \\ and\ if \left(\sum\limits_{(t=0)\to t_i} x\right) > \left(\sum\limits_{(t=0)\to t_i} \left(\frac{2 \cdot x}{1+x}\right)\right) \\ wherein\ used\ step\ size\ in\ time\ (t)\ is\ such: \\ |v| \le \left(\left(\sum\limits_{(t=0)\to t_i} x\right) - \left(\sum\limits_{(t=0)\to t_i} \left(\frac{2 \cdot x}{1+x}\right)\right)\right) \end{cases} \end{cases} \\ 0 & if\ (z < 0) \end{cases}$$

$$if \left(\left(\frac{2 \cdot s}{1+s}\right) > x\right) \left\{\left[s = \frac{x+z}{q}\right], where\ q\ is\ set\ such\ that \left(y = \left(\frac{2 \cdot s}{1+s}\right) = x\right)\right\}$$

The last line is "catch code" ensuring that total DNA damage repair cannot exceed total DNA damage.

The above uses idiosyncratic sigma notation. Which I think is clearer. If more conventional notation is wanted, please substitute the sigma notation accordingly. For the first, most principal, sigma symbol, please substitute in:

$$\sum_{n=b}^{p}$$

Where b is an "arbitrarily small" number, p is t-Δt and every instance of x falling under this sigma should instead be x_n. There are six daughter sigma systems (which too should each use x_n instead of x), which can each use the same sigma notation:

$$\sum_{n=b}^{g}$$

Where g is t_i.

Comparison with "senolytics"

	Less senescent cells	**Slightly lower body temperature**
Mouse	Transgenic mice (males and females) with less senescent cells had 27% (*or 24% in a different mouse strain*) greater median lifespan. Published in Nature [470].	Transgenic mice with 0.34°C lower mean body temperature had 20% greater median lifespan (*females. Males had 0.3°C lower, conferring 12% extension*). Published in Science [75].
Human	**No data** before senolytic drugs entered clinical trials. Since then, there has been the Phase II clinical failure of a senolytic drug (Unity Biotechnology's UBX0101 *<which is (according to its Phase II clinical study protocol) nutlin-3a in [471], which was developed by the pharmaceutical company Hoffmann-La Roche>* injected into knees with osteoarthritis) [472]. Clinical trials presently ongoing for UBX1325, fisetin	Humans with a lower body temperature have a longer lifespan [158, 170-172] and healthspan [173-174]. *Men with a body temperature below the average have a greater life expectancy (shown herein using data from [170]).*

	and for the Dasatinib+Quercetin combination [473].	
Corresponding drug success in mice?	Drugs successfully shown to decrease the number of senescent cells. *All be it only locally (because of systemic toxicity) for the first senolytic drugs that entered clinical trials, from Unity Biotechnology. Shown with senescent cells caused by injury rather than aging [353]. What distinguishes a senescent from a normal cell still isn't agreed [472].*	Drug successfully shown to dose-dependently lower body temperature (Figure 2). *Drug administered systemically.* Simple correspondence (*drug lowers body temperature of mice*) with the transgenic mice (*which have lower body temperature*).
Tractability of clinical trialling	The FDA doesn't classify aging as a disease [474]. But it can grant drug approval for treatment of an age-related disease. Unity Biotechnology showed that UBX0101 could decrease senescent cell number after knee injury in mice (but this couldn't be replicated in rats or dogs) and extrapolated that UBX0101 would treat osteoarthritis [353]. Endpoint for an osteoarthritis clinical trial is typically patient self-reporting pain (e.g., using the WOMAC scoring scale questionnaire), for which the	Alzheimer's disease can cause a higher body temperature in humans [194]. Higher body temperature accelerates disease progression in a mouse model of Alzheimer's [192]. A clinical trial can use the objective endpoint of body temperature (as an endpoint itself. Or as a surrogate endpoint for the FDA's "accelerated approval" pathway [288]). Can this drug reduce the higher body temperature of Alzheimer's patients to normality?

	placebo effect, especially for knee injections of saline [475], can be hard to surpass. Unity Biotechnology also modelled aging with injury, in its pre-clinical testing in the eye, for its follow-up drug UBX1967 [353].	
Corresponding drug extends mouse lifespan?	**No such data** before first senolytic drugs entered clinical trials. Now extended lifespan has been shown, starting with already aged mice (quicker result), with systemic administration of fisetin [476] or a Dasatinib+Quercetin combination [477]. But, conflicting, the Interventions Testing Program (ITP) [478] has tested fisetin (at the same dose as [476]) and Richard Miller (of the ITP) has said in a recent online interview that it had no lifespan effect [479]. A paper reporting this is forthcoming.	No such data to date.
Companies	Dozens [472]. Including Unity Biotechnology, which raised $222M in venture capital and then $85M in an IPO on NASDEQ, which valued the company at (pre-money)	None.

	$700M (since had up to $80M of debt financing available).	
Market size	At least some senolytic drugs, e.g. the failed and presently extant clinical drug candidates of Unity Biotechnology, are too toxic for systemic use, which restricts them to localized use [353].	Systemic drug administration anticipated possible in humans. So, (conceivably) able to slow aging throughout the body, delaying/slowing/ameliorating/treating *all* age-related diseases (simultaneously) thereby. Economists calculate that a slowdown in aging, which increases US life expectancy by one year, is worth $38T [186]. And further years accorded the multiple thereof. Local administration anticipated possible also: e.g., to the knee or eye. Market is everyone (all adults). Because everyone ages and no one wants to.
Potential	This transgenic mice result, given that *many/most* senolytic cells were eliminated [470], is probably near or at the full lifespan extending potential of this senolytic approach.	There is reason (disclosed herein) to believe that this transgenic mice result [75] is not at, or anywhere near, the full lifespan extending potential of this (*reducing metabolic heat generation, i.e. reducing metabolic rate*) approach. I believe that this intervention acts more upstream/fundamentally than the senolytic approach.
Criticism(s)	At least some senescent cells (or type[s] thereof) might be useful, not least for performing the tissue function when they are an appreciable proportion	To be seen.

	of it. “Senolytics are likely to accelerate tissue pathology, exacerbate clinical disease, and result in early morbidity and mortality” [480]. “We found that removing senescent cells, however, may be worse than leaving them to accumulate, as this can have systemic and liver-debilitating consequences”; “we show here that there are abundant $p16^{High}$ senescent cell types in an aging organism that are structurally and functionally important, while their removal has detrimental consequences”; “defined $p16^{High}$ senescent cell types are indispensable for mouse healthspan” [481]. What differentiates senescent from normal cells is contentious and so there isn’t consensus about how they can be specifically and safely targeted (“we are far from being able to define something as senescence-specific”) [472]. Studies often make the *assumption* that only senescent cells express p16 [353], which might not be correct. There might be different types of senescent	

	cells [472]. Killing senescent cells may cause them to release their contents, which are posited to be harmful, and so making things worse, not better. Senolytic drug action is often pre-clinically assayed against senescent cells caused by injury rather than aging [353] - but are these the same?	
Anticancer utility	At least some senolytic drugs are repurposed pre-clinical/clinical anticancer drugs.	Selective F_1F_0 ATP hydrolysis inhibiting drugs (*that don't inhibit F_1F_0 ATP synthesis*) have anticancer activity. This is a new finding. Patents filed (e.g. [16-17]) and so commercially viable to pursue. Clinical trials for cancer have well-defined, objective endpoints (e.g. delay of death), and surrogate endpoints (e.g. tumour shrinkage), that can be shown relatively quickly (especially in cancers that {tragically} tend to have poor prognosis, where patients only live months after diagnosis). There is a great unmet medical need, especially for a cancer drug without horrific side-effects (which often cause patients to rescind consent to treatment). Cancer cachexia (wasting/weight loss) is a huge unmet medical need. Relevantly, transgenic mice with slightly lower body temperature have higher body weight (with the same food consumption as

		control mice) [75]. Presumably because of greater metabolic efficiency, with less of the chemical energy of food dissipated as heat. Alzheimer's disease patients also suffer weight loss [296-298, 301-311], which their mortality is a function of [310-311]. Counteracting (e.g. slowing of) weight loss is a very objective, tractable clinical trial endpoint/surrogate endpoint.

COMPETING INTERESTS

The author has filed for related patents. These disclose, and protect, well beyond the scope of this present disclosure.

FUNDING

None. This work was conducted without funding.

ACKNOWLEDGEMENTS

Under the author's direction, two Contract Research Organisation (CROs) were utilized to generate the data of Figure 2, and Figures 16-50. WuXi AppTec synthesized the compounds. Crown Bioscience performed the experimentation in mice.

REFERENCES

[1] Tacutu R, Thornton D, Johnson E, Budovsky A, Barardo D, Craig T, Diana E, Lehmann G, Toren D, Wang J, Fraifeld VE, de Magalhaes JP (2018) Human Ageing Genomic Resources: new and updated databases. Nucleic Acids Research 46(D1):D1083-D1090.

[2] Denham Harman (1956) Aging: A Theory Based on Free Radical and Radiation Chemistry. Journal of Gerontology. 11:298-300.

[3] Harman D (1972) The biologic clock: the mitochondria? Journal of the American Geriatrics Society. 20(4):145-147.

[4] De Grey AD (1999) The mitochondrial free radical theory of aging. Austin, TX: RG Landes.

[5] Barja G (2013) Updating the mitochondrial free radical theory of aging: an integrated view, key aspects, and confounding concepts. Antioxidants & redox signalling. 19(12):1420-1445.

[6] Nicholls DG, Ferguson SJ (2002) Bioenergetics 3 (Vol. 3). Gulf Professional Publishing.

[7] Pullman ME, Monroy GC (1963) A naturally occurring inhibitor of mitochondrial adenosine triphosphatase. Journal of biological chemistry. 238(11):3762-3769.

[8] Runswick MJ, Bason JV, Montgomery MG, Robinson GC, Fearnley IM, Walker JE (2013) The affinity purification and characterization of ATP synthase complexes from mitochondria. Open Biology. 3(2):120160.

[9] Gledhill JR, Montgomery MG, Leslie AG, Walker JE (2007) How the regulatory protein, IF1, inhibits F1-ATPase from bovine mitochondria. Proceedings of the National Academy of Sciences. 104(40):15671-15676.

[10] Bason JV, Runswick MJ, Fearnley IM, Walker JE (2011) Binding of the inhibitor protein IF1 to bovine F1-ATPase. Journal of molecular biology. 406(3):443-453.

[11] Bason JV, Montgomery MG, Leslie AG, Walker JE (2014) Pathway of binding of the intrinsically disordered mitochondrial inhibitor protein to F1-ATPase. Proceedings of the National Academy of Sciences, 111(31):11305-11310.

[12] Mendoza-Hoffmann F, Zarco-Zavala M, Ortega R, García-Trejo JJ (2018) Control of rotation of the F1FO-ATP synthase nanomotor by an inhibitory α-helix from unfolded ε or intrinsically disordered ζ and IF1 proteins. Journal of Bioenergetics and Biomembranes. 50(5):403-24.

[13] Cabezon E, Butler PJG, Runswick MJ, Walker JE (2000) Modulation of the oligomerization state of the bovine F1-ATPase inhibitor protein, IF1, by pH. Journal of Biological Chemistry. 275(33):25460-25464.

[14] Jennings RB, Reimer KA, Steenbergen C (1991) Effect of inhibition of the mitochondrial ATPase on net myocardial ATP in total ischemia. Journal of molecular and cellular cardiology. 23(12):1383-95.

[15] Rouslin W (1983) Protonic inhibition of the mitochondrial oligomycin-sensitive adenosine 5'-triphosphatase in ischemic and autolyzing cardiac muscle. Possible mechanism for the mitigation of ATP hydrolysis under nonenergizing conditions. Journal of Biological Chemistry. 258(16):9657-61.

[16] Michael David Forrest. “Therapeutic Modulators of the Reverse Mode of ATP Synthase”. U.S. Patent Application No. 16/629,390. Published as US20200306253A1. In PDF format, on the Google Patents website:

https://patentimages.storage.googleapis.com/2b/ad/07/f9e06bda62ec75/US20200306253A1.pdf. This US patent application is a 371 national entry of PCT/EP2018/069175 (filed 13 July 2018), which published as WO2019/012149A1 (on 17 January 2019).

[17] Michael David Forrest. "Therapeutic Inhibitors of the Reverse Mode of ATP Synthase". U.S. Patent Application No. US16/478,497. Published as US20200247758A1.
In PDF format, on the Google Patents website:
https://patentimages.storage.googleapis.com/32/92/56/ffe5afbff03bf0/US20200247758A1.pdf. This US patent application is a 371 national entry of PCT/EP2018/051127 (filed 17 January 2018), which published as WO2018/134265A1 (on 26 July 2018).

[18] Forrest MD (2021) F_1F_0 ATP hydrolysis is a determinant of metabolic rate, a correlate of lifespan, and a weakness of cancer. v2. bioRxiv.

[19] Forrest MD (2021) F_1F_0 ATP hydrolysis is a determinant of metabolic rate and a correlate of lifespan. v1. bioRxiv.

[20] Figure is unmodified from that in the public domain at https://en.wikipedia.org/wiki/Pawl (accessed on 12 July 2022), where it is presented via CC BY-SA 4.0, courtesy of Antoni Espinosa.

[21] https://www.youtube.com/watch?v=5KWM9k5j_LI (accessed on 12 July 2022).

[22] Gao YQ, Yang W, Karplus M (2005) A structure-based model for the synthesis and hydrolysis of ATP by F1-ATPase. Cell. 123(2):195-205.

[23] Senior AE, Nadanaciva S, Weber J (2002) The molecular mechanism of ATP synthesis by F1F0-ATP synthase. Biochimica et Biophysica Acta (BBA)-Bioenergetics. 1553(3):188-211.

[24] Vinogradov AD (2000) Steady-state and pre-steady-state kinetics of the mitochondrial F1F0 ATPase: is ATP synthase a reversible molecular machine? Journal of Experimental Biology. 203(1):41-9.

[25] Syroeshkin AV, Vasilyeva EA, Vinogradov AD (1995) ATP synthesis catalyzed by the mitochondrial F1-F0 ATP synthase is not a reversal of its ATPase activity. FEBS letters. 366(1):29-32.

[26] Bald D, Amano T, Muneyuki E, Pitard B, Rigaud JL, Kruip J, Hisabori T, Yoshida M, Shibata M (1998) ATP synthesis by F_0F_1-ATP synthase independent of noncatalytic nucleotide binding sites and insensitive to azide inhibition. Journal of Biological Chemistry. 273(2):865-70.

[27] Tsubaki M, Yoshikawa S (1993) Fourier-transform infrared study of azide binding to the Fea3-CuB binuclear site of bovine heart cytochrome c oxidase: new evidence for a redox-linked conformational change at the binuclear site. Biochemistry. 32(1):174-82.

[28] Atwal KS, Ahmad S, Ding CZ, Stein PD, Lloyd J, Hamann LG, Green DW, Ferrara FN, Wang P, Rogers WL, Doweyko LM (2004) N-[1-Aryl-2-(1-imidazolo) ethyl]-guanidine derivatives as potent inhibitors of the bovine mitochondrial F1F0 ATP hydrolase. Bioorganic & medicinal chemistry letters. 14(4):1027-30.

[29] Bisaha SN, Malley MF, Pudzianowski A, Monshizadegan H, Wang P, Madsen CS, Gougoutas JZ, Stein PD (2005) A switch in enantiomer preference between mitochondrial F1F0-ATPase chemotypes. Bioorganic & Medicinal Chemistry Letters. 15(11):2749-51.

[30] Grover GJ, Atwal KS, Sleph PG, Wang FL, Monshizadegan H, Monticello T, Green DW (2004) Excessive ATP hydrolysis in ischemic myocardium by mitochondrial F1F0-ATPase: effect of selective pharmacological inhibition of mitochondrial ATPase hydrolase activity. American Journal of Physiology-Heart and Circulatory Physiology. 287(4):H1747-55.

[31] Cabanac A, Briese E (1992) Handling elevates the colonic temperature of mice. Physiology & behavior. 51(1):95-8.

[32] Sullivan GM, Feinn R (2012) Using effect size—or why the P value is not enough. Journal of graduate medical education. 4(3):279-82.

[33] Ialongo C (2016) Understanding the effect size and its measures. Biochemia medica. 26(2):150-63.

[34] Coe R (2002) It's the effect size, stupid. In British Educational Research Association Annual Conference (Vol. 12, p. 14).

[35] Ferguson CJ (2009) An effect size primer: a guide for clinicians and researchers. Professional Psychology: Research and Practice. 40(5):532-538.

[36] Maher JM, Markey JC, Ebert-May D (2013) The other half of the story: effect size analysis in quantitative research. CBE—Life Sciences Education. 12(3):345-51.

[37] Levine TR, Hullett CR (2002) Eta squared, partial eta squared, and misreporting of effect size in communication research. Human Communication Research. 28(4):612-25.

[38] Marschner JA, Schäfer H, Holderied A, Anders HJ (2016) Optimizing mouse surgery with online rectal temperature monitoring and preoperative heat supply. Effects on post-ischemic acute kidney injury. PLoS One. 11(2):e0149489.

[39] Hudson JW, Scott IM (1979) Daily torpor in the laboratory mouse, Mus musculus var. albino. Physiological Zoology. 52(2):205-18.

[40] Michael David Forrest. "Therapeutic Inhibitors of the Reverse Mode of ATP Synthase". Australian granted patent AU2018209175B2. In PDF format, on the Google Patents website: https://patentimages.storage.googleapis.com/44/b1/1c/441be2155c42b1/AU2018209175B2.pdf. This is a national entry of PCT/EP2018/051127 (filed 17 January 2018), which published as WO2018/134265A1 (on 26 July 2018).

[41] Wilson DJ (2019) The harmonic mean p-value for combining dependent tests. Proceedings of the National Academy of Sciences. 116(4):1195-1200.

[42] Formentini L, Pereira MP, Sánchez-Cenizo L, Santacatterina F, Lucas JJ, Navarro C, Martínez-Serrano A, Cuezva JM (2014) In vivo inhibition of the mitochondrial H+-ATP synthase in neurons promotes metabolic preconditioning. The EMBO journal. 33(7):762-78.

[43] Santacatterina F, Sánchez-Cenizo L, Formentini L, Mobasher MA, Casas E, Rueda CB, Martínez-Reyes I, de Arenas CN, García-Bermúdez J, Zapata JM, Sánchez-Aragó M (2016) Down-regulation of oxidative phosphorylation in the liver by expression of the ATPase inhibitory factor 1 induces a tumor-promoter metabolic state. Oncotarget. 7(1):490.

[44] Formentini L, Santacatterina F, de Arenas CN, Stamatakis K, López-Martínez D, Logan A, Fresno M, Smits R, Murphy MP, Cuezva JM (2017) Mitochondrial ROS production protects the intestine from inflammation through functional M2 macrophage polarization. Cell reports. 19(6):1202-13.

[45] Alpert NM, Guehl N, Ptaszek L, Pelletier-Galarneau M, Ruskin J, Mansour MC, ... & El Fakhri G (2018) Quantitative in vivo mapping of myocardial mitochondrial membrane potential. PloS one. 13(1):e0190968.

[46] Porcelli AM, Ghelli A, Zanna C, Pinton P, Rizzuto R, Rugolo M (2005) pH difference across the outer mitochondrial membrane measured with a green fluorescent protein mutant. Biochemical and biophysical research communications. 326(4):799-804.

[47] Davies KM, Strauss M, Daum B, Kief JH, Osiewacz HD, Rycovska A, ... Kühlbrandt W (2011) Macromolecular organization of ATP synthase and complex I in whole mitochondria. Proceedings of the National Academy of Sciences. 108(34):14121-14126.

[48] Llopis J, McCaffery JM, Miyawaki A, Farquhar M, Tsien RY (1998) Measurement of cytosolic, mitochondrial, and Golgi pH in single living cells with green fluorescent proteins. Proc. Natl. Acad. Sci. USA 95:6803–6808.

[49] Heidrick ML, Hendricks LC, Cook DE (1984) Effect of dietary 2-mercaptoethanol on the life span, immune system, tumor incidence and lipid peroxidation damage in spleen lymphocytes of aging BC3F1 mice. Mechanisms of ageing and development. 27(3):341-358.

[50] Milgram NW, Racine RJ, Nellis P, Mendonca A, Ivy GO (1990) Maintenance on L-deprenyl prolongs life in aged male rats. Life Sciences. 47(5):415-420.

[51] Schriner SE, Linford NJ, Martin GM, Treuting P, Ogburn CE, Emond M, Rabinovitch PS (2005) Extension of murine life span by overexpression of catalase targeted to mitochondria. Science. 308(5730):1909-1911.

[52] Podmore ID, Griffiths HR, Herbert KE, Mistry N, Mistry P, Lunec J (1998) Vitamin C exhibits pro-oxidant properties. Nature. 392(6676):559-559.

[53] Sohal RS, Orr WC (2012) The redox stress hypothesis of aging. Free Radical Biology and Medicine. 52(3):539-555.

[54] Rebrin I, Sohal RS (2008) Pro-oxidant shift in glutathione redox state during aging. Advanced drug delivery reviews. 60(13-14):1545-1552.

[55] Roberts II LJ, Reckelhoff JF (2001) Measurement of F2-isoprostanes unveils profound oxidative stress in aged rats. Biochemical and biophysical research communications. 287(1):254-6.

[56] Wood JM, Decker H, Hartmann H, Chavan B, Rokos H, Spencer JD, Schallreuter KU (2009) Senile hair graying: H2O2-mediated oxidative stress affects human hair color by blunting methionine sulfoxide repair. The FASEB Journal. 23(7):2065-2075.

[57] Shi Y, Buffenstein R, Pulliam DA, Van Remmen H (2010) Comparative studies of oxidative stress and mitochondrial function in aging. Integrative and comparative biology. 50(5):869-879.

[58] Rouslin WI (1987) The mitochondrial adenosine 5'-triphosphatase in slow and fast heart rate hearts. American Journal of Physiology-Heart and Circulatory Physiology. 252(3):H622-7.

[59] Sasaki T, Unno K, Tahara S, Shimada A, Chiba Y , Hoshino M, Kaneko T (2008) Age-related increase of superoxide generation in the brains of mammals and birds. Aging cell. 7(4):459-469.

[60] Foksinski M, Rozalski R, Guz J, Ruszkowska B, Sztukowska P, Piwowarski M, Olinski R (2004) Urinary excretion of DNA repair products correlates with metabolic rates as well as with maximum life spans of different mammalian species. Free Radical Biology and Medicine. 37(9):1449-1454.

[61] Hamilton ML, Van Remmen H, Drake JA, Yang H, Guo ZM, Kewitt K, Richardson A (2001) Does oxidative damage to DNA increase with age? Proceedings of the National Academy of Sciences. 98(18):10469-10474.

[62] Kaneo T, Tahara S, Matsuo M (1996) Non-linear accumulation of 8-hydroxy-2′-deoxyguanosine, a marker of oxidized DNA damage, during aging. Mutation Research/DNAging. 316(5-6):277-285.

[63] Barja G, Herrero A (2000) Oxidative damage to mitochondrial DNA is inversely related to maximum life span in the heart and brain of mammals. The FASEB Journal. 14(2): 312-318.

[64] Cagan A, Baez-Ortega A, Brzozowska N, Abascal F, Coorens TH, Sanders MA, ... & Martincorena I (2022) Somatic mutation rates scale with lifespan across mammals. Nature. 1-8.

[65] Pamplona R, Portero-Otın M, Ruiz C, Gredilla R, Herrero A, Barja G (2000) Double bond content of phospholipids and lipid peroxidation negatively correlate with maximum longevity in the heart of mammals. Mechanisms of ageing and development. 112(3):169-183.

[66] Swovick K, Firsanov D, Welle KA, Hryhorenko JR, Wise JP, George C, ... & Ghaemmaghami S (2021) Interspecies differences in proteome turnover kinetics are correlated with life spans and energetic demands. Molecular & Cellular Proteomics. 20.

[67] Kleiber M (1932) Body size and metabolism. Hilgardia. 6(11):315-353.

[68] Kleiber M (1947) Body size and metabolic rate. Physiological reviews. 27(4):511-541.

[69] Savage VM, Gillooly JF, Woodruff WH, West GB, Allen AP, Enquist BJ, Brown JH (2004) The predominance of quarter-power scaling in biology. Functional Ecology. 18(2):257-282.

[70] Prinzinger R (2005) Programmed ageing: the theory of maximal metabolic scope: How does the biological clock tick? EMBO reports. 6(S1):S14-S19.

[71] Porter RK, Hulbert AJ, Brand MD (1996) Allometry of mitochondrial proton leak: influence of membrane surface area and fatty acid composition. American Journal of Physiology-Regulatory, Integrative and Comparative Physiology. 271(6):R1550-R1560.

[72] Kleiber M (1941) Body size and metabolism of liver slices in vitro. Proceedings of the Society for Experimental Biology and Medicine. 48(2):419-423.

[73] Biesanz JC, Falk CF, Savalei V (2010) Assessing mediational models: Testing and interval estimation for indirect effects. Multivariate Behavioral Research. 45(4):661-701.

[74] Rosseel Y (2012) Lavaan: An R package for structural equation modeling and more. Version 0.5–12 (BETA). Journal of statistical software. 48(2):1-36.

[75] Conti B, Sanchez-Alavez M, Winsky-Sommerer R, Morale MC, Lucero J, Brownell S, Bartfai T (2006) Transgenic mice with a reduced core body temperature have an increased life span. Science. 314(5800):825-828.

[76] Conti B (2008) Considerations on temperature, longevity and aging. Cellular and Molecular Life Sciences. 65(11):1626-1630.

[77] Peto MV, De la Guardia C, Winslow K, Ho A, Fortney K, Morgen E (2017) MortalityPredictors.org: a manually-curated database of published biomarkers of human all cause mortality. Aging (Albany NY). 9(8):1916.

[78] Riely CA, Cohen G, Lieberman M (1974) Ethane evolution: a new index of lipid peroxidation. Science. 183(4121):208-210.

[79] Kneepkens CF, Lepage G, Roy CC (1994) The potential of the hydrocarbon breath test as a measure of lipid peroxidation. Free Radical Biology and Medicine. 17(2):127-160.

[80] Topp H, Vangala M, Kritzler K, Schöch G (1995) Assessment of lipid peroxidation in rats of different body weight by determining expired ethane. Biological Chemistry Hoppe-Seyler. 376(11):691-694.

[81] Sagai M, Ichinose T (1980) Age-related changes in lipid peroxidation as measured by ethane, ethylene, butane and pentane in respired gases of rats. Life sciences. 27(9):731-738.

[82] Zarling EJ, Mobarhan S, Bowen P, Kamath S (1993) Pulmonary pentane excretion increases with age in healthy subjects. Mechanisms of ageing and development. 67(1-2):141-147.

[83] Phillips M, Greenberg J, Cataneo RN (2000) Effect of age on the profile of alkanes in normal human breath. Free radical research. 33(1):57-63.

[84] Pincemail J, Deby C, Dethier A, Bertrand Y, Lismonde M, Lamy M (1987) Pentane measurement in man as an index of lipoperoxidation. Bioelectrochemistry and Bioenergetics. 18(1-3):117-126.

[85] Knutson MD, Lim AK, Viteri FE (1999) A practical and reliable method for measuring ethane and pentane in expired air from humans. Free Radical Biology and Medicine. 27(5-6):560-571.

[86] Knutson MD, Handelman GJ, Viteri FE (2000) Methods for measuring ethane and pentane in expired air from rats and humans. Free Radical Biology and Medicine. 28(4):514-519.

[87] Wade CR, van Rij A (1985) In vivo lipid peroxidation in man as measured by the respiratory excretion of ethane, pentane, and other low-molecular-weight hydrocarbons. Analytical biochemistry. 150(1):1-7.

[88] Matsuo M, Gomi F, Kuramoto K, Sagai M (1993) Food restriction suppresses an age-dependent increase in the exhalation rate of pentane from rats: a longitudinal study. Journal of gerontology. 48(4):B133-B138.

[89] Habib MP, Dickerson F, Mooradian AD (1990) Ethane production rate in vivo is reduced with dietary restriction. Journal of Applied Physiology. 68(6):2588-2590.

[90] Paredi P, Kharitonov SA, Leak D, Ward S, Cramer D, Barnes PJ (2000) Exhaled ethane, a marker of lipid peroxidation, is elevated in chronic obstructive pulmonary disease. American journal of respiratory and critical care medicine. 162(2):369-373.

[91] Kneepkens CM, Ferreira C, Lepage G, Roy CC (1992) The hydrocarbon breath test in the study of lipid peroxidation: principles and practice. Clinical and investigative medicine. Médecine clinique et experimentale. 15(2):163-186.

[92] Morrow JD, Hill KE, Burk RF, Nammour TM, Badr KF, Roberts 2nd LJ (1990) A series of prostaglandin F2-like compounds are produced in vivo in humans by a non-cyclooxygenase, free radical-catalyzed mechanism. Proceedings of the National Academy of Sciences. 87(23):9383-7.

[93] Milne GL, Musiek ES, Morrow JD (2005) F2-isoprostanes as markers of oxidative stress in vivo: an overview. Biomarkers. 10(sup1):10-23.

[94] Milne GL, Sanchez SC, Musiek ES, Morrow JD (2007) Quantification of F2-isoprostanes as a biomarker of oxidative stress. Nature protocols. 2(1):221-6.

[95] Ward WF, Qi W, Remmen HV, Zackert WE, Roberts LJ, Richardson A (2005) Effects of age and caloric restriction on lipid peroxidation: measurement of oxidative stress by F2-isoprostane levels. The Journals of Gerontology Series A: Biological Sciences and Medical Sciences. 60(7):847-51.

[96] Pratico D, Barry OP, Lawson JA, Adiyaman M, Hwang SW, Khanapure SP, Iuliano L, Rokach J, FitzGerald GA (1998) IPF2α-I: an index of lipid peroxidation in humans. Proceedings of the National Academy of Sciences. 95(7):3449-54.

[97] Montuschi P, Barnes PJ, Roberts LJ (2004) Isoprostanes: markers and mediators of oxidative stress. The FASEB journal. 18(15):1791-800.

[98] García-Bermúdez J, Sánchez-Aragó M, Soldevilla B, del Arco A, Nuevo-Tapioles C, Cuezva JM (2015) PKA phosphorylates the ATPase inhibitory factor 1 and inactivates its capacity to bind and inhibit the mitochondrial H+-ATP synthase. Cell reports. 12(12):2143-55.

[99] Simpson DJ, Chandra T (2021) Epigenetic age prediction. Aging cell. 20(9):e13452.

[100] Lu AT, Fei Z, Haghani A, Robeck TR, Zoller JA, Li CZ, Zhang J, Ablaeva J, Adams DM, Almunia J, Ardehali R (2021) Universal DNA methylation age across mammalian tissues. BioRxiv.

[101] Wilkinson GS, Adams DM, Haghani A, Lu AT, Zoller J, Breeze CE, Arnold BD, Ball HC, Carter GG, Cooper LN, Dechmann DK (2021) DNA methylation predicts age and provides insight into exceptional longevity of bats. Nature communications. 12(1):1-3.

[102] Maegawa S, Lu Y, Tahara T, Lee JT, Madzo J, Liang S, Jelinek J, Colman RJ, Issa JP (2017) Caloric restriction delays age-related methylation drift. Nature communications. 8(1):1-1.

[103] Lowe R, Barton C, Jenkins CA, Ernst C, Forman O, Fernandez-Twinn DS, Bock C, Rossiter SJ, Faulkes CG, Ozanne SE, Walter L (2018) Ageing-associated DNA methylation dynamics are a molecular readout of lifespan variation among mammalian species. Genome biology. 19(1):1-8.

[104] Matsuyama M, WuWong DJ, Horvath S, Matsuyama S (2019) Epigenetic clock analysis of human fibroblasts in vitro: effects of hypoxia, donor age, and expression of hTERT and SV40 largeT. Aging (Albany NY). 11(10):3012.

[105] Sohal RS, Weindruch R (1996) Oxidative stress, caloric restriction, and aging. Science. 273(5271):59-63.

[106] Ruggiero C, Metter EJ, Melenovsky V, Cherubini A, Najjar SS, Ble A, ... & Ferrucci L (2008) High basal metabolic rate is a risk factor for mortality: the Baltimore Longitudinal Study of Aging. The Journals of Gerontology Series A: Biological Sciences and Medical Sciences. 63(7):698-706.

[107] Buchholz AC, Rafii M, Pencharz PB (2001) Is resting metabolic rate different between men and women? British Journal of Nutrition. 86(6):641-6.

[108] Arciero PJ, Goran MI, Poehlman ET (1993) Resting metabolic rate is lower in women than in men. Journal of applied physiology. 75(6):2514-20.

[109] Ferraro R, Lillioja S, Fontvieille AM, Rising R, Bogardus C, Ravussin E (1992) Lower sedentary metabolic rate in women compared with men. The Journal of clinical investigation. 90(3):780-4.

[110] Owen OE (1988) Resting metabolic requirements of men and women. Mayo Clinic Proceedings. 63(5):503-510.

[111] Horvath S, Gurven M, Levine ME, Trumble BC, Kaplan H, Allayee H, Ritz BR, Chen B, Lu AT, Rickabaugh TM, Jamieson BD (2016) An epigenetic clock analysis of race/ethnicity, sex, and coronary heart disease. Genome biology. 17(1):1-23.

[112] Pinho GM, Martin JG, Farrell C, Haghani A, Zoller JA, Zhang J, Snir S, Pellegrini M, Wayne RK, Blumstein DT, Horvath S (2022) Hibernation slows epigenetic ageing in yellow-bellied marmots. Nature ecology & evolution. 6(4):418-26.

[113] Wu Q, Ni X (2015) ROS-mediated DNA methylation pattern alterations in carcinogenesis. Current drug targets. 16(1):13-19.

[114] Rang FJ, Boonstra J (2014) Causes and consequences of age-related changes in DNA methylation: a role for ROS? Biology. 3(2):403-425.

[115] Kietzmann T, Petry A, Shvetsova A, Gerhold JM, Görlach A (2017) The epigenetic landscape related to reactive oxygen species formation in the cardiovascular system. British journal of pharmacology. 174(12):1533-1554.

[116] Branco MR, Ficz G, Reik W (2012) Uncovering the role of 5-hydroxymethylcytosine in the epigenome. Nature Reviews Genetics. 13(1):7-13.

[117] Afanas'ev I (2014) New nucleophilic mechanisms of ros-dependent epigenetic modifications: comparison of aging and cancer. Aging and disease. 5(1):52.

[118] Horvath S (2013) DNA methylation age of human tissues and cell types. Genome biology. 14(10):1-20.

[119] Arneson A, Haghani A, Thompson MJ, Pellegrini M, Kwon SB, Vu H, Maciejewski E, Yao M, Li CZ, Lu AT, Morselli M (2022) A mammalian methylation array for profiling methylation levels at conserved sequences. Nature communications. 13(1):1-3.

[120] Horvath S, Lu AT, Cohen H, Raj K (2019) Rapamycin retards epigenetic ageing of keratinocytes independently of its effects on replicative senescence, proliferation and differentiation. Aging (Albany NY). 11(10):3238.

[121] Lujan C, Tyler EJ, Ecker S, Webster AP, Stead ER, Miguel VEM, ... & Bjedov I (2020) A CellAgeClock for expedited discovery of anti-ageing compounds. bioRxiv:803676.

[122] Warburg O (1956) On the origin of cancer cells. Science. 123(3191):309-314.

[123] Hatano E, Ikai I, Higashi T, Teramukai S, Torizuka T, Saga T, ... & Shimahara Y (2006) Preoperative positron emission tomography with fluorine-18-fluorodeoxyglucose is predictive of prognosis in patients with hepatocellular carcinoma after resection. World journal of surgery. 30(9):1736-1741.

[124] Seo S, Hatano E, Higashi T, Hara T, Tada M, Tamaki N, ... & Uemoto S (2007) Fluorine-18 fluorodeoxyglucose positron emission tomography predicts tumor differentiation, P-glycoprotein expression, and outcome after resection in hepatocellular carcinoma. Clinical cancer research. 13(2):427-433.

[125] Cerfolio RJ, Bryant AS, Ohja B, Bartolucci AA (2005) The maximum standardized uptake values on positron emission tomography of a non-small cell lung cancer predict stage, recurrence, and survival. The Journal of Thoracic and Cardiovascular Surgery. 130(1):151-159.

[126] Downey RJ, Akhurst T, Gonen M, Vincent A, Bains MS, Larson S, Rusch V (2004) Preoperative F-18 fluorodeoxyglucose-positron emission tomography maximal standardized uptake value predicts survival after lung cancer resection. Journal of Clinical Oncology. 22(16):3255-3260.

[127] il Lee M, Jung YJ, Kim DI, Lee S, Jung CS, Kang SK, ... & Kim HY (2021) Prognostic value of SUVmax in breast cancer and comparative analyses of molecular subtypes: A systematic review and meta-analysis. Medicine. 100(31).

[128] von Haehling S, Anker MS, Anker SD (2016) Prevalence and clinical impact of cachexia in chronic illness in Europe, USA, and Japan: facts and numbers update 2016.

[129] Shoemaker RH (2006) The NCI60 human tumour cell line anticancer drug screen. Nature Reviews Cancer. 6(10):813-823.

[130] Bigeleisen J (1949) The relative reaction velocities of isotopic molecules. The journal of chemical physics. 17(8):675-678.

[131] O'Ferrall RM (2010) A pictorial representation of zero-point energy and tunnelling contributions to primary hydrogen isotope effects. Journal of Physical Organic Chemistry. 23(7):572-579.

[132] Slaughter LM, Wolczanski PT, Klinckman TR, Cundari TR (2000) Inter- and Intramolecular Experimental and Calculated Equilibrium Isotope Effects for $(silox)_2(^tBu_3SiND)TiR + RH(silox= {}^tBu_3SiO)$: Inferred Kinetic Isotope Effects for RH/D Addition to Transient $(silox)_2Ti{=}NSi^tBu_3$. Journal of the American Chemical Society. 122(33):7953-7975.

[133] Holbeck SL, Collins JM, Doroshow JH (2010) Analysis of Food and Drug Administration–approved anticancer agents in the NCI60 panel of human tumor cell lines. Molecular cancer therapeutics. 9(5):1451-1460.

[134] Stryer L, Berg JM, Tymoczko JL (2002) Biochemistry, 4th Ed. New York, NY: WH Freeman.

[135] Forrest MD (2015) Why cancer cells have a more hyperpolarised mitochondrial membrane potential and emergent prospects for therapy. bioRxiv, 025197.

[136] Hanahan D, Weinberg RA (2000) The hallmarks of cancer. Cell. 100(1):57-70.

[137] Walenta S, Wetterling M, Lehrke M, Schwickert G, Sundfør K, Rofstad EK, Mueller-Klieser W (2000) High lactate levels predict likelihood of metastases, tumor recurrence, and restricted patient survival in human cervical cancers. Cancer research. 60(4):916-21.

[138] Zamzami N, Kroemer G (2001) The mitochondrion in apoptosis: how Pandora's box opens. Nature reviews Molecular cell biology. 2(1):67-71.

[139] Brizel DM, Sibley GS, Prosnitz LR, Scher RL, Dewhirst MW (1997) Tumor hypoxia adversely affects the prognosis of carcinoma of the head and neck. International Journal of Radiation Oncology* Biology* Physics. 38(2):285-289.

[140] Höckel M, Knoop C, Schlenger K, Vorndran B, Baußnann E, Mitze M, ... Vaupel P (1993) Intratumoral pO2 predicts survival in advanced cancer of the uterine cervix. Radiotherapy and Oncology. 26(1):45-50.

[141] Brizel DM, Scully SP, Harrelson JM, Layfield LJ, Bean JM, Prosnitz LR, Dewhirst MW (1996) Tumor oxygenation predicts for the likelihood of distant metastases in human soft tissue sarcoma. Cancer research. 56(5):941-943.

[142] Höckel M, Schlenger K, Aral B, Mitze M, Schäffer U, Vaupel P (1996) Association between tumor hypoxia and malignant progression in advanced cancer of the uterine cervix. Cancer research. 56(19):4509-4515.

[143] Höckel M, Schlenger K, Höckel S, Aral B, Schäffer U, Vaupel P (1998) Tumor hypoxia in pelvic recurrences of cervical cancer. International journal of cancer. 79(4):365-369.

[144] Sundfør K, Lyng H, Rofstad EK (1998) Tumour hypoxia and vascular density as predictors of metastasis in squamous cell carcinoma of the uterine cervix. British journal of cancer. 78(6):822-827.

[145] Barker HE, Paget JT, Khan AA, Harrington KJ (2015) The tumour microenvironment after radiotherapy: mechanisms of resistance and recurrence. Nature reviews Cancer. 15(7):409.

[146] Gatenby RA, Kessler HB, Rosenblum JS, Coia LR, Moldofsky PJ, Hartz WH, Broder GJ (1988) Oxygen distribution in squamous cell carcinoma metastases and its relationship to outcome of radiation therapy. International Journal of Radiation Oncology* Biology* Physics. 14(5):831-838.

[147] Sullivan R, Pare GC, Frederiksen LJ, Semenza GL, Graham CH (2008) Hypoxia induced resistance to anticancer drugs is associated with decreased senescence and requires hypoxia-inducible factor-1 activity. Molecular cancer therapeutics. 7(7):1961-73.

[148] Doktorova H, Hrabeta J, Khalil MA, Eckschlager T (2015) Hypoxia-induced chemoresistance in cancer cells: The role of not only HIF-1. Biomedical Papers of the Medical Faculty of Palacky University in Olomouc. 159(2).

[149] de Magalhães JP, Toussaint O (2004) Telomeres and telomerase: a modern fountain of youth? Rejuvenation research. 7(2):126-133.

[150] Artandi SE, Alson S, Tietze MK, Sharpless NE, Ye S, Greenberg RA, ... & DePinho RA (2002) Constitutive telomerase expression promotes mammary carcinomas in aging mice. Proceedings of the National Academy of Sciences. 99(12):8191-8196.

[151] Bernardes de Jesus B, Vera E, Schneeberger K, Tejera AM, Ayuso E, Bosch F, Blasco MA (2012) Telomerase gene therapy in adult and old mice delays aging and increases longevity without increasing cancer. EMBO molecular medicine. 4(8):691-704.

[152] Miller RA, Harrison DE, Astle CM, Fernandez E, Flurkey K, Han M, ... & Strong R (2014) Rapamycin-mediated lifespan increase in mice is dose and sex dependent and metabolically distinct from dietary restriction. Aging cell. 13(3):468-477.

[153] https://dtp.cancer.gov/dtpstandard/dwindex/index.jsp (accessed on 16 November 2021).

[154] Yuan R, Kay A, Berg WJ, Lebwohl D (2009) Targeting tumorigenesis: development and use of mTOR inhibitors in cancer therapy. Journal of hematology & oncology. 2(1):1-12.

[155] Laconi E, Marongiu F, DeGregori J (2020) Cancer as a disease of old age: changing mutational and microenvironmental landscapes. British journal of cancer. 122(7):943-952.

[156] Armstrong GT, Kawashima T, Leisenring W, Stratton K, Stovall M, Hudson MM, Sklar CA, Robison LL, Oeffinger KC (2014) Aging and risk of severe, disabling, life threatening, and fatal events in the childhood cancer survivor study. Journal of clinical oncology. 32(12):1218.

[157] Ng J, Shuryak I (2015) Minimizing second cancer risk following radiotherapy: current perspectives. Cancer management and research. 7:1.

[158] Obermeyer Z, Samra JK, Mullainathan S (2017) Individual differences in normal body temperature: longitudinal big data analysis of patient records. Bmj. 359.

[159] Foggo V, Cavenagh J (2015) Malignant causes of fever of unknown origin. Clinical Medicine. 15(3):292.

[160] Hunter WS, Croson WB, Bartke A, Gentry MV, Meliska CJ (1999) Low body temperature in long-lived Ames dwarf mice at rest and during stress. Physiology & behavior. 67(3):433-7.

[161] Brown-Borg HM (1996) Dwarf mice and the ageing process. Nature. 384:33.

[162] Miquel J, Lundgren PR, Bensch KG, Atlan H (1976) Effects of temperature on the life span, vitality and fine structure of Drosophila melanogaster. Mechanisms of ageing and development. 5:347-70.

[163] Loeb J, Northrop JH (1916) Is there a temperature coefficient for the duration of life? Proceedings of the National Academy of Sciences. 2(8):456-7.

[164] Kelly MA, Zieba AP, Buttemer WA, Hulbert AJ (2013) Effect of temperature on the rate of ageing: an experimental study of the blowfly Calliphora stygia. PLoS One. 8(9):e73781.

[165] Van Voorhies WA, Ward S (1999) Genetic and environmental conditions that increase longevity in Caenorhabditis elegans decrease metabolic rate. Proceedings of the National Academy of Sciences. 96(20):11399-403.

[166] McDougall SJ, Mills NJ (1997) The influence of hosts, temperature and food sources on the longevity of Trichogramma platneri. Entomologia Experimentalis et Applicata. 83(2):195-203.

[167] Liu RK, Walford RL (1966) Increased growth and life-span with lowered ambient temperature in the annual fish, Cynolebias adloffi. Nature. 212(5067):1277-8.

[168] Diamond A, Lye CT, Prasad D, Abbott D (2021) One size does not fit all: Assuming the same normal body temperature for everyone is not justified. Plos one. 16(2):e0245257.

[169] Sund-Levander M, Forsberg C, Wahren LK (2002) Normal oral, rectal, tympanic and axillary body temperature in adult men and women: a systematic literature review. Scandinavian journal of caring sciences. 16(2):122-8.

[170] Roth GS, Lane MA, Ingram DK, Mattison JA, Elahi D, Tobin JD, ... & Metter EJ (2002) Biomarkers of caloric restriction may predict longevity in humans. Science. 297(5582): 811-811.

[171] Protsiv M, Ley C, Lankester J, Hastie T, Parsonnet J (2020) Decreasing human body temperature in the United States since the industrial revolution. Elife. 9:e49555.

[172] Waalen J, Buxbaum JN (2011) Is older colder or colder older? The association of age with body temperature in 18,630 individuals. Journals of Gerontology Series A: Biomedical Sciences and Medical Sciences. 66(5):487-92.

[173] Simonsick EM, Meier H, Shaffer NC, Studenski SA, Ferrucci L (2016) Basal body temperature as a biomarker of healthy aging. Age. 38(5):445-54.

[174] Eggenberger P, Bürgisser M, Rossi RM, Annaheim S (2021) Body temperature is associated with cognitive performance in older adults with and without mild cognitive impairment: a cross-sectional analysis. Frontiers in Aging Neuroscience. 13:585904.

[175] Weindruch R, Walford RL, Fligiel S, Guthrie D (1986) The retardation of aging in mice by dietary restriction: longevity, cancer, immunity and lifetime energy intake. The Journal of nutrition. 116(4):641-654.

[176] Mattison JA, Colman RJ, Beasley TM, Allison DB, Kemnitz JW, Roth GS, Anderson RM (2017) Caloric restriction improves health and survival of rhesus monkeys. Nature communications. 8(1):1-12.

[177] Lane MA, Baer DJ, Rumpler WV, Weindruch R, Ingram DK, Tilmont EM, ... & Roth GS (1996) Calorie restriction lowers body temperature in rhesus monkeys, consistent with a postulated anti-aging mechanism in rodents. Proceedings of the National Academy of Sciences. 93(9):4159-4164.

[178] Rikke BA, Yerg III JE, Battaglia ME, Nagy TR, Allison DB, Johnson TE (2003) Strain variation in the response of body temperature to dietary restriction. Mechanisms of ageing and development. 124(5):663-78.

[179] Heilbronn LK, De Jonge L, Frisard MI, DeLany JP, Larson-Meyer DE, Rood J, Nguyen T, Martin CK, Volaufova J, Most MM, Greenway FL (2006) Effect of 6-month calorie restriction on biomarkers of longevity, metabolic adaptation, and oxidative stress in overweight individuals: a randomized controlled trial. JAMA. 295(13):1539-48.

[180] Soare A, Cangemi R, Omodei D, Holloszy JO, Fontana L (2011) Long-term calorie restriction, but not endurance exercise, lowers core body temperature in humans. Aging (Albany NY). 3(4):374.

[181] Rising RU, Keys AN, Ravussin ER, Bogardus CL (1992) Concomitant interindividual variation in body temperature and metabolic rate. American Journal of Physiology-Endocrinology And Metabolism. 263(4):E730-4.

[182] Tran CM, Mukherjee S, Ye L, Frederick DW, Kissig M, Davis JG, Lamming DW, Seale P, Baur JA (2016) Rapamycin blocks induction of the thermogenic program in white adipose tissue. Diabetes. 65(4):927-41.

[183] Laidler KJ (1984) The development of the Arrhenius equation. Journal of chemical Education. 61(6):494.

[184] Eyring H (1935) The activated complex in chemical reactions. The Journal of Chemical Physics. 3(2):107-15.

[185] Silcocks PB, Jenner DA, Reza R (2001) Life expectancy as a summary of mortality in a population: statistical considerations and suitability for use by health authorities. Journal of Epidemiology & Community Health. 55(1):38-43.

[186] Scott AJ, Ellison M, Sinclair DA (2021) The economic value of targeting aging. Nature Aging:1-8.

[187] Refinetti R (2010) The circadian rhythm of body temperature. Frontiers in Bioscience-Landmark. 15(2):564-94.

[188] Baker FC, Siboza F, Fuller A (2020) Temperature regulation in women: effects of the menstrual cycle. Temperature. 7(3):226-62.

[189] Harding C, Pompei F, Bordonaro SF, McGillicuddy DC, Burmistrov D, Sanchez LD (2019) The daily, weekly, and seasonal cycles of body temperature analyzed at large scale. Chronobiology International. 36(12):1646-57.

[190] Guijas C, Montenegro-Burke JR, Cintron-Colon R, Domingo-Almenara X, Sanchez-Alavez M, Aguirre CA, Shankar K, Majumder EL, Billings E, Conti B, Siuzdak G (2020) Metabolic adaptation to calorie restriction. Science signaling. 13(648):eabb2490.

[191] Olshansky SJ, Carnes BA, Cassel C (1990) In search of Methuselah: estimating the upper limits to human longevity. Science. 250(4981):634-40.

[192] Jung CG, Kato R, Zhou C, Abdelhamid M, Shaaban EI, Yamashita H, Michikawa M (2022) Sustained high body temperature exacerbates cognitive function and Alzheimer's disease-related pathologies. Scientific Reports. 12(1):1-1.

[193] Knight EM, Brown TM, Gümüsgöz S, Smith JC, Waters EJ, Allan SM, Lawrence CB (2013) Age-related changes in core body temperature and activity in triple-transgenic Alzheimer's disease (3xTgAD) mice. Disease models & mechanisms. 6(1):160-70.

[194] Klegeris A, Schulzer M, Harper DG, McGeer PL (2007) Increase in core body temperature of Alzheimer's disease patients as a possible indicator of chronic neuroinflammation: a meta-analysis. Gerontology. 53(1):7-11.

[195] Chung CW, Stephens AD, Konno T, Ward E, Avezov E, Kaminski CF, Hassanali AA, Kaminski Schierle GS (2022) Intracellular Aβ42 aggregation leads to cellular thermogenesis. Journal of the American Chemical Society.

[196] Noorani AA, Yamashita H, Gao Y, Islam S, Sun Y, Nakamura T, Enomoto H, Zou K, Michikawa M (2020) High temperature promotes amyloid β-protein production and γ-secretase complex formation via Hsp90. Journal of Biological Chemistry. 295(52):18010-22.

[197] Naiki H, Nakakuki K (1996) First-order kinetic model of Alzheimer's beta-amyloid fibril extension in vitro. Laboratory investigation; a journal of technical methods and pathology. 74(2):374-83.

[198] Kusumoto Y, Lomakin A, Teplow DB, Benedek GB (1998) Temperature dependence of amyloid β-protein fibrillization. Proceedings of the National Academy of Sciences. 95(21):12277-82.

[199] Sabaté R, Gallardo M, Estelrich J (2005) Temperature dependence of the nucleation constant rate in β amyloid fibrillogenesis. International journal of biological macromolecules. 35(1-2):9-13.

[200] Levine Iii H (2004) Alzheimer's β-peptide oligomer formation at physiologic concentrations. Analytical biochemistry. 335(1):81-90.

[201] https://www.oxfordreference.com/view/10.1093/oi/authority.20110803100428245 (accessed on 8 July 2022).

[202] Baruch-Suchodolsky R, Fischer B (2009) Aβ40, either soluble or aggregated, is a remarkably potent antioxidant in cell-free oxidative systems. Biochemistry. 48(20):4354-70.

[203] Zou K, Gong JS, Yanagisawa K, Michikawa M (2002) A novel function of monomeric amyloid β-protein serving as an antioxidant molecule against metal-induced oxidative damage. Journal of Neuroscience. 22(12):4833-41.

[204] Nadal RC, Rigby SE, Viles JH (2008) Amyloid β− Cu2+ complexes in both monomeric and fibrillar forms do not generate H2O2 catalytically but quench hydroxyl radicals. Biochemistry. 47(44):11653-64.

[205] Misonou H, Morishima-Kawashima M, Ihara Y (2000) Oxidative stress induces intracellular accumulation of amyloid β-protein (Aβ) in human neuroblastoma cells. Biochemistry. 39(23):6951-9.

[206] Pedersen JT, Chen SW, Borg CB, Ness S, Bahl JM, Heegaard NH, Dobson CM, Hemmingsen L, Cremades N, Teilum K (2016) Amyloid-β and α-synuclein decrease the level of metal-catalyzed reactive oxygen species by radical scavenging and redox silencing. Journal of the American Chemical Society. 138(12):3966-9.

[207] Nunomura A, Tamaoki T, Tanaka K, Motohashi N, Nakamura M, Hayashi T, Yamaguchi H, Shimohama S, Lee HG, Zhu X, Smith MA (2010) Intraneuronal amyloid β accumulation and oxidative damage to nucleic acids in Alzheimer disease. Neurobiology of disease. 37(3):731-7.

[208] Kontush A, Berndt C, Weber W, Akopyan V, Arlt S, Schippling S, Beisiegel U (2001) Amyloid-β is an antioxidant for lipoproteins in cerebrospinal fluid and plasma. Free Radical Biology and Medicine. 30(1):119-28.

[209] Zou K, Gong JS, Yanagisawa K, Michikawa M (2002) A novel function of monomeric amyloid β-protein serving as an antioxidant molecule against metal-induced oxidative damage. Journal of Neuroscience. 22(12):4833-41.

[210] Walter MF, Mason PE, Mason RP (1997) Alzheimer's disease amyloid β peptide 25-35 inhibits lipid peroxidation as a result of its membrane interactions. Biochemical and biophysical research communications. 233(3):760-4.

[211] Paola D, Domenicotti C, Nitti M, Vitali A, Borghi R, Cottalasso D, Zaccheo D, Odetti P, Strocchi P, Marinari UM, Tabaton M (2000) Oxidative stress induces increase in

intracellular amyloid β-protein production and selective activation of βI and βII PKCs in NT2 cells. Biochemical and biophysical research communications. 268(2):642-6.

[212] Tong Y, Zhou W, Fung V, Christensen MA, Qing H, Sun X, Song W (2005) Oxidative stress potentiates BACE1 gene expression and Aβ generation. Journal of neural transmission. 112(3):455-69.

[213] Guglielmotto M, Giliberto L, Tamagno E, Tabaton M (2010) Oxidative stress mediates the pathogenic effect of different Alzheimer's disease risk factors. Frontiers in aging neuroscience. 2010:3.

[214] Tamagno E, Guglielmotto M, Aragno M, Borghi R, Autelli R, Giliberto L, Muraca G, Danni O, Zhu X, Smith MA, Perry G (2008) Oxidative stress activates a positive feedback between the γ-and β-secretase cleavages of the β-amyloid precursor protein. Journal of neurochemistry. 104(3):683-95.

[215] Tamagno E, Parola M, Bardini P, Piccini A, Borghi R, Guglielmotto M, Santoro G, Davit A, Danni O, Smith MA, Perry G (2005) β-Site APP cleaving enzyme up-regulation induced by 4-hydroxynonenal is mediated by stress-activated protein kinases pathways. Journal of neurochemistry. 92(3):628-36.

[216] Borghi R, Patriarca S, Traverso N, Piccini A, Storace D, Garuti A, Cirmena G, Odetti P, Tabaton M (2007) The increased activity of BACE1 correlates with oxidative stress in Alzheimer's disease. Neurobiology of aging. 28(7):1009-14.

[217] Kao SC, Krichevsky AM, Kosik KS, Tsai LH (2004) BACE1 suppression by RNA interference in primary cortical neurons. Journal of Biological Chemistry. 279(3):1942-9.

[218] Bonda DJ, Wang X, Lee HG, Smith MA, Perry G, Zhu X (2014) Neuronal failure in Alzheimer's disease: a view through the oxidative stress looking-glass. Neuroscience bulletin. 30(2):243-52.

[219] Lin X, Kapoor A, Gu Y, Chow MJ, Peng J, Zhao K, Tang D (2020) Contributions of DNA damage to Alzheimer's disease. International Journal of Molecular Sciences. 21(5):1666.

[220] Wang J, Xiong S, Xie C, Markesbery WR, Lovell MA (2005) Increased oxidative damage in nuclear and mitochondrial DNA in Alzheimer's disease. Journal of neurochemistry. 93(4):953-62.

[221] Smith MA, Perry G, Richey PL, Sayrec LM, Anderson VE, Beal MF, Kowall N (1996) Oxidative damage in Alzheimer's. Nature. 382(6587):120-1.

[222] Nunomura A, Perry G, Pappolla MA, Wade R, Hirai K, Chiba S, Smith MA (1999) RNA oxidation is a prominent feature of vulnerable neurons in Alzheimer's disease. Journal of Neuroscience. 19(6):1959-64.

[223] Sayre LM, Zelasko DA, Harris PL, Perry G, Salomon RG, Smith MA (1997) 4-Hydroxynonenal-derived advanced lipid peroxidation end products are increased in Alzheimer's disease. Journal of neurochemistry. 68(5):2092-7.

[224] Mandal PK, Saharan S, Tripathi M, Murari G (2015) Brain glutathione levels–a novel biomarker for mild cognitive impairment and Alzheimer's disease. Biological psychiatry. 78(10):702-10.

[225] Wang X, Wang W, Li L, Perry G, Lee HG, Zhu X (2014) Oxidative stress and mitochondrial dysfunction in Alzheimer's disease. Biochimica et Biophysica Acta (BBA)-Molecular Basis of Disease. 1842(8):1240-7.

[226] Mecocci P, MacGarvey U, Beal MF (1994) Oxidative damage to mitochondrial DNA is increased in Alzheimer's disease. Annals of Neurology: Official Journal of the American Neurological Association and the Child Neurology Society. 36(5):747-51.

[227] Liu Q, Smith MA, Avilá J, DeBernardis J, Kansal M, Takeda A, Zhu X, Nunomura A, Honda K, Moreira PI, Oliveira CR (2005) Alzheimer-specific epitopes of tau represent lipid peroxidation-induced conformations. Free Radical Biology and Medicine. 38(6):746-54.

[228] Lovell MA, Xiong S, Xie C, Davies P, Markesbery WR (2004) Induction of hyperphosphorylated tau in primary rat cortical neuron cultures mediated by oxidative stress and glycogen synthase kinase-3. Journal of Alzheimer's Disease. 6(6):659-71.

[229] Lin MT, Beal MF (2006) Mitochondrial dysfunction and oxidative stress in neurodegenerative diseases. Nature. 443(7113):787-795.

[230] Gella A, Bolea I (2011) Oxidative stress in Alzheimer's disease: pathogenesis, biomarkers and therapy. Alzheimer's Disease Pathogenesis-Core Concepts, Shifting Paradigms and Therapeutic Targets, (contents VII, chapter 15), 319-344.

[231] Beal MF (1996) Mitochondria, free radicals, and neurodegeneration. Current opinion in neurobiology. 6(5):661-666.

[232] Dias V, Junn E, Mouradian MM (2013) The role of oxidative stress in Parkinson's disease. Journal of Parkinson's disease. 3(4):461-491.

[233] Hagemeier J, Geurts JJ, Zivadinov R (2012) Brain iron accumulation in aging and neurodegenerative disorders. Expert review of neurotherapeutics. 12(12):1467-1480.

[234] Zecca L, Youdim MB, Riederer P, Connor JR, Crichton RR (2004) Iron, brain ageing and neurodegenerative disorders. Nature Reviews Neuroscience. 5(11):863-873.

[235] Moreira PI, Smith MA, Zhu X, Nunomura A, Castellani RJ, Perry G (2005) Oxidative stress and neurodegeneration. Annals of the New York Academy of Sciences. 1043(1):545-552.

[236] Forster MJ, Dubey A, Dawson KM, Stutts WA, Lal H, Sohal RS (1996) Age-related losses of cognitive function and motor skills in mice are associated with oxidative protein damage in the brain. Proceedings of the National Academy of Sciences. 93(10):4765-4769.

[237] Halliwell B (2001) Role of free radicals in the neurodegenerative diseases. Drugs & aging. 18(9):685-716.

[238] Abou-Sleiman PM, Muqit MM, Wood NW (2006) Expanding insights of mitochondrial dysfunction in Parkinson's disease. Nature Reviews Neuroscience. 7(3):207-219.

[239] Halliwell B (1992) Reactive oxygen species and the central nervous system. Journal of neurochemistry. 59(5):1609-1623.

[240] Radi Isola RA, Castro Peyronel LA, Rodríguez Rey MI, Cassina Gómez AM, Thomson Garibotti ML, Flint Beal M, ... & Bodis-Wollner I (1997) Free radical damage to mitochondria. Mitochondria and Free Radicals in Neurodegenerative Diseases.

[241] Pope S, Land JM, Heales SJ (2008) Oxidative stress and mitochondrial dysfunction in neurodegeneration; cardiolipin a critical target? Biochimica et Biophysica Acta (BBA)-Bioenergetics. 1777(7-8):794-799.

[242] Bender A, Krishnan KJ, Morris CM, Taylor GA, Reeve AK, Perry RH, ... & Turnbull DM (2006) High levels of mitochondrial DNA deletions in substantia nigra neurons in aging and Parkinson disease. Nature genetics. 38(5):515-517.

[243] Massaad CA, Pautler RG, Klann E (2009) Mitochondrial superoxide: a key player in Alzheimer's disease. Aging (Albany NY). 1(9):758.

[244] Massaad CA, Washington TM, Pautler RG, Klann E (2009) Overexpression of SOD-2 reduces hippocampal superoxide and prevents memory deficits in a mouse model of Alzheimer's disease. Proceedings of the National Academy of Sciences. 106(32):13576-13581.

[245] Perry G, Nunomura A, Hirai K, Zhu X, Prez M, Avila J, ... & Smith MA (2002) Is oxidative damage the fundamental pathogenic mechanism of Alzheimer’s and other neurodegenerative diseases? Free Radical Biology and Medicine. 33(11):1475-1479.

[246] Harman D (2002) Alzheimer's disease: role of aging in pathogenesis. Annals of the New York Academy of Sciences. 959(1):384-395.

[247] Hardy JA, Higgins GA (1992) Alzheimer’s disease: the amyloid cascade hypothesis. Science. 256(5054):184-5.

[248] Makin S (2018) The amyloid hypothesis on trial. Nature. 559(7715):S4-.

[249] Thambisetty M, Howard R, Glymour MM, Schneider LS (2021) Alzheimer's drugs: Does reducing amyloid work? Science. 374(6567):544-5.

[250] Nunomura A, Perry G, Aliev G, Hirai K, Takeda A, Balraj EK, Jones PK, Ghanbari H, Wataya T, Shimohama S, Chiba S (2001) Oxidative damage is the earliest event in Alzheimer disease. Journal of Neuropathology & Experimental Neurology. 60(8):759-67.

[251] Arimon M, Takeda S, Post KL, Svirsky S, Hyman BT, Berezovska O (2015) Oxidative stress and lipid peroxidation are upstream of amyloid pathology. Neurobiology of disease. 84:109-19.

[252] Tamagno E, Bardini P, Obbili A, Vitali A, Borghi R, Zaccheo D, Pronzato MA, Danni O, Smith MA, Perry G, Tabaton M (2002) Oxidative stress increases expression and activity of BACE in NT2 neurons. Neurobiology of disease. 10(3):279-88.

[253] Nunomura A, Tamaoki T, Motohashi N, Nakamura M, McKeel Jr DW, Tabaton M, Lee HG, Smith MA, Perry G, Zhu X (2012) The earliest stage of cognitive impairment in transition from normal aging to Alzheimer disease is marked by prominent RNA oxidation in vulnerable neurons. Journal of Neuropathology & Experimental Neurology. 71(3):233-41.

[254] Pratico D, Uryu K, Leight S, Trojanoswki JQ, Lee VM (2001) Increased lipid peroxidation precedes amyloid plaque formation in an animal model of Alzheimer amyloidosis. Journal of Neuroscience. 21(12):4183-7.

[255] Nunomura A, Perry G, Hirai K, Aliev G, Takeda A, Chiba S, Smith MA (1999) Neuronal RNA oxidation in Alzheimer's disease and Down's syndrome. Annals of the New York Academy of Sciences. 893(1):362-4.

[256] Wang J, Markesbery WR, Lovell MA (2006) Increased oxidative damage in nuclear and mitochondrial DNA in mild cognitive impairment. Journal of neurochemistry. 96(3):825-32.

[257] Lovell MA, Markesbery WR (2008) Oxidatively modified RNA in mild cognitive impairment. Neurobiology of Disease. 29(2):169-75.

[258] Keller JN, Schmitt FA, Scheff SW, Ding Q, Chen Q, Butterfield DA, Markesbery WR (2005) Evidence of increased oxidative damage in subjects with mild cognitive impairment. Neurology. 64(7):1152-6.

[259] Markesbery WR, Kryscio RJ, Lovell MA, Morrow JD (2005) Lipid peroxidation is an early event in the brain in amnestic mild cognitive impairment. Annals of Neurology: Official Journal of the American Neurological Association and the Child Neurology Society. 58(5):730-5.

[260] Yao J, Irwin RW, Zhao L, Nilsen J, Hamilton RT, Brinton RD (2009) Mitochondrial bioenergetic deficit precedes Alzheimer's pathology in female mouse model of Alzheimer's disease. Proceedings of the National Academy of Sciences. 106(34):14670-5.

[261] Resende R, Moreira PI, Proença T, Deshpande A, Busciglio J, Pereira C, Oliveira CR (2008) Brain oxidative stress in a triple-transgenic mouse model of Alzheimer disease. Free Radical Biology and Medicine. 44(12):2051-7.

[262] Lovell MA, Markesbery WR (2007) Oxidative DNA damage in mild cognitive impairment and late-stage Alzheimer's disease. Nucleic acids research. 35(22):7497-504.

[263] Khan SM, Cassarino DS, Abramova NN, Keeney PM, Borland MK, Trimmer PA, Krebs CT, Bennett JC, Parks JK, Swerdlow RH, Parker Jr WD (2000) Alzheimer's disease cybrids replicate β-amyloid abnormalities through cell death pathways. Annals of Neurology: Official Journal of the American Neurological Association and the Child Neurology Society. 48(2):148-55.

[264] Praticò D, Clark CM, Liun F, Lee VY, Trojanowski JQ (2002) Increase of brain oxidative stress in mild cognitive impairment: a possible predictor of Alzheimer disease. Archives of neurology. 59(6):972-6.

[265] Butterfield DA, Poon HF, Clair DS, Keller JN, Pierce WM, Klein JB, Markesbery WR (2006) Redox proteomics identification of oxidatively modified hippocampal proteins in mild cognitive impairment: insights into the development of Alzheimer's disease. Neurobiology of disease. 22(2):223-32.

[266] Torres LL, Quaglio NB, de Souza GT, Garcia RT, Dati LM, Moreira WL, de Melo Loureiro AP, de Souza-Talarico JN, Smid J, Porto CS, de Campos Bottino CM (2011) Peripheral oxidative stress biomarkers in mild cognitive impairment and Alzheimer's disease. Journal of Alzheimer's Disease. 26(1):59-68.

[267] Rinaldi P, Polidori MC, Metastasio A, Mariani E, Mattioli P, Cherubini A, Catani M, Cecchetti R, Senin U, Mecocci P (2003) Plasma antioxidants are similarly depleted in mild cognitive impairment and in Alzheimer's disease. Neurobiology of aging. 24(7):915-9.

[268] Lovell MA, Markesbery WR (2007) Oxidative damage in mild cognitive impairment and early Alzheimer's disease. Journal of neuroscience research. 85(14):3036-40.

[269] Williams TI, Lynn BC, Markesbery WR, Lovell MA (2006) Increased levels of 4-hydroxynonenal and acrolein, neurotoxic markers of lipid peroxidation, in the brain in Mild Cognitive Impairment and early Alzheimer's disease. Neurobiology of aging. 27(8):1094-9.

[270] Bradley-Whitman MA, Timmons MD, Beckett TL, Murphy MP, Lynn BC, Lovell MA (2014) Nucleic acid oxidation: an early feature of Alzheimer's disease. Journal of neurochemistry. 128(2):294-304.

[271] Praticò D, Clark CM, Liun F, Lee VY, Trojanowski JQ (2002) Increase of brain oxidative stress in mild cognitive impairment: a possible predictor of Alzheimer disease. Archives of neurology. 59(6):972-6.

[272] Dumont M, Wille E, Stack C, Calingasan NY, Beal MF, Lin MT (2009) Reduction of oxidative stress, amyloid deposition, and memory deficit by manganese superoxide dismutase overexpression in a transgenic mouse model of Alzheimer's disease. The FASEB Journal. 23(8):2459-66.

[273] Mao P, Manczak M, Calkins MJ, Truong Q, Reddy TP, Reddy AP, Shirendeb U, Lo HH, Rabinovitch PS, Reddy PH (2012) Mitochondria-targeted catalase reduces abnormal APP processing, amyloid β production and BACE1 in a mouse model of Alzheimer's disease: implications for neuroprotection and lifespan extension. Human Molecular Genetics. 21(13):2973-90.

[274] McManus MJ, Murphy MP, Franklin JL (2011) The mitochondria-targeted antioxidant MitoQ prevents loss of spatial memory retention and early neuropathology in a transgenic mouse model of Alzheimer's disease. Journal of Neuroscience. 31(44):15703-15.

[275] Young ML, Franklin JL (2019) The mitochondria-targeted antioxidant MitoQ inhibits memory loss, neuropathology, and extends lifespan in aged 3xTg-AD mice. Molecular and Cellular Neuroscience. 101:103409.

[276] Lee HP, Pancholi N, Esposito L, Previll LA, Wang X, Zhu X, Smith MA, Lee HG (2012) Early induction of oxidative stress in mouse model of Alzheimer disease with reduced mitochondrial superoxide dismutase activity. PloS one. 7(1):e28033.

[277] Leuner K, Schütt T, Kurz C, Eckert SH, Schiller C, Occhipinti A, Mai S, Jendrach M, Eckert GP, Kruse SE, Palmiter RD (2012) Mitochondrion-derived reactive oxygen species lead to enhanced amyloid beta formation. Antioxidants & redox signaling. 16(12):1421-33.

[278] Li F, Calingasan NY, Yu F, Mauck WM, Toidze M, Almeida CG, Takahashi RH, Carlson GA, Flint Beal M, Lin MT, Gouras GK (2004) Increased plaque burden in brains of APP mutant MnSOD heterozygous knockout mice. Journal of neurochemistry. 89(5):1308-12.

[279] Melov S, Adlard PA, Morten K, Johnson F, Golden TR, Hinerfeld D, Schilling B, Mavros C, Masters CL, Volitakis I, Li QX (2007) Mitochondrial oxidative stress causes hyperphosphorylation of tau. PloS one. 2(6):e536.

[280] Esposito L, Raber J, Kekonius L, Yan F, Yu GQ, Bien-Ly N, Puoliväli J, Scearce-Levie K, Masliah E, Mucke L (2006) Reduction in mitochondrial superoxide dismutase modulates Alzheimer's disease-like pathology and accelerates the onset of behavioral changes in human amyloid precursor protein transgenic mice. Journal of Neuroscience. 26(19):5167-79.

[281] Sung S, Yao Y, Uryu K, Yang H, Lee VM, Trojanowski JQ, Praticò D (2004) Early vitamin E supplementation in young but not aged mice reduces Aβ levels and amyloid deposition in a transgenic model of Alzheimer's disease. The FASEB journal. 18(2):323-5.

[282] Sano M, Ernesto C, Thomas RG, Klauber MR, Schafer K, Grundman M, Woodbury P, Growdon J, Cotman CW, Pfeiffer E, Schneider LS (1997) A controlled trial of selegiline, alpha-tocopherol, or both as treatment for Alzheimer's disease. New England Journal of Medicine. 336(17):1216-22.

[283] Zandi PP, Anthony JC, Khachaturian AS, Stone SV, Gustafson D, Tschanz JT, Norton MC, Welsh-Bohmer KA, Breitner JC, Cache County Study Group (2004) Reduced risk of Alzheimer disease in users of antioxidant vitamin supplements: the Cache County Study. Archives of neurology. 61(1):82-8.

[284] Morris MC, Evans DA, Bienias JL, Tangney CC, Wilson RS (2002) Vitamin E and cognitive decline in older persons. Archives of neurology. 59(7):1125-32.

[285] Engelhart MJ, Geerlings MI, Ruitenberg A, van Swieten JC, Hofman A, Witteman JC, Breteler MM (2002) Dietary intake of antioxidants and risk of Alzheimer disease. Jama. 287(24):3223-9.

[286] Sevigny J, Chiao P, Bussière T, Weinreb PH, Williams L, Maier M, Dunstan R, Salloway S, Chen T, Ling Y, O'Gorman J (2016) The antibody aducanumab reduces Aβ plaques in Alzheimer's disease. Nature. 537(7618):50-6.

[287] Kastanenka KV, Bussiere T, Shakerdge N, Qian F, Weinreb PH, Rhodes K, Bacskai BJ (2016) Immunotherapy with aducanumab restores calcium homeostasis in Tg2576 mice. Journal of Neuroscience. 36(50):12549-58.

[288] https://www.fda.gov/drugs/information-health-care-professionals-drugs/accelerated-approval-program (accessed on 31 July 2022).

[289] Tagliavini F, Tiraboschi P, Federico A (2021) Alzheimer's disease: The controversial approval of Aducanumab. Neurological Sciences. 42(8):3069-70.

[290] Howard R, Liu KY (2020) Questions EMERGE as Biogen claims aducanumab turnaround. Nature Reviews Neurology. 16(2):63-4.

[291] Knopman DS, Jones DT, Greicius MD (2021) Failure to demonstrate efficacy of aducanumab: An analysis of the EMERGE and ENGAGE trials as reported by Biogen, December 2019. Alzheimer's & Dementia. 17(4):696-701.

[292] Montine TJ, Markesbery WR, Morrow JD, Roberts III LJ (1998) Cerebrospinal fluid F2-isoprostane levels are increased in Alzheimer's disease. Annals of neurology. 44(3):410-3.

[293] Praticò D, Sung S (2004) Lipid peroxidation and oxidative imbalance: early functional events in Alzheimer's disease. Journal of Alzheimer's Disease. 6(2):171-5.

[294] Praticò D, Clark CM, Lee VM, Trojanowski JQ, Rokach J, FitzGerald GA (2000) Increased 8, 12-iso-iPF2α-VI in Alzheimer's disease: Correlation of a noninvasive index of lipid peroxidation with disease severity. Annals of neurology. 48(5):809-12.

[295] Patel NV, Gordon MN, Connor KE, Good RA, Engelman RW, Mason J, Morgan DG, Morgan TE, Finch CE (2005) Caloric restriction attenuates Aβ-deposition in Alzheimer transgenic models. Neurobiology of aging. 26(7):995-1000.

[296] Singh S, Mulley GP, Losowsky MS (1988) Why are Alzheimer patients thin? Age and ageing. 17(1):21-8.

[297] Burns A, Marsh A, Bender DA (1989) Dietary intake and clinical, anthropometric and biochemical indices of malnutrition in elderly demented patients and non-demented subjects. Psychological medicine. 19(2):383-91.

[298] Venturelli M, Cè E, Limonta E, Muti E, Scarsini R, Brasioli A, Schena F, Esposito F (2016) Possible predictors of involuntary weight loss in patients with Alzheimer's disease. PLoS One. 11(6):e0157384.

[299] Keene JM, Hope T. Hyperphagia in dementia: 1 (1997) The use of an objective and reliable method for measuring hyperphagia in people with dementia. Appetite. 28(2):151-65.

[300] Keene JM, Hope T (1997) Hyperphagia in dementia: 2. Food choices and their macronutrient contents in hyperphagia, dementia and ageing. Appetite. 28(2):167-75.

[301] Guérin O, Andrieu S, Schneider SM, Milano M, Boulahssass R, Brocker P, Vellas B (2005) Different modes of weight loss in Alzheimer disease: a prospective study of 395 patients–. The American journal of clinical nutrition. 82(2):435-41.

[302] Gillette-Guyonnet S, Nourhashémi F, Andrieu S, de Glisezinski I, Ousset PJ, Rivière D, Albarède JL, Vellas B (2000) Weight loss in Alzheimer disease. The American journal of clinical nutrition. 71(2):637S-42S.

[303] Gillette-Guyonnet S, Van Kan GA, Alix E, Andrieu S (2007) IANA (International Academy on Nutrition and Aging) Expert Group: weight loss and Alzheimer's disease. The journal of nutrition, health & aging. 11(1):38.

[304] Tjahyo AS, Gandy J, Porter J, Henry CJ (2021) Is weight loss more severe in older people with dementia?. Journal of Alzheimer's Disease. 81(1):57-73.

[305] Sergi G, De Rui M, Coin A, Inelmen EM, Manzato E (2013) Weight loss and Alzheimer's disease: temporal and aetiologic connections. Proceedings of the Nutrition Society. 72(1):160-5.

[306] Wolf-Klein GP, Silverstone FA, Lansey SC, Tesi D, Ciampaglia C, O'Donnell M, Galkowski J, Jaeger A, Wallenstein S, Leleiko NS (1995) Energy requirements in Alzheimer's disease patients. Nutrition (Burbank, Los Angeles County, Calif.). 11(3):264-8.

[307] Wang PN, Yang CL, Lin KN, Chen WT, Chwang LC, Liu HC (2004) Weight loss, nutritional status and physical activity in patients with Alzheimer's disease. Journal of neurology. 251(3):314-20.

[308] Wolf-Klein GP, Silverstone FA, Levy AP (1992) Nutritional patterns and weight change in Alzheimer patients. International Psychogeriatrics. 4(1):103-18.

[309] Cova I, Clerici F, Rossi A, Cucumo V, Ghiretti R, Maggiore L, Pomati S, Galimberti D, Scarpini E, Mariani C, Caracciolo B (2016) Weight loss predicts progression of mild cognitive impairment to Alzheimer's disease. PloS one. 11(3):e0151710.

[310] White H, Pieper C, Schmader K (1998) The association of weight change in Alzheimer's disease with severity of disease and mortality: a longitudinal analysis. Journal of the American Geriatrics Society. 46(10):1223-7.

[311] White HK, McConnell ES, Bales CW, Kuchibhatla M (2004) A 6-month observational study of the relationship between weight loss and behavioral symptoms in institutionalized Alzheimer's disease subjects. Journal of the American Medical Directors Association. 5(2):89-97.

[312] Knight EM, Verkhratsky A, Luckman SM, Allan SM, Lawrence CB (2012) Hypermetabolism in a triple-transgenic mouse model of Alzheimer's disease. Neurobiology of aging. 33(1):187-93.

[313] Vloeberghs E, Van Dam D, Franck F, Serroyen J, Geert M, Staufenbiel M, De Deyn PP (2008) Altered ingestive behavior, weight changes, and intact olfactory sense in an APP overexpression model. Behavioral neuroscience. 122(3):491.

[314] Morgan D, Gordon MN (2008) Amyloid, hyperactivity, and metabolism: theoretical comment on Vloeberghs et al.(2008).

[315] Pugh PL, Richardson JC, Bate ST, Upton N, Sunter D (2007) Non-cognitive behaviours in an APP/PS1 transgenic model of Alzheimer's disease. Behavioural brain research. 178(1):18-28.

[316] Cummings J, Feldman HH, Scheltens P (2019) The “rights” of precision drug development for Alzheimer’s disease. Alzheimer’s research & therapy. 11(1):1-14.

[317] Mather M, Jacobsen LA, Pollard KM (2015) Aging in the United States: population bulletin. Population Reference Bureau.

[318] Tahami Monfared AA, Byrnes MJ, White LA, Zhang Q (2022) The Humanistic and Economic Burden of Alzheimer’s Disease. Neurology and Therapy. 1-27.

[319] Alzheimer’s Study Group. A national Alzheimer’s strategic plan: The report of the Alzheimer’s study group.

[320] Urquhart L (2021) Top companies and drugs by sales in 2020. Nature reviews. Drug discovery. 20(4):253.

[321] Birnbaum H, Pike C, Kaufman R, Maynchenko M, Kidolezi Y, Cifaldi M (2010) Societal cost of rheumatoid arthritis patients in the US. Current medical research and opinion. 26(1):77-90.

[322] Mundim KC, Baraldi S, Machado HG, Vieira FM (2020) Temperature coefficient (Q10) and its applications in biological systems: Beyond the Arrhenius theory. Ecological Modelling. 431:109127.

[323] Sterratt DC (2015) Q10: the effect of temperature on ion channel kinetics. In Encyclopedia of Computational Neuroscience. 2551-2552.
Springer New York.

[324] Tsai SP, Hardy RJ, Wen CP (1992) The standardized mortality ratio and life expectancy. American journal of epidemiology. 135(7):824-31.

[325] Redman LM, Smith SR, Burton JH, Martin CK, Il'yasova D, Ravussin E (2018) Metabolic slowing and reduced oxidative damage with sustained caloric restriction support the rate of living and oxidative damage theories of aging. Cell metabolism. 27(4):805-15.

[326] Il'yasova D, Fontana L, Bhapkar M, Pieper CF, Spasojevic I, Redman LM, Das SK, Huffman KM, Kraus WE, CALERIE Study Investigators (2018) Effects of 2 years of caloric restriction on oxidative status assessed by urinary F2-isoprostanes: The CALERIE 2 randomized clinical trial. Aging Cell. 17(2):e12719.

[327] Wilkinson GS, Adams DM (2019) Recurrent evolution of extreme longevity in bats. Biology letters. 15(4):20180860.

[328] Turbill C, Bieber C, Ruf T (2011) Hibernation is associated with increased survival and the evolution of slow life histories among mammals. Proceedings of the Royal Society B: Biological Sciences. 278(1723):3355-63.

[329] Blanco MB, Zehr SM (2015) Striking longevity in a hibernating lemur. Journal of Zoology. 296(3):177-88.

[330] Lyman CP, O'Brien RC, Greene GC, Papafrangos ED (1981) Hibernation and longevity in the Turkish hamster Mesocricetus brandti. Science. 212(4495):668-70.

[331] Turbill C, Smith S, Deimel C, Ruf T (2012) Daily torpor is associated with telomere length change over winter in Djungarian hamsters. Biology Letters. 8(2):304-7.

[332] Puspitasari A, Cerri M, Takahashi A, Yoshida Y, Hanamura K, Tinganelli W (2021) Hibernation as a tool for radiation protection in space exploration. Life. 11(1):54.

[333] Gordon CJ (2012) Thermal physiology of laboratory mice: defining thermoneutrality. Journal of thermal biology. 37(8):654-685.

[334] Pennycuik PR (1967) A comparison of the effects of a variety of factors on the metabolic rate of the mouse. Australian Journal of Experimental Biology and Medical Science. 45(4):331-346.

[335] Kingma B, Frijns A, van Marken Lichtenbelt W (2012) The thermoneutral zone: implications for metabolic studies. Frontiers in Bioscience-Elite. 4(5):1975-85.

[336] State of the Tropics (2020) State of the Tropics 2020 Report. James Cook University, Townsville, Australia.

[337] Papa S, Zanotti F, Cocco T, Perrucci C, Candita C, Minuto M (1996) Identification of functional domains and critical residues in the adenosinetriphosphatase inhibitor protein of mitochondrial F0F1 ATP synthase. European journal of biochemistry. 240(2):461-7.

[338] Zanotti F, Raho G, Vuolo R, Gaballo A, Papa F, Papa S (2000) Functional domains of the ATPase inhibitor protein from bovine heart mitochondria. FEBS letters. 482(1-2):163-6.

[339] Zanotti F, Raho G, Gaballo A, Papa S (2004) Inhibitory and anchoring domains in the ATPase inhibitor protein IF1 of bovine heart mitochondrial ATP synthase. Journal of bioenergetics and biomembranes. 36(5):447-57.

[340] de Chiara C, Nicastro G, Spisni A, Zanotti F, Cocco T, Papa S (2002) Activity and NMR structure of synthetic peptides of the bovine ATPase inhibitor protein, IF1. Peptides. 23(12):2127-41.

[341] Rothbard JB, Garlington S, Lin Q, Kirschberg T, Kreider E, McGrane PL, ... & Khavari PA (2000) Conjugation of arginine oligomers to cyclosporin A facilitates topical delivery and inhibition of inflammation. Nature medicine. 6(11):1253-1257.

[342] Altschul SF, Gish W, Miller W, Myers EW, Lipman DJ (1990) Basic local alignment search tool. Journal of molecular biology. 215(3):403-410.

[343] Michael David Forrest. "Inhibitors of ATP synthase - cosmetic and therapeutic uses". International Patent Cooperation Treaty (PCT) application PCT/IB2021/050529 (filed 24 January 2021), which published as WO2022157548 (on 28 July 2022). *At the time of writing, not yet available on the google patents website.*

[344] Berg JM, Tymoczko JL, Stryer L (2002) Biochemistry. 5th edition. New York: WH Freeman.

[345] Meyer AS, McCain MD, Fang Q, Pegg AE, Spratt TE (2003) O 6-Alkylguanine− DNA Alkyltransferases Repair O 6-Methylguanine in DNA with Michaelis−Menten-like Kinetics. Chemical research in toxicology. 16(11):1405-1409.

[346] Blainey PC, van Oijen AM, Banerjee A, Verdine GL, Xie XS (2006) A base-excision DNA-repair protein finds intrahelical lesion bases by fast sliding in contact with DNA. Proceedings of the National Academy of Sciences. 103(15):5752-5757.

[347] Gorman J, Chowdhury A, Surtees JA, Shimada J, Reichman DR, Alani E, Greene EC (2007) Dynamic basis for one-dimensional DNA scanning by the mismatch repair complex Msh2-Msh6. Molecular cell. 28(3):359-370.

[348] Hobbs JK, Jiao W, Easter AD, Parker EJ, Schipper LA, Arcus VL (2013) Change in heat capacity for enzyme catalysis determines temperature dependence of enzyme catalyzed rates. ACS chemical biology. 8(11):2388-2393.

[349] Jones HB, Crean RM, Matthews C, Troya AB, Danson MJ, Bull SD, ... & Pudney CR (2018) Uncovering the relationship between the change in heat capacity for enzyme catalysis and vibrational frequency through isotope effect studies. ACS Catalysis. 8(6):5340-5349.

[350] Arcus VL, Mulholland AJ (2020) Temperature, dynamics, and enzyme-catalyzed reaction rates. Annual review of biophysics. 49:163-180.

[351] Arcus VL, Prentice EJ, Hobbs JK, Mulholland AJ, Van der Kamp MW, Pudney CR, ... & Schipper LA (2016) On the temperature dependence of enzyme-catalyzed rates. Biochemistry. 55(12):1681-1688.

[352] Waring MJ, Arrowsmith J, Leach AR, Leeson PD, Mandrell S, Owen RM, Pairaudeau G, Pennie WD, Pickett SD, Wang J, Wallace O (2015) An analysis of the attrition of drug candidates from four major pharmaceutical companies. Nature reviews Drug discovery. 14(7):475-86.

[353] https://www.sec.gov/Archives/edgar/data/1463361/000119312518125773/d535851ds1a.htm (accessed on 25 July 2022).

[354] Naoi M, Maruyama W (1999) Cell death of dopamine neurons in aging and Parkinson's disease. Mechanisms of ageing and development. 111(2):175-88.

[355] Bender A, Krishnan KJ, Morris CM, Taylor GA, Reeve AK, Perry RH, Turnbull DM (2006) High levels of mitochondrial DNA deletions in substantia nigra neurons in aging and Parkinson disease. Nature genetics. 38(5):515-517.

[356] Kraytsberg Y, Kudryavtseva E, McKee AC, Geula C, Kowall NW, Khrapko K (2006) Mitochondrial DNA deletions are abundant and cause functional impairment in aged human substantia nigra neurons. Nature genetics. 38(5):518-520.

[357] Wong WL, Su X, Li X, Cheung CM, Klein R, Cheng CY, Wong TY (2014) Global prevalence of age-related macular degeneration and disease burden projection for 2020 and 2040: a systematic review and meta-analysis. The Lancet Global Health. 2(2):e106-16.

[358] Austad SN, Fischer, KE (1991) Mammalian aging, metabolism, and ecology: evidence from the bats and marsupials. Journal of Gerontology. 46(2):B47-B53.

[359] Burbank RC, Young JZ (1934) Temperature changes and winter sleep of bats. The Journal of physiology. 82(4):459.

[360] Pearson OP (1947) The rate of metabolism of some small mammals. Ecology. 28(2):127-145.

[361] Siegel JM (2005) Clues to the functions of mammalian sleep. Nature. 437(7063):1264-1271.

[362] Wilkinson GS, South JM (2002) Life history, ecology and longevity in bats. Aging cell. 1(2):124-131.

[363] Meyer GA, Senulis JA, Reinartz JA (2016) Effects of temperature and availability of insect prey on bat emergence from hibernation in spring. Journal of Mammalogy. 97(6):1623-1633.

[364] Podlutsky AJ, Khritankov AM, Ovodov ND, Austad SN (2005) A new field record for bat longevity. The Journals of Gerontology Series A: Biological Sciences and Medical Sciences. 60(11):1366-1368.

[365] Studier EH, Wilson DE (1970) Thermoregulation in some neotropical bats. Comparative Biochemistry and Physiology. 34(2):251-262.

[366] Brunet-Rossinni AK (2004) Reduced free-radical production and extreme longevity in the little brown bat (Myotis lucifugus) versus two non-flying mammals. Mechanisms of ageing and development. 125(1):11-20.

[367] Buffenstein R, Yahav S (1991) Is the naked mole-rat Hererocephalus glaber an endothermic yet poikilothermic mammal? Journal of Thermal Biology. 16(4):227-32.

[368] Smith ESJ, Schuhmacher L, Husson Z (2015) The naked mole-rat as an animal model in biomedical research: current perspectives. Open Access Animal Physiology. (7): 137-148.

[369] McNab BK (1966) The metabolism of fossorial rodents: a study of convergence. Ecology. 47(5):712-733.

[370] Gordon CJ (1990) Thermal biology of the laboratory rat. Physiology & behavior. 47(5):963-991.

[371] Dawson TJ, Hulbert AJ (1969) Standard energy metabolism of marsupials. Nature. 221(5178):383-383.

[372] Huxley AF (1959) Ion movements during nerve activity. Annals of the New York Academy of Sciences. 81(2):221-46.

[373] Chapman RA (1967) Dependence on temperature of the conduction velocity of the action potential of the squid giant axon. Nature. 213(5081):1143.

[374] Maldonado CA, Wooley BD, Pancrazio JJ. The excitatory effect of temperature on the Hodgkin-Huxley model.

[375] Fitzhugh R (1966) Theoretical effect of temperature on threshold in the Hodgkin-Huxley nerve model. The Journal of general physiology. 49(5):989-1005.

[376] Kuang S, Wang J, Zeng T, Cao A (2008) Thermal impact on spiking properties in Hodgkin-Huxley neuron with synaptic stimulus. Pramana. 70(1):183-90.

[377] Goldin MA, Mindlin GB (2017) Temperature manipulation of neuronal dynamics in a forebrain motor control nucleus. PLoS computational biology. 13(8):e1005699.

[378] Ronchi JA, Henning B, Ravagnani FG, Figueira TR, Castilho RF, Dos Reis SF, Vercesi AE (2015) Increased susceptibility of Gracilinanus microtarsus liver mitochondria to Ca2+-induced permeability transition is associated with a more oxidized state of NAD(P). Oxidative medicine and cellular longevity.

[379] Austad SN (1993) Retarded senescence in an insular population of Virginia opossums (Didelphis virginiana). Journal of Zoology. 229(4):695-708.

[380] Austad SN, Fischer KE (2016) Sex differences in lifespan. Cell metabolism. 23(6):1022-33.

[381] Data from the World Bank website, e.g. for female, from https://data.worldbank.org/indicator/SP.DYN.LE00.FE.IN (accessed on 20 July 2022).

[382] Geneva II, Cuzzo B, Fazili T, Javaid W (2019) Normal body temperature: a systematic review. Open forum infectious diseases. 6(4):1-7.

[383] Karanjawala ZE, Murphy N, Hinton DR, Hsieh CL, Lieber MR (2002) Oxygen metabolism causes chromosome breaks and is associated with the neuronal apoptosis observed in DNA double-strand break repair mutants. Current biology. 12(5):397-402.

[384] Barnes DE (2002) DNA damage: air-breaks? Current biology. 12(7):R262-R264.

[385] Yim MB, Chock PB, Stadtman ER (1993) Enzyme function of copper, zinc superoxide dismutase as a free radical generator. Journal of Biological Chemistry. 268(6):4099-4105.

[386] Peled-Kamar M, Lotem J, Wirguin I, Weiner L, Hermalin A, Groner Y (1997) Oxidative stress mediates impairment of muscle function in transgenic mice with elevated level of wild-type Cu/Zn superoxide dismutase. Proceedings of the National Academy of Sciences. 94(8):3883-3887.

[387] Yim MB, Chock PB, Stadtman ER (1990) Copper, zinc superoxide dismutase catalyzes hydroxyl radical production from hydrogen peroxide. Proceedings of the National Academy of Sciences. 87(13):5006-5010.

[388] Ansenberger-Fricano K, Ganini D, Mao M, Chatterjee S, Dallas S, Mason RP, Bonini MG (2013) The peroxidase activity of mitochondrial superoxide dismutase. Free Radical Biology and Medicine. 54:116-124.

[389] Li Y, Huang TT, Carlson EJ, Melov S, Ursell PC, Olson JL, ... & Epstein CJ (1995) Dilated cardiomyopathy and neonatal lethality in mutant mice lacking manganese superoxide dismutase. Nature genetics. 11(4):376-381.

[390] Thomas CE, Morehouse LA, Aust SD (1985) Ferritin and superoxide-dependent lipid peroxidation. Journal of Biological Chemistry. 260(6):3275-3280.

[391] Liochev SI (1996) Commentary: The Role of Iron-Sulfur Clusters in In Vivo Hydroxyl Radical Production. Free radical research. 25(5):369-384.

[392] Liochev SI, Fridovich I (1999) Superoxide and iron: partners in crime. IUBMB life. 48(2):157-161.

[393] Liochev SI, Fridovich I (1994) The role of $O_2^{\cdot -}$ in the production of $HO^{\cdot}$: in vitro and in vivo. Free Radical Biology and Medicine. 16(1):29-33.

[394] Gardner PR, Raineri I, Epstein LB, White CW (1995) Superoxide radical and iron modulate aconitase activity in mammalian cells. Journal of Biological Chemistry. 270(22):13399-13405.

[395] Ganini D, Santos JH, Bonini MG, Mason RP (2018) Switch of mitochondrial superoxide dismutase into a prooxidant peroxidase in manganese-deficient cells and mice. Cell chemical biology. 25(4):413-425.

[396] Orr WC, Sohal RS (1994) Extension of life-span by overexpression of superoxide dismutase and catalase in Drosophila melanogaster. Science. 263(5150):1128-1130.

[397] Mitsui A, Hamuro J, Nakamura H, Kondo N, Hirabayashi Y, Ishizaki-Koizumi S, Yodoi J (2002) Overexpression of human thioredoxin in transgenic mice controls oxidative stress and life span. Antioxidants and Redox Signaling. 4(4):693-696.

[398] Umeda-Kameyama Y, Tsuda M, Ohkura C, Matsuo T, Namba Y, Ohuchi Y, Aigaki T (2007) Thioredoxin suppresses Parkin-associated endothelin receptor-like receptor-induced neurotoxicity and extends longevity in Drosophila. Journal of Biological Chemistry. 282(15):11180-11187.

[399] Orr WC, Radyuk SN, Prabhudesai L, Toroser D, Benes JJ, Luchak JM, Sohal RS (2005) Overexpression of glutamate-cysteine ligase extends life span in Drosophila melanogaster. Journal of Biological Chemistry. 280(45):37331-37338.

[400] Nóbrega-Pereira S, Fernandez-Marcos PJ, Brioche T, Gomez-Cabrera MC, Salvador-Pascual A, Flores JM, Serrano M (2016) G6PD protects from oxidative damage and improves healthspan in mice. Nature communications. 7(1):1-9.

[401] Legan SK, Rebrin I, Mockett RJ, Radyuk SN, Klichko VI, Sohal RS, Orr WC (2008) Overexpression of glucose-6-phosphate dehydrogenase extends the life span of Drosophila melanogaster. Journal of Biological Chemistry. 283(47):32492-32499.

[402] Quick KL, Ali SS, Arch R, Xiong C, Wozniak D, Dugan LL (2008) A carboxyfullerene SOD mimetic improves cognition and extends the lifespan of mice. Neurobiology of aging. 29(1):117-28.

[403] Wu S, Li Q, Du M, Li SY, Ren J (2007) Cardiac-specific overexpression of catalase prolongs lifespan and attenuates ageing-induced cardiomyocyte contractile dysfunction and protein damage. Clinical and experimental pharmacology and physiology. 34(1-2):81-7.

[404] De Luca G, Ventura I, Sanghez V, Russo MT, Ajmone-Cat MA, Cacci E, Martire A, Popoli P, Falcone G, Michelini F, Crescenzi M (2013) Prolonged lifespan with enhanced exploratory behavior in mice overexpressing the oxidized nucleoside triphosphatase hMTH1. Aging cell. 12(4):695-705.

[405] Michael David Forrest. “Therapeutic Modifiers of the Reverse Mode of ATP Synthase”. Australian Patent Application Number AU2019208238A1. Filed on 26 July 2019. Published on 11 February 2021.

[406] Michael David Forrest. "Therapeutic Modifiers of the Reverse Mode of ATP Synthase". Canadian Patent Application Number CA3050553. Filed on 25 July 2019. Published on 25 January 2021.

[407] Rieger B, Arroum T, Villalta J, Busch KB (2021) Mitochondrial F_1F_O ATP synthase determines the local proton motive force in cristae tips. bioRxiv.

[408] McCullough L, Arora S (2004) Diagnosis and treatment of hypothermia. American family physician. 70(12):2325-32.

[409] Gaskill BN, Rohr SA, Pajor EA, Lucas JR, Garner JP (2009) Some like it hot: mouse temperature preferences in laboratory housing. Applied Animal Behaviour Science. 116(2):279-85.

[410] Gordon CJ, Puckett ET, Repasky ES, Johnstone AF (2017) A Device that Allows Rodents to Behaviorally Thermoregulate when Housed in Vivariums. Journal of the American Association for Laboratory Animal Science. 56(2):173-6.

[411] Boily P (2009) Role of voluntary motor activity on menthol-induced hyperthermia in mice. Journal of Thermal Biology. 34(8):420-5.

[412] Tomlinson S, Withers PC, Cooper C (2007) Hypothermia versus torpor in response to cold stress in the native Australian mouse Pseudomys hermannsburgensis and the introduced house mouse Mus musculus. Comparative Biochemistry and Physiology Part A: Molecular & Integrative Physiology. 148(3):645-50.

[413] LaMorte, W: Sample Size calculations: Excel spreadsheet downloadable from webpage: https://www.bu.edu/researchsupport/compliance/animal-care/working-with-animals/research/sample-size-calculations-iacuc/ (accessed on 31/07/2022).

[414] PS Power and Sample size. Hosted by the Department of Biostatistics at Vanderbilt University. https://vbiostatps.app.vumc.org/ps/ (accessed on 31/07/2022).

[415] Russell WM, Burch RL (1959) The principles of humane experimental technique. Methuen.

[416] https://www.nhs.uk/live-well/healthy-weight/understanding-calories/ (accessed on 16 August 2021).

[417] Magalhães JPD, Costa J, Church GM (2007) An analysis of the relationship between metabolism, developmental schedules, and longevity using phylogenetic independent contrasts. The Journals of Gerontology Series A: Biological Sciences and Medical Sciences. 62(2):149-160.

[418] Barja G (2007) Mitochondrial oxygen consumption and reactive oxygen species production are independently modulated: implications for aging studies. Rejuvenation research. 10(2):215-224.

[419] Barja G, Cadenas S, Rojas C, Perez-Campo R, Lopez-Torres M (1994) Low mitochondrial free radical production per unit O2 consumption can explain the simultaneous presence of high longevity and high aerobic metabolic rate in birds. Free radical research. 21(5):317-327.

[420] Lambert AJ, Buckingham JA, Boysen HM, Brand MD (2010) Low complex I content explains the low hydrogen peroxide production rate of heart mitochondria from the long-lived pigeon, Columba livia. Aging cell. 9(1):78-91.

[421] Pamplona R, Portero-Otín M, Sanz A, Ayala V, Vasileva E, Barja G (2005) Protein and lipid oxidative damage and complex I content are lower in the brain of budgerigar and canaries than in mice. Relation to aging rate. Age. 27(4):267-280.

[422] Miwa S, Jow H, Baty K, Johnson A, Czapiewski R, Saretzki G, Von Zglinicki T (2014) Low abundance of the matrix arm of complex I in mitochondria predicts longevity in mice. Nature communications. 5(1):1-12.

[423] Pamplona R, Jové M, Mota-Martorell N, Barja G (2021) Is the NDUFV2 subunit of the hydrophilic complex I domain a key determinant of animal longevity? The FEBS Journal.

[424] Hulbert AJ, Pamplona R, Buffenstein R, Buttemer WA (2007) Life and death: metabolic rate, membrane composition, and life span of animals. Physiological reviews. 87(4):1175-1213.

[425] Pamplona R, Prat J, Cadenas S, Rojas C, Perez-Campo R, Torres ML, Barja G (1996) Low fatty acid unsaturation protects against lipid peroxidation in liver mitochondria from long-lived species: the pigeon and human case. Mechanisms of ageing and development. 86(1):53-66.

[426] Pamplona R, Portero-Otın M, Requena JR, Thorpe SR, Herrero A, Barja G (1999) A low degree of fatty acid unsaturation leads to lower lipid peroxidation and lipoxidation-derived protein modification in heart mitochondria of the longevous pigeon than in the short-lived rat. Mechanisms of ageing and development. 106(3):283-296.

[427] Pamplona R, Portero-Otin M, Riba D, Ledo F, Gredilla R, Herrero A, Barja G (1999) Heart fatty acid unsaturation and lipid peroxidation, and aging rate, are lower in the canary and the parakeet than in the mouse. Aging Clinical and Experimental Research. 11(1):44-49.

[428] Buttemer WA, Battam H, Hulbert AJ (2008) Fowl play and the price of petrel: long-living Procellariiformes have peroxidation-resistant membrane composition compared with short-living Galliformes. Biology Letters. 4(4):351-354.

[429] Hulbert AJ, Faulks S, Buttemer WA, Else PL (2002) Acyl composition of muscle membranes varies with body size in birds. Journal of Experimental Biology. 205(22):3561-3569.

[430] Major SS Flower (1925) Contributions to our Knowledge of the Duration of Life in Vertebrate Animals. - IV. Birds. Proceedings of the Zoological Society of London. 95(4):1365-1422. Blackwell Publishing Ltd.

[431] Rouslin W, Frank GD, Broge CW (1995) Content and binding characteristics of the mitochondrial ATPase inhibitor, IF1 in the tissues of several slow and fast heart-rate homeothermic species and in two poikilotherms. Journal of bioenergetics and biomembranes. 27(1):117-125.

[432] Rouslin W, Pullman ME (1987) Protonic inhibition of the mitochondrial adenosine 5′-triphosphatase in ischemic cardiac muscle. Reversible binding of the ATPase inhibitor protein to the mitochondrial ATPase during ischemia. Journal of molecular and cellular cardiology. 19(7):661-668.

[433] Rouslin W (1988) Factors affecting the loss of mitochondrial function during zero-flow ischemia (autolysis) in slow and fast heart-rate hearts. Journal of molecular and cellular cardiology. 20(11):999-1007.

[434] Rouslin W, Broge CW, Grupp IL (1990) ATP depletion and mitochondrial functional loss during ischemia in slow and fast heart-rate hearts. American Journal of Physiology-Heart and Circulatory Physiology. 259(6):H1759-H1766.

[435] Rouslin W, Broge CW (1989) Regulation of mitochondrial matrix pH and adenosine 5′-triphosphatase activity during ischemia in slow heart-rate hearts: Role of Pi/H+ symport. Journal of Biological Chemistry. 264(26):15224-15229.

[436] Satre M, De Jerphanion MB, Huet J, Vignais PV (1975) ATPase inhibitor from yeast mitochondria. Purification and properties. Biochimica et Biophysica Acta (BBA)-Bioenergetics. 387(2):241-55.

[437] Hill AB (1965) The environment and disease: association or causation?

[438] Lourenço dos Santos S, Petropoulos I, Friguet B (2018) The oxidized protein repair enzymes methionine sulfoxide reductases and their roles in protecting against oxidative stress, in ageing and in regulating protein function. Antioxidants. 7(12):191.

[439] Whittemore K, Vera E, Martínez-Nevado E, Sanpera C, Blasco MA (2019) Telomere shortening rate predicts species life span. Proceedings of the National Academy of Sciences. 116(30):15122-15127.

[440] Barnes RP, Fouquerel E, Opresko PL (2019) The impact of oxidative DNA damage and stress on telomere homeostasis. Mechanisms of ageing and development. 177:37-45.

[441] Oikawa S, Kawanishi S (1999) Site-specific DNA damage at GGG sequence by oxidative stress may accelerate telomere shortening. FEBS letters. 453(3):365-368.

[442] Von Zglinicki T (2002) Oxidative stress shortens telomeres. Trends in biochemical sciences. 27(7):339-344.

[443] von Zglinicki T, Saretzki G, Döcke W, Lotze C (1995) Mild hyperoxia shortens telomeres and inhibits proliferation of fibroblasts: a model for senescence? Experimental cell research. 220(1):186-193.

[444] Qian W, Kumar N, Roginskaya V, Fouquerel E, Opresko PL, Shiva S, ... & Van Houten B (2019) Chemoptogenetic damage to mitochondria causes rapid telomere dysfunction. Proceedings of the National Academy of Sciences. 116(37):18435-18444.

[445] Passos JF, Nelson G, Wang C, Richter T, Simillion C, Proctor CJ, ... & Von Zglinicki T (2010) Feedback between p21 and reactive oxygen production is necessary for cell senescence. Molecular systems biology. 6(1):347.

[446] Correia-Melo C, Marques FD, Anderson R, Hewitt G, Hewitt R, Cole J, ... & Passos JF (2016) Mitochondria are required for pro-ageing features of the senescent phenotype. The EMBO journal. 35(7):724-742.

[447] Hütter E, Unterluggauer H, Überall F, Schramek H, Jansen-Dürr P (2002) Replicative senescence of human fibroblasts: the role of Ras-dependent signaling and oxidative stress. Experimental gerontology. 37(10-11):1165-1174.

[448] Blander G, De Oliveira RM, Conboy CM, Haigis M, Guarente L (2003) Superoxide dismutase 1 knock-down induces senescence in human fibroblasts. Journal of Biological Chemistry. 278(40):38966-38969.

[449] Chen Q, Fischer A, Reagan JD, Yan LJ, Ames BN (1995) Oxidative DNA damage and senescence of human diploid fibroblast cells. Proceedings of the National Academy of Sciences. 92(10):4337-4341.

[450] Packer L, Fuehr K (1977) Low oxygen concentration extends the lifespan of cultured human diploid cells. Nature. 267(5610):423-425.

[451] Parrinello S, Samper E, Krtolica A, Goldstein J, Melov S, Campisi J (2003) Oxygen sensitivity severely limits the replicative lifespan of murine fibroblasts. Nature cell biology. 5(8):741-747.

[452] Lee AC, Fenster BE, Ito H, Takeda K, Bae NS, Hirai T, ... & Finkel T (1999) Ras proteins induce senescence by altering the intracellular levels of reactive oxygen species. Journal of Biological Chemistry. 274(12):7936-7940.

[453] Catalano A, Rodilossi S, Caprari P, Coppola V, Procopio A (2005) 5-Lipoxygenase regulates senescence-like growth arrest by promoting ROS-dependent p53 activation. The EMBO journal. 24(1):170-179.

[454] Macip S, Igarashi M, Berggren P, Yu J, Lee SW, Aaronson SA (2003) Influence of induced reactive oxygen species in p53-mediated cell fate decisions. Molecular and cellular biology. 23(23):8576-8585.

[455] Niedernhofer LJ, Daniels JS, Rouzer CA, Greene RE, Marnett LJ (2003) Malondialdehyde, a product of lipid peroxidation, is mutagenic in human cells. Journal of Biological Chemistry. 278(33):31426-33.

[456] Breimer LH (1990) Molecular mechanisms of oxygen radical carcinogenesis and mutagenesis: the role of DNA base damage. Molecular carcinogenesis. 3(4):188-97.

[457] Hsie AW, Recio L, Katz DS, Lee CQ, Wagner M, Schenley RL (1986) Evidence for reactive oxygen species inducing mutations in mammalian cells. Proceedings of the National Academy of Sciences. 83(24):9616-20.

[458] Cooke MS, Evans MD, Dizdaroglu M, Lunec J (2003) Oxidative DNA damage: mechanisms, mutation, and disease. The FASEB Journal. 17(10):1195-214.

[459] Hulbert AJ, Pamplona R, Buffenstein R, Buttemer WA (2007) Life and death: metabolic rate, membrane composition, and life span of animals. Physiological reviews. 87(4):1175-213.

[460] Musatov A (2006) Contribution of peroxidized cardiolipin to inactivation of bovine heart cytochrome c oxidase. Free Radical Biology and Medicine. 41(2):238-246.

[461] Moosmann B, Behl C (2008) Mitochondrially encoded cysteine predicts animal lifespan. Aging cell. 7(1):32-46.

[462] Aledo JC, Li Y, de Magalhães JP, Ruíz-Camacho M, Pérez-Claros JA (2011) Mitochondrially encoded methionine is inversely related to longevity in mammals. Aging cell. 10(2):198-207.

[463] Samuels DC (2005) Life span is related to the free energy of mitochondrial DNA. Mechanisms of ageing and development. 126(10):1123-9.

[464] Skujina I, McMahon R, Lenis VPE, Gkoutos GV, Hegarty M (2016) Duplication of the mitochondrial control region is associated with increased longevity in birds. Aging (Albany NY). 8(8):1781.

[465] Eberhard JR, Wright TF (2016) Rearrangement and evolution of mitochondrial genomes in parrots. Molecular phylogenetics and evolution. 94:34-46.

[466] Perez-Campo R, Lopez-Torres M, Cadenas S, Rojas C, Barja G (1998) The rate of free radical production as a determinant of the rate of aging: evidence from the comparative approach. Journal of Comparative Physiology B. 168(3):149-58.

[467] Pamplona R, Costantini D (2011) Molecular and structural antioxidant defenses against oxidative stress in animals. American Journal of Physiology-Regulatory, Integrative and Comparative Physiology. 301(4):R843-63.

[468] Calder III WA (1985) The comparative biology of longevity and lifetime energetics. Experimental gerontology. 20(3-4):161-70.

[469] Porter RK, Brand MD (1995) Causes of differences in respiration rate of hepatocytes from mammals of different body mass. American Journal of Physiology-Regulatory, Integrative and Comparative Physiology. 269(5):R1213-R1224.

[470] Baker DJ, Childs BG, Durik M, Wijers ME, Sieben CJ, Zhong J, Van Deursen JM (2016) Naturally occurring p16 Ink4a-positive cells shorten healthy lifespan. Nature. 530(7589):184-189.

[471] Vassilev LT, Vu BT, Graves B, Carvajal D, Podlaski F, Filipovic Z, Kong N, Kammlott U, Lukacs C, Klein C, Fotouhi N (2004) In vivo activation of the p53 pathway by small-molecule antagonists of MDM2. Science. 303(5659):844-8.

[472] Dolgin E (2020) Send in the senolytics. Nature Biotechnology. 38(12):1371-1378.

[473] https://clinicaltrials.gov (accessed on 25 July 2022).

[474] Hall SS (2015) The man who wants to beat back aging. Science. 16.

[475] Previtali D, Merli G, Di Laura Frattura G, Candrian C, Zaffagnini S, Filardo G (2021) The long-lasting effects of "placebo injections" in knee osteoarthritis: a meta-analysis. Cartilage. 13(1_suppl):185S-96S.

[476] Yousefzadeh MJ, Zhu YI, McGowan SJ, Angelini L, Fuhrmann-Stroissnigg H, Xu M, Ling YY, Melos KI, Pirtskhalava T, Inman CL, McGuckian C (2018) Fisetin is a senotherapeutic that extends health and lifespan. EBioMedicine. 36:18-28.

[477] Xu M, Pirtskhalava T, Farr JN, Weigand BM, Palmer AK, Weivoda MM, Inman CL, Ogrodnik MB, Hachfeld CM, Fraser DG, Onken JL (2018) Senolytics improve physical function and increase lifespan in old age. Nature medicine. 24(8):1246-56.

[478] Miller RA, Harrison DE, Astle CM, Floyd RA, Flurkey K, Hensley KL, Javors MA, Leeuwenburgh C, Nelson JF, Ongini E, Nadon NL (2007) An aging interventions testing program: study design and interim report. Aging cell. 6(4):565-75.

[479] https://www.youtube.com/watch?v=42PzfNs9egA (accessed on 2 August 2022).

[480] Fossel M (2019) Cell senescence, telomerase, and senolytic therapy. OBM Geriatrics. 3(1):1-.

[481] Grosse L, Wagner N, Emelyanov A, Molina C, Lacas-Gervais S, Wagner KD, Bulavin DV (2020) Defined p16^{High} senescent cell types are indispensable for mouse healthspan. Cell Metabolism. 32(1):87-99.